

# Development and Evaluation of Monolithic Columns for Protein Analysis

## Dissertation

zur Erlangung des akademischen Grades

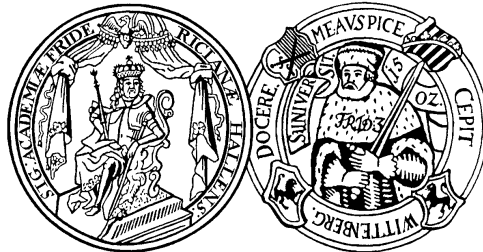
doctor rerum naturalium

(Dr. rer. nat.)

vorgelegt der

Naturwissenschaftlichen Fakultät I – Biowissenschaften

Martin-Luther-Universität Halle-Wittenberg



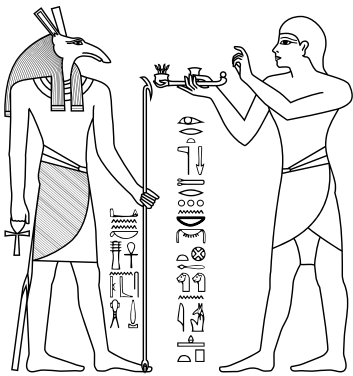
von

Jens Sproß

geboren am 20.11.1981 in VS-Villingen

GutachterInnen:

1. Prof. Dr. Andrea Sinz
  2. Prof. Dr. Hans-Herrmann Rüttinger
  3. Prof. Dr. Frank-Michael Matysik
- Halle (Saale), den 26. Februar 2013



---

**Contents**

Contents	I
Abbreviations	IV
1 Summary	1
2 Basic Principles	3
2.1 Principles of Liquid Chromatography	3
2.2 Monolithic Materials – Definition, History and Platforms	4
2.2.1 Preparation of Organic Monoliths	7
2.2.2 Preparation of Inorganic Monoliths	10
2.2.3 Functionalization of Monoliths	11
2.2.4 Characterization of MSPs	14
2.2.5 Applications of Monoliths – Challenges and Benefits	17
2.3 Mass Spectrometry	19
2.3.1 Ionization Mechanisms	19
2.3.1.1 Matrix-Assisted Laser Desorption/Ionization (MALDI)	19
2.3.1.2 Electrospray Ionization (ESI) and nano-ESI	21
2.3.2 Time-of-Flight (TOF) Mass Spectrometry	23
2.3.3 Q-TOF Mass Spectrometry	25
2.3.4 Linear Ion Trap (LIT)-Orbitrap Mass Spectrometry	27
2.3.5 Peptide Sequencing by Mass Spectrometry	30
2.4 Chemical Cross-Linking	31
2.4.1 Cross-Linking Reagents	33
2.4.2 Strategies for Identification of Cross-Linked Products	34

---

3	Publications	38
3.1	Review Article 1 (Trend Article including Preliminary Results):	38
	<b>Immobilized monolithic enzyme reactors for application in proteomics and pharmaceuticals</b>	
3.2	Original Paper 1:	39
	<b>A Capillary Monolithic Trypsin Reactor for Efficient Protein Digestion in <i>Online</i> and <i>Offline</i> Coupling to ESI and MALDI Mass Spectrometry</b>	
3.3	Review Article 2:	40
	<b>Monolithic media for applications in affinity chromatography</b>	
3.4	Original Paper 2:	41
	<b>Monolithic columns with immobilized monomeric avidin: preparation and application for affinity chromatography</b>	
3.5	Original Paper 3:	42
	<b>Multi-dimensional Nano-HPLC Coupled with Tandem Mass Spectrometry for Analyzing Biotinylated Proteins</b>	
4	Discussion	43
4.1	Monolithic Trypsin Reactor	43
4.2	Monolithic Affinity Column with Immobilized Monomeric Avidin	44
4.3	Online 3D and 2D nano-LC/nano-ESI/MS/MS Set-ups	46
5	Literature References	48
	Supplemental Material	61
	Acknowledgement	VI
	Publication List	VIII

Curriculum Vitae	XI
Selbständigkeitserklärung	XII

## Abbreviations

AAm	-	acrylamide
AC	-	alternating current
ACN	-	acetonitrile
AIBN	-	$\alpha,\alpha'$ -azoisobutyronitrile
BS <sup>3</sup>	-	bis(sulfosuccinimidyl)suberate
C-trap	-	curved ion trap
CCCA	-	$\alpha$ -cyano-4-chlorocinnamic acid
CHCA	-	$\alpha$ -cyano-4-hydroxycinnamic acid
CID	-	collision-induced dissociation
Co-IP	-	protein complex immunoprecipitation
DC	-	direct current
DHB	-	2,5-dihydroxybenzoic acid
EDMA	-	ethylene glycol dimethacrylate
ESI	-	electrospray ionization
FA	-	frontal analysis
FSC	-	fused silica capillary
GC	-	gas chromatography
GMA	-	glycidyl methacrylate
HIC	-	hydrophobic interaction chromatography
HPLC	-	high-performance liquid chromatography
IEX	-	ion exchange chromatography
IMER	-	immobilized monolithic enzyme reactor
ISEC	-	inverse size exclusion chromatography
LID	-	laser-induced dissociation
LIT	-	linear ion trap
<i>m/z</i>	-	mass-to-charge ratio
MACMA	-	monolithic affinity columns with immobilized monomeric avidin
MALDI	-	matrix-assisted laser desorption/ionization
$\gamma$ -MAPS	-	$\gamma$ -methacryloxypropyl trimethoxysilane
MS	-	mass spectrometry
MSP	-	monolithic stationary phase
NHS	-	<i>N</i> -hydroxysuccinimide

---

NIR	-	near infrared
NMR	-	nuclear magnetic resonance
LC	-	liquid chromatography
<i>oa</i> -TOF	-	orthogonal acceleration time-of-flight
PEEK	-	polyether ether ketone
PEG	-	poly(ethylene glycol)
PTFE	-	poly(tetrafluoroethylene)
Q	-	quadrupole
RF	-	radio frequency
ROMP	-	ring-opening metathesis polymerization
RP	-	reversed phase
SEC	-	size exclusion chromatography
SEM	-	scanning electron microscopy
skMLCK	-	skeletal muscle myosin light chain kinase
SP	-	stationary phase
SPE	-	solid phase extraction
TEM	-	transmission electron microscopy
TIS	-	timed ion selector
TLC	-	thin layer chromatography
TOF	-	time-of-flight
UHPLC	-	ultra-high-performance liquid chromatography
UV	-	ultraviolet
Y2H	-	yeast two-hybrid

## Proteinogenic amino acids:

A	-	Ala	-	alanine	M	-	Met	-	methionine
C	-	Cys	-	cysteine	N	-	Asn	-	asparagine
D	-	Asp	-	aspartate	P	-	Pro	-	proline
E	-	Glu	-	glutamate	Q	-	Gln	-	glutamine
F	-	Phe	-	phenylalanine	R	-	Arg	-	arginine
G	-	Gly	-	glycine	S	-	Ser	-	serine
H	-	His	-	histidine	T	-	Thr	-	threonine
I	-	Ile	-	isoleucine	V	-	Val	-	valine
K	-	Lys	-	lysine	W	-	Trp	-	tryptophane
L	-	Leu	-	leucine	Y	-	Tyr	-	tyrosine

## 1 Summary

Proteins play a key role in all processes of living organisms. Biological processes, such as supplying an organism with energy, repairing damages, producing compounds for sustaining the cell cycle, disposing threats to the organism or signal transduction would be impossible without proteins [1]. Despite this multitude of tasks all proteins are composed of only 20 amino acids, the so called proteinogenic amino acids. The high diversity of proteins is realized by their primary structures (amino acid sequences) resulting in different secondary structures (*e.g.*  $\alpha$ -helices,  $\beta$ -sheets), tertiary structures (3D conformation), and quaternary structure. Most tasks cannot be performed by a single protein alone, but proteins act as part of complexes, composed of only two proteins or creating huge assemblies [1].

In the course of this work, monolithic stationary phases (MSPs) were developed and validated for improving protein analysis using multi-dimensional liquid chromatography coupled with mass spectrometry (LC/MS/MS). Monolithic columns possess an enhanced mass transfer compared to particle based stationary phases resulting in an improved performance [2, 3]. Based on existing preparation protocols [4-6] an immobilized monolithic enzyme reactor (IMER) with trypsin was prepared and digestion conditions were optimized using simple protein systems [7]. Recent reports on trypsin IMERs only optimized certain aspects of digestion conditions, such as content of chaotropic agent [4, 8] or digestion temperature [9]. Here, all relevant parameters (protein concentration, interaction time, concentration and type of chaotropic agent, and digestion temperature) were optimized. Complete digestion of cytochrome *c* and BSA was achieved within only 80 s. The trypsin IMER presented herein exhibited a high tolerance for acetonitrile (ACN) and urea. Integration of the trypsin reactor into an online 2D nano-HPLC/nano-ESI-LTQ-Orbitrap-MS/MS system enabled an automated digestion, separation, and analysis of proteins within 90 minutes.

For the targeted enrichment of biotinylated proteins and peptides, avidin was immobilized onto a monolithic column and monomerized in an additional step [10]. Biotin binding capacities were determined using fluorescein-labeled biotin as well as biotin- and fluorescein-labeled BSA. Additionally, the latter served to determine non-specific binding of the monolithic affinity columns. The enrichment parameters were optimized using biotinylated cytochrome *c* and biotinylated cytochrome *c* peptides. Enrichment performance of the monomeric avidin immobilized on the monolithic medium was superior compared to that of commercially available monomeric avidin beads.

For the enrichment of cross-linked peptides, a novel trifunctional cross-linker with a biotin moiety and two amine reactive *N*-hydroxysuccinimide (NHS) esters was used [11]. After the cross-linking reaction, the protein of interest was digested in solution and the resulting peptide mixtures were analyzed using a 2D nano-HPLC/nano-ESI-LTQ-Orbitrap-MS/MS system with the monomeric avidin affinity column in the first dimension. The second dimension consisted of a reversed phase (RP) column for the separation of enriched cross-linked peptides. Several cross-links were identified within cytochrome *c* as well as within a complex of calmodulin and a peptide derived from skeletal muscle myosin light chain kinase (skMLCK). Finally, both monolithic columns (trypsin IMER and affinity column) were successfully integrated into an online 3D nano-HPLC/nano-ESI-Q-TOF-MS/MS system for an automated digestion of biotinylated protein, an enrichment of biotinylated peptides, and a subsequent separation by RP chromatography and MS analysis.

## 2 Basic Principles

### 2.1 Liquid Chromatography (LC)

In chromatography, analytes are percolated through a stationary phase (SP) by a mobile phase. In case of LC, the SP is commonly placed within a column, while the analyte is dissolved in the mobile phase. Thereby, LC is suitable for the separation of non-volatile substances in contrast to gas chromatography (GC), which is only capable to separate volatile compounds [12].

LC was introduced by the Russian Mikhail Tsvett at the beginning of the 20<sup>th</sup> century who separated leaf extracts using inulin as SP [13, 14]. In the middle of the 20<sup>th</sup> century, Martin and Synge investigated chromatographic separations of amino acids [15-17] laying the path for the advent of modern high-performance liquid chromatography (HPLC), which was introduced in the late 1960s by Huber [18], Horvath [19], and Kirkland [20].

The mode of action in LC is quite simple. The analyte is delivered through the column containing the SP and is allowed with the SP. An equilibrium is established between the analyte that is absorbed on the SP and the analyte that is dissolved in the mobile phase. The analyte moves through the column more slowly compared to a compound that does not, or only to a limited extent, interact with the SP. Thus, it is possible to separate compounds with different physicochemical properties from each other. Most commonly, ultraviolet (UV) detectors are employed for monitoring the separation [21]. HPLC can also be coupled to MS analysis, which will give additional structural information about the analyte [21]. The most important components of an HPLC system are indicated in Figure 1.

The SP usually consists of silica gel particles, which carry modifications on their surface determining the separation mechanism [21]. For RP applications, silica gel particles are modified with alkylsilanes, such as octadecylsilane, for the separation of small molecules or peptides. As separation efficiencies are improved when using small particles, a pump is required to percolate the mobile phase through the SP. In the early years of HPLC, the particle size was limited to 3  $\mu\text{m}$  as most HPLC systems did not withstand the high backpressure generated by smaller

particles. This was overcome at the beginning of the 21<sup>st</sup> century with the development of chromatographic equipment capable of withstanding pressures up to 1,000 bar. This enabled to use particles with diameters smaller than 2  $\mu\text{m}$ , which further increased separation efficiency. The term ultra-high-performance liquid chromatography (UHPLC) was established for this development [22]. The invention of monolithic materials also resulted in better separation efficiencies, without the need for special instrumentation because of the lower backpressure of these SPs. Over the recent years, monolithic stationary phases MSPs have advanced into a valid alternative to particle columns [23, 24].

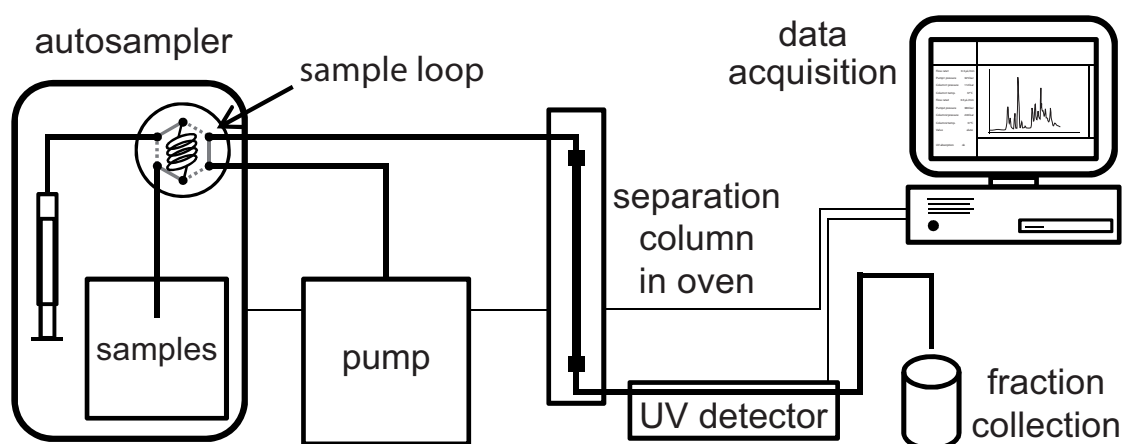


Figure 1: Scheme of an HPLC setup.

## 2.2 Monolithic Materials – Definition, History, and Platforms

The term ‘monolith’ is derived from the Greek expression ‘ $\mu\text{o}\nu\text{o}$ ’ (mono) – ‘single’ and ‘ $\lambda\acute{\iota}\theta\omicron\varsigma$ ’ (lithos) – ‘stone’, reflecting the idea of a chromatographic medium that is derived from a single piece of material. However, this definition hints a solid medium, which would not be suitable for LC as it lacks pores. In contrast to particulate SPs where the mobile phase is flowing around the particles, MSPs exhibit a highly interconnected network of pores, similar to that of leuconoid sponges (Figure 2). Therefore, the mobile phase flows through the skeleton of the monolith and the analytes that are transported by the mobile phase come into close contact with the monolith’s

surface. This and the tortuosity of the pores are responsible for the exceptionally fast mass transfer kinetics of monolithic columns [3, 25]. Monoliths are prepared from monomers using polymerization reactions in the presence of inert solvents, the so called porogens.

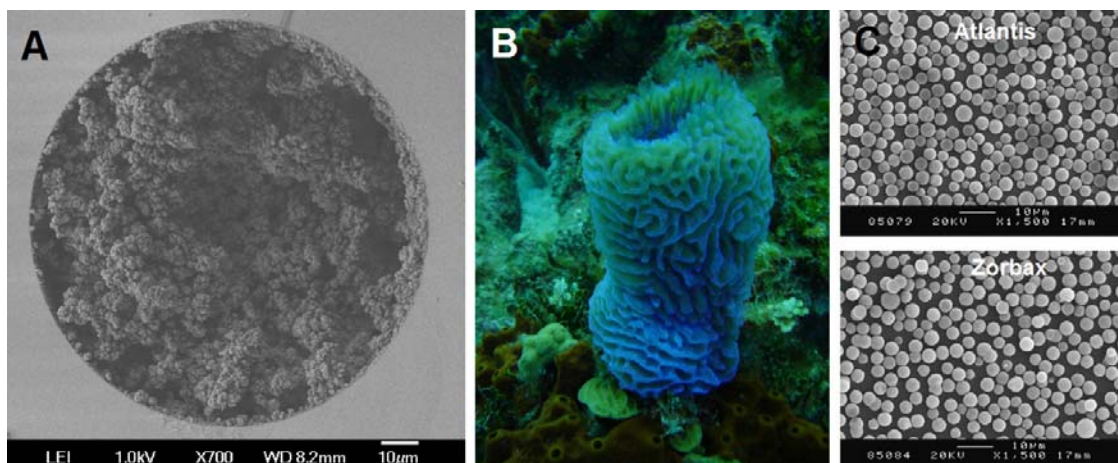


Figure 2: (A) Organic monolith in a fused silica capillary; (B) sponge, with kind permission of Mr. E. Murkett ([www.emmette.com](http://www.emmette.com)); (C) sub 2- $\mu\text{m}$  silica particles, reproduced with permission from [26], copyright 2007, Elsevier.

The idea of monolithic beds for the separation of compounds dates back to the 1950s when Nobel Prize laureate Robert Synge postulated materials with similar characteristics as they are realized in monolithic materials [27, 28]. Initial efforts using polyurethane foams did not yield high separation efficiencies as the structures were not sufficiently rigid and tended to collapse under the pressure induced by the flow of a mobile phase [29, 30]. At the beginning of the 1990s, several novel separation media emerged: Hjerten *et al.* performed separations with compressed acrylamide gels, however, the preparation of the separation beds was barely reproducible [31-33]. The group of Švec developed methacrylate-based monolithic columns, a highly versatile and successful subset of monolithic materials [23, 34-36], and in 1996 monoliths prepared from inorganic silica were reported by the group of Tanaka [24, 37]. Polymeric and silica-based monoliths have been patented and are now commercially available: Polymeric monoliths can be obtained from BIA Separations (CIM<sup>®</sup>), Agilent Technologies (Bio-Monolith<sup>®</sup>), and Dionex (now

ThermoFisher Scientific; ProtSwift<sup>®</sup> and PepSwift<sup>®</sup>); silica monoliths are commercialized by Merck KgA (Chromolith<sup>®</sup>) and Phenomenex (Onyx<sup>®</sup>). However, available surface chemistries are limited to mainly RP and ion exchange (IEX) materials. Therefore, when specific analytical needs have to be met, researchers have to access either unmodified MSPs as they are sold by Merck and BIA Separations or, alternatively, they have to prepare MSPs by themselves.

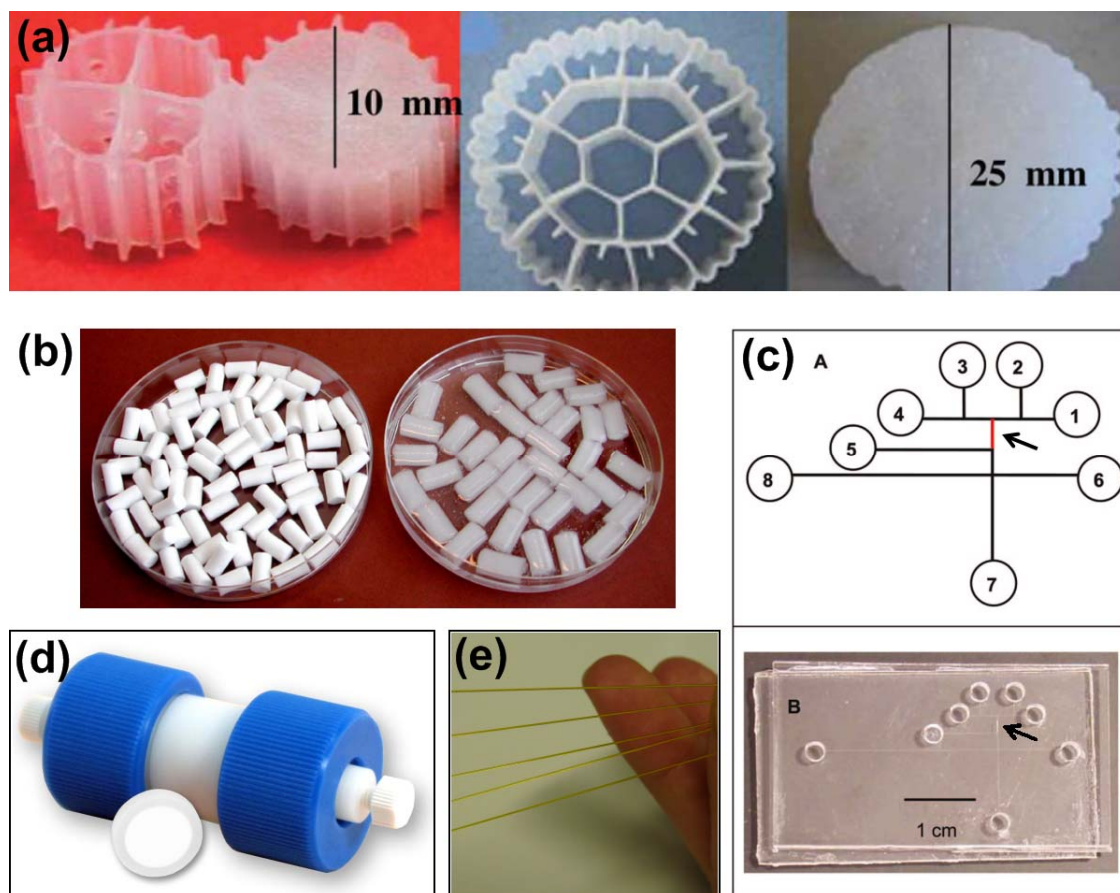


Figure 3: Formats of monoliths for AC: (a) cryogel in carrier; (b) cryogel microcolumns; (c) capillary electrophoresis microchip, position of monolith marked red; (d) CIM<sup>®</sup> disc and holder (image kindly provided by BIA Separations); (e) monoliths prepared in fused silica capillaries. Reproduced with permission from [38], copyright 2010, John Wiley and Sons.

To date, monolithic columns are used in numerous applications in all fields of LC and electrochromatography with a great variety of surface chemistries [25, 38-47]. They have been reported in column [3, 48, 49], capillary [3, 44, 48, 50], chip [51-54], pipette tip [52, 55-58], solid phase

extraction (SPE) spin bars [59-64], and thin layer chromatography (TLC) plate formats [65-67]. In order to combine advantages of particulate SPs and MSPs, hybrid materials have been prepared, in which the monolithic structure fixes the particles [68-72]. Several examples of housings for MSPs are presented in Figure 3.

### 2.2.1 Preparation of Organic Monoliths

Monoliths prepared from organic monomers were the first MSPs to emerge and up to date, they present the most versatile platform for chromatographic applications [23, 38, 73, 74]. The preparation process is straightforward and a multitude of monomers can be incorporated into the MSP. Glycidyl methacrylate (GMA) and ethylene glycol dimethacrylate (EDMA) were among the first monomers to be used for the preparation of monoliths (Figure 4) [34]. These two monomers are still widely used as they enable the introduction of a great variety of surface chemistries resulting in a multitude of chromatographic applications [38, 42]. However, the range of monomers is not limited to methacrylates. Every vinyl containing compound (e.g. divinyl benzene, acrylamide) can be copolymerized if it can be dissolved in the polymerization mixture [75]. Although a large number of preparation protocols exist for various monomers, conditions, especially the porogenic solvent mixture, have to be carefully optimized for each application to obtain optimum results [74, 75].

Generally, monoliths are prepared via polymerization reactions; radical polymerization is most commonly employed for polymeric monoliths [23, 34, 75], but alternative strategies, such as addition polymerization [76] and ring-opening metathesis polymerization (ROMP) [77-79], have been reported. At least two monomers are necessary: the functional monomer, which carries the functionality needed for LC (e.g. butyl methacrylate) [80] or a reactive group for ligand immobilization (e.g. GMA) [5, 7, 10], and the cross-linker (in most cases EDMA), which determines rigidity and mechanical properties of the MSP.

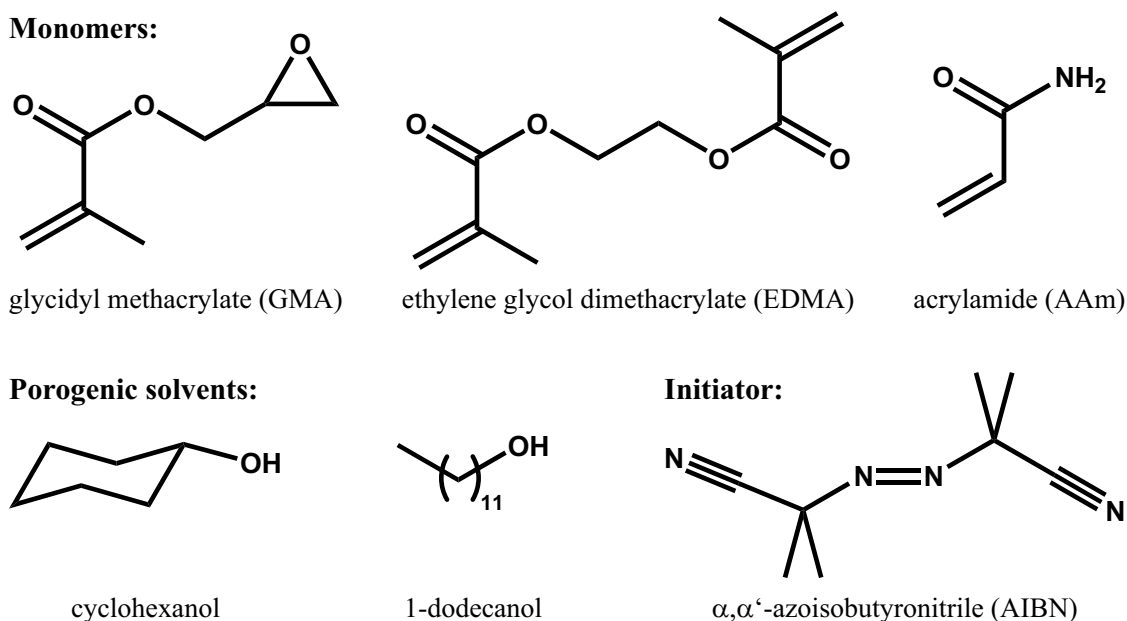


Figure 4: Monomers, porogenic solvents, and initiator used in this work.

When initializing the polymerization reaction, the monomers are dissolved in the porogenic solvents, which are responsible for creating the porous structure of the monolith [81]. Usually, mixtures of two solvents are used (Figure 4) [3, 75], but for tailoring the porous properties of the MSP the use of polymers, such as polyethylene glycols (PEGs) of varying chain lengths, has also been reported [82-84]. Free radical polymerization can be initiated by a multitude of strategies [75]: The routinely employed UV light-induced polymerization [85] and heat-induced polymerization [23] require initiators, such as  $\alpha, \alpha'$ -azoisobutyronitrile (AIBN; Figure 4). Less commonly used initiation by  $\gamma$ -rays [86-88] or electrons [89-92] results in polymers that are absent of any functional groups at the chain ends as these are introduced by the initiator.

Usually, the polymerization mixture is a homogeneous solution and phase separation determines the final pore structure of the MSP. However, monoliths can in principle be obtained from biphasic systems. Monolithic cryogels are prepared at sub-zero temperatures and the resulting ice crystals as well as the freezing and thawing speed determine the porous properties of the MSP [93-95]. Monoliths prepared from high internal phase emulsions also rely on a biphasic system

[96, 97]. The small droplets of the aqueous phase serve as a template resulting in MSPs with high surface areas [98].

During the preparation process, several parameters influence the porous properties of the MSP. As all parameters highly affect each other, manipulating one parameter can result in a completely different morphology of the MSP and subtle changes can have a huge impact on the MSP's structure and properties [99]. A multitude of studies have been published to elucidate the influences of specific parameters [3, 44, 75, 82, 99, 100], which can be divided into four main groups:

- I.) The porogenic solvents, their ratio in respect to each other and to the monomers – Each porogenic solvent mixture consists of a thermodynamically poorer solvent (the so called macroporogen) and a thermodynamically favored solvent for the polymer chains, which keeps them in solution for a longer period of time. If a larger amount of macroporogen is present, the through pores become large (due to an earlier onset of phase separation) and *vice versa*. Higher amounts of macroporogen also result in large microglobules, and therefore lower surface areas [3, 75, 99, 101].
- II.) The monomers, their ratio in respect to each other and to the porogenic solvents – The monomers also act as thermodynamically favorable solvents for the polymer chains, which results in a delayed onset of phase separation. If high amounts of cross-linker are present, phase separation starts earlier, but due to the higher number of initial polymer nuclei the resulting microglobules and through pores are smaller. As such, this effect is opposite to that when using high amounts of macroporogen, which will also result in an early onset of phase separation [85, 100, 102].
- III.) Polymerization temperature – UV light-initiated polymerization usually takes place at ambient temperature, whereas heat-induced polymerization requires temperatures between 50°C and 70°C. Higher temperature corresponds to a better solubility and therefore a later onset of phase separation. The resulting through pores are smaller as are the microglobules,

and higher surface areas are obtained. Additionally, the kinetics of the polymerization reaction and that of the transfer of monomers from solution into the growing nuclei are affected [81, 100].

- IV.) The polymerization initiation method and the reaction rate – The impact of the reaction kinetics can be easily determined by initiating the polymerization reaction with UV light. The reaction proceeds much faster compared to heat-initiated reactions indicating a larger amount of nuclei to be formed. However, differences in the separation performance of MSPs prepared via photo-initiation and temperature-initiation are insignificant [80, 103].

Organic monoliths have been prepared in a great variety of sizes, ranging from capillary format up to columns with a volume of 8 liters. This impressively demonstrates the high flexibility of the preparation process, but one should note that temperature control during the synthesis of large monolithic columns is challenging.

### 2.2.2 Preparation of Inorganic Monoliths

To date, silica particles are state-of-the-art SPs in LC and consequently, the first monoliths synthesized from inorganic precursors were silica monoliths [24, 37, 104]. The first generation of silica monoliths was prepared from aqueous solutions of tetraalkoxysilanes (Figure 5) in a sol-gel process via condensation polymerization in the presence of water, which served as porogenic solvent and for generating silanol groups via hydrolysis of the precursors, polymers, such as PEG (to determine the pore structure of the monolith), and acid (catalyst) [24, 41, 104]. Recently, trialkoxy(methyl)silane precursors (Figure 5) have gained increasing importance [41, 105, 106]. Compared to monoliths prepared from tetraalkoxysilanes, better separation performance is obtained using trialkoxy(methyl)silanes [105].

Mesopores are introduced in a second step by etching the silica network with a basic solution resulting in the large surface areas of silica monoliths [24, 104]. The resulting monoliths are highly hydrophilic due to the presence of surface hydroxyl groups, which serve to immobilize

functional groups in an additional step. In contrast to silica monoliths prepared within fused silica capillaries (FSCs), larger silica monoliths with diameters of several mm are prepared in molds and have to be clad in a polyether ether ketone (PEEK) or poly(tetrafluoroethylene) (PTFE) tube to obtain the final separation column [24, 104].

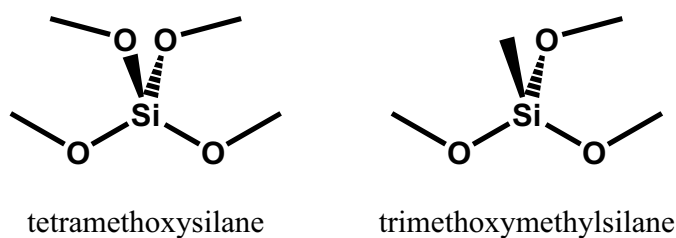


Figure 5: Precursors for silica monolith preparation.

Shrinking of the monolith during the aging step is still a major issue as radial inhomogeneities are created in the MSP, which detrimentally affect separation efficiencies of the columns [3]. Additionally, silica materials are not stable at elevated pH values. Therefore, other metal oxides have moved into the focus of research [107, 108]. Monoliths have been prepared from titania ( $\text{TiO}_2$ ) [109], zirconia ( $\text{ZrO}_2$ ) [110, 111] and hafnia ( $\text{HfO}_2$ ) [108], however, hydrolysis rates of their precursors is faster as for silanes and make the preparation process even more difficult to handle. So far, separations of small molecules have been reported using these novel monolithic materials [108, 110].

### 2.2.3 Functionalization of Monoliths

Surface functionalization is an important topic as each chromatographic application requires a different functional group to be attached to the MSP [38, 42]. The simplest way to introduce a functional group is the copolymerization of a monomer bearing the required functionality, such as alkyl methacrylates [80, 112, 113]. Yet, this strategy is not always applicable when preparing monolithic media for affinity chromatography. It is only beneficial when the functional monomer is sufficiently stable during the polymerization process and readily available, as a certain amount

of functional groups are buried within the monolithic matrix during the preparation process and do not take part in the chromatographic separation [76, 114]. Additionally, preparation conditions of the MSP have to be optimized for each individual functional monomer. The attachment of proteins onto the monolith's surface is virtually impossible with this strategy as the proteins will denature in the polymerization mixture.

Therefore, the use of template MSPs, which are subsequently derivatized based on the needs of a specific application, is receiving increasing attention [38, 42, 45]. Three main strategies for the introduction of functional groups on MSPs have evolved over the recent years:

- I.) Preparation of MSPs using living polymerization, such as ROMP, enables the introduction of a functional monomer after the polymerization of the template MSP as the catalyst/initiator remains on the surface of the monolith [101, 115, 116].
- II.) Different functionalities can be immobilized even in different regions of a monolithic column using photografting and photomasks [117, 118]. However, as UV light cannot penetrate into the center of the MSP, the homogeneity of the surface modification is a matter of debate.
- III.) Immobilization of functional groups using reactive groups on the MSP's surface is the most commonly used strategy [38, 42, 45]. Usually, *poly*(GMA-*co*-EDMA) monoliths are employed because of the high reactivity of the epoxy groups with a multitude of functional groups, *e.g.* primary amines or  $H^+$  [5, 7, 10, 38]. Other reactive groups, such as 2-vinyl-4,4-dimethylazlactone, have also been reported [119, 120]. Although a single-step immobilization of ligands is possible, higher ligand densities are obtained when employing more elaborate and time consuming multi-step immobilization strategies [121, 122].

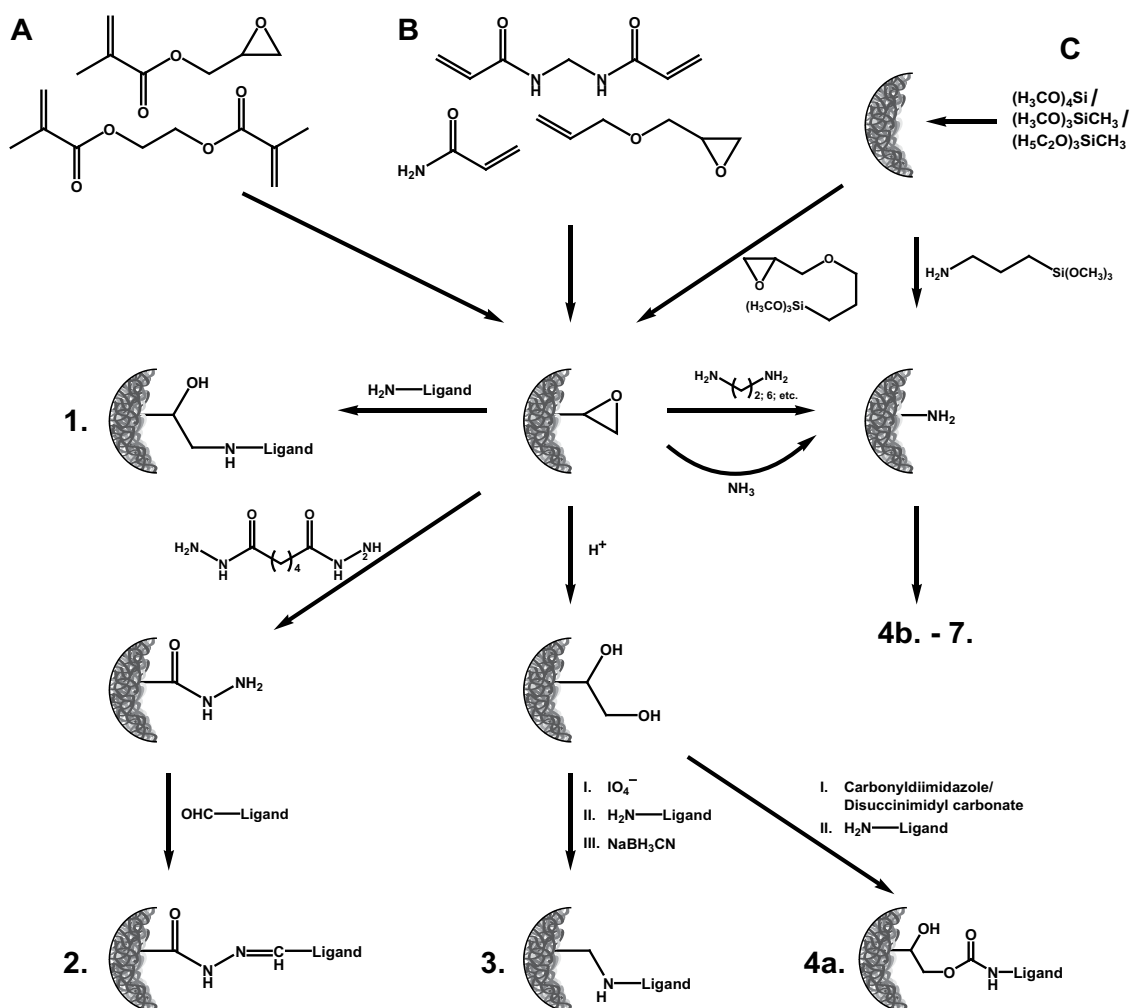
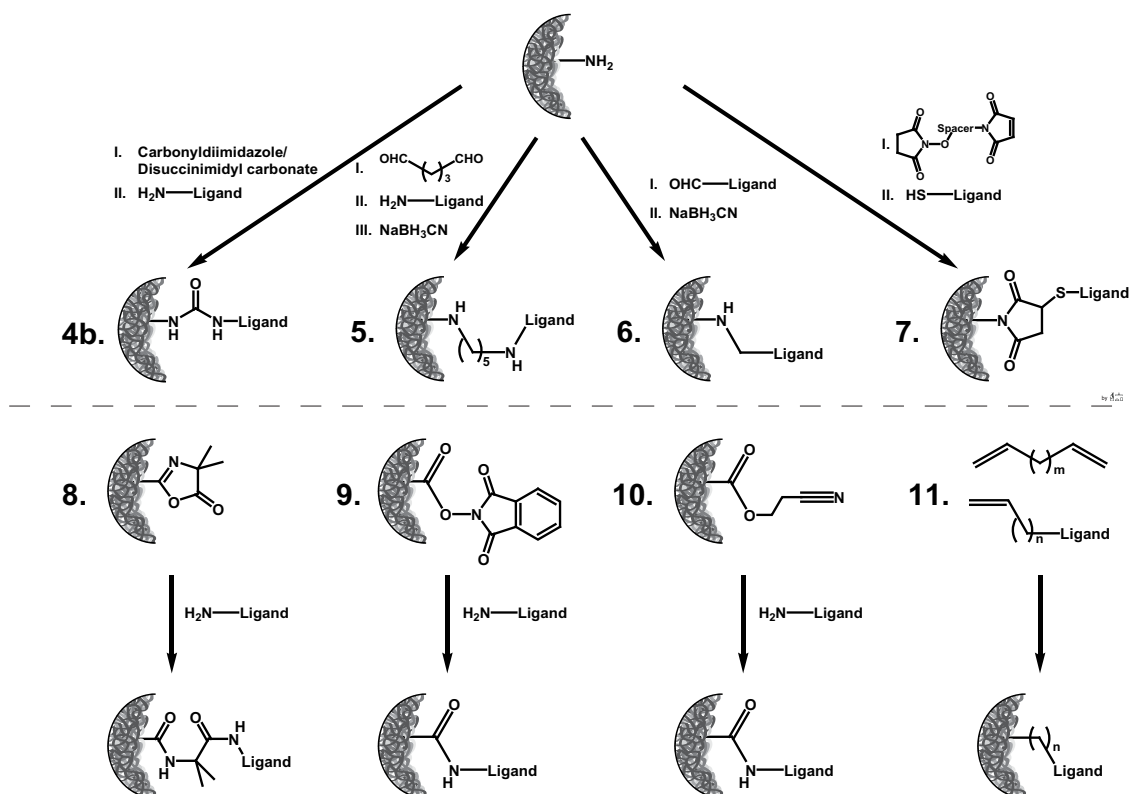


Figure 6: Overview of immobilization strategies for the preparation of affinity chromatography media from (A) organic monoliths, (B) monolithic cryogels, and (C) silica monoliths. 1, epoxy method; 2, hydrazide method; 3, Schiff base method; 4a, carbonyldiimidazole.

An overview of different immobilization strategies is presented in Figure 6. In contrast to organic MSPs, inorganic monoliths usually have to be modified after the preparation of the monolithic matrix. Direct entrapment of proteins in silica monoliths has been reported, but the release of alcohols during the hydrolysis of the alkoxy silane precursors might denature the protein [123-126]. For the derivatization of silica monoliths, the silanol groups on the surface are used for immobilizing functional groups [24, 105, 127]. This enables the preparation of monolithic

columns for a large variety of applications from a single MSP, thereby eliminating the need to optimize the MSP for every application.



#### 2.2.4 Characterization of MSPs

The chromatographic performance of an MSP is directly related to its porous properties. The size of the through pores and the mesopores, the pore size distribution, their geometry, and the surface area influence the hydrodynamic properties, column capacity or ligand density, and the mass transfer kinetics [3, 75]. A brief overview of the most important methods providing insight into the physical properties of the MSPs is presented below.

**Morphology:** This feature is commonly studied by scanning electron microscopy (SEM) [3, 84, 105, 114, 128] and to a lesser extent by transmission electron microscopy (TEM) [129, 130]. As the images obtained by these methods are acquired in the dry state they only provide an estimation of the morphology.

**Porosity and pore size distribution:** Mercury porosimetry [81, 84, 100, 130, 131], inverse size exclusion chromatography (ISEC) [98, 130-133], near infrared (NIR) spectroscopy [134, 135], and (ultra) small angle neutron scattering [136] have been used for the investigation of porosity, determination of pore sizes, and pore size distribution. ISEC is the only method where these parameters can be assessed under chromatographic conditions, the other methods are employed in the dry state.

**Specific surface area:** This parameter is determined by nitrogen adsorption via the Brunauer-Emmett-Teller method [84, 98, 130, 133]. Mercury porosimetry [84], ISEC [130], and NIR spectroscopy [134] also yield information about the surface area of MSPs.

**Permeability:** The permeability  $K$  of an MSP directly depends on the macroporous structure. Although ISEC [130, 131] can be used, *Darcy's law* (E1.1) [137, 138] is commonly used for calculating the permeability:

$$K = \frac{u\eta L}{\Delta p} \quad (\text{E1.1})$$

$u$  – linear velocity,  $\eta$  – viscosity of the solvent,  $L$  – length of the column, and  $\Delta p$  – pressure drop across the chromatographic medium.

**Separation efficiency:** For the separation of analytes, by *e.g.* RP-LC, the efficiency of the SP is commonly described by the parameters summarized below. It should be noted that these parameters do not describe the properties of enzyme reactors or affinity media, described in this work.

The *number of theoretical plates* ( $N$ ) and their respective *heights* ( $H$ ) give insight into the efficiency of a separation medium. The column performance depends on the flow velocity ( $u$ ) and is estimated by the *van Deemter* equation (E1.2) [80, 139].

---

$$H = A + \frac{B}{u} + C \cdot u \quad (\text{E1.2})$$

This equation summarizes the parameters that contribute to peak broadening with A – Eddy diffusion, B – longitudinal diffusion, and C – resistance to mass transfer.

The minimum of the curve described by the *van Deemter* equation represents the optimum flow velocity.

For comparing separation efficiencies of particle-packed columns and monolithic columns column impedance (quotient of plate height square  $H^2$  and permeability K) has gained popularity over the recent years [3, 140].

**Loading capacity:** The loading capacity is determined by elution chromatography and frontal analysis (FA; dynamic binding capacity). In contrast to FA, the first method is not compatible with affinity chromatographic media. However, the amount of non-specific binding is difficult to assess by FA [141]. The *binding capacity* of affinity media can also be determined by tagging specific binding partners of the ligand, *e.g.* with a fluorescent dye [10]. The labeled binding partner is infused into the affinity column and non-bound and non-specifically retained molecules are removed. In the next step, the specifically retained binding partner is eluted, collected, and quantified.

**Enzyme activity:** In case enzymes are immobilized onto an MSP, the enzyme activity is commonly investigated using a model substrate [7, 119, 120, 142]. The substrate is flushed through the reactor and collected before spectroscopic methods are used to quantify the created product and to estimate the enzyme activity. Additionally, kinetic parameters of the enzymatic reaction can be investigated [119, 121]. However, in many cases enzyme activities were not determined, but only the ability of the prepared enzyme reactors to proteolytically cleave proteins was evaluated [9, 143].

### 2.2.5 Applications of Monoliths – Benefits and Challenges

The first applications of MSPs to be published in the first half of the 1990s were protein separations by IEX [23, 36], RP [36, 112, 144], and hydrophobic interaction chromatography (HIC) [36], as well as the use of molecularly imprinted (MIP) monolithic materials for separating regioisomers or enantiomers of template molecules [145]. Over the following two decades, the scope of applications was extended over all fields of LC: separation of small molecules [3, 44, 146], SEC [77, 147], SPE [52], enzyme reactors [6, 45], affinity enrichment [38, 42, 49, 148, 149] (using aptamers [150, 151], metal ions [152, 153], or binding proteins such as antibodies [154-156], lectins [157] or avidin [10]), and chiral separations [47]. Due to the ease of preparation and the great variety of available modification methods monoliths prepared from organic monomers are especially popular. Monolithic cryogels and hydrogels constitute a subclass of organic monoliths, which are usually prepared from acrylamides. Because of their large pores they find numerous applications for the enrichment of large analytes, *e.g.* viruses and bacteria [93, 158-161], or for the analysis of particle containing solutions [162], which would result in column blocking if conventional monoliths were used.

Silica monoliths are commonly used for RP separations [3, 41], but affinity separations and applications as enzyme reactors have also been reported [38, 42, 45, 127]. Due to the low back pressure of MSPs, very long columns (up to 4 m have been reported) can be used without the need of using equipment that is able to withstand the high pressures as they are required in UHPLC [163-166]. Monoliths are not limited to LC applications. MSPs have also been employed for capillary electrochromatography [47, 146, 167-169] and GC applications [170-172].

Compared to particulate SPs, all monolithic applications benefit from the fast mass transfer kinetics characteristic of MSPs [2, 173-175]. The life times of monolithic columns are high (in the order of months or even years) without losing their separation efficiency [80, 176-178]. The trypsin reactors prepared in the course of this work were operated for several months and were shown to be active even after two years of storage [7, 11]. Although the surface area of organic

MSPs is rather low compared to particulate SPs, similar ligand densities have been reported for *poly*(GMA-*co*-EDMA) monoliths [179, 180].

Almost all our knowledge about physicochemical and chromatographic properties of monolithic columns is derived from monolithic silica columns. However, separation performance of the 1.7  $\mu\text{m}$  particulate separation media used in UHPLC is superior [181] compared to monolithic columns, which are comparable with 3 to 5  $\mu\text{m}$  particles [3, 104, 182, 183]. For improved separation efficiencies smaller domain sizes (*i.e.* sum of the average through pore size and skeleton thickness) are required, however, this leads to higher back pressures. Using these monolithic silica materials, efficiencies are comparable to particle-based columns packed with 2-2.5  $\mu\text{m}$  particles [184, 185].

Previous experiments indicate that silica monoliths exhibit a certain degree of radial inhomogeneity, with domain size (average of skeleton thickness plus through pore size) varying over the column cross section [175, 186]. This negatively affects the separation performance of monolithic columns, mainly in ‘classical’ applications, *i.e.* RP separations of small molecules [3]. For other applications, such as affinity chromatography, where the analyte of interest is retained on the MSP and contaminating molecules are removed, radial inhomogeneity does not give rise to lower separation efficiencies.

For both particle-based and monolithic columns it is crucial that the total mobile phase is percolated through the SP. In the case of particle columns, channeling is the main problem, while the weakest point for monolithic columns is the interface between the wall of the support and the MSP. When glass containers are used, such as FSCs, this challenge can be easily met by a direct attachment of the MSP to the wall using trialkoxy silanes with vinyl groups, e.g.  $\gamma$ -methacryloxypropyl trimethoxysilane ( $\gamma$ -MAPS, Figure 7) [187, 188]. Silica monoliths with diameters of several millimeters are commonly clad in heat-shrinkable PEEK or PTFE tubes, which ensure for a tight seal between the tubing material and the MSP [24, 104]. In case other containers are employed, such as stainless steel tubes, the authors do not give detailed

information about how they prevented the formation of void volumes between the MSP and the container wall [5, 23, 189].

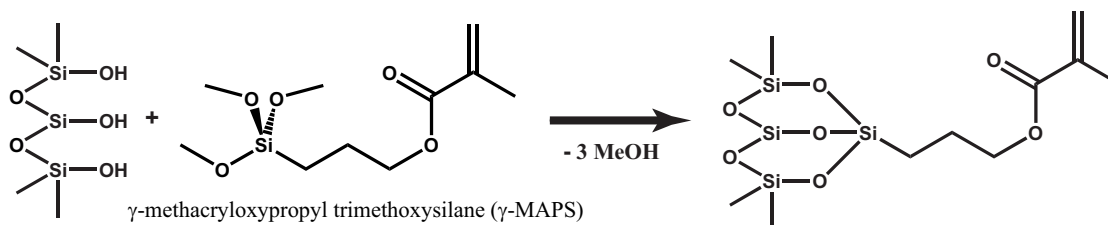


Figure 7: Glass wall modification with  $\gamma$ -MAPS.

### 2.3 Mass Spectrometry

Mass spectrometers enable the analysis of ionized molecules yielding information that assist in the identification of analytes. Fragmentation of the molecular ion is an important technique as it enables the identification of functional groups or, in case proteins or peptides are analyzed, the assignment of the amino acid sequence. In the following, only the mass spectrometric techniques are described that were used in the course of this work.

#### 2.3.1 Ionization Mechanisms

For protein and peptide analysis, matrix-assisted laser desorption/ionization (MALDI) and electrospray ionization (ESI) are the most commonly used ionization methods as they enable the “soft ionization” of these macromolecules.

##### 2.3.1.1 Matrix-Assisted Laser Desorption/Ionization (MALDI)

To enable the ionization of biopolymers by MALDI, the analyte molecules have to be embedded into a matrix compound, which is usually achieved by the dried-droplet method [190-192]. The analyte solution is mixed with the matrix solution at a ratio of 1:100 to 1:10,000 and spotted onto a target plate. When a laser shot hits the crystals matrix molecules absorb the laser energy, are

excited, and transfer the laser energy into the crystal structure causing local disruptions [193]. Eventually, excited matrix and analyte molecules are liberated into the gas phase [190]. During this process, only a small part of the energy seems to be transferred into vibrational energy as even labile biopolymers remain intact.

Commonly used matrices for protein analysis are sinapinic acid [194] and 2,5-dihydroxybenzoic acid (DHB, Figure 8) [195, 196], while peptide analysis is usually performed using  $\alpha$ -cyano-4-hydroxycinnamic acid (CHCA, Figure 8) [197]. Higher sensitivity is achieved when using matrices with lower proton affinity, such as  $\alpha$ -cyano-4-chlorocinnamic acid (CCCA, Figure 8) [198, 199]. However, due to the hypsochromic shift of the absorption maximum upon introduction of the halogen substituent ND:YAG-lasers ( $\lambda = 355$  nm) are not suitable. Instead,  $N_2$  lasers ( $\lambda = 337$  nm) have to be used in order to benefit from the improved ionization efficiencies of halogen substituted matrices [199].

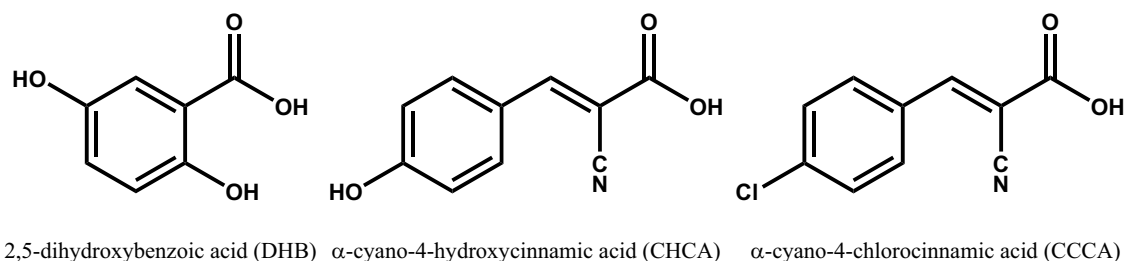


Figure 8: MALDI matrices DHB and CHCA that were used in this work and the novel matrix CCCA.

During the MALDI process, mainly singly charged ions are generated. Experimental observations confirmed not only a contribution of matrix molecules during the ionization process (proton transfer) [200-202], but suggested that analyte ions are already transferred into the gas phase (therefore called “lucky survivor”) [202]. When peptides are analyzed with CHCA as matrix, about 90% of the analyte ions are generated according to the “lucky survivor mechanism” [202].

MALDI is not suitable for *online* coupling with LC as the analytes have to be crystallized on the target plate prior to analysis, however, *offline* LC/MALDI coupling is performed via spotting robots.

#### 2.3.1.2 Electrospray Ionization (ESI) and Nano-ESI

ESI was introduced in the late 1980s by John B. Fenn [203-205] based on previous observations made by Malcolm Dole [206]. In contrast to MALDI, ESI is readily coupled with HPLC as it continuously generates ions from a stream of liquid that is delivered by an HPLC system or syringe pump with a flow rate of up to several hundreds of  $\mu\text{L}/\text{min}$  [204]. The ion source consists of the spray emitter, *e.g.* a stainless steel or metal-coated glass capillary ending in a tip with an orifice of several tens of  $\mu\text{m}$ , and a supply for a heated drying gas (Figure 9A). High voltage (3-5 kV) is applied between the spray emitter and the sample inlet of the mass spectrometer a resulting in the formation of an electric field, which assists in the generation of charged droplets (several  $\mu\text{m}$  diameter) and guides them towards the orifice of the mass spectrometer.

As in LC applications, miniaturization of ESI results in increased sensitivity [207]. For nano-ESI, the inner diameter of the spray emitter is decreased to ca. 20  $\mu\text{m}$  with an orifice diameter of several  $\mu\text{m}$  [208, 209]. Lower flow rates (100-300 nL/min) as delivered by a nano-HPLC system are sufficient for creating a stable electrospray. In static nano-ESI, the orifice is even smaller (approximately 2  $\mu\text{m}$ ) allowing capillary forces that are created by the release of droplets to deliver the analyte solution towards the spray emitter tip [208]. As the droplets formed by nano-ESI are one order of magnitude smaller than in ESI, the ionization efficiency is significantly increased [210].

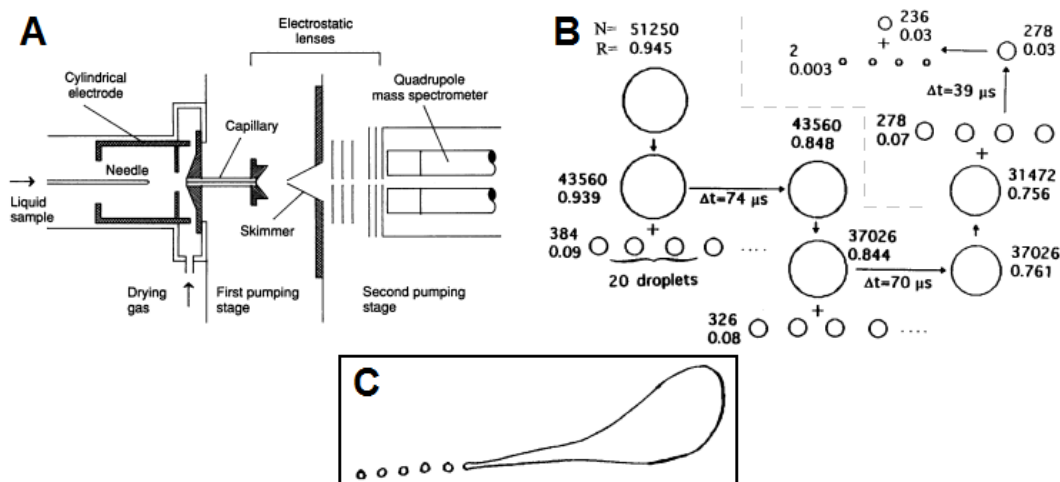


Figure 9: (A) Scheme of an ESI-source coupled to a quadrupole mass spectrometer, reproduced with permission from [205], copyright 1989, AAAS; (B) ESI process, illustrating several fission steps;  $N$  – number of elementary charges,  $R$  – droplet radius [ $\mu\text{m}$ ], adapted with permission from [211], copyright 2000, John Wiley and Sons; (C) outline of a flash shadowgraph showing a droplet during the fission process, adapted with permission from [212], copyright 1994, American Institute of Physics.

In contrast to MALDI, ESI creates multiply charged species. In the positive ionization mode, which is commonly employed for analyzing proteins and peptides, positively charged ions move to the end of the spray emitter tip causing the meniscus of the liquid to be warped into the so called Taylor cone [213]. From the tip of the Taylor cone small droplets are ejected due to the charge rejection that is caused by an excess of positively charged ions [214, 215]. These droplets are attracted by the counter electrode and travel in its direction. In ESI, a stream of gas is commonly employed to assist the nebulization and evaporation of the droplets, however, for nano-ESI this is not required due to the smaller droplet size. As the diameter of the droplets decreases upon evaporation, the charge density of the droplets increases until it reaches the Rayleigh limit and the droplets become unstable (Figure 9B) [216, 217]. Then, smaller droplets are released from the end of a droplet filament (Figure 9C) [218-220]. Several fissions have to take place until solvent-free ions are formed.

Formation of the solvent-free ions can be explained by the *charged residue model* by Dole [206, 221, 222] (small droplets of approximately 1 nm diameter contain only one remaining analyte ion) and the *ion evaporation model* by Iribarne and Thomson [223, 224] (ions are ejected from droplets with radii of  $\sim 8$  nm). Experiments revealed that solvent-free ions of small analytes are predominantly formed by the ion evaporation model. For large analytes, such as proteins, the charged residue model is favored for the generation of solvent-free ions [221, 222].

### 2.3.2 Time-of-Flight (TOF) Mass Spectrometry

TOF analyzers make use of the kinetic energy  $E_{\text{kin}}$  of ions (E2.1) and the fact that heavy ions possess lower velocities than light ions (when both ions have the same charge; E2.2).

$$E_{\text{kin}} = \frac{mv^2}{2} = \frac{mL^2}{2t^2} = qU \quad (\text{E2.1})$$

$$t = \sqrt{\frac{m}{2qU}} \cdot L \quad (\text{E2.2})$$

with  $m$  – mass of the analyte,  $v$  – velocity,  $L$  – length of the flight path,  $t$  – time of flight,  $q$  – elementary charge, and  $U$  – acceleration voltage.

To ensure that heavy ions are not overtaken by light ions it is of crucial importance that ions enter the TOF analyzer at defined time intervals. This makes TOF analyzers highly compatible with MALDI, a pulsed ionization technique [225].

The simplest TOF analyzers exhibit a linear geometry. The generated ions are accelerated by an electrode at a given voltage until they reach a certain kinetic energy (E2.1). By measuring the time interval necessary for the ions to reach the detector at the end of the flight tube their  $m/z$  values can be calculated (E2.2) [226, 227]. For the protein analysis, linear TOF analyzers are commonly used as they guarantee high sensitivity. Fragment ions and/or neutrals originating from

one precursor ion conserve the kinetic energy of the precursor ion and therefore reach the detector at the same time [228]. However, resolution is limited in the linear mode.

In order to enable higher resolution and better mass accuracy, state-of-the-art TOF instruments, such as the Ultraflex III MALDI-TOF/TOF mass spectrometer (Figure 10; Bruker Daltonik, Bremen) can be operated in the reflectron mode [229-231]. The reflectron compensates for differences in starting time, starting point, kinetic energy, and drift vectors of the generated ions and increases the flight path of ions resulting in multiplying the achievable resolution [232]. It is located at the end of the field-free drift region of the flight tube and consists of several ring electrodes. These ring electrodes are operated with increasing voltage, generating an electric field that decelerates ions until their kinetic energies reach zero. The ions are ejected and reach their initial kinetic energies when leaving the reflectron. As ions of higher kinetic energy penetrate deeper into the reflectron's electric field they also take longer to leave the reflectron compared to ions of the same  $m/z$  value, but lower kinetic energy (Figure 10). Ions of the same  $m/z$  value, but with different kinetic energies reach the reflectron detector at the same time. Usually, the reflectron voltage is 1.05 to 1.1 times higher than the acceleration voltage to ensure that all ions are ejected from the reflectron [227].

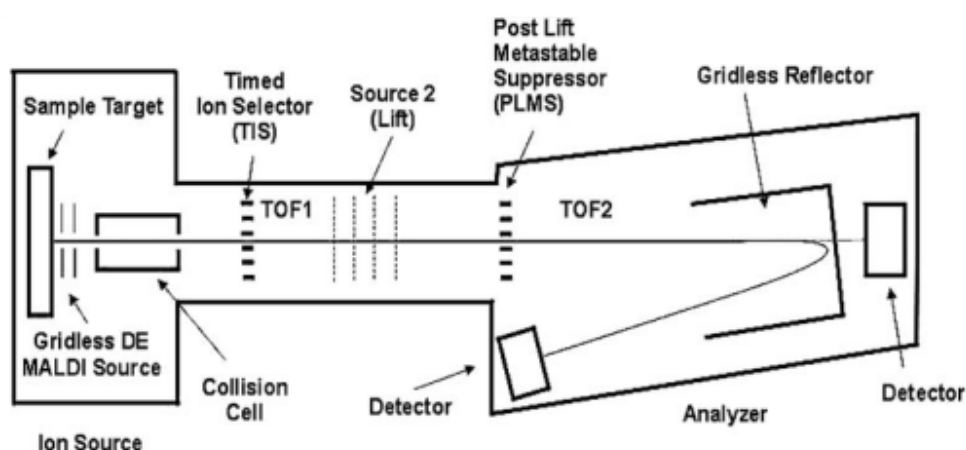


Figure 10: Scheme of the MALDI-TOF/TOF mass spectrometer Ultraflex III (Bruker Daltonik), reproduced with permission from [229], copyright 1993, Springer.

An additional strategy to obtain high resolution mass spectra is the application of delayed extraction. This technique compensates for initial differences in the kinetic energy of the generated ions. Instead of switching on the acceleration voltage during the ion formation process, the acceleration voltage is applied after a short time interval in the 100-200 ns range after ionization has already taken place.

### 2.3.3 Q-TOF Mass Spectrometry

Q-TOF mass spectrometers belong to the family of hybrid instruments comprised of two mass analyzers, which can be operated independently: a quadrupole mass analyzer with limited mass accuracy and resolution and a TOF analyzer with high mass accuracy and resolution [233, 234]. During the acquisition of mass spectra the quadrupole is operated in RF (radio frequency)-only mode and ions are analyzed in the TOF analyzer. When tandem MS experiments are performed, the quadrupole is used for the isolation of precursor ions, which are fragmented in the hexapole collision cell by collision-induced dissociation (CID) using a collision gas, *e.g.* nitrogen and analyzed in the TOF analyzer (Figure 11). Q-TOF mass spectrometers are usually equipped with ESI ion sources.

Quadrupole mass analyzers consist of four rods with either cylindrical or hyperbolic cross section (Figure 12) [235, 236]. The rod pairs, which are opposite to each other, are held at the same potential containing a direct current (DC) and an alternating current (AC) component. Ions entering the quadrupole experience an attractive force by the rods exhibiting the opposite charge. As the AC component changes periodically, the charge of the rods does the same and the ions are forced on an oscillating flight path along the axis of the quadrupole [237]. In RF-only mode the DC component equals zero making the quadrupole function as ion guide [238, 239]. When the quadrupole is used as a mass analyzer, the DC component is ramped and only trajectories of ions

with defined  $m/z$  values remain stable according to the *Mathieu equations* allowing them to pass the quadrupole towards the detector or the collision cell [240].

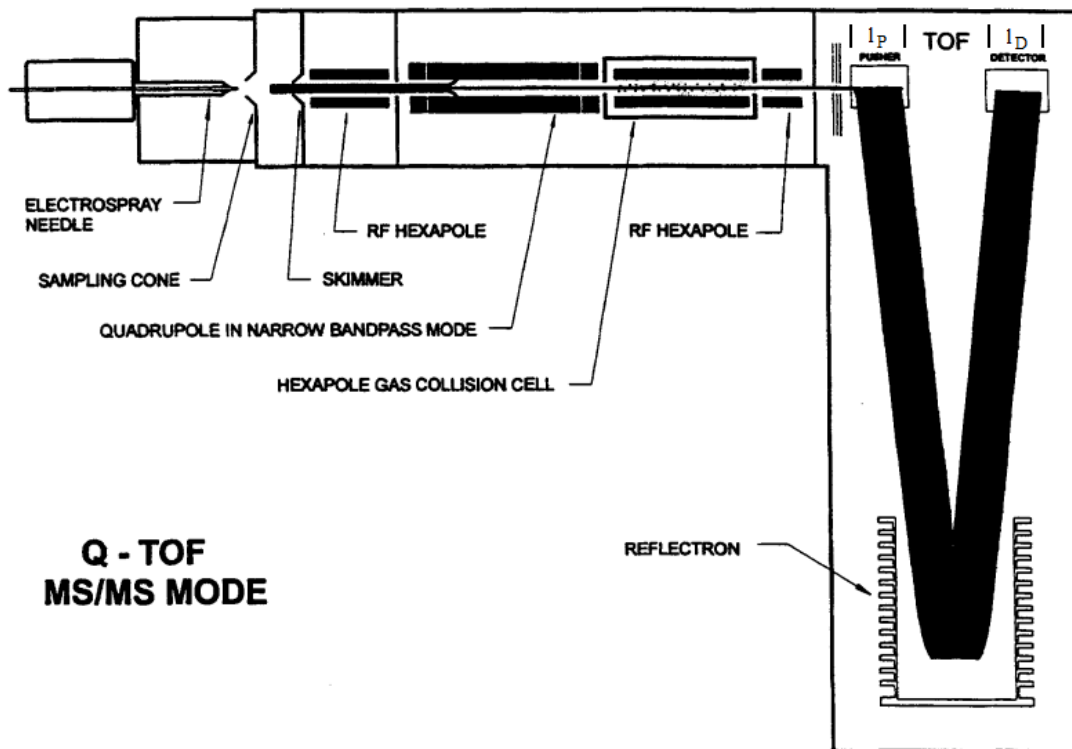


Figure 11: Schematic illustration of a Q-TOF mass spectrometer. Reproduced with permission from [233], copyright 1996, Wiley-VCH.

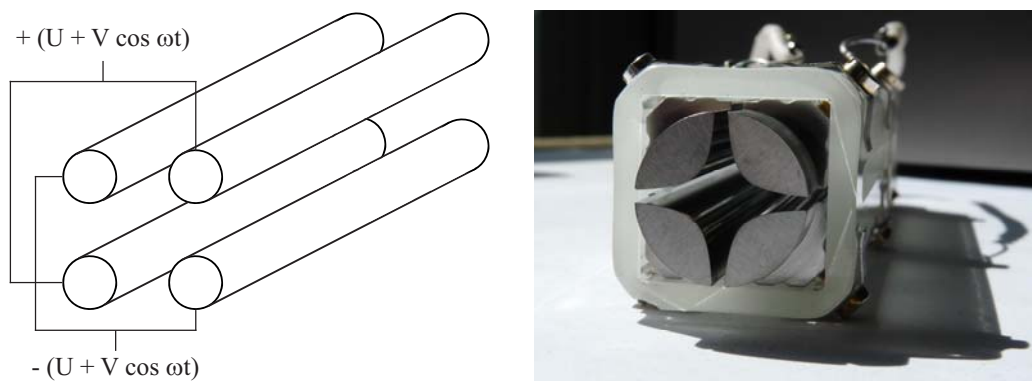


Figure 12: Scheme of a linear quadrupole mass analyzer with cylindrical rods (left) and image of a quadrupole from a Thermo Finnigan TSQ 700 triple quadrupole mass spectrometer with hyperbolic rods (right).

As described in section 2.3.2, TOF analyzers require a pulsed ion source. ESI sources and quadrupole mass analyzers deliver ions continuously making axial acceleration TOF analyzers less suitable for Q-TOF instruments. In order to render TOF analyzers compatible with continuous ion sources, the orthogonal acceleration TOF analyzer (*oa*-TOF) was developed [241-243]. Here, a certain length of the ion beam ( $l_p$ ) is accelerated in orthogonal direction to its flight path into the flight tube by applying an acceleration voltage at a sharp pulse of 2-4 kV (Figure 11). During the ions' drift time they still move in their original direction requiring detectors of a certain length ( $l_D$ ) and wider flight tubes to ensure a high sensitivity. Reflectrons are used to improve the resolution. Additional strategies for enhancing the resolution are focusing the ion beam by collisional cooling with residual gas molecules in the quadrupole and/or hexapole of the instrument, and by electrostatic lenses [244, 245].

#### 2.3.4 Linear Ion Trap (LIT)-Orbitrap Mass Spectrometry

As the Q-TOF mass spectrometer the LTQ-Orbitrap instrument (ThermoFisher Scientific) is a hybrid instrument composed of a linear ion trap (LIT, or LTQ – the trade name by ThermoFisher Scientific) and an orbitrap mass analyzer (Figure 13).

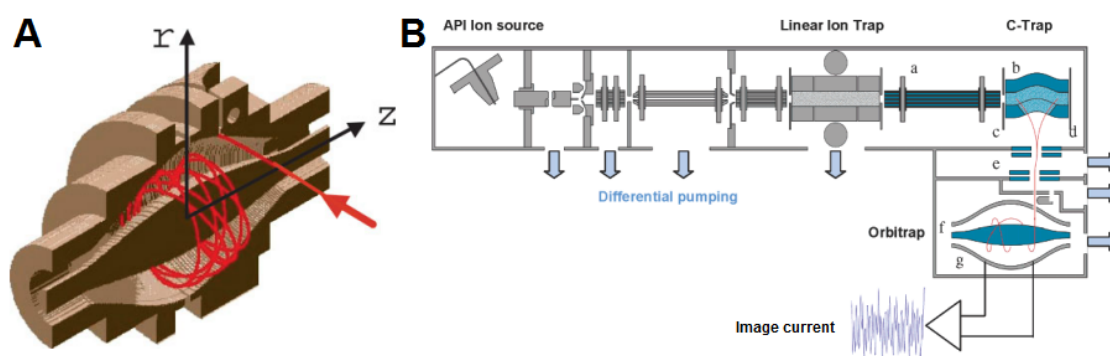


Figure 13: (A) cut-away view of the orbitrap, Reproduced with permission from [246], copyright 2005, John Wiley and Sons; (B) scheme of the hybrid LTQ-Orbitrap mass spectrometer. Reproduced with permission from [247], copyright 2006, American Chemical Society.

The LIT is used for accumulation of ion packages, precursor ion isolation, and CID fragmentation, which is not possible in the orbitrap. It also shields the ultrahigh vacuum that is necessary for optimum performance of the orbitrap analyzer. The analysis of MS and MS/MS data can be performed either in the LIT or the orbitrap analyzer. Mass accuracy and resolution of the LIT are limited, which is in sharp contrast to the high mass accuracy and excellent resolution of the orbitrap.

The LIT represents a quadrupole mass analyzer with additional cap electrodes at the entry and the exit of the quadrupole (Figure 14) [239, 248]. By applying a voltage between these two electrodes ions are trapped in an RF quadrupole field, leading to an oscillating ion movement. To avoid overfilling of the LIT the LTQ-Orbitrap instrument uses automatic gain control. In short prescans the total ion current is determined in a pre-set mass range, thus regulating the filling time of the LIT. For generating a homogeneous electric field, the quadrupole is separated in three segments with the first and last segments taking over the part of the trapping electrodes. This enables detection of ions by radial excitation. An additional AC voltage is applied on two rods opposite to each other, by which ions are selected, activated, and ejected towards the detectors. Ions are transferred towards the orbitrap analyzer by axial ejection after lowering the potential of the back section trapping electrode (Figure 14) [248].

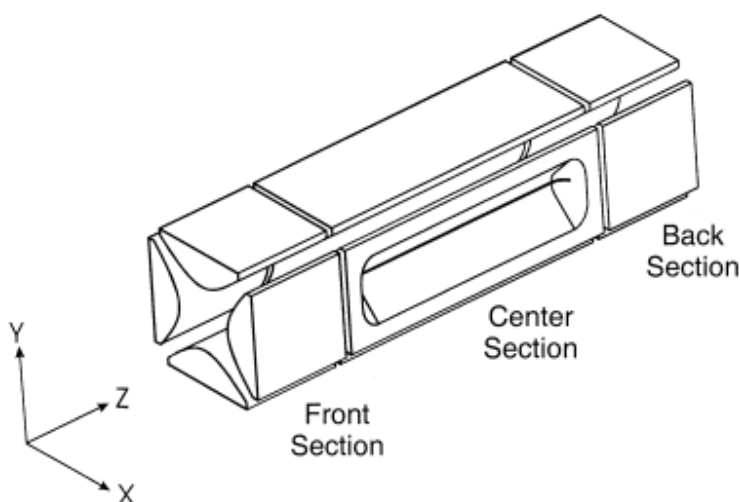


Figure 14: Scheme of the 2D-linear ion trap of the LTQ mass spectrometer. By ion ejection along the x-axis (radial ejection) through the slits in the centre section detection of the ions is performed. Ions are transmitted to the orbitrap analyzer by axial ejection along the z-axis. Reproduced with permission from [248], copyright 2002, Elsevier.

Another attractive feature of quadrupole ion traps is the option to focus ions into packets by collisional cooling [239, 244]. This is not only achieved in the LIT, but also in the C-trap (a curved quadrupole ion trap), and is of major importance as the ions have to be injected as small ion packet into the orbitrap to ensure maximum performance. A nitrogen pressure of 1 mbar in the C-trap ensures that no CID takes place.

The orbitrap belongs to the group of electrostatic traps. It was developed based on the work of Kingdon who was the first one to describe ion trapping on orbits around a central electrode [249] and Knight who optimized the outer electrode of the Kingdon trap [250]. However, no mass spectra were recorded with these first traps. The design was further optimized by Makarov and consists of a barrel-shaped outer electrode (split into two symmetrical halves) and a spindle-shaped inner electrode (Figure 13A) [246, 247, 251]. These electrodes generate an electrostatic quadrupole field. Ions are injected tangential to the inner electrode into the orbitrap and start oscillating in axial direction in the orbitrap while rotating around the inner electrode. The frequency of an ion oscillating axially within the orbitrap is proportional to its  $m/z$  value (equation E2.3) [246, 251].

$$\omega = \sqrt{\frac{k}{m/q}} \quad (\text{E2.3})$$

with  $\omega$  - frequency,  $k$  – instrument constant,  $m$  – mass of the analyte,  $q$  – elementary charge.

Mass spectra are obtained by a fast Fourier transformation of the image current, which is induced in the outer electrodes, and recorded. As the axial frequency is independent of the energy and spatial distribution of the ions, high mass resolution and accuracy can be obtained in the orbitrap. Resolution can be increased by recording the image current for a longer time or by increasing the size of the inner electrode, while sensitivity can be increased by using compact orbitraps or by optimizing the ion transfer optics [252, 253].

### 2.3.5 Peptide Sequencing by Mass Spectrometry

In this work, peptides were fragmented by laser-induced dissociation (LID) in the MALDI-TOF/TOF mass spectrometer and by CID in the Q-TOF and LTQ-Orbitrap mass spectrometers. Both techniques generate similar fragment ions, mainly y- and b-type-ions by fragmentation of the labile peptide bonds (Figure 15).

For LID, laser fluency is increased resulting in higher ion yields. The initial acceleration voltage is lower (8 kV), ensuring longer drift times of the ions (10 to 20  $\mu$ s) during which fragmentations take place [229]. All precursor ions move at velocities determined by equation E2.1, which is also the case for all fragment ions formed after acceleration. Therefore, a precursor ion and its fragment ions comprise an “*ion family*” as they reach the timed ion selector (TIS) together. By switching off the TIS, the selected ion family enters the LIFT cell (Laser-induced fragmentation technology, trade name by Bruker Daltoniks) where the ions are focused according to their velocity by applying a potential lift. Finally, the ions are accelerated towards the detector where they are focused in the reflectron.

CID requires a collision gas (nitrogen in the Q-TOF and helium in the LTQ) with which the isolated precursor ions collide [254, 255]. This results in the conversion of a part of the precursor ion's kinetic energy into internal energy, *e.g.* vibrational energy, causing the generation of fragment ions.

For the denomination of fragment ions, the *Roepstorff-Biemann* nomenclature was used [256, 257]. If the charge resides on the *N*-terminal fragment, the ions are termed a-, b- and c-type fragment ions, while the corresponding *C*-terminal fragments are named x-, y- and z-type fragment ions. To allow for a straightforward distinction between different cross-linked peptides (section 2.4), fragment ions created from the heavier peptide chain are marked with the index  $\alpha$ , while the fragment ions of the peptide chain with lower molecular weight are denoted with  $\beta$  (Figure 15) [258].

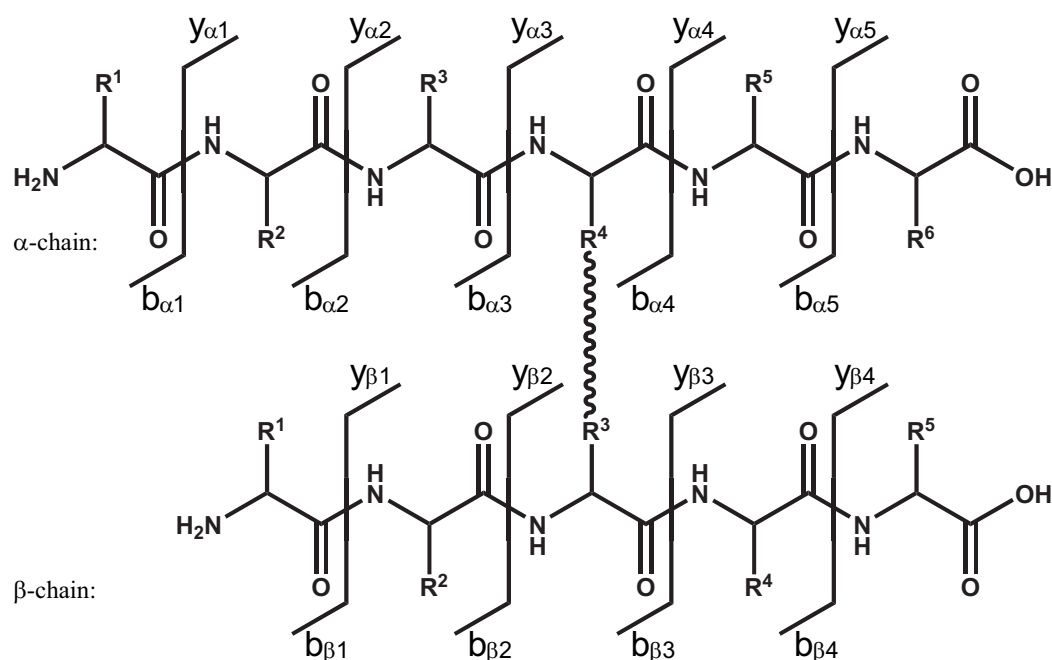


Figure 15: Nomenclature of peptide fragments according to Roepstorff [256], Biemann [257], and Schilling [258].

## 2.4 Chemical Cross-Linking

For a detailed understanding of cellular processes it is essential to gain insight into the interactions of proteins – the nature of their binding partners, the stoichiometry of the complexes, their topologies, and their kinetic data [259, 260].

Several methods are employed to answer these questions, among the most popular are protein complex immunoprecipitation (Co-IP) [261, 262] and the yeast two-hybrid system (Y2H) [263–265], which are employed for the identification of protein interaction partners. However, neither method yields information about the stoichiometry and the 3D-structure of the protein complexes and especially the Y2H method is prone to identifying false positives. On the other hand, weakly binding interaction partners might be lost during washing steps in Co-IP experiments.

X-ray crystallography [266] and nuclear magnetic resonance (NMR) spectroscopy [267, 268] yield highly resolved 3D structures of protein complexes, but both methods require large amounts

of purified protein. To make things worse, not all proteins or protein complexes can be investigated using these high-resolution techniques. For X-ray crystallographic studies, proteins have to form highly ordered structures to yield analyzable spectra. The high protein concentrations as well as the fact that 3D structures are determined in the solid state may result in artifacts. For NMR, the protein has to be present in mM concentrations, which might not be available for low-abundant proteins.

Chemical cross-linking employs chemical reagents that are able to form covalent bonds between amino acid side chains and as such can be used to derive low-resolution information. Artificial amino acids with photo-reactive diazirine moieties can be incorporated *in vivo* into proteins by the cell's translation machinery and upon irradiation with UV-light, spatially close reactive groups are cross-linked [269]. Other strategies for the *in vivo* cross-linking of proteins have been reported [270, 271] but to date *in vivo* cross-linking is challenging.

In more commonly used *in vitro* experiments, solutions with protein concentrations in the  $\mu\text{M}$  range yield low-resolution protein 3D structures. A great variety of cross-linking reagents are available for this task, in most studies homobifunctional amine-reactive compounds are used, which target nucleophilic groups in the proteins, *e.g.* the *N*-terminus or lysine side chains [272-276]. The cross-linked proteins are commonly analyzed using a "bottom-up" strategy (a proteolytic peptide mixture is generated and analyzed by MS and MS/MS) [259, 260, 276-279]. The advantage of the bottom-up approach consists in the fact that it does not pose high demands for MS instrumentation. Yet, for the bottom-up strategy it is crucial to separate the complex peptide mixtures prior to MS by gel electrophoresis and/or LC [260, 273, 280].

The obtained distance constraints can be used to confirm existing models of protein complexes or can serve as basis to create 3D structures by molecular modeling [281-283]. Cross-linking has successfully been employed to characterize small proteins and protein complexes (*e.g.* 20 kDa-complexes of calmodulin with its target peptides) [272, 278, 284-287] as well as protein assemblies with sizes of several 100 kDa to MDa [273, 282, 288]. Its low protein consumption

makes chemical cross-linking an affordable method and the analysis of cross-linking products by MS and MS/MS allows for a high throughput. To date, the bottleneck of this approach is the identification of cross-linked peptides and the assignment of the amino acid residues, which are connected with each other.

#### 2.4.1 Cross-Linking Reagents

Cross-linking reagents consist of two reactive groups connected by a spacer and can be divided into three groups: *Homobifunctional* reagents possess only one type of reactive group (*e.g.* NHS esters) and target specific functional groups of amino acid side chains (in case of NHS esters: nucleophilic groups, such as amines or alcohols) [273, 277, 284, 289, 290]. *Heterobifunctional* reagents possess two different reactive groups. Very common are combinations of amine-reactive with photo-reactive groups, which allow conducting the cross-linking reaction in a two-step fashion [278]. *Trifunctional* reagents consist of a homo- or heterobifunctional body bearing the reactive groups for the cross-linking reaction and a third group, *e.g.* biotin, which allows for a subsequent enrichment of cross-linked species [275, 291]. Cross-linkers facilitating identification of cross-linked products, such as chemically or MS/MS cleavable reagents might also be considered to be trifunctional reagents, however, they are usually classified according to their reactive groups [289, 292-294]. In this work, the following cross-linkers were used:

$BS^3$  – Bis(sulfosuccinimidyl)suberate is a homobifunctional reagent (Figure 16A), which mainly reacts with lysine residues or the protein's *N*-terminus [272, 273, 284]. Reactions with other nucleophilic amino acids (tyrosine, threonine, serine) occur to a lower extent [277, 295]. The spacer length of  $BS^3$  is 11.4 Å, but  $C_\alpha$  distances of up to 25 Å can be assumed for cross-linked amino acids.

$PEG_4$ -biotin-(NHS)<sub>2</sub> is a novel trifunctional cross-linker with two amine reactive NHS-esters and a biotin group connected via a PEG-linker of four units (Figure 16B). The  $PEG_4$ -linker enhances

the reagent's solubility, while the biotin group enables the enrichment of cross-linked species by affinity chromatography. The cross-linker possesses a spacer length of 16.5 Å.

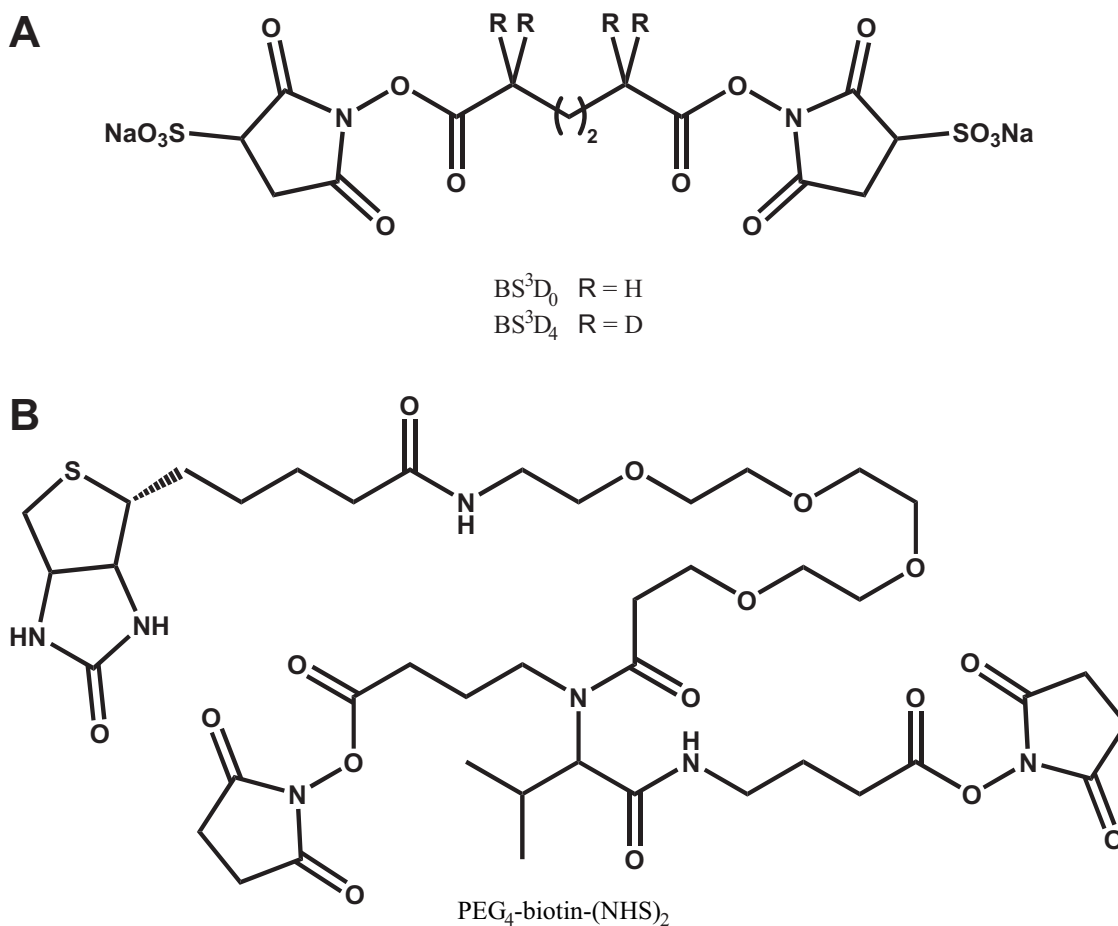


Figure 16: Cross-linkers used in this work.

#### 2.4.2 Strategies for Identification of Cross-Linked Products

Three types of cross-links are found after the reaction (Figure 17): *Type 0* cross-links are mere modifications of single amino acids as the second reactive group of the cross-linker has been hydrolyzed or aminolyzed. These modifications give information about the solvent accessibility of the respective amino acid residue [296]. In *Type 1* cross-links, the reagent has reacted with two amino acid residues, however, both residues are located on a single proteolytic peptide. In *Type 2* cross-links two different proteolytic peptides are linked to each other. This can either occur

intramolecularly (within on protein) or intermolecularly (between interaction partners), therefore these cross-links carry the most valuable information in regard to 3D structure determination of the protein or the protein complex. The strategies described below aim for an easier identification of the Type 2 cross-links.

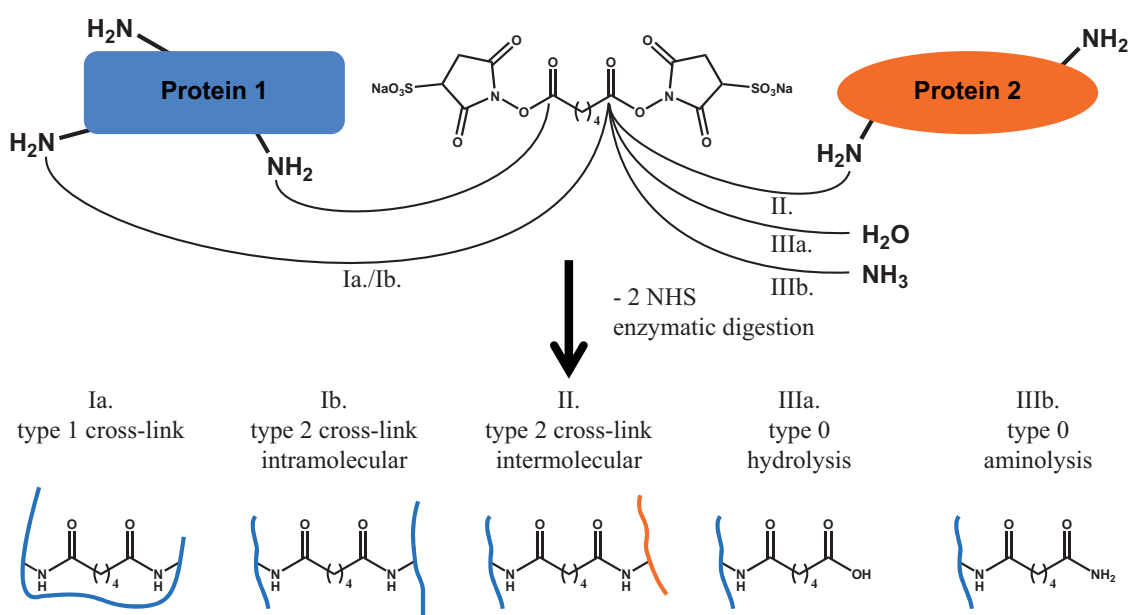


Figure 17: Different types of cross-links.

Cross-linked peptides are usually of low abundance in the proteolytic peptide mixtures. Therefore, methods to facilitate identification or enrichment of the cross-linked species have gained importance over the last years. Cross-linking reagents with stable isotope labels (*e.g.* deuterium or <sup>13</sup>C) enable the identification of cross-linked peptides based on their characteristic isotopic patterns in the mass spectra [274, 278, 284, 297]. As MS signals of all cross-linker-containing fragment ions also exhibit this characteristic pattern, this strategy also helps to pinpoint the cross-linked amino acids by MS/MS experiments. A similar approach makes use of cross-linkers, which fragment preferentially upon activation by CID in MS/MS experiments. This results in a characteristic fragment ion pattern, by which cross-linked peptides are identified [289,

290, 292, 293, 298]. Finally, MS<sup>3</sup> experiments of these fragment ions yield the sequence information needed for the assignment of amino acids that have been cross-linked.

Enrichment of cross-linked peptides using cation exchange chromatography makes use of the high charge state of type 2 cross-links [273, 297]. As proteolytic cleavage is usually performed with the serine protease trypsin, cleaving C-terminally at lysines and arginines, the resulting tryptic peptides exhibit at least two groups which can be protonated – the N-terminus and the C-terminal basic amino acid. Therefore type 2 cross-links usually carry three or more charges, while unmodified peptides, type 0, and type 1 cross-links are less charged and are therefore not enriched.

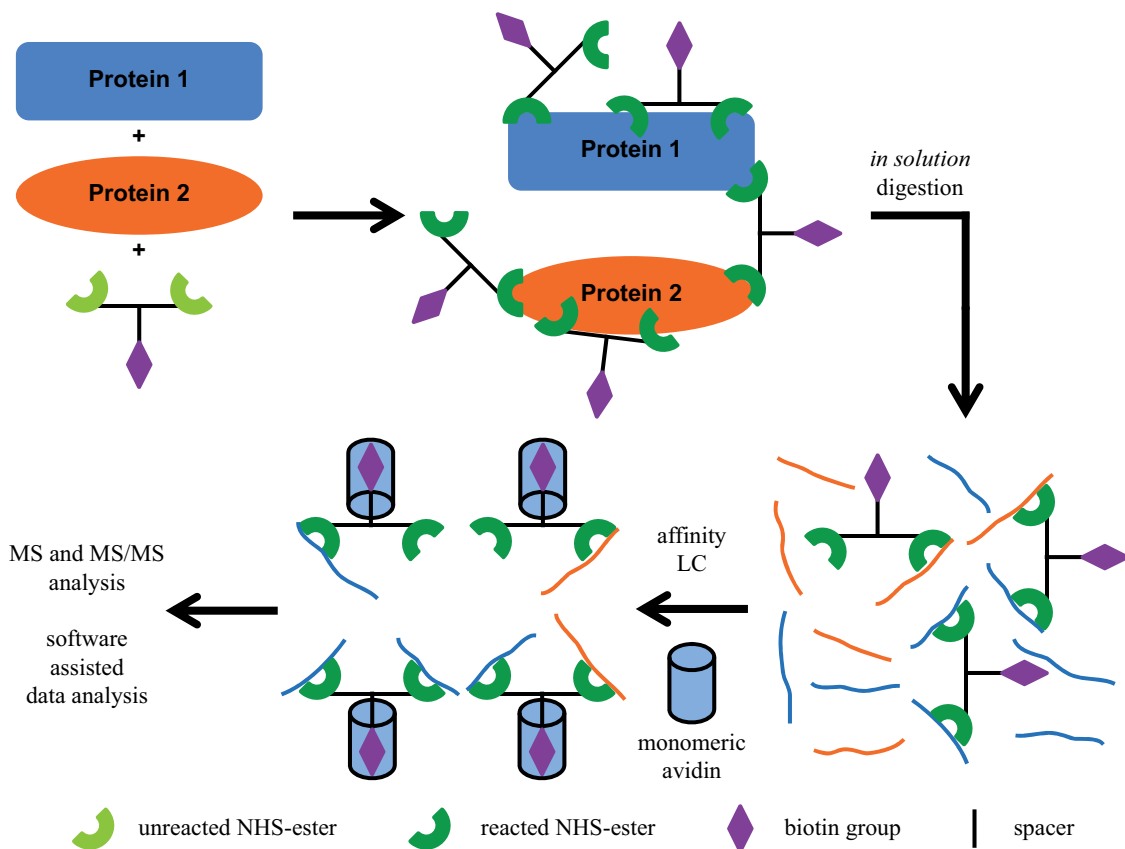


Figure 18: Cross-linking strategy used in this work.

In this thesis, the novel three-functional cross-linker PEG<sub>4</sub>-biotin-(NHS)<sub>2</sub> was used for the enrichment of cross-linked species by affinity chromatography using immobilized monomeric avidin (Figure 18) [10]. Similar approaches using particle-based affinity media have been published [274, 275, 291].

Identification of cross-links from the large MS data sets is assisted by specific software tools [299, 300]. An *in-silico* cross-linking experiment is performed and the theoretical masses of cross-linking products are compared with experimental MS data. However, this step is still time-consuming and requires the skilled eye of the researcher [299-301]. Especially the assignment of the MS/MS signals to the corresponding fragment ion is difficult to automate. Assignments of the software tools offer mere hints [300] and have to be reviewed carefully.

### 3 Publications

In the following sections, three original papers and two review articles are summarized, which are the basis of this work.

#### 3.1 Review Article 1 (Trend Article including Preliminary Results):

##### **Immobilized monolithic enzyme reactors for application in proteomics and pharmaceuticals**

Jens Sproß and Andrea Sinz

*Analytical and Bioanalytical Chemistry*, 2009, **6**, 1583–1588

**Abstract:** The use of monolithic supports for a wide variety of applications has rapidly expanded during the past few years. The examples for applications of monoliths presented herein show that the chromatographic performance of bioreactors and affinity media prepared from monolithic media is superior to that of conventional particle-based systems. The ease of fabrication and modification combined with the long lifetime of the monolithic columns and their potential to be used in fully automated analytical systems make them attractive tools for an increasing number of applications.

3.2 Original Paper 1:

**A Capillary Monolithic Trypsin Reactor for Efficient Protein Digestion in *Online* and *Offline* Coupling to ESI and MALDI Mass Spectrometry**

Jens Sproß and Andrea Sinz

Analytical Chemistry, 2010, **82**, 1434–1443

**Abstract:** We describe the preparation of a capillary trypsin immobilized monolithic enzyme reactor (IMER) for a rapid and efficient digestion of proteins down to the femtomole level. Trypsin was immobilized on a *poly*(glycidyl methacrylate-*co*-acrylamide-*co*-ethylene glycol dimethacrylate) monolith using the glutaraldehyde technique. Digestion efficiencies of the IMER were evaluated using model proteins and protein mixtures as well as chemically cross-linked lysozyme regarding the addition of denaturants and increasing digestion temperature. The trypsin IMER described herein is applicable for the digestion of protein mixtures. Even at a 1000-fold molar excess of one protein, low-abundance proteins are readily identified, in combination with MS/MS analysis. An online setup of the IMER with reversed phase nano-HPLC separation and nano-ESI-MS/MS analysis was established. The great potential of the trypsin IMER for proteomics applications comprise short digestion times in the range of seconds to minutes, in addition to improved digestion efficiencies, compared to in-solution digestion.

### 3.3 Review Article 2:

#### **Monolithic media for applications in affinity chromatography**

Jens Sproß and Andrea Sinz

Journal of Separation Science, 2011, **34**, 1958–1973

**Abstract:** Affinity chromatography presents a highly versatile analytical tool, which relies on exploiting highly specific interactions between molecules and their ligands. This review covers the most recent literature on the application of monoliths as stationary phases for various affinity-based chromatographic applications. Different affinity approaches as well as separations using molecularly imprinted monoliths are discussed. Hybrid stationary phases created by embedding of particles or nanoparticles into a monolithic stationary phase are also considered in this review article. The ease of preparation of monoliths and the multitude of functionalization techniques, which have matured during the past years, make monoliths interesting for an increasing number of biochemical and medical applications.

3.4 Original Paper 2:

**Monolithic Columns with Immobilized Monomeric Avidin: Preparation and Application for Affinity Chromatography**

Jens Sproß and Andrea Sinz

Analytical and Bioanalytical Chemistry, 2012, **402**, 2395–2405

**Abstract:** A *poly*(glycidyl methacrylate-*co*-acrylamide-*co*-ethylene dimethacrylate) monolith and a *poly*(glycidyl methacrylate-*co*-ethylene dimethacrylate) monolith were prepared in fused silica capillaries (100 µm ID) and modified with monomeric avidin using the glutaraldehyde technique. The biotin binding capacity of monolithic affinity columns with immobilized monomeric avidin (MACMAs) was determined by fluorescence spectroscopy using biotin (5-fluorescein) conjugate, as well as biotin- and fluorescein-labeled bovine serum albumin (BSA). The affinity columns were able to bind 16.4 and 3.7 µmol biotin/mL, respectively. Columns prepared using the *poly*(glycidyl methacrylate-*co*-ethylene dimethacrylate) monolith retained 7.1 mg BSA/mL, almost six times more than commercially available monomeric avidin beads. Protocols based on MALDI-TOF mass spectrometry monitoring were optimized for the enrichment of biotinylated proteins and peptides. A comparison of enrichment efficiencies between MACMAs and commercially available monomeric avidin beads yielded superior results for our novel monolithic affinity columns. However, the affinity medium presented in this work suffers from a significant degree of nonspecific binding, which might hamper the analysis of more complex mixtures. Further modifications of the monolith's surface are envisaged for the future development of monoliths with improved enrichment characteristics.

3.5 Original Paper 3:

**Multi-dimensional Nano-HPLC Coupled with Tandem Mass Spectrometry for Analyzing Biotinylated Proteins**

Jens Sproß\*, Sebastian Brauch, Friedrich Mandel, Moritz Wagner, Stephan Buckenmaier, Bernhard Westermann and Andrea Sinz\*

\* Corresponding authors

Analytical and Bioanalytical Chemistry, 2013, **405**, 2163–2173

**Abstract:** Multidimensional high-performance liquid chromatography (HPLC) is a key method in shotgun proteomics approaches for analyzing highly complex protein mixtures by complementary chromatographic separation principles. Here, we describe an integrated 3D-nano-HPLC/nano-electrospray ionization quadrupole time-of-flight mass spectrometry system that allows an enzymatic digestion of proteins followed by an enrichment and subsequent separation of the created peptide mixtures. The *online* 3D-nano-HPLC system is composed of a monolithic trypsin reactor in the first dimension, a monolithic affinity column with immobilized monomeric avidin in the second dimension, and a reversed phase C18 HPLC-Chip in the third dimension that is coupled to a nano-ESI-Q-TOF mass spectrometer. The 3D-LC/MS setup is exemplified for the identification of biotinylated proteins from a simple protein mixture. Additionally, we describe an *online* 2D-nano-HPLC/nano-ESI-LTQ-Orbitrap-MS/MS setup for the enrichment, separation, and identification of cross-linked, biotinylated species from chemical cross-linking of cytochrome c and a calmodulin/peptide complex using a novel trifunctional cross-linker with two amine-reactive groups and a biotin label.

---

## 4 Discussion

### 4.1 Monolithic Trypsin Reactor

Trypsin IMERs are the most commonly reported monolithic enzyme reactors with trypsin activity being the only parameter, which was investigated by all researchers. Digestion performance is usually assessed by proteolytic cleavage of a simple protein without considering parameters [119], which are state-of-the-art in protocols for *in-solution* digestion, such as concentration of chaotropic agent [9] or digestion temperature [302, 8, 4]. In this work, digestion conditions were optimized for a trypsin IMER prepared according to the protocol published by Duan *et al.* [4]. The *poly*(GMA-co-AAm-co-EDMA) monolith reported by Duan *et al.* contains acrylamide for a more hydrophilic surface. Using  $N_{\alpha}$ -benzoyl-L-arginine ethyl ester the enzymatic activity of the immobilized trypsin was determined in dependence of interaction time, i.e. flow rate, and temperature. The prepared reactors were 420 time more active than a solution containing 1  $\mu\text{g}$  trypsin/mL and more than twice as active as the trypsin IMER reported by Duan *et al.* [4]. Using cytochrome *c* the protein concentration was adjusted and digestion efficiency was evaluated in the presence of different chaotropic agents using bovine serum albumin. Optimum results were obtained when using 2 M urea and 10% ACN in the protein solution.

By integrating the trypsin IMER into an online 2D-nano-HPLC/nano-ESI-MS/MS system, the process of analyzing proteins was automated and cytochrome *c* or bovine serum albumin were enzymatically cleaved, separated and analyzed within two hours. In comparison, *in-solution* protein digestion and mass spectrometric analysis require up to 18 hours. By minimizing the need for manual sample handling, potential sample contamination during the digestion step is largely eliminated.

Using the optimized digestion conditions simple protein mixtures were digested and analyzed by offline MALDI-TOF/TOF-MS/MS resulting in an identification of all proteins from a simple mixture. The same was true when analyzing a mixture, in which one protein was present in a 1000-fold molar excess. However, the performance of trypsin IMER was not equally convincing

when analyzing cross-linked lysozyme. Only two cross-links originating from the *N*-terminus of the protein were identified although the flow rate was reduced to 100 nL/min, thereby increasing the interaction time from 232 seconds to 693 seconds. There are two potential explanations for this finding:

- I.) Potential trypsin cleavage sites are blocked by reaction with the amine-reactive cross-linker BS<sup>3</sup> making cross-linked proteins difficult to digest.
- II.) The protein's 3D structure is fixed by the introduction of chemical cross-links. Therefore, potential cleavage sites remain buried within the protein and are not accessible to the enzyme.

Although the proteolytic cleavage of cross-linked proteins has to be optimized, the prepared trypsin IMERs exhibited a high enzymatic activity and were successfully used for protein digestion. Low abundant proteins were identified even in the presence of on protein in a 1000-fold molar excess.

#### 4.2 Monolithic Affinity Column with Immobilized Monomeric Avidin

Although the interaction of avidin and biotin is highly specific, the avidin/biotin pair cannot be used for the enrichment of analytes because of the tight binding of biotin to avidin. Therefore, avidin and the closely related bacterial protein streptavidin are commonly used for the immobilization of ligands for affinity chromatography [38, 151, 303]. The avidin/biotin interaction is only weakened in the presence of strong denaturing agents, such as 8 M guanidinium chloride [304, 305]. However, biotinylated analytes can be eluted without the addition of denaturants when monomeric avidin is employed as its association constant for biotin is significantly lower compared to native avidin in its tetrameric form [306, 307]. Therefore, avidin was immobilized onto a SP and subsequently monomerized using denaturing agents.

Based on the experience gained during preparation of the trypsin IMERs we chose the same MSP for the preparation of monolithic affinity columns with immobilized monomeric avidin

(MACMAs). In addition to the acrylamide-containing monolith that was used for preparing the trypsin IMER, a *poly*(GMA-*co*-EDMA) monolith was employed for preparing the affinity columns. Immobilization of avidin was performed via the glutaraldehyde technique according to the protocol established for the immobilization of trypsin.

For the assessment of reversible biotin and protein binding capacities a novel assay was established using fluorescein as probe and fluorescence spectroscopy for quantification eliminating the use of radioactive  $^{14}\text{C}$  labeled biotin [307, 308]. Reversible biotin and protein binding was highly reproducible, however, affinity columns prepared using the *poly*(GMA-*co*-EDMA) monolith suffered from a high degree of non-specific protein binding, most likely because of the hydrophobicity of the monolith's backbone. Pretreatment of the MACMAs with bovine serum albumin in order to minimize non-specific binding was not successful. Nonetheless, when analyzing a mixture of biotinylated and non-biotinylated cytochrome *c*, no biotinylated cytochrome *c* was found in flow-through and washing fractions. Acetonitrile was used to reduce non-specific binding, but when more than 5% ACN were present in the solution, biotinylated cytochrome *c* was eluted during the washing step. For unknown reasons protein enrichment of MACMAs prepared from the *poly*(GMA-*co*-AAM-*co*-EDMA) monolith was insufficient and they were excluded from further experiments.

Enrichment on the peptide level was far more successful. Biotinylated peptides were rarely present in the flow-through and during the washing step 15% ACN were tolerated with hardly any elution of biotinylated peptides, which were almost exclusively present in the elution fraction. The enrichment efficiency was further investigated using five pairs of peptides, which were found to be both biotinylated and non-biotinylated. In most cases, a complete depletion of unmodified peptides was achieved during the enrichment procedure. It has to be noted that biotinylated peptides were also identified with an additional oxidation. Using fragmentation experiments the location of the oxidation was pinpointed to the biotin group itself. However, the oxidation of the biotin tag did not hamper the enrichment of the respective peptides. Our hypothesis that the heme

group of cytochrome *c* is involved in the oxidation of the biotin label was supported by observation of oxidations in myoglobin (another heme-containing protein) and their absence in the case of lysozyme (contains no heme group). This hypothesis was further validated during online 3D-nano-HPLC/nano-ESI-MS/MS analysis of biotinylated cytochrome *c*, where oxidized biotin modifications were only identified in peptides containing the heme group.

Compared to commercially available particle based monomeric avidin, protein binding capacity of the MACMAs was six times higher, whereas information about non-specific binding of the commercial product is not available. When biotinylated cytochrome *c* peptides were enriched using monomeric avidin beads, biotinylated peptides were identified in all fractions and no enrichment was achieved. Although sample preparation was the same as for the experiments using the MACMAs and benzamidine was used to inhibit residual trypsin, mass spectra obtained from the enrichment using the monomeric avidin beads were dominated by signals, which were assigned to tryptic avidin peptides. In contrast, only a few low-intensity signals of avidin peptides were identified in mass spectra from the enrichment on the MACMAs.

It can be concluded that the prepared MACMAs show a better performance when enriching biotinylated peptides, compared to a commercially available particle based affinity medium. However, choosing a more hydrophilic monolith or using deglycosylated avidin might be advantageous in respect to the rather high degree of non-specific binding.

#### 4.3 Online 3D- and 2D-nano-HPLC/nano-ESI-MS/MS Setups

As for the trypsin IMER, integration of the MACMAs into a 2D-nano-HPLC/nano-ESI-MS/MS system enables an automated enrichment and analysis of cross-linked peptides minimizing manual sample treatment. For testing the applicability of this setup for analysis of cross-linked proteins, the novel trifunctional cross-linker PEG<sub>4</sub>-biotin-(NHS)<sub>2</sub> was used, possessing two amine-reactive NHS-esters and a biotin group for the affinity enrichment. Several cross-links were identified in cytochrome *c* and a complex between calmodulin and a peptide derived from

skMLCK. Tandem mass spectrometry experiments allowed to pinpoint the cross-linked amino acids. The bridged distances were in agreement with existing crystal structures, however, because of the inherent flexibility of its spacer, this novel cross-linker is not perfectly suited for obtaining distance restraints to model protein 3D structures.

Analysis of biotinylated proteins was further automated by establishing an online 3D-nano-HPLC/nano-ESI-MS/MS system, comprised of the trypsin IMER as the first dimension, the MACMA as the second dimension, and a reversed phase separation as the third dimension. A Q-TOF mass spectrometer was used for analysis of the generated, enriched, and separated biotinylated peptides. Using the optimized instrument configuration, injection of a protein mixture in 2 M urea containing 20% ACN and 0.1 M ammonium bicarbonate was sufficient as pretreatment prior to the identification of ca. 20 biotinylated cytochrome *c* peptides. A sequence coverage of almost 100% was achieved for cytochrome *c*. Automation was further improved by increasing the temperature in the trypsin IMER compartment to 50°C resulting in the identification of more than 30 biotinylated cytochrome *c* peptides. All non-biotinylated peptides that were identified in these experiments were modified by a heme group and were thus rather hydrophobic.

When analyzing a simple a protein mixture composed of biotinylated cytochrome *c*, lysozyme,  $\beta$ -lactoglobulin, and bovine serum albumin, mainly biotinylated cytochrome *c* peptides were identified. A maximum of three peptides were observed that did not originate from cytochrome *c*; two peptides originated from lysozyme, one peptide originated from  $\beta$ -lactoglobulin. Using the automated setup, analysis and identification of biotinylated peptides was performed within 125 minutes compared to 24 hours using *in-solution* digestion and commercially available monomeric avidin beads.

## 5 Literature References

1. Lodish H, Berk A, Kaiser CA, Krieger M, Scott MP, Bretscher A, Ploegh H, Matsudaira PT; Molecular Cell Biology, 2007. W. H. Freeman & Co Ltd, New York. 1150
2. Gritti F, Piatkowski W, Guiochon G; J Chromatogr A, 2003, **983**, (1-2), 51-71
3. Guiochon G; J Chromatogr A, 2007, **1168**, (1-2), 101-168
4. Duan J, Liang Z, Yang C, Zhang J, Zhang L, Zhang W, Zhang Y; Proteomics, 2006, **6**, (2), 412-419
5. Petro M, Svec F, Frechet JMJ; Biotechnol Bioeng, 1996, **49**, (4), 355-363
6. Krenkova J, Svec F; J Sep Sci, 2009, **32**, (5-6), 706-718
7. Sproß J, Sinz A; Anal Chem, 2010, **82**, (4), 1434-1443
8. Feng S, Ye ML, Jiang XG, Jin WH, Zou HF; J Proteome Res, 2006, **5**, (2), 422-428
9. Krenkova J, Bilkova Z, Foret F; J Sep Sci, 2005, **28**, (14), 1675-1684
10. Sproß J, Sinz A; Anal Bioanal Chem, 2012, **402**, (7), 2395-2405
11. Sproß J, Brauch S, Mandel F, Wagner M, Buckenmaier S, Westermann B, Sinz A; Anal Bioanal Chem, 2013, **405**, 2163-2173
12. Bartle KD, Myers P; TrAC, Trends Anal Chem, 2002, **21**, (9-10), 547-557
13. Tsvett M; Berichte der Deutschen Botanischen Gesellschaft, 1906, **24**, 316-323
14. Tsvett M; Berichte der Deutschen Botanischen Gesellschaft, 1906, **24**, 384-393
15. Martin AJ, Synge RL; The Biochemical journal, 1941, **35**, (12), 1358-1368
16. Consden R, Gordon AH, Martin AJP; Biochem J, 1948, **42**, (3), 443-447
17. Synge RLM; Analyst, 1946, **71**, (843), 256-258
18. Huber JFK, Hulsman JAR; Anal Chim Acta, 1967, **38**, (1-2), 305-313
19. Horvath CG, Preiss BA, Lipsky SR; Anal Chem, 1967, **39**, (12), 1422-1428
20. Kirkland JJ; Anal Chem, 1969, **41**, (1), 218-220
21. Snyder LR, Kirkland JJ, Dolan JW; Introduction to Modern Liquid Chromatography, 2011. John Wiley & Sons, New York. 960
22. Xiang Y, Liu Y, Lee ML; J Chromatogr A, 2006, **1104**, (1&2), 198-202
23. Svec F, Frechet JMJ; Anal Chem, 1992, **64**, (7), 820-822
24. Minakuchi H, Nakanishi K, Soga N, Ishizuka N, Tanaka N; Anal Chem, 1996, **68**, (19), 3498-3501
25. Svec F; J Sep Sci, 2004, **27**, (17-18), 1419-1430
26. Gritti F, Guiochon G; J Chromatogr A, 2007, **1166**, (1-2), 30-46
27. Mould DL, Synge RLM; Analyst, 1952, **77**, (921), 964-969

28. Mould DL, Synge RLM; *Biochem J*, 1954, **58**, (4), 571-585
29. Ross WD, Jefferson RT; *J Chromatogr Sci*, 1970, **8**, (7), 386-389
30. Schnecko H, Bieber O; *Chromatographia*, 1971, **4**, (3), 109-112
31. Hjerten S, Liao JL, Zhang R; *J Chromatogr*, 1989, **473**, (1), 273-275
32. Hjerten S, Li YM, Liao JL, Mohammad J, Nakazato K, Pettersson G; *Nature*, 1992, **356**, (6372), 810-811
33. Hjerten S, Nakazato K, Mohammad J, Eaker D; *Chromatographia*, 1993, **37**, (5-6), 287-294
34. Tennikova TB, Belenkii BG, Svec F; *J Liq Chromatogr*, 1990, **13**, (1), 63-70
35. Frechet JMJ; *Makromolekulare Chemie-Macromolecular Symposia*, 1993, **70-1**, 289-301
36. Tennikova TB, Svec F; *J Chromatogr*, 1993, **646**, (2), 279-288
37. Ishizuka N, Minakuchi H, Nakanishi K, Soga N, Hosoya K, Tanaka N; *HRC J High Resolut Chromatogr*, 1998, **21**, (8), 477-479
38. Sproß J, Sinz A; *J Sep Sci*, 2011, **34**, (16-17), 1958-1973
39. Svec F, Frechet JMJ; *Science*, 1996, **273**, (5272), 205-211
40. Buchmeiser MR; *J Chromatogr A*, 2001, **918**, (2), 233-266
41. Tanaka N, Kobayashi H, Ishizuka N, Minakuchi H, Nakanishi K, Hosoya K, Ikegami T; *J Chromatogr A*, 2002, **965**, (1-2), 35-49
42. Mallik R, Hage DS; *J Sep Sci*, 2006, **29**, (12), 1686-1704
43. Buchmeiser MR; *J Sep Sci*, 2008, **31**, (11), 1907-1922
44. Urban J, Jandera P; *J Sep Sci*, 2008, **31**, (14), 2521-2540
45. Ma JF, Zhang LH, Liang Z, Zhang WB, Zhang YK; *Anal Chim Acta*, 2009, **632**, (1), 1-8
46. Bakry R, Huck CW, Bonn GK; *J Chromatogr Sci*, 2009, **47**, (6), 418-431
47. Lammerhofer M, Gargano A; *J Pharm Biomed Anal*, 2010, **53**, (5), 1091-1123
48. Svec F, Tennikova TB, Deyl Ze; *Monolithic Materials*, 2003, vol 67. *Journal of Chromatography Library*. Elsevier, Amsterdam
49. Jungbauer A, Hahn R; *J Chromatogr A*, 2008, **1184**, (1-2), 62-79
50. Wu R, Hu LG, Wang FJ, Ye ML, Zou H; *J Chrom A*, 2008, **1184**, (1-2), 369-392
51. Stachowiak TB, Svec F, Frechet JMJ; *J Chromatogr A*, 2004, **1044**, (1-2), 97-111
52. Svec F; *J Chromatogr B*, 2006, **841**, (1-2), 52-64
53. Ro KW, Nayalk R, Knapp DR; *Electrophoresis*, 2006, **27**, (18), 3547-3558
54. Sun XH, Yang WC, Pan T, Woolley AT; *Anal Chem*, 2008, **80**, (13), 5126-5130
55. Miyazaki S, Morisato K, Ishizuka N, Minakuchi H, Shintani Y, Furuno M, Nakanishi K; *J Chromatogr A*, 2004, **1043**, (1), 19-25

56. Altun Z, Blomberg LG, Abdel-Rehim M; *Journal of Liquid Chromatography & Related Technologies*, 2006, **29**, (10), 1477-1489
57. Abdel-Rehim M, Persson C, Altun Z, Blomberg L; *J Chromatogr A*, 2008, **1196**, 23-27
58. Altun Z, Skoglund C, Abdel-Rehim M; *J Chromatogr A*, 2010, **1217**, (16), 2581-2588
59. Hu YL, Li JW, Hu YF, Li GK; *Talanta*, 2010, **82**, (2), 464-470
60. Si BJ, Zhou J; *Chin J Chem* 2011, **29**, (11), 2487-2494
61. Gomez-Caballero A, Guerreiro A, Karim K, Piletsky S, Aranzazu Goicolea M, Barrio RJ; *Biosensors & Bioelectronics*, 2011, **28**, (1), 25-32
62. Huang X, Lin J, Yuan D; *J Chromatogr A*, 2010, **1217**, (30), 4898-4903
63. Huang X, Qiu N, Yuan D, Huang B; *Talanta*, 2009, **78**, (1), 101-106
64. Huang X, Yuan D; *J Chromatogr A*, 2007, **1154**, (1-2), 152-157
65. Hauck HE, Schulz M; *Chromatographia*, 2003, **57**, S313-S315
66. Bakry R, Bonn GK, Mair D, Svec F; *Anal Chem*, 2007, **79**, (2), 486-493
67. Frolova AM, Konovalova OY, Loginova LP, Bulgakova AV, Boichenko AP; *J Sep Sci*, 2011, **34**, (16-17), 2352-2361
68. Bakry R, Stoeggl WM, Hochleitner EO, Stecher G, Huck CW, Bonn GK; *J Chromatogr A*, 2006, **1132**, (1-2), 183-189
69. Zhu GJ, Zhang LH, Yuan HM, Liang Z, Zhang WB, Zhang YK; *J Sep Sci*, 2007, **30**, (6), 792-803
70. Koerner T, Xie R, Sheng F, Oleschuk R; *Anal Chem*, 2007, **79**, (9), 3312-3319
71. Gibson GTT, Koerner TB, Xie R, Shah K, de Korompay N, Oleschuk RD; *J Colloid Interface Sci*, 2008, **320**, (1), 82-90
72. Fan Y, Rubakhin SS, Sweedler JV; *Anal Chem*, 2011, **83**, (24), 9557-9563
73. Svec F, Huber CG; *Anal Chem*, 2006, **78**, (7), 2100-2107
74. Vlakh EG, Tennikova TB; *J Sep Sci*, 2007, **30**, (17), 2801-2813
75. Svec F; *J Chromatogr A*, 2010, **1217**, (6), 902-924
76. Ren LB, Liu Z, Liu YC, Dou P, Chen HY; *Angew Chem Int Ed*, 2009, **48**, (36), 6704-6707
77. Lubbad S, Buchmeiser MR; *Macromol Rapid Commun*, 2002, **23**, (10-11), 617-621
78. Buchmeiser MR; *J Chromatogr A*, 2004, **1060**, (1-2), 43-60
79. Gatschelhofer C, Magnes C, Pieber TR, Buchmeiser MR, Sinner FM; *J Chromatogr A*, 2005, **1090**, (1-2), 81-89
80. Geiser L, Eeltink S, Svec F, Frechet JMJ; *J Chromatogr A*, 2007, **1140**, (1-2), 140-146
81. Svec F, Frechet JMJ; *Chem Mater*, 1995, **7**, (4), 707-715

82. Horak D, Labsky J, Pilar J, Bleha M, Pelzbauer Z, Svec F; *Polymer*, 1993, **34**, (16), 3481-3489
83. Palm A, Novotny MV; *Anal Chem*, 1997, **69**, (22), 4499-4507
84. Courtois J, Bystrom E, Irgum K; *Polymer*, 2006, **47**, (8), 2603-2611
85. Viklund C, Ponten E, Glad B, Irgum K, Horstedt P, Svec F; *Chem Mater*, 1997, **9**, (2), 463-471
86. Grasselli M, Smolko E, Hargittai N, Safrany A; *Nucl Instrum Methods Phys Res Sect B-Beam Interact Mater Atoms*, 2001, **185**, 254-261
87. Yone A, Rusell ML, Grasselli M, Vizioli NM; *Electrophoresis*, 2007, **28**, (13), 2216-2218
88. Safrany A, Beiler B, Laszlo K, Svec F; *Polymer*, 2005, **46**, (9), 2862-2871
89. Bandari R, Knolle W, Prager-Duschke A, Glasel H-J, Buchmeiser MR; *Macromol Chem Phys*, 2007, **208**, (13), 1428-1436
90. Schlemmer B, Gatschelhofer C, Pieber TR, Sinner FA, Buchmeiser MR; *J Chromatogr A*, 2006, **1132**, (1-2), 124-131
91. Bandari R, Eisner C, Knolle W, Kuehnel C, Decker U, Buchmeiser MR; *J Sep Sci*, 2007, **30**, (17), 2821-2827
92. Bandari R, Knolle W, Buchmeiser MR; *J Chromatogr A*, 2008, **1191**, (1-2), 268-273
93. Galaev IY, Dainiak MB, Plieva F, Mattiasson B; *Langmuir*, 2007, **23**, (1), 35-40
94. Kubin M, Spacek P, Chromece R; *Collect Czech Chem Commun*, 1967, **32**, (11), 3881-3887
95. Plieva FM, Galaev IY, Mattiasson B; *J Sep Sci*, 2007, **30**, (11), 1657-1671
96. Hainey P, Huxham IM, Rowatt B, Sherrington DC, Tetley L; *Macromolecules*, 1991, **24**, (1), 117-121
97. Small PW, Sherrington DC; *J Chem Soc-Chem Commun*, 1989, (21), 1589-1591
98. Jerabek K, Pulko I, Soukupova K, Stefanec D, Krajnc P; *Macromolecules*, 2008, **41**, (10), 3543-3546
99. Jiang T, Mallik R, Hage DS; *Anal Chem*, 2005, **77**, (8), 2362-2372
100. Viklund C, Svec F, Frechet JMJ, Irgum K; *Chem Mater*, 1996, **8**, (3), 744-750
101. Peters EC, Svec F, Frechet JMJ, Viklund C, Irgum K; *Macromolecules*, 1999, **32**, (19), 6377-6379
102. Santora BP, Gagne MR, Moloy KG, Radu NS; *Macromolecules*, 2001, **34**, (3), 658-661
103. Bernabe-Zafon V, Canto-Mirapeix A, Simo-Alfonso EF, Ramis-Ramos G, Herrero-Martinez JM; *Electrophoresis*, 2009, **30**, (11), 1929-1936
104. Minakuchi H, Nakanishi K, Soga N, Ishizuka N, Tanaka N; *J Chromatogr A*, 1997, **762**, (1-2), 135-146

105. Motokawa M, Kobayashi H, Ishizuka N, Minakuchi H, Nakanishi K, Jinnai H, Hosoya K, Ikegami T, Tanaka N; *J Chromatogr A*, 2002, **961**, (1), 53-63
106. Siouffi AM; *J Chromatogr A*, 2003, **1000**, (1-2), 801-818
107. Miyazaki S, Miah MY, Morisato K, Shintani Y, Kuroha T, Nakanishi K; *J Sep Sci*, 2005, **28**, (1), 39-44
108. Hoth DC, Rivera JG, Colon LA; *J Chromatogr A*, 2005, **1079**, (1-2), 392-396
109. Randon J, Guerrin JF, Rocca JL; *J Chromatogr A*, 2008, **1214**, (1-2), 183-186
110. Randon J, Huguet S, Demesmay C, Berthod A; *J Chromatogr A*, 2010, **1217**, (9), 1496-1500
111. Randon J, Huguet S, Piram A, Puy G, Demesmay C, Rocca JL; *J Chromatogr A*, 2006, **1109**, (1), 19-25
112. Wang QC, Svec F, Frechet JMJ; *Anal Chem*, 1993, **65**, (17), 2243-2248
113. Eeltink S, Geiser L, Svec F, Frechet JMJ; *J Sep Sci*, 2007, **30**, (17), 2814-2820
114. Tetala KKR, Chen B, Visser GM, van Beek TA; *J Sep Sci*, 2007, **30**, (17), 2828-2835
115. Meyer U, Svec F, Frechet JMJ, Hawker CJ, Irgum K; *Macromolecules*, 2000, **33**, (21), 7769-7775
116. Gatschelhofer C, Mautner A, Reiter F, Pieber TR, Buchmeiser MR, Sinner FM; *J Chromatogr A*, 2009, **1216**, (13), 2651-2657
117. Rohr T, Hilder EF, Donovan JJ, Svec F, Frechet JMJ; *Macromolecules*, 2003, **36**, (5), 1677-1684
118. Krenkova J, Lacher NA, Svec F; *Anal Chem*, 2009, **81**, (5), 2004-2012
119. Peterson DS, Rohr T, Svec F, Frechet JMJ; *Anal Chem*, 2002, **74**, (16), 4081-4088
120. Xie SF, Svec F, Frechet JMJ; *Biotechnol Bioeng*, 1999, **62**, (1), 30-35
121. Luo QZ, Mao XQ, Kong L, Huang XD, Zou HF; *J Chromatogr B*, 2002, **776**, (2), 139-147
122. Josic D, Buchacher A; *J Biochem Bioph Methods*, 2001, **49**, (1-3), 153-174
123. Brennan JD; *Acc Chem Res*, 2007, **40**, (9), 827-835
124. Lin T-Y, Wu C-H, Brennan JD; *Biosensors & Bioelectronics*, 2007, **22**, (9-10), 1861-1867
125. Wang G-H, Zhang L-M; *J Phys Chem B*, 2009, **113**, (9), 2688-2694
126. Lu S-Y, Jiang S-L, Qian J-Q, Guo H; *Journal of Liquid Chromatography & Related Technologies*, 2011, **34**, (9), 690-704
127. Ma JF, Liang Z, Qiao XQ, Deng QL, Tao DY, Zhang LH, Zhang YK; *Anal Chem*, 2008, **80**, (8), 2949-2956
128. Ishizuka N, Kobayashi H, Minakuchi H, Nakanishi K, Hirao K, Hosoya K, Ikegami T, Tanaka N; *J Chromatogr A*, 2002, **960**, (1-2), 85-96
129. Courtois J, Szumski M, Georgsson F, Irgum K; *Anal Chem*, 2007, **79**, (1), 335-344

130. Lubda D, Lindner W, Quaglia M, von Hohenesche CD, Unger KK; *J Chromatogr A*, 2005, **1083**, (1-2), 14-22
131. Urban J, Eeltink S, Jandera P, Schoenmakers PJ; *J Chromatogr A*, 2008, **1182**, (2), 161-168
132. Grimes BA, Skudas R, Unger KK, Lubda D; *J Chromatogr A*, 2007, **1144**, (1), 14-29
133. Lubbad SH, Buchmeiser MR; *J Chromatogr A*, 2010, **1217**, (19), 3223-3230
134. Huck CW, Bittner L; *Chromatographia*, 2011, **73**, S29-S34
135. Petter CH, Heigl N, Bonn GK, Huck CW; *J Sep Sci*, 2008, **31**, (14), 2541-2550
136. Ford KM, Konzman BG, Rubinson JF; *Anal Chem*, 2011, **83**, (24), 9201-9205
137. Darcy H; *Les Fontaines Publiques de la Ville de Dijon*, 1856. Dalmont, V. Paris. 647 p + atlas
138. Guiochon G, Felinger A, Katti AM, Shirazi D (2006). In: *Fundamentals of Preparative and Nonlinear Chromatography*. Elsevier, Amsterdam,
139. Van Deemter JJ, Zuiderweg FJ, Klinkenberg A; *Chem Eng Sci*, 1956, **5**, (6), 271-289
140. Bristow PA, Knox JH; *Chromatographia*, 1977, **10**, (6), 279-289
141. Kasai K, Oda Y, Nishikata M, Ishii S; *J Chromatogr*, 1986, **376**, 33-47
142. Sakai-Kato K, Kato M, Toyo'oka T; *Anal Chem*, 2002, **74**, (13), 2943-2949
143. Lin W, Skinner CD; *J Sep Sci*, 2009, **32**, (15-16), 2642-2652
144. Wang QC, Svec F, Frechet JMJ; *J Chromatogr A*, 1994, **669**, (1-2), 230-235
145. Matsui J, Kato T, Takeuchi T, Suzuki M, Yokoyama K, Tamiya E, Karube I; *Anal Chem*, 1993, **65**, (17), 2223-2224
146. Tanaka N, Nagayama H, Kobayashi H, Ikegami T, Hosoya K, Ishizuka N, Minakuchi H, Nakanishi K, Cabrera K, Lubda D; *HRC J High Resolut Chromatogr*, 2000, **23**, (1), 111-116
147. Li Y, Tolley HD, Lee ML; *J Chromatogr A*, 2010, **1217**, (52), 8181-8185
148. Kumar A, Bhardwaj A; *Biomed Mater*, 2008, **3**, (3), 1-11
149. Josic D, Clifton JG; *J Chromatogr A*, 2007, **1144**, (1), 2-13
150. Su XY, Hu LH, Kong L, Lei XY, Zou HF; *J Chromatogr A*, 2007, **1154**, (1-2), 132-137
151. Zhao Q, Li XF, Le XC; *Anal Chem*, 2008, **80**, (10), 3915-3920
152. Cheeks MC, Kamal N, Sorrell A, Darling D, Farzaneh F, Slater NKH; *J Chromatogr A*, 2009, **1216**, (13), 2705-2711
153. Feng S, Pan CS, Jiang XG, Xu SY, Zhou HJ, Ye ML, Zou HF; *Proteomics*, 2007, **7**, (3), 351-360
154. Brne R, Lim YP, Podgornik A, Barut M, Pihlar B, Strancar A; *J Chromatogr A*, 2009, **1216**, (13), 2658-2663

155. Calleri E, Marrubini G, Brusotti G, Massolini G, Caccialanza G; *J Pharm Biomed Anal*, 2007, **44**, (2), 396-403
156. Chen HX, Huang T, Zhang XX; *Talanta*, 2009, **78**, (1), 259-264
157. Okanda FM, El Rassi Z; *Electrophoresis*, 2006, **27**, (5-6), 1020-1030
158. Dainiak MB, Galaev IY, Mattiasson B; *Enzyme Microb Technol*, 2007, **40**, (4), 688-695
159. Galaev IY, Mattiasson B; *Methods Mol Biol*, 2008, **421**, 247-255
160. Peskoller C, Niessner R, Seidel M; *J Chromatogr A*, 2009, **1216**, (18), 3794-3801
161. Kumar A, Srivastava A; *Nature Protocols*, 2010, **5**, (11), 1737-1747
162. Önnby L, Giorgi C, Plieva FM, Mattiasson B; *Biotechnol Progr*, 2010, **26**, (5), 1295-1302
163. Eeltink S, Dolman S, Detobel F, Swart R, Ursem M, Schoenmakers PJ; *J Chromatogr A*, 2010, **1217**, (43), 6610-6615
164. Eghbali H, Sandra K, Detobel F, Lynen F, Nakanishi K, Sandra P, Desmet G; *J Chromatogr A*, 2011, **1218**, (21), 3360-3366
165. Iwasaki M, Miwa S, Ikegami T, Tomita M, Tanaka N, Ishihama Y; *Anal Chem*, 2010, **82**, (7), 2616-2620
166. Miyamoto K, Hara T, Kobayashi H, Morisaka H, Tokuda D, Horie K, Koduki K, Makino S, Nunez O, Yang C, Kawabe T, Ikegami T, Takubo H, Ishihama Y, Tanaka N; *Anal Chem*, 2008, **80**, (22), 8741-8750
167. Okanda FM, El Rassi Z; *Electrophoresis*, 2007, **28**, (1-2), 89-98
168. Gubitzi G, Schmid MG; *Biopharm Drug Dispos*, 2001, **22**, (7-8), 291-336
169. Zhang ZB, Wu RA, Wu MH, Zou HF; *Electrophoresis*, 2010, **31**, (9), 1457-1466
170. Kanat'eva AY, Korolev AA, Shiryaeva VE, Popova TP, Kurganov AA; *Polym Sci Ser A*, 2009, **51**, (10), 1060-1067
171. Kanatyeva A, Korolev A, Shiryaeva V, Popova T, Kurganov A; *J Sep Sci*, 2009, **32**, (15-16), 2635-2641
172. Tian H, Li Y, Chen J; *Se pu / Chin J Chromatogr*, 2010, **28**, (11), 1011-1014
173. Gritti F, Guiochon G; *J Chromatogr A*, 2009, **1216**, (23), 4752-4767
174. Hahn R, Panzer M, Hansen E, Mollerup J, Jungbauer A; *Sep Sci Technol*, 2002, **37**, (7), 1545-1565
175. Gritti F, Guiochon G; *J Chromatogr A*, 2012, **1221**, 2-40
176. Zheng JJ, Patel D, Tang QL, Markovich RJ, Rustum AM; *J Pharm Biomed Anal*, 2009, **50**, (5), 815-822
177. Bartolini M, Cavrini V, Andrisano V; *J Chromatogr A*, 2007, **1144**, (1), 102-110
178. Mancini F, Naldi M, Cavrini V, Andrisano V; *J Chromatogr A*, 2007, **1175**, (2), 217-226

179. Mallik R, Xuan H, Hage DS; *J Chromatogr A*, 2007, **1149**, (2), 294-304
180. Mallik R, Hage DS; *J Pharm Biomed Anal*, 2008, **46**, (5), 820-830
181. Guillarme D, Ruta J, Rudaz S, Veuthey JL; *Anal Bioanal Chem*, 2010, **397**, (3), 1069-1082
182. Leinweber FC, Lubda D, Cabrera K, Tallarek U; *Anal Chem*, 2002, **74**, (11), 2470-2477
183. Tallarek U, Leinweber FC, Seidel-Morgenstern A; *Chem Eng Technol*, 2002, **25**, (12), 1177-1181
184. Hara T, Kobayashi H, Ikegami T, Nakanishi K, Tanaka N; *Anal Chem*, 2006, **78**, (22), 7632-7642
185. Miyazaki S, Takahashi M, Ohira M, Terashima H, Morisato K, Nakanishi K, Ikegami T, Miyabe K, Tanaka N; *J Chromatogr A*, 2011, **1218**, (15), 1988-1994
186. Miyabe K, Cavazzini A, Gritti F, Kele M, Guiochon G; *Anal Chem*, 2003, **75**, (24), 6975-6986
187. Courtois J, Szumski M, Bystrom E, Iwasiewicz A, Shchukarev A, Irgum K; *J Sep Sci*, 2006, **29**, (1), 14-24
188. Vidic J, Podgornik A, Strancar A; *J Chromatogr A*, 2005, **1065**, (1), 51-58
189. Luo QZ, Zou HF, Xiao XZ, Guo Z, Kong L, Mao XQ; *J Chromatogr A*, 2001, **926**, (2), 255-264
190. Karas M, Hillenkamp F; *Anal Chem*, 1988, **60**, (20), 2299-2301
191. Vorm O, Mann M; *J Am Soc Mass Spectrom*, 1994, **5**, (11), 955-958
192. Cohen SL, Chait BT; *Anal Chem*, 1996, **68**, (1), 31-37
193. Karas M, Bachmann D, Hillenkamp F; *Anal Chem*, 1985, **57**, (14), 2935-2939
194. Beavis RC, Chait BT; *Rapid Commun Mass Spectrom*, 1989, **3**, (12), 432-435
195. Strupat K, Karas M, Hillenkamp F; *Int J Mass Spectrom Ion Processes*, 1991, **111**, 89-102
196. Hillenkamp F, Karas M, Beavis RC, Chait BT; *Anal Chem*, 1991, **63**, (24), A1193-A1202
197. Beavis RC, Chaudhary T, Chait BT; *Org Mass Spectrom*, 1992, **27**, (2), 156-158
198. Jaskolla TW, Lehmann WD, Karas M; *Proc Natl Acad Sci U S A*, 2008, **105**, (34), 12200-12205
199. Jaskolla TW, Papasotiriou DG, Karas M; *J Proteome Res*, 2009, **8**, (7), 3588-3597
200. Zenobi R, Knochenmuss R; *Mass Spectrom Rev*, 1998, **17**, (5), 337-366
201. Knochenmuss R, Zenobi R; *Chem Rev*, 2003, **103**, (2), 441-452
202. Jaskolla TW, Karas M; *J Am Soc Mass Spectrom*, 2011, **22**, (6), 976-988
203. Yamashita M, Fenn JB; *J Phys Chem*, 1984, **88**, (20), 4451-4459
204. Whitehouse CM, Dreyer RN, Yamashita M, Fenn JB; *Anal Chem*, 1985, **57**, (3), 675-679
205. Fenn JB, Mann M, Meng CK, Wong SF, Whitehouse CM; *Science*, 1989, **246**, (4926), 64-71

206. Dole M, Mack LL, Hines RL; *J Chem Phys*, 1968, **49**, (5), 2240-2249
207. Wilm M, Shevchenko A, Houthaeve T, Breit S, Schweigerer L, Fotsis T, Mann M; *Nature*, 1996, **379**, (6564), 466-469
208. Wilm MS, Mann M; *Int J Mass spectrom*, 1994, **136**, (2-3), 167-180
209. Wilm M, Mann M; *Anal Chem*, 1996, **68**, (1), 1-8
210. Juraschek R, Dulcks T, Karas M; *J Am Soc Mass Spectrom*, 1999, **10**, (4), 300-308
211. Kebarle P; *J Mass Spectrom*, 2000, **35**, (7), 804-817
212. Gomez A, Tang KQ; *Phys Fluids*, 1994, **6**, (1), 404-414
213. de la Mora JF (2007) The fluid dynamics of Taylor cones. In: *Annual Review of Fluid Mechanics*, vol 39. *Annual Review of Fluid Mechanics*. Annual Reviews, Palo Alto, pp 217-243
214. Taylor G; *Proc R Soc Lond A-Math Phys Sci*, 1964, **280**, (1382), 383-397
215. Cloupeau M, Prunetfoch B; *J Aerosol Sci*, 1994, **25**, (6), 1021-1036
216. Smith JN, Flagan RC, Beauchamp JL; *J Phys Chem A*, 2002, **106**, (42), 9957-9967
217. Peschke M, Verkerk UH, Kebarle P; *J Am Soc Mass Spectrom*, 2004, **15**, (10), 1424-1434
218. Kebarle P, Tang L; *Anal Chem*, 1993, **65**, (22), 972A-986A
219. Duft D, Achtzehn T, Muller R, Huber BA, Leisner T; *Nature*, 2003, **421**, (6919), 128-128
220. Konermann L; *J Am Soc Mass Spectrom*, 2009, **20**, (3), 496-506
221. Winger BE, Lightwahl KJ, Loo RRO, Udseth HR, Smith RD; *J Am Soc Mass Spectrom*, 1993, **4**, (7), 536-545
222. de la Mora JF; *Anal Chim Acta*, 2000, **406**, (1), 93-104
223. Iribarne JV, Thomson BA; *J Chem Phys*, 1976, **64**, (6), 2287-2294
224. Thomson BA, Iribarne JV; *J Chem Phys*, 1979, **71**, (11), 4451-4463
225. Stephens WE; *Physical Review*, 1946, **69**, (11-1), 691-691
226. Cotter RJ; *Anal Chim Acta*, 1987, **195**, 45-59
227. Guilhaus M; *J Mass Spectrom*, 1995, **30**, (11), 1519-1532
228. Beavis RC, Chait BT; *Rapid Commun Mass Spectrom*, 1989, **3**, (7), 233-237
229. Suckau D, Resemann A, Schuerenberg M, Hufnagel P, Franzen J, Holle A; *Anal Bioanal Chem*, 2003, **376**, (7), 952-965
230. Mamyurin BA, Karataev VI, Shmikk DV, Zagulin VA; *Sov Phys JETP*, 1973, **37**, (1), 45-48
231. Mamyurin BA; *Int J Mass Spectrom Ion Processes*, 1994, **131**, 1-19
232. Cotter RJ; *Anal Chem*, 1992, **64**, (21), A1027-A1039
233. Morris HR, Paxton T, Dell A, Langhorne J, Berg M, Bordoli RS, Hoyes J, Bateman RH; *Rapid Commun Mass Spectrom*, 1996, **10**, (8), 889-896

234. Morris HR, Paxton T, Panico M, McDowell R, Dell A; *J Protein Chem*, 1997, **16**, (5), 469-479
235. Paul W, Raether M; *Zeitschrift Für Physik*, 1955, **140**, (3), 262-273
236. Paul W, Steinwedel H; *Z Naturfors Sect A-J Phys Sci*, 1953, **8**, (7), 448-450
237. Blaum K, Geppert C, Muller P, Nortershauser W, Otten EW, Schmitt A, Trautmann N, Wendt K, Bushaw BA; *Int J Mass spectrom*, 1998, **181**, 67-87
238. Huang YL, Guan SH, Kim HS, Marshall AG; *Int J Mass Spectrom Ion Processes*, 1996, **152**, (2-3), 121-133
239. Douglas DJ, Frank AJ, Mao DM; *Mass Spectrom Rev*, 2005, **24**, (1), 1-29
240. Douglas DJ; *Mass Spectrom Rev*, 2009, **28**, (6), 937-960
241. Verentchikov AN, Ens W, Standing KG; *Anal Chem*, 1994, **66**, (1), 126-133
242. Mirgorodskaya OA, Shevchenko AA, Chernushevich IV, Dodonov AF, Miroshnikov AI; *Anal Chem*, 1994, **66**, (1), 99-107
243. Guilhaus M, Selby D, Mlynski V; *Mass Spectrom Rev*, 2000, **19**, (2), 65-107
244. Douglas DJ, French JB; *J Am Soc Mass Spectrom*, 1992, **3**, (4), 398-408
245. Giles K, Pringle SD, Worthington KR, Little D, Wildgoose JL, Bateman RH; *Rapid Commun Mass Spectrom*, 2004, **18**, (20), 2401-2414
246. Hu QZ, Noll RJ, Li HY, Makarov A, Hardman M, Cooks RG; *J Mass Spectrom*, 2005, **40**, (4), 430-443
247. Makarov A, Denisov E, Kholomeev A, Baischun W, Lange O, Strupat K, Horning S; *Anal Chem*, 2006, **78**, (7), 2113-2120
248. Schwartz JC, Senko MW, Syka JEP; *J Am Soc Mass Spectrom*, 2002, **13**, (6), 659-669
249. Kingdon KH; *Physical Review*, 1923, **21**, (4), 408-418
250. Knight RD; *Appl Phys Lett*, 1981, **38**, (4), 221-223
251. Makarov A; *Anal Chem*, 2000, **72**, (6), 1156-1162
252. Makarov A, Denisov E, Lange O; *J Am Soc Mass Spectrom*, 2009, **20**, (8), 1391-1396
253. Michalski A, Damoc E, Lange O, Denisov E, Nolting D, Muller M, Viner R, Schwartz J, Remes P, Belford M, Dunyach J-J, Cox J, Horning S, Mann M, Makarov A; *Mol Cell Proteomics*, 2012, **11**, (3)
254. McLafferty FW, Bente PF, Kornfeld R, Tsai SC, Howe I; *J Am Chem Soc*, 1973, **95**, (7), 2120-2129
255. Cooks RG; *J Mass Spectrom*, 1995, **30**, (9), 1215-1221
256. Roepstorff P, Fohlman J; *Biomedical Mass Spectrometry*, 1984, **11**, (11), 601-601
257. Biemann K; *Biomedical and Environmental Mass Spectrometry*, 1988, **16**, (1-12), 99-111

258. Schilling B, Row RH, Gibson BW, Guo X, Young MM; *J Am Soc Mass Spectrom*, 2003, **14**, (8), 834-850
259. Sinz A; *J Mass Spectrom*, 2003, **38**, (12), 1225-1237
260. Sinz A; *Mass Spectrom Rev*, 2006, **25**, (4), 663-682
261. Phizicky EM, Fields S; *Microbiol Rev*, 1995, **59**, (1), 94-123
262. Johansen K, Svensson L; *Methods in Molecular Medicine*, 1998, **13**, 15-28
263. Fields S, Song O-k; *Nature*, 1989, **340**, (6230), 245-246
264. Young KH; *Biology of Reproduction*, 1998, **58**, (2), 302-311
265. Joung JK, Ramm EI, Pabo CO; *Proc Natl Acad Sci U S A*, 2000, **97**, (13), 7382-7387
266. Kendrew JC, Bodo G, Dintzis HM, Parrish RG, Wyckoff H, Phillips DC; *Nature*, 1958, **181**, (4610), 662-666
267. Fiaux J, Bertelsen EB, Horwich AL, Wüthrich K; *Nature*, 2002, **418**, (6894), 207-211
268. Wüthrich K; *J Biomol NMR*, 2003, **27**, (1), 13-39
269. Xie J, Schultz PG; *Nature Reviews Molecular Cell Biology*, 2006, **7**, (10), 775-782
270. Lomant AJ, Fairbanks G; *J Mol Biol*, 1976, **104**, (1), 243-261
271. Hermanson GT; *Bioconjugate techniques*, 1996. Academic Press, San Diego, CA
272. Dimova K, Kalkhof S, Pottratz I, Ihling C, Rodriguez-Castaneda F, Liepold T, Griesinger C, Brose N, Sinz A, Jahn O; *Biochemistry*, 2009, **48**, (25), 5908-5921
273. Chen ZA, Jawhari A, Fischer L, Buchen C, Tahir S, Kamenski T, Rasmussen M, Lariviere L, Bukowski-Wills JC, Nilges M, Cramer P, Rappsilber J; *EMBO J*, 2010, **29**, (4), 717-726
274. Sinz A; *Angew Chem Int Ed*, 2007, **46**, (5), 660-662
275. Sinz A, Kalkhof S, Ihling C; *J Am Soc Mass Spectrom*, 2005, **16**, (12), 1921-1931
276. Lee YJ; *Mol Biosyst*, 2008, **4**, (8), 816-823
277. Kalkhof S, Sinz A; *Anal Bioanal Chem*, 2008, **392**, (1-2), 305-312
278. Krauth F, Ihling CH, Rüttinger HH, Sinz A; *Rapid Commun Mass Spectrom*, 2009, **23**, (17), 2811-2818
279. Trakselis MA, Alley SC, Ishmael FT; *Bioconjugate Chem*, 2005, **16**, (4), 741-750
280. Ihling C, Schmidt A, Kalkhof S, Schulz DM, Stingl C, Mechtler K, Haack M, Beck-Sickingler AG, Cooper DMF, Sinz A; *J Am Soc Mass Spectrom*, 2006, **17**, (8), 1100-1113
281. Kalkhof S, Haehn S, Paulsson M, Smyth N, Meiler J, Sinz A; *Proteins: Struct, Funct, Bioinf*, 2010, **78**, (16), 3409-3427
282. Schulz DM, Kalkhof S, Schmidt A, Ihling C, Stingl C, Mechtler K, Zschoernig O, Sinz A; *Proteins: Struct, Funct, Bioinf*, 2007, **69**, 254-269
283. Back JW, de Jong L, Muijsers AO, de Koster CG; *J Mol Biol*, 2003, **331**, (2), 303-313

284. Müller MQ, de Koning LJ, Schmidt A, Ihling C, Syha Y, Rau O, Mechtler K, Schubert-Zsilavecz M, Sinz A; *J Med Chem*, 2009, **52**, (9), 2875-2879
285. Kalkhof S, Ihling C, Mechtler K, Sinz A; *Anal Chem*, 2005, **77**, (2), 495-503
286. Schulz DM, Ihling C, Clore GM, Sinz A; *Biochemistry*, 2004, **43**, (16), 4703-4715
287. Sinz A, Wang K; *Biochemistry*, 2001, **40**, (26), 7903-7913
288. Kalisman N, Adams CM, Levitt M; *Proc Natl Acad Sci U S A*, 2012
289. Dreiocker F, Müller MQ, Sinz A, Schäfer M; *J Mass Spectrom*, 2010, **45**, (2), 178-189
290. Müller MQ, Dreiocker F, Ihling CH, Schäfer M, Sinz A; *J Mass Spectrom*, 2010, **45**, (8), 880-891
291. Hurst GB, Lankford TK, Kennel SJ; *J Am Soc Mass Spectrom*, 2004, **15**, (6), 832-839
292. Müller MQ, Dreiocker F, Ihling CH, Schäfer M, Sinz A; *Anal Chem*, 2010, **82**, (16), 6958-6968
293. Müller MQ, Zeiser JJ, Dreiocker F, Pich A, Schäfer M, Sinz A; *Rapid Commun Mass Spectrom*, 2011, **25**, (1), 155-161
294. Petrotchenko EV, Olkhovik VK, Borchers CH; *Mol Cell Proteomics*, 2005, **4**, (8), 1167-1179
295. Mädler S, Bich C, Touboul D, Zenobi R; *J Mass Spectrom*, 2009, **44**, (5), 694-706
296. Novak P, Kruppa GH, Young MM, Schoeniger J; *J Mass Spectrom*, 2004, **39**, (3), 322-328
297. Fritzsche R, Ihling CH, Götze M, Sinz A; *Rapid Commun Mass Spectrom*, 2012, **26**, (6), 653-658
298. Soderblom EJ, Goshe MB; *Anal Chem*, 2006, **78**, (23), 8059-8068
299. Peri S, Steen H, Pandey A; *Trends Biochem Sci*, 2001, **26**, (11), 687-689
300. Götze M, Pettelkau J, Schaks S, Bosse K, Ihling C, Krauth F, Fritzsche R, Kühn U, Sinz A; *J Am Soc Mass Spectrom*, 2012, **23**, (1), 76-87
301. de Koning LJ, Kasper PT, Back JW, Nessen MA, Vanrobaeys F, Van Beeumen J, Gherardi E, de Koster CG, de Jong L; *Febs J*, 2006, **273**, (2), 281-291
302. Palm AK, Novotny MV; *Rapid Commun Mass Spectrom*, 2004, **18**, (12), 1374-1382
303. Delmotte N, Kobold U, Meier T, Gallusser A, Strancar A, Huber CG; *Anal Bioanal Chem*, 2007, **389**, (4), 1065-1074
304. Green NM; *Biochem J*, 1963, **89**, (3), 609-620
305. Green NM, Toms EJ; *Biochem J*, 1972, **130**, (3), 707-711
306. Green NM, Toms EJ; *Biochem J*, 1973, **133**, (4), 687-698
307. Gravel RA, Lam KF, Mahuran D, Kronis A; *Arch Biochem Biophys*, 1980, **201**, (2), 669-673

308. Green NM; *Biochem J*, 1963, **89**, (3), 585-599

## Supplemental Material

- I. Immobilized monolithic enzyme reactors for application in proteomics and pharmaceuticals  
Jens Sproß and Andrea Sinz  
*Analytical and Bioanalytical Chemistry*, 2009, **6**, 1583–1588  
Reprinted with permission, copyright (2009), Springer
  
- II. A Capillary Monolithic Trypsin Reactor for Efficient Protein Digestion in *Online* and *Offline* Coupling to ESI and MALDI Mass Spectrometry  
Jens Sproß and Andrea Sinz  
*Analytical Chemistry*, 2010, **82**, 1434–1443  
Reprinted with permission, copyright (2010), American Chemical Society
  
- III. Monolithic media for applications in affinity chromatography  
Jens Sproß and Andrea Sinz  
*Journal of Separation Science*, 2011, **34**, 1958–1973  
Reprinted with permission, copyright (2010), Wiley and Sons
  
- IV. Monolithic Columns with Immobilized Monomeric Avidin: Preparation and Application for Affinity Chromatography  
Jens Sproß and Andrea Sinz  
*Analytical and Bioanalytical Chemistry*, 2012, **402**, 2395–2405  
Reprinted with permission, copyright (2012), Springer
  
- V. Multi-dimensional Nano-HPLC Coupled with Tandem Mass Spectrometry for Analyzing Biotinylated Proteins  
Jens Sproß, Sebastian Brauch, Friedrich Mandel, Moritz Wagner, Stephan Buckenmaier, Bernhard Westermann and Andrea Sinz  
*Analytical and Bioanalytical Chemistry*, 2013, **405**, 2163–2173  
Reprinted with permission, copyright (2012), Springer

# Immobilized monolithic enzyme reactors for application in proteomics and pharmaceuticals

Jens Sproß · Andrea Sinz

Received: 4 May 2009 / Revised: 17 July 2009 / Accepted: 20 July 2009 / Published online: 9 August 2009  
© Springer-Verlag 2009

**Abstract** The use of monolithic supports for a wide variety of applications has rapidly expanded during the past few years. The examples for applications of monoliths presented herein show that the chromatographic performance of bioreactors and affinity media prepared from monolithic media is superior to that of conventional particle-based systems. The ease of fabrication and modification combined with the long lifetime of the monolithic columns and their potential to be used in fully automated analytical systems make them attractive tools for an increasing number of applications.

**Keywords** Monolithic column · Enzymatic digestion · Trypsin · Proteome analysis

## Abbreviations

ASP	affinity stationary phase
CYP	cytochrome P450
ESI-MS/MS	electrospray ionization tandem mass spectrometry
HPLC	high-performance liquid chromatography
IMER	immobilized monolithic enzyme reactor
MS	mass spectrometry
MSP	monolithic stationary phase
PEGMA	polyethoxylated hydroxyethyl methacrylate
RP	reversed phase

## Introduction

For proteome analysis, high-throughput methods for protein analysis are of outstanding importance. This has led to novel developments, such as immobilizing enzymes on a solid support, so-called enzyme reactors, that allow an efficient and rapid digestion of protein mixtures. Enzyme immobilization with the aim of preparing bioreactors is a technique that was introduced almost 100 years ago, whereas the immobilization of ligands for affinity chromatography can be traced back to the early 1950s [1, 2]. Initially, particle materials were used as a stationary phase [3, 4]; yet these materials suffer from several deficiencies. Firstly, particle-based stationary phases exhibit a high back pressure limiting the flow rates to be applied. Secondly, because of diffusion-limited interaction of sample molecules with the stationary phase or an immobilized molecule, particle-based systems are characterized by a flow rate giving optimal interaction of the analyte with the stationary phase as is determined by the van Deemter equation. Finally, the preparation of microfluidic systems, using column inner diameters below 200  $\mu\text{m}$ , is challenging owing to the rather complicated packing procedure. Microfluidic devices, however, are of enormous interest in the field of analytical sciences, where only minute amounts of analyte might be available for one experiment. Microfluidic devices are also essential in fields of biological research dealing with low sample amounts where samples are often difficult to obtain—as in proteomics or metabolomics. They are also required for high-throughput applications using a microflow apparatus to save costs when enzymes are expensive and/or difficult to handle or to obtain.

Especially for microfluidic applications, the development of monolithic stationary phases (MSPs) in the early 1990s proved to be highly beneficial for overcoming these

J. Sproß · A. Sinz (✉)  
Department of Pharmaceutical Chemistry & Bioanalytics,  
Institute of Pharmacy, Martin-Luther-Universität  
Halle-Wittenberg,  
Wolfgang-Langenbeck-Straße 4,  
06120 Halle / Saale, Germany  
e-mail: andrea.sinz@pharmazie.uni-halle.de

limitations [5, 6]. MSPs exhibit low back pressure even at high flow rates owing to their spongelike constitution composed of mesopores (approximately 50 nm) providing a large surface area and macropores (1–3 μm) for the transport of the mobile phase. The dominating transport mechanisms of analytes towards the monolith are determined by a rapid mass transfer caused by the convective flow. Therefore, chromatographic systems and bioreactors based on monolithic materials maintain their excellent performance over a wide range of flow rates, making these materials extremely useful for high-throughput applications. Moreover, MSPs are made from homogenous solutions, which can be transferred with ease in housings of nearly any desired shape and dimension, making microfluidic applications straightforward.

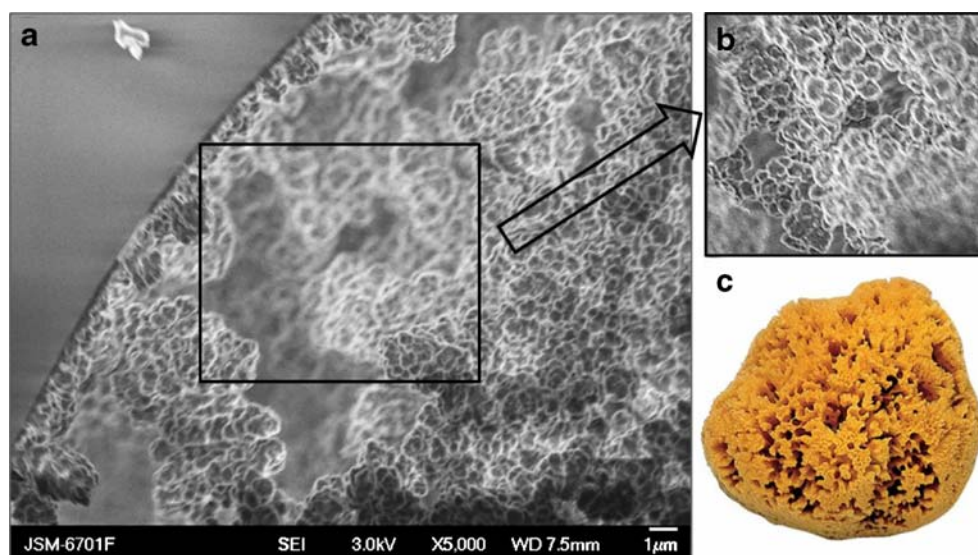
### Modification of MSPs

MSPs are highly interconnected, macroporous polymeric materials (Fig. 1) prepared from inorganic (e.g., tetramethoxysilane) or organic (e.g., styrene, acrylates, or methacrylates) precursors dissolved in an inert porogenic solvent. Inorganic silica monoliths offer excellent separation power in reversed-phase (RP) high-performance liquid chromatography (HPLC); in contrast, organic monoliths can be directly prepared using the desired functional monomer [5, 7, 8]. At present, monolithic RP separation media are commercially available, whereas MSPs for affinity chromatography or for application as immobilized monolithic enzyme reactors (IMERs) are prepared in a number of laboratories worldwide. Immobilization of the respective affinity ligands, such as small molecules or antibodies, or enzymes is achieved by matrix entrapment during the preparation process of the monolith or a

subsequent physical adsorption or covalent bonding of the ligand to the MSP after polymerization. There are only a few examples using inorganic, silica-based monolithic materials for immobilization owing to their difficult preparation; yet, immobilization of affinity ligands or enzymes via matrix entrapment is easily achieved because of the mild preparation conditions [9]. Organic methacrylate-based monoliths are more commonly used for the preparation of affinity stationary phases (ASPs) or IMERs, in which the respective functional species is covalently bound to the surface of the monolith. For this, a reactive monomer—usually glycidyl methacrylate—is copolymerized in the MSP. Afterwards, the epoxy group can be derivatized using several chemistries. Most common is the aminolysis of the epoxide and coupling of the functional species via a dialdehyde linker, which is followed by a subsequent reduction of the imine to a secondary amine, but other techniques have also been reported (Fig. 2) [6, 10–12]. By attaching the functional species via an inert covalent bond to the MSP, one eliminates leaching of the functional species. Also, the ASP or IMER can be used several times or even over a period of several months because most proteins exhibit an enhanced stability after immobilization [10, 11].

ASPs and IMERs prepared in capillaries offer the advantage of direct coupling with HPLC and mass spectrometry (MS), thus eliminating sample loss and contamination caused by manual handling and adsorption to surfaces. Because of the convective flow within the monolithic material and the resulting high mass transfer, the local concentrations of immobilized affinity ligands or enzymes are used to their utmost extent. Although the residence time of the analyte within an ASP or IMER is only in the range of seconds to several minutes, complete binding to the affinity ligand (in the ASP) or high sequence coverage after enzymatic cleavage of the protein (in the IMER) is readily obtained. Compared with classic digestion

**Fig. 1** Scanning electron micrograph of a poly(glycidyl methacrylate-co-acrylamide-co-ethylene dimethacrylate) monolith (a) and insight into a macropore (b). The structure and mode of operation of a monolith exhibit strong similarities to those of a sponge (c)



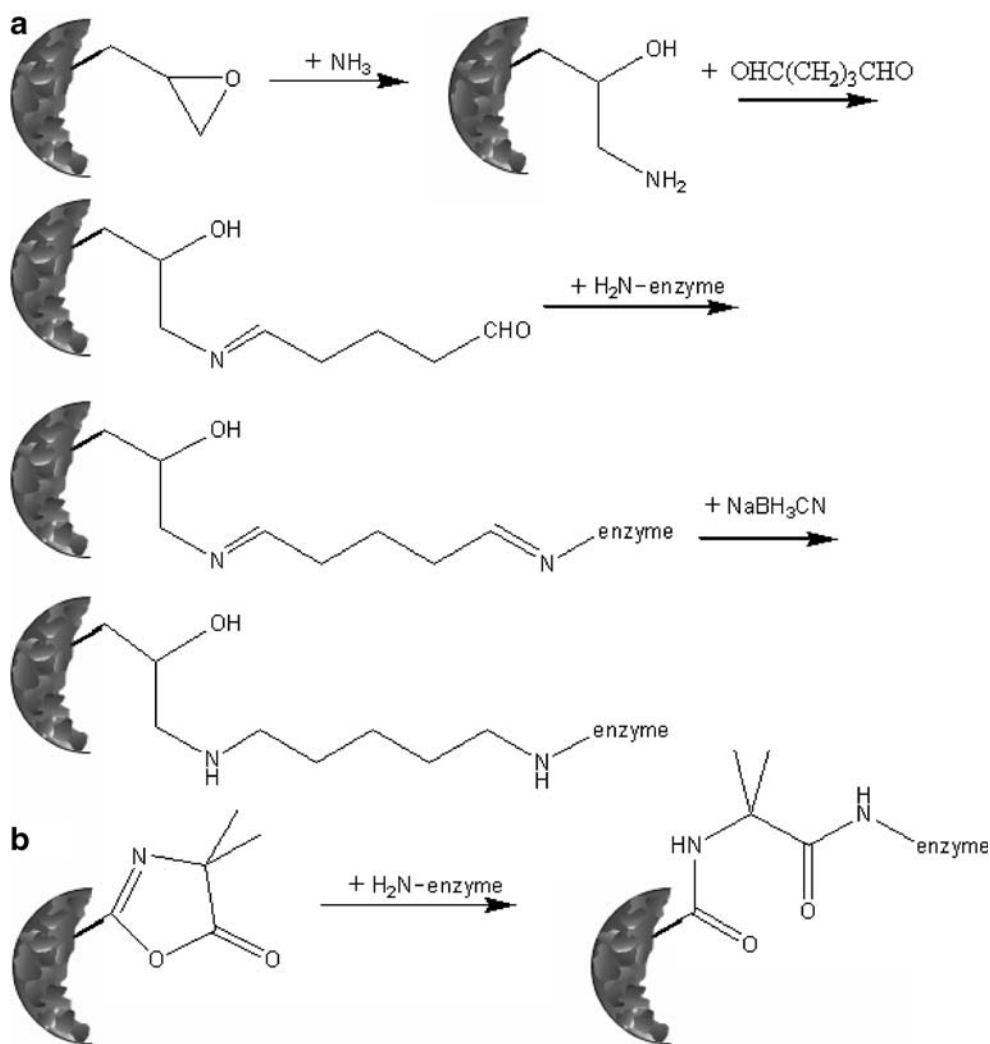
protocols employing soluble proteases with incubation times of approximately 12 h, a drastic decrease in digestion time is achieved using IMERs. The enzyme activity is important for the evaluation of the IMER performance. Recently, it was shown by Ma et al. [13] that there is no difference between  $k_M$  of trypsin *in solution* and immobilized on a MSP, whereas  $V_{max}$  of the immobilized trypsin is 6,600 times higher than for the free trypsin. Moreover, autodigestion of the enzyme is completely eliminated when the enzyme is immobilized on a solid support.

### IMERs in proteomics

At present, trypsin is the most commonly used protease in proteomics and therefore several reports dealing with the preparation of trypsin-IMERs have been published [6, 10]. The advantages of using trypsin are its high specificity of cleaving peptide bonds at the C-terminal side of lysine and

arginine and the fact that a reversible inhibitor, benzamidine, is known to prevent autodigestion of the enzyme during the immobilization, yielding an IMER with high activity. Also, automated protein identification using customized software applications is well established. However, trypsin may not be the protease of choice for lysine- and arginine-rich proteins, for which a large number of small peptides are obtained that are difficult to separate and therefore to identify. Smaller peptides have fewer internal ionizable basic groups, making electrospray ionization tandem MS (ESI-MS/MS) analysis difficult. However, only a few other proteases, such as chymotrypsin, pepsin, and papain, and the protease mixture pronase have been introduced for the preparation of IMERs [14–17]. Chymotrypsin has a lower specificity than trypsin for cleaving at the C-terminal side of phenylalanine, tyrosine, tryptophan, methionine, valine, and leucine. Pepsin (at pH values between 1.5 and 2), papain, and pronase exhibit only low specificities, so short residence times have to be used to

**Fig. 2** Immobilization of an enzyme to a monolithic stationary phase using **a** the glutardialdehyde method or **b** the azlactone method. Alternative methods have been described in the literature



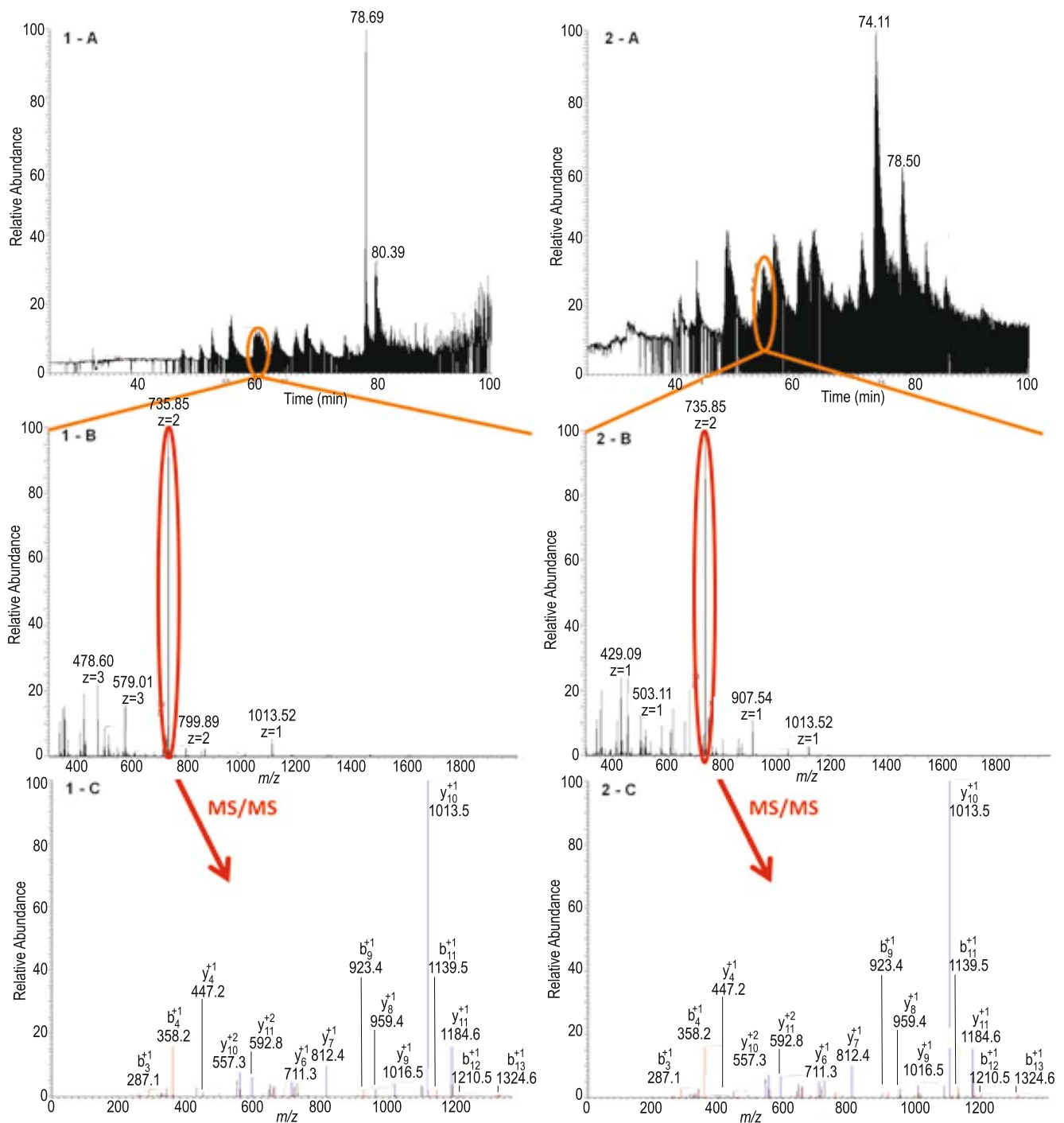


**Fig. 3** *Left*: 5 pmol cytochrome *c* after in-solution digestion (20 h). Thirty-five peptides were identified, yielding a sequence coverage of 91%; Mascot score 3,415. *Right*: 5 pmol cytochrome *c* was digested within 231 s using a trypsin-immobilized monolithic enzyme reactor (210 mm×100µm). Twenty-nine peptides were identified, giving a

sequence coverage of 94%; Mascot score: 4, 493. *Top*: chromatograms of the total ion current. *Middle*: mass spectrometry (MS) survey scans. *Bottom*: tandem mass spectra (MS/MS) of the precursor ion at *m/z* 735.85 corresponding to peptide TGQAPGFTYTDANK, amino acids 40–53

obtain analyzable, longer peptides. One should consider that identification of the digested protein(s) is difficult if enzymes with low specificity are employed.

Fused-silica capillaries are a common housing of IMERs for microfluidic applications. A trypsin-IMER

(210 mm×100µm) was prepared in our laboratory and integrated into a fully automated nano HPLC/nano ESI-MS/MS system. The protein solution was directly injected onto the trypsin-IMER and the resulting peptide mixture was loaded on a C18 trapping column. Afterwards, the

peptides were separated on a RP-C18 capillary column (75- $\mu\text{m}$  inner diameter) and analyzed by nano ESI-MS/MS. This setup of a fully automated and integrated protein identification workflow minimizes manual handling and can be used for high-throughput applications. The residence time of the proteins on the IMER was just 231 s. The analysis of 5 pmol cytochrome *c* is presented in Fig. 3. A sequence coverage of 94% was obtained, compared with 91% sequence coverage by analysis of the same amount of cytochrome *c* that was digested in-solution for 20 h.

Recently, Krenkova et al. [11] reported the preparation of an IMER with immobilized LysC that cleaves highly specifically at the C-terminal side of lysine residues. To prevent unspecific protein adsorption to the MSP leading to sample carryover, the monolith's surface was first hydrophilized by photografting of polyethoxylated hydroxyethyl methacrylate (PEGMA) ( $n=11$ ). After the PEGMA modification, the monolith had to be activated by photografting of 2-vinyl-4,4-dimethylazlactone, which reacts with primary amines by a ring-opening transamidation (Fig. 2b). Using the LysC-IMER, three model proteins (cytochrome *c*, bovine serum albumin, and polyclonal human immunoglobulin G) were digested and the resulting peptide mixtures were analyzed using matrix-assisted laser desorption/ionization time-of-flight MS. Although reasonable sequence coverages were obtained, a trypsin-IMER prepared in the same manner showed better performance in all cases. Compared with the same enzymes in solution, similar sequence coverages were obtained with the IMERs at residence times of 270 s. Further optimization of the immobilization process of LysC might yield better results, yet the great potential of the LysC-IMER for proteomics applications is apparent.

Furthermore, complex mixtures of proteins can be handled with IMERs. The excellent performance of a trypsin-IMER based on a silica monolith was shown by Ma et al. [13] by digestion of 20  $\mu\text{g}$  *Escherichia coli* protein extract: 208 proteins were identified after a digestion time of 150 s, compared with 176 proteins after 24 h of in-solution digestion.

### IMERs in pharmaceuticals

Additional enzymes have been immobilized on MSPs as well. Recently, IMERs containing pharmaceutically relevant enzymes such as cytochrome P450 (CYP) isoforms,  $\beta$ -secretase, acetylcholinesterase, and butyrylcholinesterase have been described [18–21]. Whereas CYP-IMERs have been employed for the evaluation of drug metabolites,  $\beta$ -secretase, acetylcholinesterase and butyrylcholinesterase have been used for inhibitory studies of drugs employing affinity chromatography.  $\text{IC}_{50}$  values were obtained for a variety of

drugs, such as donepezil, physostigmine, and bisnorcymserine. The CYP-IMERs and the three IMERs used for affinity chromatography showed great potential for the pharmaceutical industry since they are reusable (e.g., the acetylcholinesterase ASP was continuously employed for 7 months) and coupling with HPLC offers the possibility of an almost fully automated screening process.

For investigating unspecific interactions of drugs with nontarget proteins, affinity chromatography is employed [22]. For this reason, human serum albumin was immobilized on monolithic silica columns [23]. Human serum albumin is known to nonspecifically interact with drugs, such as the calcium antagonist verapamil [22, 24–26]. These studies are of great value as they may lead to improved models for the mechanisms underlying drug transport in body fluids, e.g., blood, or to further characterization of drug-drug interactions.

### Future applications

In conclusion, MSPs are a versatile tool which can be designed to fit the needs of nearly every application. The examples presented herein prove that the chromatographic performance of bioreactors and affinity media prepared from monolithic media is superior to that of conventional particle-based systems. Also, the ease of fabrication and modification combined with a long lifetime of the columns prepared and their potential to be used in fully automated analytical systems make them not only interesting for proteomics research, but also for pharmaceutical research.

**Acknowledgement** The authors thank A. Wolfsteller for providing scanning electron microscopy images. M. Müller is acknowledged for graphical assistance.

### References

1. Nelson JM, Griffin EG (1916) *J Am Chem Soc* 38:1109–1115
2. Lerman LS (1953) *Proc Natl Acad Sci USA* 39:232–236
3. Mosbach K (1976) *Immobilized enzymes*. Academic, New York
4. Mosbach K (1987) *Immobilized enzymes*. Academic, New York
5. Minakuchi H, Nakanishi K, Soga N, Ishizuka N, Tanaka N (1996) *Anal Chem* 68:3498–3501
6. Petro M, Svec F, Frechet JMJ (1996) *Biotechnol Bioeng* 49:355–363
7. Grafnetter J, Coufal P, Tesarova E, Suchankova J, Bosakova Z, Sevcik J (2004) *J Chromatogr A* 1049(1–2):43–49
8. Sproß J (2007) Diploma thesis, Jena
9. Kawakami K, Abe D, Urakawa T, Kawashima A, Oda Y, Takahashi R, Sakai S (2007) *J Sep Sci* 30:3077–3084
10. Duan J, Liang Z, Yang C, Zhang J, Zhang L, Zhang W, Zhang Y (2006) *Proteomics* 6:412–419

11. Krenkova J, Lacher NA, Svec F (2009) *Anal. Chem* 81:2004–2012
12. Mallik R, Hage DS (2006) *J Sep Sci* 29:1686–1704
13. Ma J, Liang Z, Qiao X, Deng Q, Tao D, Zhang L, Zhang Y (2008) *Anal Chem* 80:2949–2956
14. Temporini C, Calleri E, Campese D, Cabrera K, Felix G, Massolini G (2007) *J Sep Sci* 30:3069–3076
15. Temporini C, Perani E, Calleri E, Dolcini L, Lubda D, Caccialanza G, Massolini G (2007) *Anal Chem* 79:355–363
16. Schoenherr RM, Ye M, Vannatta M, Dovichi N (2007) *J Anal Chem* 79:2230–2238
17. Luo QZ, Mao XQ, Kong L, Huang XD, Zou HF (2002) *J Chromatogr B* 776(2):139–147
18. Nicoli R, Bartolini M, Rudaza S, Andrisano V, Veutheya J-L (2008) *J Chromatogr A* 1206:2–10
19. Bartolini M, Cavrini V, Andrisano V (2007) *J Chromatogr A* 1144:102–110
20. Mancini F, Naldi M, Cavrini V, Andrisano V (2007) *J Chromatogr A* 1175:217–226
21. Bartolini M, Greig NH, Yu Q-S, Andrisano V (2009) *J Chromatogr A* 1216:2730–2738
22. Mallik R, Yoo MJ, Chen S, Hage DS (2008) *J Chromatogr B* 876:69–75
23. Mallik R, Hage DS (2008) *J Pharm Biomed Anal* 46:820–830
24. Ding YS, Zhu XF, Lin BC (1999) *Electrophoresis* 20:1890
25. Jia Z, Ramstad T, Zhong M (2002) *J Pharm Biomed Anal* 30:405
26. Lee K-J, Park H-J, Shin Y-H, Lee C-H (2004) *Arch Pharm Res* 27:978

# A Capillary Monolithic Trypsin Reactor for Efficient Protein Digestion in *Online* and *Offline* Coupling to ESI and MALDI Mass Spectrometry

Jens Sproß and Andrea Sinz\*

Department of Pharmaceutical Chemistry & Bioanalytics, Institute of Pharmacy, Martin-Luther-Universität Halle-Wittenberg, Wolfgang-Langenbeck-Str. 4, D-06120 Halle (Saale), Germany

We describe the preparation of a capillary trypsin immobilized monolithic enzyme reactor (IMER) for a rapid and efficient digestion of proteins down to the femtomole level. Trypsin was immobilized on a poly(glycidyl methacrylate-co-acrylamide-co-ethylene glycol dimethacrylate) monolith using the glutaraldehyde technique. Digestion efficiencies of the IMER were evaluated using model proteins and protein mixtures as well as chemically cross-linked lysozyme regarding the addition of denaturants and increasing digestion temperature. The trypsin IMER described herein is applicable for the digestion of protein mixtures. Even at a 1000-fold molar excess of one protein, low-abundance proteins are readily identified, in combination with MS/MS analysis. An *online* setup of the IMER with reversed phase nano-HPLC separation and nano-ESI-MS/MS analysis was established. The great potential of the trypsin IMER for proteomics applications comprise short digestion times in the range of seconds to minutes, in addition to improved digestion efficiencies, compared to *in-solution* digestion.

## INTRODUCTION

The aim of proteome research consists of a comprehensive identification of the proteins that are present in a cell or an organism at a specified state under specific conditions. To achieve this goal, a variety of methods are available. Separation of the complex protein mixtures is usually achieved using gel electrophoretic or liquid chromatographic techniques. One strategy for protein identification, which is only briefly mentioned herein, because it has not yet developed into a generally applicable technique for global proteomics studies, is the so-called “top-down” approach. This strategy is based on the identification of a protein by measuring the mass of the intact protein using matrix-assisted laser desorption/ionization (MALDI) or electrospray ionization (ESI) mass spectrometry (MS) and a subsequent fragmentation of the protein inside the mass spectrometer using different fragmentation techniques.<sup>1</sup> Despite its elegance by eliminating the need for an enzymatic digestion of the intact protein, the “top-down” approach has special demands on the scientist and instrumentation, which usually requires Fourier transform ion cyclotron resonance (FTICR) or orbitrap mass spectrometry.

For the majority of proteomics studies, a so-called “bottom-up” approach is employed for protein identification, which involves *in-solution* or *in-gel* digestion of proteins by a proteolytic enzyme before the resulting peptide mixtures are analyzed by mass spectrometry.<sup>2</sup> The respective protein is identified by comparison of the experimental peptide masses with *in-silico* digestions of proteins deposited in protein databases by peptide mass fingerprint (PMF) analysis. Tandem mass spectrometry (MS/MS) experiments confirm the identity of the peptides.<sup>3</sup> The mainly used enzyme in proteomics studies is trypsin—in rare cases, LysC and AspN also might be used—which is characterized by highly specific cleavage sites. Most digestion protocols employ extended incubation times to achieve the best possible digestion of the protein(s) of interest. Also, only minute amounts of enzyme are used to avoid the detection of peptides originating from trypsin proteolysis.

To circumvent long digestion times, the proteolytic enzyme can alternatively be immobilized on a solid support. Enzyme immobilization has been performed as early as 1916 by Nelson and Griffin, who used charcoal particles.<sup>4</sup> Since the introduction of monolithic stationary phases (MSPs) in the 1990s by Svec and Tanaka, these have been employed for the immobilization of several different enzymes.<sup>5–14</sup> MSPs combine the advantages of low back pressure at high flow rates with an excellent mass transfer, thus allowing the reduction of digestion times from several hours to a few minutes or even seconds. Today, trypsin immobilized on particles is commercially available by several companies, whereas monolith-based products are not available yet.

- (2) Shevchenko, A.; Tomas, H.; Havlis, J.; Olsen, J. V.; Mann, M. *Nat. Protocol* **2006**, *1*, 2856–2860.
- (3) Lottspeich, F. *Angew. Chem., Int. Ed.* **1999**, *38*, 2476–2492.
- (4) Nelson, J. M.; Griffin, E. G. *J. Am. Chem. Soc.* **1916**, *38*, 1109–1115.
- (5) Svec, F.; Frechet, J. *Anal. Chem.* **1992**, *64*, 820–822.
- (6) Minakuchi, H.; Nakanishi, K.; Soga, N.; Ishizuka, N.; Tanaka, N. *Anal. Chem.* **1996**, *68*, 3498–3501.
- (7) Petro, M.; Svec, F.; Frechet, J. M. J. *Biotechnol. Bioeng.* **1996**, *49*, 355–363.
- (8) Duan, J.; Liang, Z.; Yang, C.; Zhang, J.; Zhang, L.; Zhang, W.; Zhang, Y. *Proteomics* **2006**, *6*, 412–419.
- (9) Krenkova, J.; Lacher, N. A.; Svec, F. *Anal. Chem.* **2009**, *81*, 2004–2012.
- (10) Ma, J.; Liang, Z.; Qiao, X.; Deng, Q.; Tao, D.; Zhang, L.; Zhang, Y. *Anal. Chem.* **2008**, *80*, 2949–2956.
- (11) Sproß, J.; Sinz, A. *Anal. Bioanal. Chem.* **2009**, *395*, 1583–1588.
- (12) Nicoli, R.; Rudaz, S.; Stella, C.; Veuthey, J.-L. *J. Chromatogr., A* **2009**, *1216*, 2695–2689.
- (13) Krenkova, J.; Svec, F. *J. Sep. Sci.* **2009**, *32*, 706–718.
- (14) Ma, J.; Zhang, L.; Liang, Z.; Zhang, W.; Zhang, Y. *Anal. Chim. Acta* **2009**, *632*, 1–8.

\* Author to whom correspondence should be addressed. Tel.: +49-345-5525170. Fax: +49-345-5527026. E-mail: andrea.sinz@pharmazie.uni-halle.de.

(1) Kelleher, N. L.; Lin, H. Y.; Valaskovic, G. A.; Aaserud, D. J.; Fridrikson, E. K.; McLafferty, F. W. *J. Am. Chem. Soc.* **1999**, *121*, 806–812.

In a recent publication, Nicoli et al. compared the digestion performance of their in-lab-prepared monolithic trypsin reactor with that of one of these products.<sup>12</sup> With their monolithic trypsin reactor, a higher sequence coverage was obtained for all five model proteins, compared to the particle-based trypsin reactor. The integration of an immobilized monolithic enzyme reactor (IMER) into an HPLC system coupled to a mass spectrometer allows further automation of the analysis and diminishes sample contamination caused by manual handling.

For functional proteomics studies, which intend to gain insight into the specific interactions of a specific protein with its binding partners, chemical cross-linking of proteins, combined with a subsequent digestion of the cross-linked protein(s) and a mass spectrometric analysis of the created peptide mixture, presents a valid strategy.<sup>15,16</sup> By identifying intermolecular crosslinks between two proteins, interaction regions are determined, whereas intramolecular cross-links within one protein offer insights into its three-dimensional structure. For the digestion of cross-linked protein(s), short digestion times, using immobilized enzymes, should be beneficial, because they would allow the cross-linking approach to be conducted in a high-throughput fashion for determining low-resolution three-dimensional protein structures and for mapping protein interfaces.

In this study, a poly(glycidyl methacrylate-co-acrylamide-co-ethylene glycol dimethacrylate) monolith was used for the trypsin immobilization. Digestion conditions were optimized with *N*<sub>α</sub>-benzoyl-L-arginine ethyl ester (BAEE), cytochrome c, and bovine serum albumin (BSA) as model compounds. The effects of the chaotropic agents, urea and guanidinium hydrochloride (GdnHCl), as well as acetonitrile (ACN), in the protein-containing solution on the digestion efficiencies were evaluated, as only a few publications exist that evaluated the influence of digestion temperature on IMER performance so far.<sup>17,18</sup> Optimized digestion conditions served as the basis for identifying proteins down to low femtomole amounts from protein mixtures and for identifying cross-linked products from hen egg lysozyme, combining IMER digestion with a direct analysis of the digestion products by reversed phase (RP)-HPLC-MS/MS.

## EXPERIMENTAL SECTION

**Materials.** Fused-silica capillaries (outer diameter (OD) of 360 μm, inner diameter (ID) of 100 μm) were obtained from Ziemer Chromatographie (Mannheim, Germany). Ethylene glycol dimethacrylate (EDMA, 98%), γ-methacryloxypropyl trimethoxysilane (γ-MAPS, 98%), cyclohexanol (99%), glutaraldehyde solution (50%), bovine serum albumin (BSA), cytochrome c (horse heart), lysozyme (chicken egg white), β-lactoglobulin B (bovine milk), myoglobin (horse heart), tris(hydroxymethyl) aminomethane hydrochloride (TRIS, 99%), potassium phosphate (98+%), ammonium bicarbonate (99%), 4-(2-hydroxyethyl)-1-piperazineethanesulfonic acid (HEPES, 99.5%), dimethyl sulfoxide (99.5%), DL-dithiothreitol (DTT, 99%), iodoacetamide (99%), formic acid (FA, mass spectrometry grade), and 2,5-dihydroxy benzoic acid (gen-

tisic acid, DHB, 99+%) were from Sigma (Taufkirchen, Germany). Benzamidine hydrochloride (97%) was obtained from Calbiochem (Darmstadt, Germany). Acrylamide (AAM, 99.5%), glycidyl methacrylate (GMA, 97%), sodium cyanoborohydride (>95%), and 1-dodecanol (99.5%) were purchased from Fluka (Buchs, Switzerland). *N*<sub>α</sub>-benzoyl-L-arginine ethyl ester (BAEE) was obtained from Applichem (Darmstadt, Germany) and trypsin (bovine pancreas) from VWR (Darmstadt, Germany). α,α'-Azobisisobutyronitrile (AIBN) was purified via recrystallization from ethanol. Ammonia solution (30%–33%) and guanidinium hydrochloride (GdnHCl, 99%) were from Roth (Karlsruhe, Germany) and trypsin (sequencing grade) from Roche Diagnostics (Mannheim, Germany). Urea (99.5%), trifluoroacetic acid (TFA, UvaSolv), and acetonitrile (ACN, LiChroSolv) were obtained from Merck (Darmstadt, Germany). Potassium hydroxide (85%) was obtained from Grüssing (Filsulm, Germany). *Bis*(sulfosuccinimidyl)suberate (BS<sup>3</sup>) was obtained as nondeuterated (*D*<sub>0</sub>) and four-times-deuterated (*D*<sub>4</sub>) derivative from Pierce, Inc. (Rockford, IL). Water was purified using a Milli-Q5 system and YM-10 Microcon filtration units were from Millipore (Schwalbach, Germany). The C-terminally His-tagged ligand-binding domain of the human peroxisome proliferator-activated receptor α (hPPARα) was expressed in *Escherichia coli* as previously published.<sup>19</sup>

**Preparation of Monolithic Columns.** Fused-silica capillaries (FSCs) were prepared according to a previously published report, in which different silanization procedures were evaluated.<sup>20</sup> First, the capillaries were rinsed with ACN and water before they were activated with 1 M potassium hydroxide at 120 °C for 3 h, and flushed with water and acetone. Afterward, a 10% (v/v) solution of γ-MAPS in dry toluene was filled into the capillaries and incubated overnight at room temperature, followed by washing with acetone and water. The capillaries were dried and stored at 4 °C.

The composition of the polymerization mixture has been published elsewhere:<sup>8</sup> 90 mg GMA, 150 mg EDMA, 60 mg AAM, 595 mg cyclohexanol, 105 mg 1-dodecanol, and 3.0 mg AIBN (1 wt %, with respect to the monomers) were mixed, followed by degassing and sonicating the solution for 15 min. Subsequently, the solution was manually filled into the pretreated capillaries (30 cm length) by a syringe. Both ends of the capillaries were sealed with silicon rubbers and the capillaries were heated at 55 °C in a water bath for 16 h. After the polymerization was complete, each column was inspected under a light microscope to check the homogeneity of the stationary phase. ACN was pumped through the monoliths to wash out porogenic solvents and other compounds. Further investigation of the monolithic support was performed via scanning electron microscopy (SEM), using a JEOL Model JSM-6701F scanning electron microscope (JEOL, Tokyo, Japan).

**Immobilization of Trypsin.** Trypsin was immobilized on the monolithic support, according to an existing procedure that was used with slight modifications.<sup>8</sup> The monolithic columns were flushed overnight with 15% (v/v) ammonium hydroxide solution containing 50% (v/v) ACN. After a 2-h wash with a 25% (v/v) ACN

(15) Sinz, A. *J. Mass Spectrom.* **2003**, *38*, 1225–1237.

(16) Sinz, A. *Mass Spectrom. Rev.* **2006**, *25*, 663–682.

(17) Krenkova, J.; Bilkova, Z.; Foret, F. *J. Sep. Sci.* **2005**, *28*, 1675–1684.

(18) Calleri, E.; Temporini, C.; Perani, E.; De Palma, A.; Lubda, D.; Mellero, G.; Sala, A.; Galliano, M.; Caccialanza, G.; Massolini, G. *J. Protein Res.* **2005**, *4*, 481–490.

(19) Müller, M. Q.; Roth, C.; Sträter, N.; Sinz, A. *Protein Expression Purif.* **2008**, *62*, 185–189.

(20) Courtois, J.; Szumski, M.; Byström, E.; Iwasiewicz, A.; Schukarev, A.; Irgum, K. *J. Sep. Sci.* **2006**, *29*, 14–24.

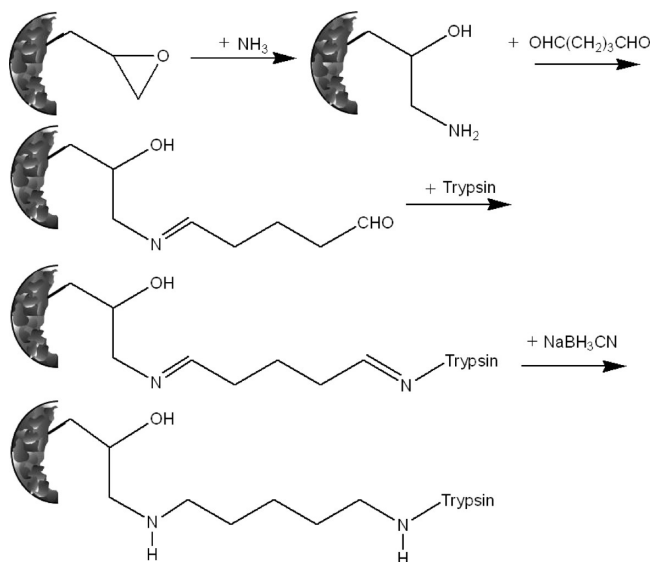


**Figure 1.** Immobilization of trypsin on a monolithic stationary phase (MSP) using the glutaraldehyde method.

solution, a 10% (v/v) glutaraldehyde solution in 25% (v/v) ACN was pumped through the columns for 4 h. The activated support was equilibrated by pumping 100 mM phosphate buffer (pH 8.0) through the capillaries for 2 h. Trypsin was coupled to the support by continuously introducing 2.5 mg/mL trypsin in 100 mM phosphate buffer (pH 8.0) containing 50 mM benzamidine into the capillaries overnight. To prevent leaching of trypsin from the column, the labile Schiff base was reduced with an 80 mM sodium borohydride solution (6 h) to form a stable secondary amine (see Figure 1). All steps were performed at room temperature. Glass syringes from ILS (Stützerbach, Germany) and a Fusion400 syringe pump from Chemyx (Stafford, TX) were used to deliver the liquids through the capillaries. The capillaries were filled with 100 mM ammonium bicarbonate, cut to a length of 7 or 21 cm, and stored at 4 °C before use.

**Enzymatic Activity Assay.** The enzymatic activity of soluble trypsin (1  $\mu\text{g}/\text{mL}$ ) in 100 mM sodium bicarbonate (pH 8.0) was determined spectrophotometrically at 253 nm with 0.1 mM BAEE as the substrate. Activity of the immobilized enzyme was determined by the hydrolysis of 20 mM BAEE in 100 mM sodium bicarbonate (pH 8.0) at volumetric flow rates—generated with a syringe pump—ranging between 200 nL/min to 600 nL/min at 22 °C. The generated product was separated from nonreacted BAEE by capillary electrophoresis (CE). CE experiments were performed using an *in-house* system equipped with a fused-silica capillary of 75 cm length and 75  $\mu\text{m}$  ID/360  $\mu\text{m}$  OD (detection window after 50 cm). The samples were injected hydrodynamically for 10 s, separated at a voltage of 21 kV, and detected at 253 nm using a 50 mM Tris-HCl buffer (pH 7.5). The activity of the immobilized trypsin was also determined spectrophotometrically, using an Ultrospec 1100pro (GE Healthcare, Munich, Germany). Enzymatic activity was expressed in BAEE-units (BAEE-U), which is defined as  $\Delta A_{253}$  of 0.001 AU/min.

**Protein Preparation Prior to IMER Digestion.** The performance of the IMER was evaluated by digesting cytochrome c solutions (0.01  $\mu\text{M}$  to 10  $\mu\text{M}$ ) in 100 mM sodium bicarbonate buffer (pH 8.0). Digestion efficiencies were first evaluated by MALDI-TOF-MS measurements (see below) in the linear mode

**Table 1. Denaturants Added to Protein Solutions<sup>a</sup>**

protein	denaturant	$T$ [°C]	offline MALDI-MS	online ESI-MS
cytochrome c		22	×	×
cytochrome c	2 M urea	37	×	×
cytochrome c	2 M urea + 10% ACN	37		×
BSA		22	×	
BSA	5%, 10%, and 20% ACN	22	×	
BSA	2 M, 4 M, 6 M urea	22	×	×
BSA	1 M, 2 M, 3 M GdnHCl	22	×	
BSA	2 M urea + 10% ACN	22 and 37	×	×
PM-1	2 M urea + 10% ACN	37	×	
PM-2	2 M urea + 10% ACN	37	×	
lysozyme (cross-linked)	2 M urea + 10% ACN	37	×	

<sup>a</sup> PM-1: BSA, lysozyme, cytochrome c, hPPAR $\alpha$ ,  $\beta$ -lactoglobulin, and myoglobin in equal molar ratios; PM-2: BSA, lysozyme, cytochrome c, hPPAR $\alpha$ , and  $\beta$ -lactoglobulin with molar ratios of 1000:1:1:1:1. All solutions contained 0.1 M  $\text{NH}_4\text{HCO}_3$ , flow rate through the IMER 300 nL/min.

by checking for the presence of residual intact cytochrome c. A comparative study of protein digestion in 100 mM sodium bicarbonate buffer (pH 8.0) containing different denaturants (ACN, urea, GdnHCl) was performed with a 0.1  $\mu\text{M}$  BSA solution. The compositions of the solutions are given in Table 1. Prior to digestion, BSA was reduced and alkylated using the following protocol: 10  $\mu\text{L}$  of a 10  $\mu\text{M}$  aqueous BSA solution were mixed with 20  $\mu\text{L}$  0.4 M ammonium bicarbonate and 5  $\mu\text{L}$  8 M urea. Disulfide bridges in BSA were reduced with 5  $\mu\text{L}$  of a solution containing 45 mM DTT and 0.4 M ammonium bicarbonate (15 min at 50 °C) and free sulfhydryl groups were alkylated with 5  $\mu\text{L}$  of a solution containing 0.1 M iodoacetamide and 0.4 M ammonium bicarbonate (15 min at room temperature in the dark). For detergent removal, C4-ZipTips (Millipore, Schwalbach, Germany) were used, according to the procedure suggested by the manufacturer. After digestion of BSA in the IMER, digests were collected, desalted with C18-ZipTips (Millipore), directly spotted onto an AnchorChip target (Bruker Daltonik, Bremen, Germany), and analyzed via MALDI-TOF/TOF-MS/MS (see below).

**IMER Digestion of Protein Mixtures.** Two protein mixtures were subjected to digestion with the trypsin IMER. The first protein mixture (PM-1) contained the proteins BSA, lysozyme, cytochrome c, hPPAR $\alpha$ ,  $\beta$ -lactoglobulin, and myoglobin, while the second protein mixture (PM-2) contained all proteins of PM-1, except myoglobin. For PM-1, 100 pmol of each protein were added to 5  $\mu\text{L}$  of 8 M urea and 20  $\mu\text{L}$  of 0.4 M ammonium bicarbonate. For PM-2, 500 pmol BSA and 500 fmol of lysozyme, cytochrome c, hPPAR $\alpha$ , and  $\beta$ -lactoglobulin were added to 5  $\mu\text{L}$  of 8 M urea and 20  $\mu\text{L}$  of 0.4 M ammonium bicarbonate, yielding a 1000-fold molar excess of BSA over the other four proteins in the mixture. All proteins were reduced and alkylated as described above, and the volume was adjusted to 100  $\mu\text{L}$  with 20  $\mu\text{L}$  of 8 M urea, 10  $\mu\text{L}$  of ACN, and 29  $\mu\text{L}$  of water. Conclusively, final protein concentrations of 1  $\mu\text{M}$  for each protein (in mixture PM-1), as well as 5  $\mu\text{M}$  BSA and 5 nM for the four other proteins (in PM-2) were obtained. Both mixtures were digested on a 21-cm trypsin IMER at 37 °C, and the resulting peptides were analyzed by *offline* nano-HPLC/MALDI-TOF/TOF-MS/MS (see below).

**In-Solution Protein Digestion.** Ten microliters (10  $\mu\text{L}$ ) of a 10  $\mu\text{M}$  protein solution (cytochrome c or BSA) were mixed with 20  $\mu\text{L}$  of 0.4 M ammonium bicarbonate and 5  $\mu\text{L}$  of 8 M urea. Before in-solution digestion, BSA was reduced and alkylated following the procedure described above and 60  $\mu\text{L}$  of water were added after the alkylation. No reduction and alkylation was performed in case of cytochrome c; instead, 70  $\mu\text{L}$  water were added to the digestion mixture. In-solution digestion was performed by adding trypsin (sequencing grade) at an enzyme-to-substrate ratio of 1:60 (w/w) and incubating the mixture at 37  $^{\circ}\text{C}$  for 16 h.

**Chemical Crosslinking.** Hen egg lysozyme (10  $\mu\text{M}$ ) in a solution containing 20 mM HEPES (pH 7.5) was chemically cross-linked with a 50-fold molar excess of BS<sup>3</sup>-D<sub>0</sub>/D<sub>4</sub> at room temperature. The ratio of nondeuterated (D<sub>0</sub>) to deuterated (D<sub>4</sub>) BS<sup>3</sup> was 2:1. After 45 min, the reaction was stopped with 20 mM ammonium bicarbonate and the cross-linking reaction mixture was reduced and alkylated as described above. The detergents were removed through the use of Microcon filtration units (YM-10), employing the protocol provided by the manufacturer (Millipore). After adjusting the protein concentration to  $\sim 1 \mu\text{M}$  and adding the denaturants (Table 1), cross-linked lysozyme was digested on the trypsin reactor (37  $^{\circ}\text{C}$ ) and the resulting peptides were analyzed by *offline* nano-HPLC/MALDI-TOF/TOF-MS/MS (see below).

**MALDI-TOF-MS.** MALDI-TOF-MS measurements for the detection of undigested cytochrome c were performed by spotting 1  $\mu\text{L}$  of the desalted mixture onto a polished stainless steel target (Bruker Daltonik). The samples were mixed with 1  $\mu\text{L}$  of matrix solution (50 mg/mL DHB in 50% (v/v) ACN/0.1% (v/v) TFA). Mass spectra were externally calibrated using a mixture of cytochrome c and myoglobin (10  $\mu\text{M}$  each). MS analyses were conducted with an Ultraflex III MALDI-TOF/TOF mass spectrometer equipped with a 200 Hz SmartBeam Laser (Bruker Daltonik) in the positive ionization and linear mode by accumulating 5000 laser shots in the range of  $m/z$  5000–30000 into one mass spectrum. Data acquisition was done manually with FlexControl 1.3, and data processing was performed with FlexAnalysis 3.0 (both Bruker Daltonik).

Proteolytic peptide mixtures of BSA and cytochrome c from the trypsin IMER were also analyzed with the Ultraflex III MALDI-TOF/TOF mass spectrometer. One microliter (1  $\mu\text{L}$ ) of the desalted peptide mixtures (between 100 fmol and 2 pmol) were spotted onto an 384 MTP 800- $\mu\text{m}$  AnchorChip target (Bruker Daltonik) and mixed with matrix solution (0.7 mg/mL  $\alpha$ -cyano-4-hydroxycinnamic acid (CHCA) in 95% (v/v) ACN/0.1% (v/v) TFA, 1 mM  $\text{NH}_4\text{H}_2\text{PO}_4$ ). MS analyses were conducted in the positive ionization and reflectron mode by accumulating 5000 laser shots in the range  $m/z$  700–5500 into one mass spectrum. Mass spectra were externally calibrated using Peptide Calibration Standard II delivered from the manufacturer (Bruker Daltonik). Data acquisition was done manually with the MS data acquisition (FlexControl 1.3) and data processing (FlexAnalysis 3.0) software.

**Offline Nano-HPLC/MALDI-TOF/TOF-MS/MS.** Analyses of protein mixtures and cross-linked lysozyme that had been digested with the trypsin IMERs were performed by *offline* coupling of a nano-HPLC system (Ultimate 3000, Dionex, Idstein,

Germany) to the MALDI-TOF/TOF mass spectrometer. Samples were injected onto a precolumn (Acclaim PepMap, C18, 300  $\mu\text{m}$   $\times$  5 mm, 5  $\mu\text{m}$ , 100  $\text{\AA}$ , Dionex) and desalted by washing the precolumn for 15 min with 0.1% TFA before the peptides were eluted onto the separation column (Acclaim PepMap, C18, 75  $\mu\text{m}$   $\times$  150 mm, 3  $\mu\text{m}$ , 100  $\text{\AA}$ , Dionex), which had been equilibrated with 95% solvent A (A: 5% (v/v) ACN, 0.05% (v/v) TFA). Peptides of mixture PM-1 and cross-linked lysozyme were separated with gradient A (0–30 min, 5%–50% B; 30–33 min, 50%–100% B; 33–38 min, 100% B; 38–39 min, 100%–5% B; and 39–45 min: 100% B, with solvent B: 80% ACN, 0.04% TFA) at a flow rate of 300 nL/min with UV detection at 214 and 280 nm. Eluates were fractionated into 24-s fractions using the fraction collector Proteiner fc (Bruker Daltonik), mixed with 1.1  $\mu\text{L}$  of CHCA matrix solution, and directly prepared onto a 384 MTP 800- $\mu\text{m}$  AnchorChip target (Bruker Daltonik). The peptides originating from mixture PM-2 were separated with gradient B (0–50 min, 5%–50% B; 50–53 min, 50%–100% B; 53–58 min, 100% B; 58–59 min, 100%–5% B; and 59–65 min, 100% B, with solvent B: 80% ACN, 0.04% TFA), using the flow rates and UV detection previously described. Fractionation of the eluates into 21-s fractions was performed as described above. All devices were controlled using HyStar 3.2 (Bruker Daltonik). MS data were acquired using the Ultraflex III MALDI-TOF/TOF mass spectrometer in the positive ionization and reflectron mode by accumulating 2000 laser shots in the range  $m/z$  700–5500 into one mass spectrum. Signal selection for laser-induced fragmentation was performed manually for cross-linked lysozyme and PM-2. For mixture PM-1, all signals with a signal-to-noise ratio of  $>15$  were subjected to laser-induced fragmentation. Data acquisition was done automatically by the WarpLC 1.1 software (Bruker Daltonik) coordinating MS data acquisition (FlexControl 1.3) and data processing (FlexAnalysis 3.0) software.

**Online IMER-Nano-HPLC/Nano-ESI-MS/MS.** *Online* digestion experiments were performed on a nano-HPLC system consisting of a Famos autosampler, a Switchos II (loading pump and valves), the Ultimate (two nano-HPLC pumps, all Dionex LC Packings, Idstein, Germany), and an U3000 variable wavelength UV detector (Dionex). Five microliters (5  $\mu\text{L}$ ) of the protein solution in 0.1 M sodium bicarbonate (pH 8.0) containing different amounts of denaturant (see Table 1) were injected into a 5  $\mu\text{L}$ -sample loop and digested on the trypsin IMER at a flow rate of 300 nL/min. Digestion temperatures were 22 or 37  $^{\circ}\text{C}$ , respectively. Directly after the IMER, the flow of the loading pump (15  $\mu\text{L}/\text{min}$ , 0.1% (v/v) TFA) was added to the flow from the IMER with a T-shaped connection, and the digestion mixture was loaded onto the C18 trapping column (Acclaim PepMap, C18, 300  $\mu\text{m}$   $\times$  5 mm, 5  $\mu\text{m}$ , 100  $\text{\AA}$ , Dionex). The scheme of the *online* IMER-nano-HPLC/nano-ESI-MS/MS setup is presented in Figure 2. After 25 min, the 10-port valve was switched to elute the peptide mixture from the trapping column onto the 75- $\mu\text{m}$  ID separation column (Acclaim PepMap, C18, 75  $\mu\text{m}$   $\times$  150 mm, 3  $\mu\text{m}$ , 100  $\text{\AA}$ , Dionex) where it was separated by RP-nano-HPLC at 37  $^{\circ}\text{C}$  using a gradient with solvent C (5% ACN, 0.1% FA) and solvent D (80% ACN, 0.1% FA). The linear gradient started with 100% C for 25 min, from 0% D to 50% D in 50 min, to 100% D in 2 min, 100% D for 20 min, to 100% C in 2 min, and then 100% C for 21 min at a flow rate of 300 nL/min. Peptides were detected by their UV absorption at 214 nm.

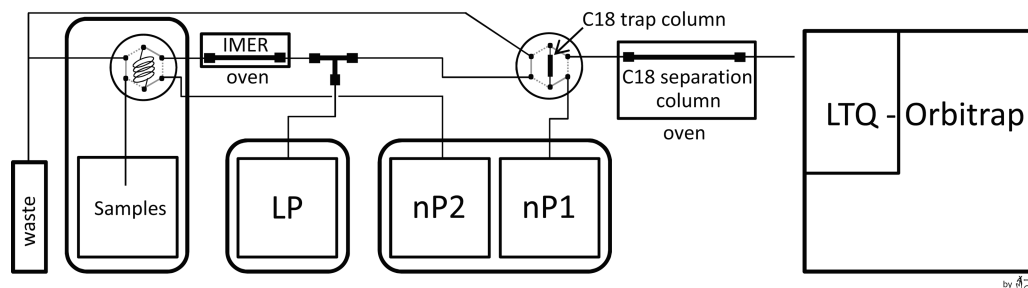


**Figure 2.** Scheme of the *online* IMER-nano-HPLC/nano-ESI-MS/MS setup; “LP” denotes loading pump, and “nP” denotes nano pump.

Nano-ESI-MS/MS was performed on a LTQ-Orbitrap XL mass spectrometer (ThermoFisher Scientific, San Jose, CA) equipped with a nano electrospray ionization source (Proxeon, Odense, Denmark). A spray voltage of 1.6 kV was employed and the temperature of the transfer capillary was set to 200 °C. MS data were acquired over 95 min in data-dependent MS/MS mode. The full-scan mode in the orbitrap analyzer covered the range  $m/z$  300–2000 at a resolution of 60 000 and was followed by product ion scans of the five most-intense signals in the full-scan mass spectrum (isolation window 2 u). Dynamic exclusion with a duration of 180 s (exclusion window  $-1/+2$  Th) was used to detect less-abundance ions. All signals with a charge state of +1 were rejected from collision-induced dissociation (CID) in the linear ion trap (LTQ). MS/MS collision energy was set to 35%, and the fragment ions were detected either in the orbitrap analyzer at a resolution of 7500 or in the LTQ, respectively. Chromatograms of the total ion current (TIC) and mass spectra were recorded on a personal computer with the Xcalibur software version 2.07 (ThermoFisher Scientific). Mass calibration and tuning of the mass spectrometer were performed in the positive ionization mode, using the ESI source delivered by the manufacturer by direct infusion (3  $\mu$ L/min) of a solution of caffeine (Sigma), methionyl-arginyl-phenylalanyl-alanine, and Ultramark 1621 (both ThermoFisher Scientific).

**Protein Identification.** PMF and PFF (peptide fragment fingerprint) MALDI-MS and MS/MS analyses for protein identification were performed with BioTools 3.1 (Bruker Daltonik) using the Mascot software and the SwissProt database (www.expasy.ch). Protein identification based on *online* nano-HPLC/nano-ESI-MS/MS experiments was achieved by conversion of raw data to mgf-files, using the Proteome Discoverer 1.0 SP1 (ThermoFisher Scientific). The mgf-files were used to search the SwissProt database with BioTools 3.1 (Bruker Daltonik). MS/MS data were also included in the Mascot search. For database searches of digested cytochrome c, the heme modification (with a formal charge of +1, a sum formula of  $C_{34}H_{31}N_4O_4Fe$ , and a mass of 615.1694) was included as modification. Cross-linking products were identified using the GPMAW (General Protein Mass Analysis for Windows, version 8.10) software by Light-house Data (Odense, Denmark, available at www.welcome.to/gpmaw).

## RESULTS AND DISCUSSION

**IMER Preparation and Characterization.** The monolithic mixture optimized by Duan et al. was used for IMER preparation.<sup>8</sup> The resulting MSP is composed of GMA for trypsin immobilization and AAm, which is copolymerized for obtaining a more hydrophilic

surface. This results in a better accessibility of the reaction sites on the monolithic support and, thus, in higher digestion efficiencies. SEM was employed to examine the morphology of the prepared trypsin IMER (see Figure 3). Apparently, the monolith is perfectly anchored to the inner wall of the fused-silica capillary and exhibits a highly interconnected network of macropores with small-sized microglobules, providing an optimal interaction of the proteins with the immobilized trypsin. The trypsin IMERs were able to withstand flow rates up to 600 nL/min at back pressures of  $\sim$ 60 bar.

The immobilization of enzymes on GMA-based monoliths via aminolysis of the oxirane groups, followed by modification with glutaraldehyde, coupling of the enzyme, and reduction of the labile imine groups to secondary amines, is a commonly used technique.<sup>7,8</sup> Although this presents a time-consuming multistep procedure, it allows for a high capacity of the immobilized enzyme. Moreover, the glutaraldehyde spacer yields an optimum accessibility of the protein for the enzyme. Both features present keystones for a high proteolytic activity of the prepared IMER.

**IMER Digestion Efficiency.** For a detailed evaluation of the IMER’s proteolytic activity,  $N_\alpha$ -benzoyl-L-arginine ethyl ester (BAEE) was digested at different flow rates between 200 and 600 nL/min. As trypsin possesses a pH optimum between pH 7.5 and 8.5, all solutions contained 0.1 M  $NH_4HCO_3$  for pH adjustment. The digests were collected and analyzed by CE (see Figure 4A). The peak height ratios of digestion product  $N_\alpha$ -benzoyl-L-arginine (BA) and substrate BAEE (BA/BAEE) were taken as criterion to measure the digestion efficiencies of the IMERs. BA/BAEE ratios exhibited their optima between 250 nL/min and 350 nL/min, with the product peak exhibiting an intensity that was  $\sim$ 2.4 times higher than the substrate peak (see Figure 4B). To maintain short digestion times, a flow rate of 300 nL/min was used for all further experiments. Using UV spectroscopy, the enzymatic activity for the trypsin IMERs at a flow rate of 300 nL/min and 22 °C was determined to be 6300 BAEE-U (RSD 10%; see Table 2). As direct comparison, trypsin was used for an enzymatic digestion *in-solution* (1  $\mu$ g/mL), yielding an activity of 15 BAEE-U. This result indicates a  $\sim$ 420 times higher enzymatic activity of the immobilized trypsin, compared to that of trypsin in solution at a digestion temperature of 22 °C. Accordingly, the enzymatic activity of the trypsin IMER is equivalent to that of a trypsin solution with a concentration of 420  $\mu$ g/mL. Raising the temperature to 37 °C increased the enzymatic activity to 9600 BAEE-U (RSD 3%; see Table 2 and Figure 4B), corresponding to an increase in enzymatic activity of more than 50%, compared to that at 22 °C.

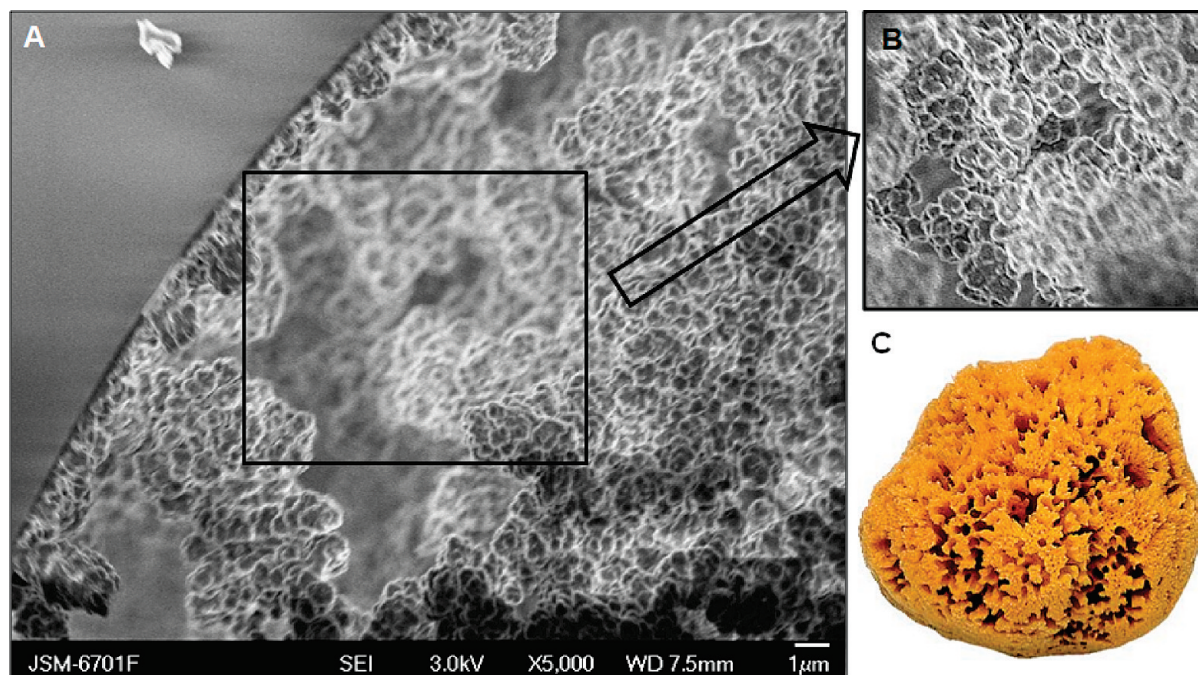


**Figure 3.** Scanning electron microscopy (SEM) image of (A) a poly(glycidyl methacrylate-co-acrylamide-co-ethylene glycol dimethacrylate) monolith and (B) insight into a macropore. (C) The structure of the monolith exhibits strong similarities to a sponge. Reprinted, with permission, from ref 11. (Copyright 2009, Springer, Berlin, Germany).

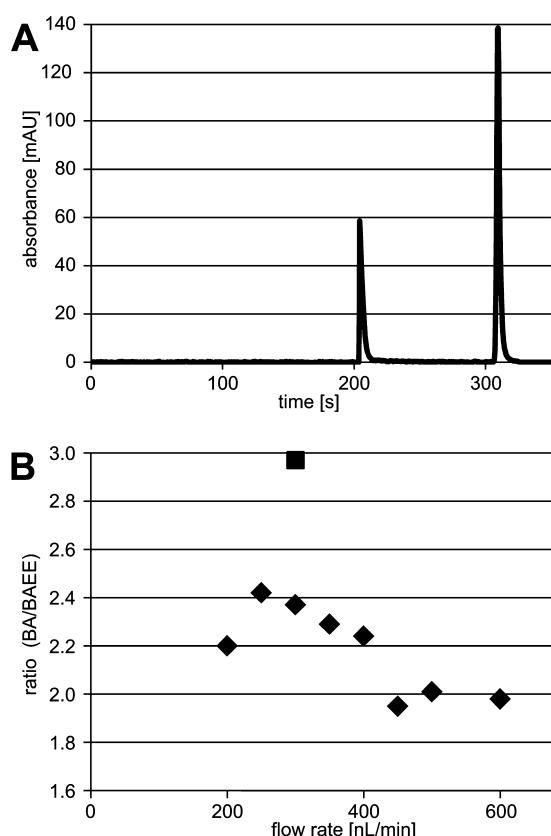


**Figure 4.** (A) Electropherogram of the CE separation of a 20 mM BAEE digest (digestion time = 77 s). The peak at ~210 s corresponds to unreacted BAEE, whereas the peak at ~315 s presents the digestion product BA. Details of CE separation conditions are described in the text. (B) Dependence of digestion product to substrate (BA/BAEE) ratios on the flow rate during IMER digestion (legend for digestion temperature data points: (◆) 22 °C and (■) 37 °C).

**Table 2. Enzymatic Activities of Three Trypsin IMERs (15-1, 15-2, and 15-3) at 22 and 37 °C, Determined with a Solution Containing 20 mM BAEE and 0.1 M NH<sub>4</sub>HCO<sub>3</sub> Using a Flow Rate of 300 nL/min (Digestion Time = 77 s)**

IMER	activity at 22 °C [BAEE-U]	activity at 37 °C [BAEE-U]
15-1	7200	9300
15-2	5610	9600
15-3	6100	9980

**Optimization of Protein Digestion Conditions.** Cytochrome c is a small protein (~12.4 kDa) that is frequently used for evaluating enzymatic digestion efficiencies. Cytochrome c contains 104 amino acids and 21 tryptic cleavage sites (i.e., Arg and Lys residues). To evaluate the optimal protein concentration to be used with the prepared IMERs, cytochrome c was dissolved in 0.1 M sodium bicarbonate at concentrations ranging from 0.01 μM to 10 μM. The flow rate of 300 nL/min resulted in a residence time of 77 s in the trypsin IMER. The effluent from the microreactor was collected and analyzed by MALDI-TOF-MS in the linear mode, to determine if intact protein was still present, and in the reflectron mode, to analyze the proteolytic peptides. While protein concentrations above 2 μM yielded intense cytochrome c signals in the mass spectra, intact protein was hardly detected below a protein concentration of 1.5 μM. In the MALDI-TOF mass spectra of the peptide mixtures obtained from the digestion of a 1–2 μM cytochrome c solution, more than 10 signals were routinely assigned to cytochrome c. At a protein concentration of 1 μM, sequence coverages ranged between 60% and 70%. Protein concentrations as low as 0.1 μM yielded signals that were still sufficient for a correct identification of cytochrome c. Note that, for MALDI-MS experiments, 1 μL of the digest was directly spotted onto a MALDI target, demonstrating an efficient and rapid

**Table 3. Results of the Offline Digestion of BSA by Adding Different Denaturants (Flow Rate = 300 nL/min, Digestion Time = 77 s)<sup>a</sup>**

conditions	Ø sequence coverage (%)	number of peptides
pure BSA	18.2	10
5% ACN	22.1	9
10% ACN	19.1	7
20% ACN	23.7	12
2 M urea	26.2	13
4 M urea	25.0	13
6 M urea	25.9	12
1 M GdnHCl	6.5	3
2 M GdnHCl	5.3	2
3 M GdnHCl	12.1	4
10% ACN/2 M urea	24.0	12
10% ACN/2 M urea (37 °C)	41.6	23

<sup>a</sup> Values are averages from three experiments. All solutions contained 0.1 M NH<sub>4</sub>HCO<sub>3</sub>.

protein identification by *offline* IMER/MALDI-TOF/TOF-MS analyses.

For an optimum digestion of large and folded proteins, the addition of denaturing agents, such as urea or GdnHCl, is essential. However, most enzymes used for proteomic studies have a limited tolerance against denaturants.<sup>21</sup> Immobilization of enzymes has been shown to be useful to increase the tolerance of the enzyme against denaturing agents.<sup>22</sup> Therefore, the influence of urea, GdnHCl, and ACN on the digestion efficiency of the 66.4 kDa protein BSA was tested. Because BSA contains 17 disulfide bridges, the protein was reduced and alkylated prior to digestion on the trypsin IMER. To exclude a potential inactivation of immobilized trypsin by DTT and iodoacetamide, BSA samples were purified with C4-ZipTips, dried under vacuum, and reconstituted in the digestion solution containing 0.1 M NH<sub>4</sub>HCO<sub>3</sub> and the denaturant, giving a BSA concentration of 0.1 μM (Table 1). After digestion on the trypsin IMER (flow rate = 300 nL/min, residence time = 77 s), the peptide mixtures were desalted with C18-ZipTips and analyzed via MALDI-TOF/TOF-MS and a database search was performed.

The digestion of BSA on the trypsin IMER without the addition of a denaturant resulted in an average sequence coverage of 18%, with an average of 10 peptides identified per measurement (see Table 3). The presence of ACN or urea gave a slightly higher sequence coverage (Table 3) with a reasonably high number of peptides (~12) identified in most cases. However, the use of GdnHCl as denaturant resulted in an unsatisfying sequence coverage (Table 3). This decrease in enzymatic activity caused by GdnHCl was not permanent, and the original activity of the IMERs was easily restored by flushing the IMERs with a 0.1 M NH<sub>4</sub>HCO<sub>3</sub> solution. The presence of both ACN and urea in the BSA solution yielded improved results (see Table 3), compared to BSA without denaturing agents, but did not exceed the digestion efficiencies obtained with only one of the two denaturants present. Increasing the digestion temperature from 22 °C to 37 °C yielded a significantly higher sequence coverage and the number of identified BSA peptides was almost doubled (see Table 3).

(21) Harris, J. I. *Nature* **1956**, *177*, 471–473.

(22) Puvanakrishnan, R.; Bose, S. M. *Biotechnol. Bioeng.* **1980**, *22*, 2449–2453.

**Online IMER-Nano-HPLC/nano-ESI-MS/MS.** The integration of the trypsin IMER into a nano-HPLC system allows a more straightforward workflow. By directly coupling the separation system to a mass spectrometer equipped with a nano-ESI source, the resulting peptides can be analyzed using MS<sup>n</sup>-experiments, yielding further information about the analyte. This *online* setup allows for an automated high-throughput analysis of protein samples for fast identification. To test our setup (see Figure 2), 1.3 pmol of reduced and alkylated BSA was desalted with C4-ZipTips and injected onto the IMER (see Table 1). The liquid that contained the tryptic BSA peptides (digestion time 231 s) was mixed with the loading pump flow, transporting the peptides to the C18-trapping column. In the second step, the trapped peptides were separated and analyzed using a LTQ-Orbitrap XL mass spectrometer that was equipped with a nano-ESI source. At a digestion temperature of 22 °C, an average sequence coverage of 49% was obtained for BSA with ~27 peptides identified. By raising the temperature of the trypsin IMER to 37 °C, a mean number of 43 peptides was identified, with a sequence coverage of ~67% (see Figure 5). These results clearly demonstrate the beneficial influence of an elevated digestion temperature on IMER digestion efficiency.

Using the *online* setup for the analysis of 5 pmol cytochrome c, ~25 peptides were identified, giving a sequence coverage of 85% without the addition of denaturants. By adding urea (at a concentration of 2 M) or ACN (10% (v/v) in combination with 2 M urea) to the cytochrome c solution, a sequence coverage of 100% was routinely obtained, with the number of identified peptides increasing to ~36. *In-solution* digestion of cytochrome c yielded 38 peptides with a sequence coverage of 90% (see Figure 6).<sup>11</sup> In summary, the trypsin IMER gives better results, with shorter incubation times (by a factor of 250), compared to standard *in-solution* digestion protocols.

**IMER Digestion of Protein Mixtures.** The trypsin IMER performance was further evaluated with respect to its general applicability to proteomics studies, where low-abundance proteins must be digested in the presence of dominating proteins. For this, two protein mixtures (PM-1 and PM-2) were digested with the IMER. Mixture PM-1 contained six proteins: cytochrome c (12.4 kDa), lysozyme (14.3 kDa), myoglobin (16.9 kDa), β-lactoglobulin (18.3 kDa), hPPARα (32.1 kDa), and BSA (66.4 kDa). The proteins were reduced and alkylated prior to digestion, and the concentration was adjusted to 1 μM for each protein, as described previously. Optimized digestion conditions were used (flow rate = 300 nL/min, 2 M urea, 10% ACN, and 37 °C; see Table 1) with a digestion time of 231 s. For separation and identification of the six proteins, 1 μL of the digestion mixture containing 1 pmol of each protein was diluted and analyzed by *offline* nano-HPLC/MALDI-TOF/TOF-MS/MS, as described previously. All six proteins were identified with excellent Mascot scores (see Table 4); only myoglobin gave a low sequence coverage, with three peptides identified.

To mimic serum samples, protein mixture PM-2 contained BSA at a molar excess of 1000, compared to the other proteins in the mixture. As such, BSA concentration was adjusted to 5 μM, whereas cytochrome c, lysozyme, β-lactoglobulin, and hPPARα were present at 5 nM. The digestion conditions were identical to those used for protein mixture PM-1 (see Table

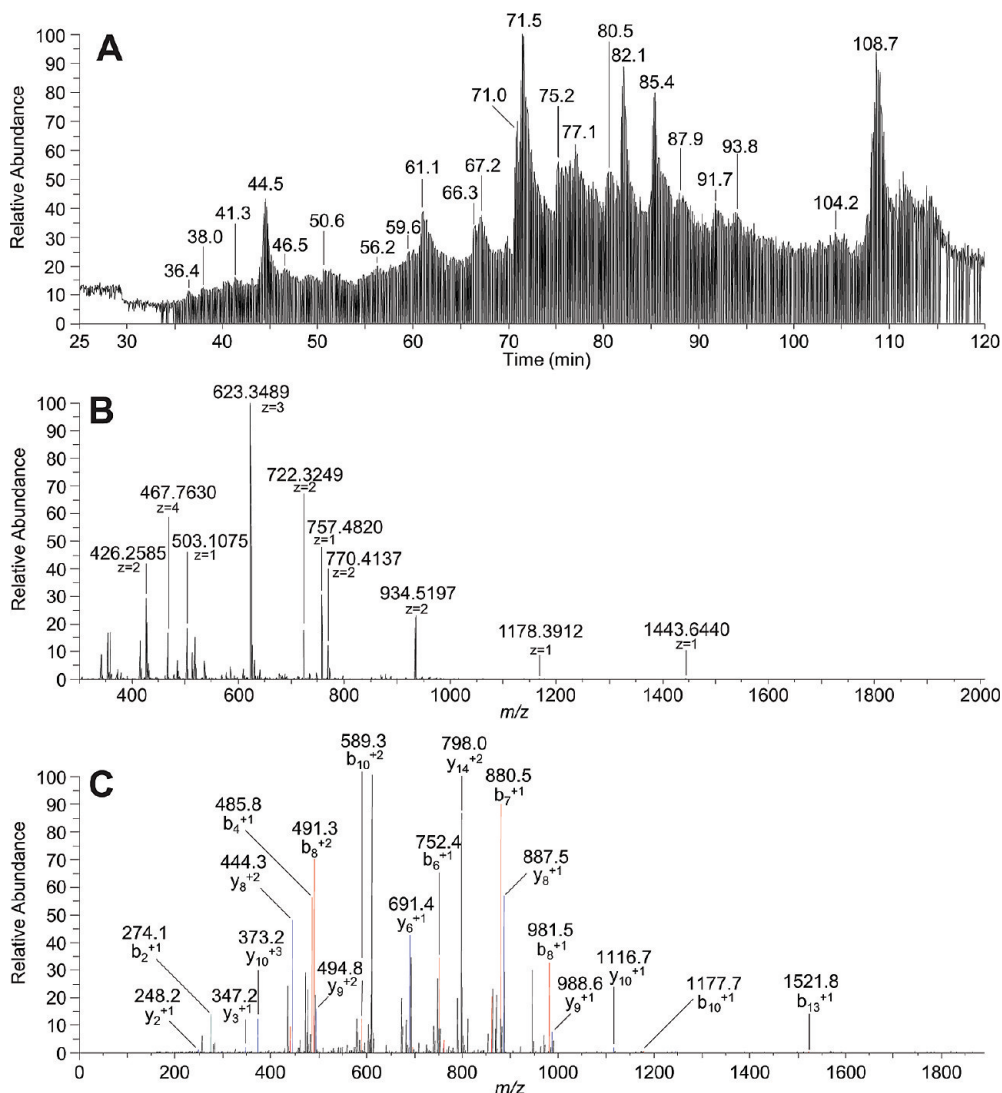


**Figure 5.** (A) Chromatogram of the total ion current (TIC) of a separation of 1.3 pmol *online* digested BSA (denaturants: 2 M urea and 10% ACN, digestion temperature = 37 °C) with the trypsin IMER (digestion time = 231 s). (B) MS survey scan at a retention time of 44.5 min. (C) Fragment ion mass spectrum (MS/MS) of the precursor ion  $[M+3H]^{3+}$  at  $m/z$  623.349 (peptide LCVLHEKTPVSEKVTK, corresponding to BSA amino acids 482–497).

1). Two microliters ( $2 \mu\text{L}$ ) of the digest were diluted, and the peptides were analyzed by *offline* nano-HPLC/MALDI-TOF/TOF-MS/MS. With only 10 femtomoles of each low-abundance protein being loaded onto the separation column, all four proteins were readily identified, showing the excellent performance of the trypsin IMER, even at very low protein amounts in the presence of a highly abundant protein (see Table 4). Figure 7 exemplarily shows a mass spectrum of one HPLC fraction that is dominated by signals of BSA peptides; yet, peptides from the four low-abundance proteins were successfully identified.

**Digestion of Cross-Linked Lysozyme.** To evaluate the digestion efficiency of the IMER on a cross-linked protein, hen egg lysozyme was cross-linked with the amine-reactive homobifunctional cross-linker BS<sup>3</sup>. Because lysozyme contains four disulfide bridges, it was reduced and alkylated prior to digestion on the trypsin IMER. Urea and ACN were added to the protein solution (see Table 1) and the IMER digestion was performed at 37 °C. However, the flow rate of 300 nL/min

that had been determined to be optimal for the digestion of single proteins and protein mixtures was not sufficient to create enough peptides for an analysis of cross-linked products. This is due to the modification of lysine residues by the amine-reactive cross-linking agent: after the cross-linking reaction, modified lysines are no longer available for tryptic cleavage. Moreover, intramolecular crosslinks hamper the unfolding of the protein upon the addition of denaturant and, thus, obstruct the accessibility of trypsin at potential cleavage sites. Therefore, the flow rate was reduced to 100 nL/min, prolonging the digestion time to 11 min and 33 s for the cross-linked protein. *Offline* nano-HPLC/MALDI-TOF/TOF-MS/MS experiments were performed to identify two cross-linking products in lysozyme: an intrapeptide and an interpeptide one (see Table 5). The use of a mixture of nondeuterated and four-times-deuterated BS<sup>3</sup> further aided in the confirmation of potential cross-linked products, based on the distinct 4-u isotopic pattern.

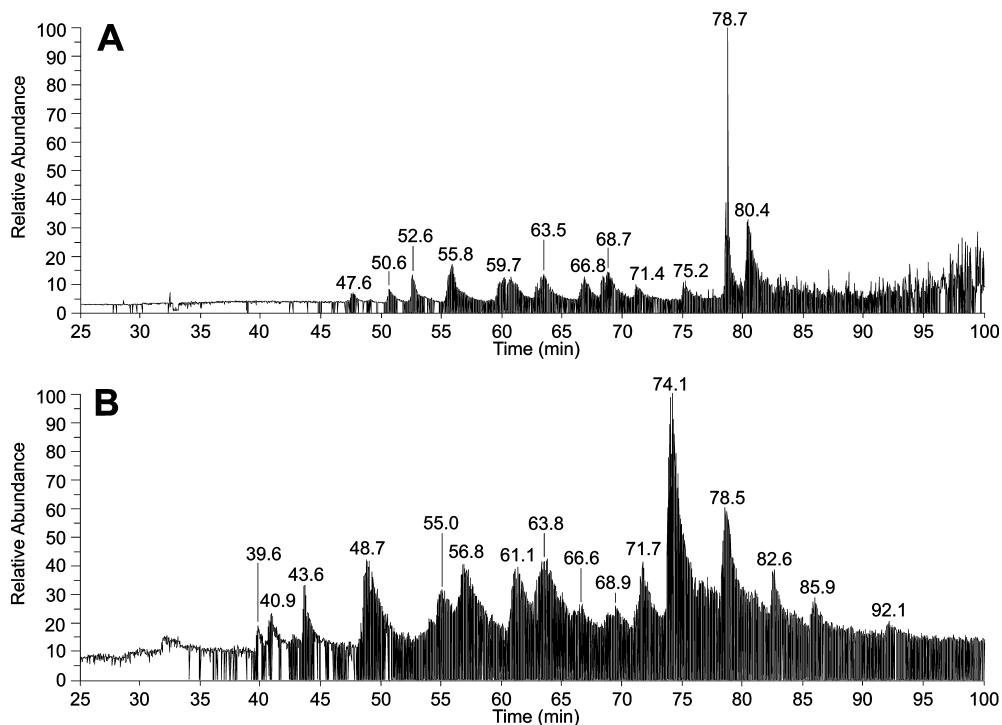


**Figure 6.** TIC chromatograms of (A) a separation of 5 pmol cytochrome c *in-solution* digestion mixture and (B) an *online* digestion using the trypsin IMER with a digestion time of 231 s. See text for details on the LC/MS/MS method.

**Table 4. Results of Protein Identification by Database Search after the Digestion of Protein Mixtures**

parameter	cytochrome c	lysozyme	myoglobin	lactoglobulin	hPPAR $\alpha$	BSA
<b>Protein Mixture PM-1</b>						
sequence coverage	73%	94%	26%	51%	34%	41%
MS/MS score	836	1113	67	532	352	915
number of peptides	17	19	3	15	10	28
<b>Protein Mixture PM-2<sup>a</sup></b>						
sequence coverage	46%	57%		17%	26%	n.a. <sup>b</sup>
MS/MS score	124	248		11	157	n.a. <sup>b</sup>
number of peptides	6	11		2	6	n.a. <sup>b</sup>

<sup>a</sup> No myoglobin was present in protein mixture PM-2. <sup>b</sup> Not applicable, because BSA was present in 1000-fold molar excess to lysozyme, cytochrome c, hPPAR $\alpha$ , and  $\beta$ -lactoglobulin in mixture PM-2 and was not subjected to PMF and PFF analysis.

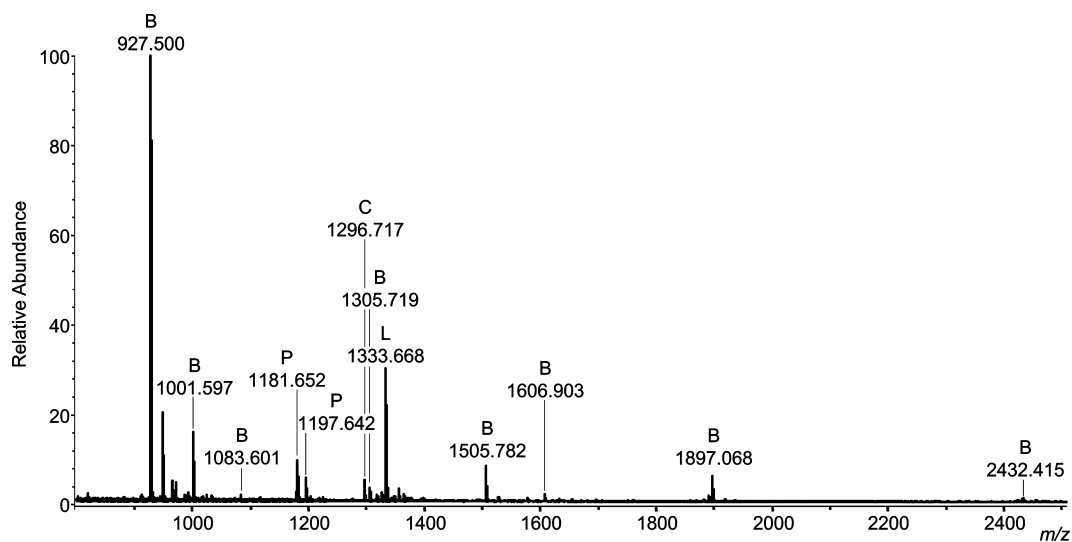


**Figure 7.** MALDI-TOF mass spectrum of the HPLC fraction at  $t_R = 48.8$  min. The spectrum is dominated by signals of BSA peptides (B); yet, peptides originating from three of the four low-abundance proteins were identified (C, cytochrome c; L, lysozyme; P, hPPAR $\alpha$ ).

**Table 5. Identified Cross-Linked Products within Hen Egg Lysozyme after IMER Digestion**

cross-linking product	observed mass [M+H] <sup>+</sup>	sequence (aa)
N-terminus - K1	744.43	KVFGR + XL
K13 - N-terminus	2132.01	CELAAAMKRHGLDNYR/K + XL

## CONCLUSIONS

The trypsin IMERs described herein, which are based on a poly(GMA-co-EDMA-co-AAm) monolith, allow for a rapid and efficient digestion of proteins. The enzymatic activity of immobilized trypsin activity was determined to be ~6300 BAEE-U at a digestion temperature of 22 °C, compared to the previously reported of 2800 BAEE-U.<sup>8</sup> We believe that the presence of ammonium bicarbonate (pH 8) is responsible for the improved performance of the trypsin IMERs. By raising the temperature to 37 °C, the activity of immobilized trypsin was determined to be ~9600 BAEE-U, which is equivalent to a trypsin solution containing the enzyme at a concentration of 640 µg/mL. Digestion of cytochrome c gave sequence coverages of 60%–70% in our *offline* setup, using MALDI-TOF/TOF-MS/MS, and up to 100% in the *online* IMER-nano-HPLC/nano-ESI-MS/MS setup. ACN and urea (up to 6 M) in the protein mixture were observed to increase digestion efficiencies without damaging the trypsin IMERs. Also, the combination of urea and ACN yielded better results, compared to protein digestion in an aqueous buffer. IMER digestion of BSA using the *online* setup yielded sequence coverages of 49% at 22 °C and 67% at 37 °C, stressing the importance of elevated temperatures for digestion. The trypsin IMERs are applicable for the digestion of protein mixtures: even at a 1000-fold molar excess of one protein, low-abundance proteins were readily identified by MS/MS experiments, down to low-femtomole levels. Also, the enzymatic digestion of the intramolecularly cross-linked protein lysozyme was successfully conducted, resulting in the identification of two cross-linked products. The greatest advantages of the trypsin IMERs comprise their short digestion times in the range of seconds to minutes with improved digestion efficiencies, compared to *in-solution* digestion procedures over several hours. Further optimization of the *online* IMER-LC/MS setup and evaluation of the IMERs for digesting highly complex cross-linked protein mixtures are currently performed.

## ACKNOWLEDGMENT

The authors thank Mr. A. Wolfsteller for providing SEM images, Dr. C. H. Ihling for assistance with HPLC and MS, Dr. H. H. Rüttinger for assistance with CE experiments, and Ms. J. Legler and Ms. A. Sleinitz for their help with initial experiments.

Ms. B. Brandt and Ms. S. Knies are acknowledged for excellent technical support. Mr. M. Q. Müller kindly provided the hPPAR $\alpha$ .

## APPENDIX

### Abbreviations

AAm	acrylamide
ACN	acetonitrile
AIBN	$\alpha,\alpha'$ -azobisisobutyronitrile
BA	$N_{\alpha}$ -benzoyl-L-arginine
BAEE	$N_{\alpha}$ -benzoyl-L-arginine ethyl ester
BS <sup>3</sup>	<i>bis</i> (sulfosuccinimidyl)suberate
BSA	bovine serum albumin
CE	capillary electrophoresis
CID	collision-induced dissociation
DHB	2,5-dihydroxy benzoic acid (gentisic acid)
DTT	DL-dithiothreitol
EDMA	ethylene glycol dimethacrylate
ESI	electrospray ionization
FA	formic acid
FSC	fused silica capillary
FTICR	Fourier transform ion cyclotron resonance
GdnHCl	guanidinium hydrochloride
GMA	glycidyl methacrylate
HEPES	4-(2-hydroxyethyl)-1-piperazineethanesulfonic acid
HPLC	high-performance liquid chromatography
hPPAR $\alpha$	human peroxisome proliferator-activated receptor $\alpha$
ID	inner diameter
IMER	immobilized monolithic enzyme reactor
LTQ	linear ion trap (ThermoFisher Scientific)
MALDI	matrix-assisted laser desorption/ionization
$\gamma$ -MAPS	$\gamma$ -methacryloxypropyl trimethoxysilane
MS	mass spectrometry
MS/MS	tandem mass spectrometry
MSP	monolithic stationary phase
OD	outer diameter
PFF	peptide fragment fingerprint
PMF	peptide mass fingerprint
RP	reversed phase
SEM	scanning electron microscopy
TIC	total ion current
TFA	trifluoroacetic acid
TRIS	tris(hydroxymethyl) aminomethane hydrochloride
TOF	time-of-flight

Received for review November 5, 2009. Accepted January 4, 2010.

AC9025362

Jens Sproß  
Andrea Sinz

Department of Pharmaceutical  
Chemistry and Bioanalytics,  
Institute of Pharmacy, Martin-  
Luther-Universität Halle-  
Wittenberg, Halle (Saale),  
Germany

Received May 6, 2011  
Revised May 19, 2011  
Accepted May 19, 2011

## Review Article

# Monolithic media for applications in affinity chromatography

Affinity chromatography presents a highly versatile analytical tool, which relies on exploiting highly specific interactions between molecules and their ligands. This review covers the most recent literature on the application of monoliths as stationary phases for various affinity-based chromatographic applications. Different affinity approaches as well as separations using molecularly imprinted monoliths are discussed. Hybrid stationary phases created by embedding of particles or nanoparticles into a monolithic stationary phase are also considered in this review article. The ease of preparation of monoliths and the multitude of functionalization techniques, which have matured during the past years, make monoliths interesting for an increasing number of biochemical and medical applications.

**Keywords:** Affinity purification / Monolith / Preparation  
DOI 10.1002/jssc.201100400

## 1 Introduction

Monolithic columns are used in a multitude of analytical fields covering applications that rely on reversed phase (RP) [1–3], ion exchange [4], size exclusion [1, 5], and affinity chromatography (AC) [6, 7]. Monolithic materials have also been successfully introduced as basis for immobilized enzyme reactors [8–10]. In this review, we focus on monolithic media for affinity-based chromatography as this presents one of the most versatile fields for the application of monoliths. There have been a number of excellent reviews dealing with the various applications of monolithic columns for AC. Specifically mentioned in this context should be the reviews by Mallik and Hage covering the basic principles and monolithic applications of AC [6], by Tetala and Beek on bioaffinity chromatography [11] and by Haginaka on the topics of molecular imprinting and chiral separation [12, 13]. This review summarizes and discusses

the original literature on all of these topics published in the years between 2007 and the beginning of 2011. Additionally, functionalized particles embedded into monolithic materials are reviewed.

### 1.1 Principles of AC

The term “affinity” is derived from the Latin word “affinitas” for “close relationship”. In biochemistry, the expression “affinity” is used for describing the interaction of biomolecules, i.e., proteins, carbohydrates, polynucleotides, with their ligands. Interactions of proteins with their binding partners play a major role in various cellular events, such as signal transduction and cell proliferation. Of course, biomolecules do not exclusively interact with other biomolecules, but they also undergo highly specific binding to metal ions or artificial ligands, such as small-molecule drugs [14–16]. The underlying molecular recognition mechanisms are highly selective and as such, serve as basis for the various affinity-based chromatographic methods.

AC makes use of specific interactions between analytes and their ligands for enrichment, purification, or separation of a target compound from a complex matrix, such as blood or plasma. AC methods that rely on the numerous interaction mechanisms between biomolecules are often referred to as “bioaffinity” methods. The exploitation of interactions between antibodies and their corresponding antigens is summarized as “immunoaffinity” methods – an important subclass of AC [6, 11].

In AC, one partner of the affinity pair is immobilized on the stationary phase. This attachment should be covalent in order to avoid leakage of the ligand from the stationary phase and moreover, it should not affect the binding site required for complex formation. Also mentioned in this

---

**Correspondence:** Professor Andrea Sinz, Department of Pharmaceutical Chemistry and Bioanalytics, Institute of Pharmacy, Martin-Luther-Universität Halle-Wittenberg, Wolfgang-Langenbeck-Str. 4, D-06120 Halle (Saale), Germany  
**E-mail:** andrea.sinz@pharmazie.uni-halle.de  
**Fax:** +49-345-5527026

**Abbreviations:** **AAM**, acrylamide; **AC**, affinity chromatography; **AGE**, allyl glycidyl ether; **CIM**<sup>®</sup>, convective interaction media; **EDMA**, ethylene glycol dimethacrylate; **FITC**, fluorescein-5-isothiocyanate; **GMA**, glycidyl methacrylate; **HEMA**, 2-hydroxyethyl methacrylate; **IDA**, iminodiacetic acid; **IMAC**, immobilized metal-ion affinity chromatography; **MAA**, methacrylic acid; **MAC**, *N*-methacryloyl-(L)-cysteine methylester; **MAH**, *N*-methacryloyl-(L)-histidine methylester; **MIP**, molecularly imprinted phase; **MSP**, monolithic stationary phase

context should be molecular imprinting, a technique in which the stationary phase itself exhibits cavities for specific interactions. This is achieved by polymerization of the monolith-forming monomers in the presence of a template molecule, which is incorporated into the stationary phase exclusively by noncovalent interactions [17].

Nonspecific binding presents a major challenge for the preparation of affinity supports, resulting in most cases from a nonspecific interaction of molecules, present in the sample matrix other than the analyte, with the immobilized ligand or the stationary phase [18, 19]. Nonspecifically bound substances are usually removed by several washing steps. Elution of the analyte is mostly achieved either by changing the polarity, pH value, and/or ionic strength of the buffer (nonspecific elution) or by adding a competitor of the analyte to the loading buffer (biospecific elution) [6]. The elution method used has to be specifically adapted to each case.

Originally, particles mainly prepared from agarose or silica were used for AC [15, 20, 21], but since the emergence of monolithic stationary phases (MSPs) with their advantageous properties, such as rapid mass transfer, high porosity, and low backpressure at high flow rates, these materials are becoming more and more popular [7, 22, 23]. Also, miniaturization is easily achieved when MSPs are chosen as supports for AC [24, 25].

## 2 MSPs

Monoliths are highly porous stationary phases. They are prepared from monomeric precursors, which form a skeleton with interconnected pores upon polymerization

in a solvent mixture. The pore size distribution and thereby the chromatographic properties of the MSP are tailored by the solvents, which are commonly referred to as porogens. Monoliths exhibit a bimodal pore size distribution with throughpores in the micrometer and mesopores in the nanometer range, which are responsible for their high surface area. Monolithic separation media possess a low resistance to mass transfer resulting in exceptionally fast mass transfer kinetics. A great variety of MSPs are available for preparing the numerous affinity supports, which has been the topic of a number of review articles [6, 11, 12, 26–30]. Therefore, the most popular MSPs will only be briefly discussed in this section and the reader is referred to the existing body of literature for more extensive information.

### 2.1 Organic monoliths

Organic monoliths were introduced by the group of Svec almost 30 years ago and up to date, they present the most popular MSPs [6, 8, 11, 31, 32]. Their main advantage is their straightforward preparation from a multitude of monomers in a great variety of desired dimensions [33]. Glycidyl methacrylate (GMA) and ethylene glycol dimethacrylate (EDMA) are the most commonly employed monomers for the preparation of organic MSPs, which are subsequently functionalized (Fig. 1A). The procedures for preparing these monoliths are well established and the epoxide group of GMA allows for a multitude of immobilization strategies for various ligands (Fig. 2) [6, 11]. In addition to monolithic columns, commercially available

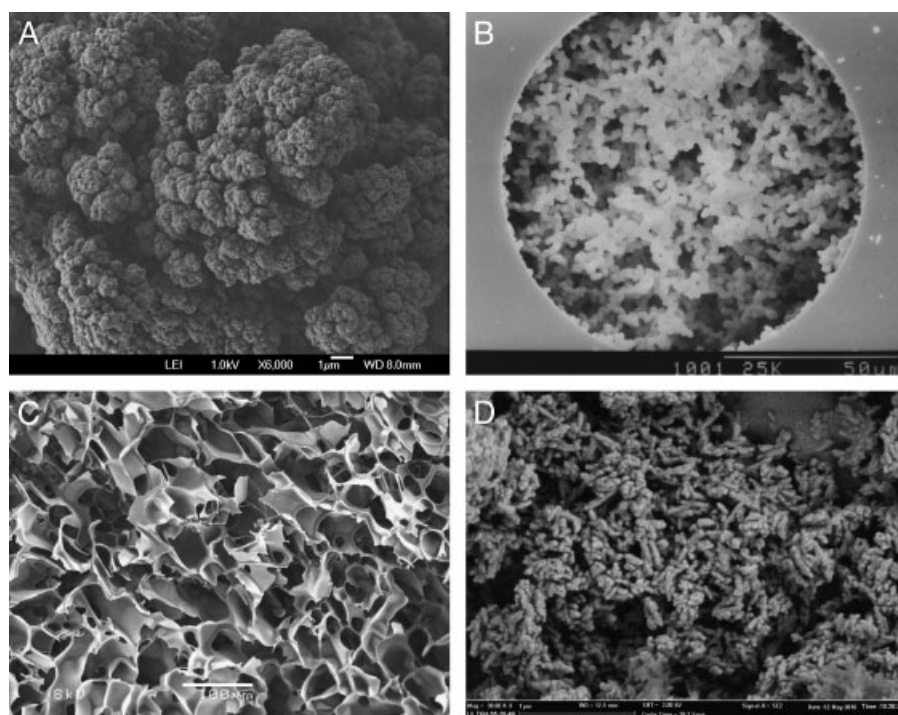


**Figure 1.** Scanning electron microscopy images showing (A) poly-GMA-co-EDMA monolith, (B) monolithic silica (reproduced with permission from [59], copyright 1998, Wiley-VCH), (C) monolithic cryogel (reproduced with permission from [143], copyright 2010, Am. Inst. of Chem. Engineers), and (D) particles embedded in a MSP (reproduced with permission from [57], copyright 2010, Am. Chem. Soc.).

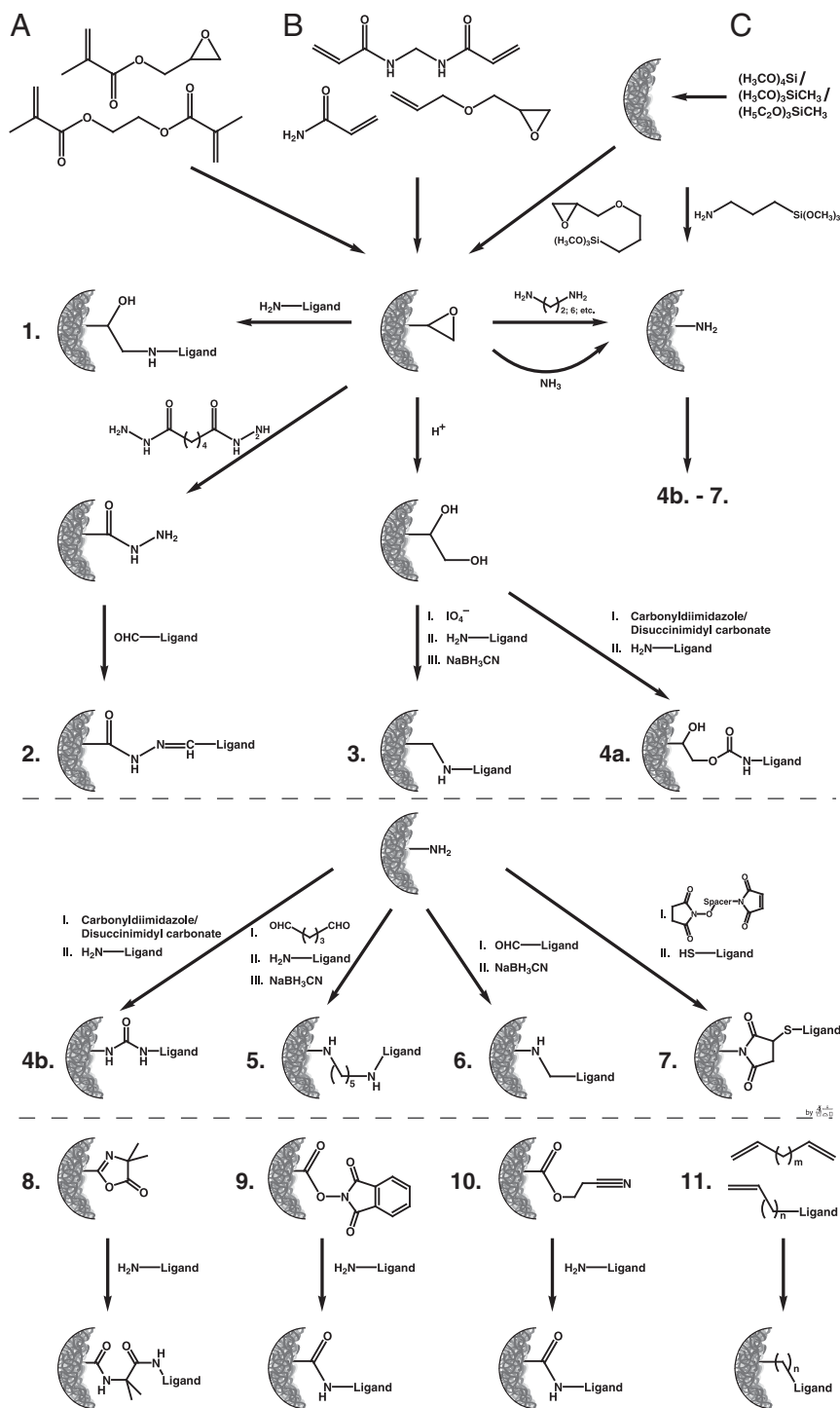


**Figure 2.** Overview of immobilization strategies for the preparation of AC media from (A) organic monoliths, (B) monolithic cryogels, and (C) silica monoliths. 1, Epoxy method; 2, hydrazide method; 3, Schiff base method; 4a and b, carbonyldiimidazole or disuccinimidyl carbonate method; 5, glutaraldehyde method; 6, reductive amination; 7, maleimide method; 8, azlactone method; immobilization using 9, *N*-hydroxyphthalimide ester or 10, 2-cyanoethanol ester as leaving group; 11, direct copolymerization of (e.g. vinyl terminated) ligand.

monolithic discs (convective interaction media – CIM<sup>®</sup>, BIA Separations) of poly(GMA-*co*-EDMA) are commonly employed [34]. Other monomers, such as 2-vinyl-4,4-dimethylazlactone (VDA) [35, 36] and 2-cyanoethyl methacrylate (CEMA) [37, 38], are also used for MSP preparation and even a direct copolymerization of functional monomers

is feasible [39, 40], yielding monolithic affinity columns in a single step.

In order to prevent leakage of the monolithic support and to enable high flow rates, it is crucial to covalently attach the MSP to the container wall. In these cases where the monolith is prepared in glass and fused silica containers, a

covalent attachment is usually done by silanization of the container walls using (meth)acryl terminated trialkoxysilanes [41]. Organic monoliths have smaller surface areas compared with silica monoliths (Section 2.2), resulting in a lower ligand density, which might hamper separation efficiency [42]. This can be circumvented by embedding of particles or nanoparticles into the monolithic support (Section 2.1.2) [43].

### 2.1.1 Monolithic cryogels and hydrogels

Cryogels and hydrogels are two similar classes of macroporous continuous chromatographic supports, which present a subclass of organic monoliths [44, 45]. They are usually hydrophilic stationary phases prepared from acrylamide (AAm), *N,N'*-methylenebisacrylamide (Bis), and allyl glycidyl ether (AGE) in an aqueous buffer (Fig. 1C). During the preparation of hydrogels, the buffer itself acts as porogen, whereas in cryogels ice crystals, produced by freezing the polymerization mixture, define the porous properties of the stationary phase [44, 46, 47]. Ammonium persulfate and *N,N,N',N'*-tetramethyl ethylenediamine are commonly used to initiate the polymerization reaction underlining the similarity between cryogels and hydrogels with acrylamide gels used for SDS-PAGE [48]. After preparation of the monolithic cryogels, ligand immobilization is commonly achieved using the epoxy group of AGE (Fig. 2).

In contrast to methacrylate or silica monoliths (Section 2.2), cryogels and hydrogels are not rigid. This enables the use of alternative elution strategies, such as mechanical compression or temperature-induced shrinkage of the monolithic supports. Especially for the elution of large particles, such as whole cells or viruses, these elution strategies have proven beneficial [49–51]. Also, the pores of monolithic cryogels and hydrogels are larger compared to those of methacrylate and silica monoliths. This enables the investigation of particle-containing fluids, such as tap water, milk, serum or blood, without clogging of the column [31, 50, 52, 53]. Surface areas of these MSPs are generally small resulting in relatively low amounts of ligand to be immobilized on these supports. As for organic methacrylate monoliths, embedding of particles or nanoparticles into the cryogel or the hydrogel will result in a higher density of ligand (Section 2.1.2) [54].

### 2.1.2 Hybrid materials – particles embedded into monoliths

The small surface areas of organic monoliths and macroporous cryogels compared with silica monoliths or particles result in lower ligand densities and limit their separation efficiency. On the other side, nanoparticles have high surface areas, but the preparation of analytical columns using nanoparticles is not feasible. Therefore, hybrid materials, in which nanoparticles are embedded into monolithic matrices, can circumvent these drawbacks and

combine the advantages of both materials. The hybrid materials reviewed herein are mainly prepared by entrapment of particles during the polymerization of the monolithic support (Fig. 1D) [43, 55]. The introduction of nanoparticles after MSP preparation was also exemplified for thiol groups on the MSP's surface and gold nanoparticles [56].

The monolithic bed minimizes leakage of particles from the column and allows for an extensive interaction of analytes in the mobile phase with the ligands introduced by embedding of the particles. In the case of using nanoparticles, preparation of the hybrid material in capillary columns is a straightforward procedure [57]. Also, particles prepared from crushed monoliths have been incorporated into monolithic cryogels [55]. The latter approach makes additional use of the pores in the monolithic particles, which further increases the surface area of the hybrid MSP.

## 2.2 Silica monoliths

Tanaka et al. first described silica monoliths in the mid-1990s (Fig. 1B) [58, 59]. They are commonly prepared from silane precursors, such as tetramethoxysilane, tetraethoxysilane, or methyl(trimethoxy)silane. The resulting bare silica monoliths have become commercially available (e.g. Chromolith-Si<sup>®</sup>, Merck) and can be used for ligand immobilization. Therefore, modification of silanol groups on the surface of the monolithic silica skeleton by silylation reagents, such as (3-aminopropyl)trimethoxysilane or (3-glycidyloxypropyl)trimethoxysilane, is crucial (Fig. 2) [60–62]. Alternatively, grafting of the monolithic surface can be employed to introduce a variety of functionalities [63]. Silica monoliths possess an excellent mechanical stability and a high surface area, but their preparation is challenging due to shrinking of the MSP during the gelation process. In order to avoid disintegration of the MSP, the pH has to be limited to a range between 2 and 8 [64]. Entrapment of ligands in silica monoliths is also feasible; however, the release of alcohols during the gelation process is not always compatible with labile proteins [65, 66].

## 3 Format of monolithic supports

One of the most striking advantages of monolithic supports is that they are readily prepared in any container suitable for the needs of the experiment (Fig. 3). As the main use of MSPs is LC, these containers are mainly columns with varying diameters. Not surprisingly, almost 75% of the applications reviewed herein rely on monolithic supports in column format (Fig. 3B and E), with almost one quarter of the applications dealing with the preparation of MSPs in capillaries. The latter is preferable when precious or rare ligands have to be immobilized or when sample amount is limited (Figs. 3C and E). Most of the remaining applications (ca. 25%) use commercially available monolithic CIM discs

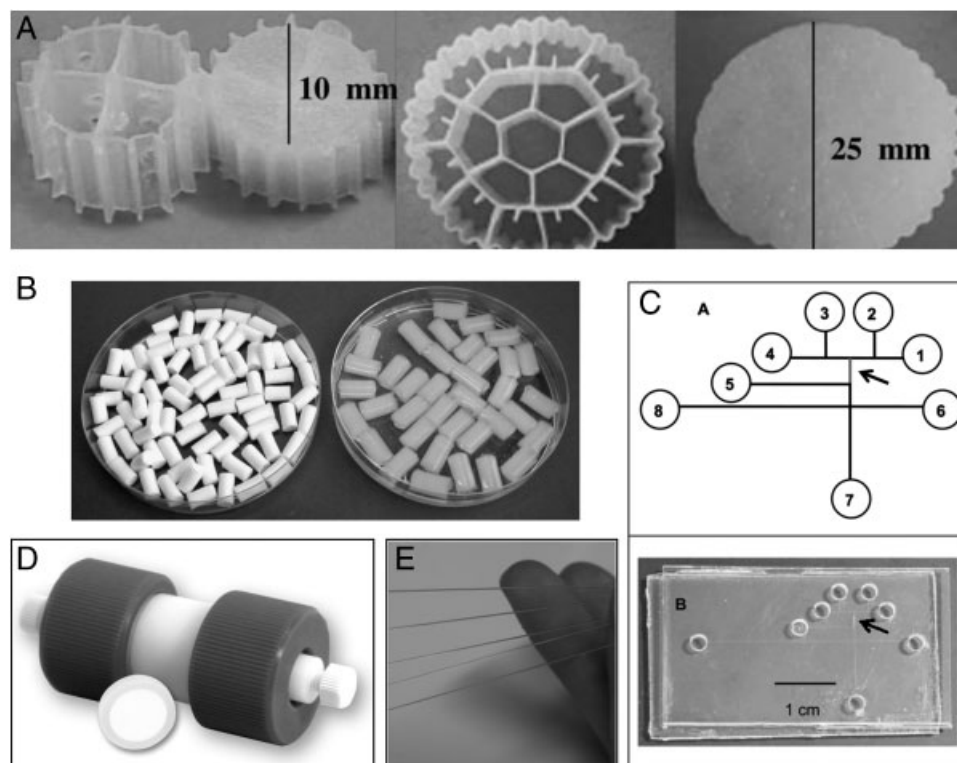


**Figure 3.** Formats of monoliths for AC; (A) cryogel in carrier (reproduced with permission from [143], copyright 2010, Am. Inst. of Chem. Engineers); (B) cryogel microcolumns (reproduced with permission from [50], copyright 2010, Am. Inst. of Chem. Engineers); (C) CE microchip, position of monolith marked with arrow (reproduced with permission from [73], copyright 2010, Am. Chem. Soc.); (D) CIM disc and holder (image kindly provided by BIA Separations); (E) monoliths prepared in fused silica capillaries.

(Fig. 3D). These are easily coupled to HPLC systems and present an alternative format of monolithic supports.

Formats of monolithic supports used for batch-mode applications are not as restricted as the ones used for continuous-mode applications. Functionalized monoliths prepared in carriers (Fig. 3A) enable a straightforward removal of contaminants from stirred solutions, e.g. bioreactors [67]. Polymerization of MSPs in pipet tips allows a rapid manual sample preparation [43] and microarrays using monolithic supports exhibit an excellent sensitivity due to the higher ligand density of a porous monolith compared with a modified glass plate [68].

## 4 Types of AC

### 4.1 Immunoaffinity chromatography

Interactions between antibodies and their antigens are highly selective and therefore immensely popular for AC. Proteins as well as small molecules are common haptens, which are targeted in immunoaffinity chromatography. Immobilized protein A and protein G are used for capturing antibodies. In the following, various immunoaffinity chromatographic applications are discussed; an overview of applications is presented in Table 1.

#### 4.1.1 Antibodies

A large number of applications have been reported in the past years on immobilizing antibodies on MSPs (Table 1).

An oriented immobilization of antibodies makes use of the hydrazide strategy, which attaches the antibody via its carbohydrate chains to the monolithic support. Human serum albumin (HSA) and inter- $\alpha$  inhibitor protein were selectively captured by specific antibodies that had been immobilized on the MSP in this manner [69]. In addition to the direct immobilization of antibodies via the monolith's epoxy groups, immobilization was performed via streptavidin using biotinylated antibodies (for comparison, see Section 4.2.2) [70], resulting in the enrichment of myoglobin and *N*-terminal pronatriuretic peptide from serum.

A number of reports describe the use of immobilized mouse IgG and fluorescent dye-labeled goat anti-mouse IgG for optimizing monolithic supports and experimental conditions [37, 38, 68, 71]. The optimized conditions served to detect osteopontin in cell culture medium [68].

Specific antibodies against fluorescein-5-isothiocyanate (FITC) were used for the enrichment of FITC-labeled amino acids [72] and proteins [73] by microchip CE (Figs. 3C and 4). Enrichment of V5-tagged blood-group antigens was performed via their V5-tag [74]. The antibody directed against the V5-tag was immobilized on a CIM disc. Several groups investigated the enrichment of contaminants, such as the mycotoxins ochratoxin A [75], aflatoxin B1 [76], and bisphenol A [77], by immunoaffinity approaches. A 2-D HPLC system was introduced by Liang et al., in which a monolithic immunoaffinity column was used as the first dimension for specifically capturing pyrethroids [78]. The captured compounds were subsequently separated using RP-HPLC.

**Table 1.** Applications of immunoaffinity chromatography using monolithic supports

Ligand	Analyte	Monolithic support	Ref.
Antibodies	HSA, inter- $\alpha$ inhibitor protein	GMA/EDMA	[69]
	Myoglobin, N-terminal pronatriuretic peptide	GMA/EDMA	[70]
	Polyclonal antibody	HPIEAA/GMA/EDMA	[38]
	Polyclonal antibody	CEMA/EDMA and GMA/EDMA	[68]
	Polyclonal antibody	GMA/EDMA	[71]
	FITC-labeled amino acids	GMA/EDMA	[72]
	FITC-labeled proteins	GMA/EDMA	[73]
	V5-tagged proteins	GMA/EDMA	[74]
	Mycotoxins	GMA/EDMA	[75, 76]
	Bisphenol A	GMA/EDMA	[77]
	Pyrethroids	GMA/EDMA	[78]
	Testosterone	VDA/HEMA/EDMA	[35]
	Erythropoietin	Not reported	[79]
Protein G	Immunoglobulin	GMA/EDMA	[82–84]
Protein A	Immunoglobulin	GMA/EDMA	[85]
	IgG-labeled inclusion bodies	Cryogel	[51]
Protein A, Protein G, antibodies	Stem cells, lymphocytes	Cryogel	[86]
	Immunoglobulins, serum albumin, transferrin, haptoglobin, $\alpha_1$ -antitrypsin, $\alpha_2$ -macroglobulin (all human)	GMA/EDMA	[87–89]

CEMA, 2-Cyanoethyl methacrylate; HPIEAA, *N*-hydroxyphthalimide ester of acrylic acid; VDA, 2-vinyl-4,4-dimethylazlactone.

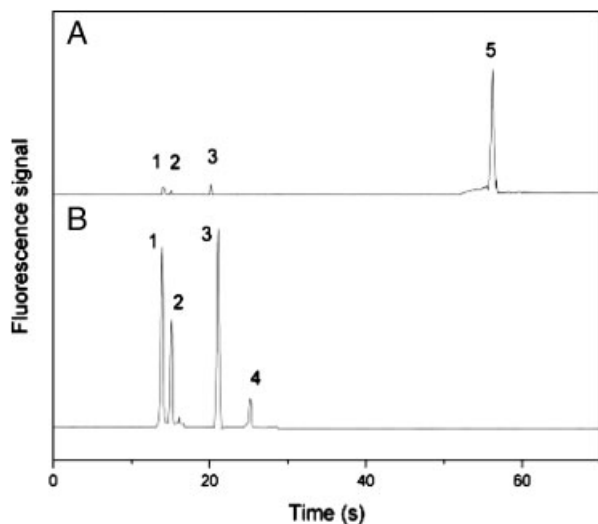


**Figure 4.** Microchip CE of FITC-labeled amino acids and green fluorescent protein (GFP). (A) Before and (B) after affinity column extraction. 1, FITC-Gly; 2, FITC-Phe; 3, FITC-Arg; 4, FITC; 5, green fluorescent protein (reproduced with permission from [72], copyright 2008, Wiley).

A monolithic column with an immobilized polyclonal antibody has been prepared for the quantification of testosterone [35]. Testosterone was labeled with a fluorescent dye; yet, the site that was modified with the label had to be carefully chosen because it influenced the interaction with the antibody. Also, the purification of erythropoietin and several analogues was investigated using monolithic microcolumns with immobilized antibodies, yielding higher recoveries than conventional strategies relying on ultrafiltration [79].

#### 4.1.2 Proteins A and G

The bacterial immunoglobulin-binding proteins protein A (from *Staphylococcus aureus*) and protein G (from *Streptococci*) are commonly used for the isolation or depletion of antibodies. These proteins are able to bind to the  $F_c$  region of different classes of antibodies, however, mainly IgGs are captured by these two proteins [80, 81].

Direct coupling of monolithic discs with immobilized protein G and a monolithic ion-exchange disc allowed capturing bovine serum albumin (BSA) and IgG from serum [82]. Using the same approach, insulin and transferrin were separated from IgG in cell culture medium, additionally enabling a direct quantification of IgG [83]. Coupling of a monolithic RP C4-column with a monolithic protein G column was highly effective for the depletion of immunoglobulins and simultaneous enrichment of low-abundant proteins [84].

A commercially available CIM disc with immobilized protein A was used for the rapid quantification of IgG from supernatants of Chinese hamster ovary cells [85]. Protein A that had been immobilized on monolithic cryogels allowed capturing IgG-labeled inclusion bodies [51], B lymphocytes, and stem cells [86]. Compared with the biospecific elution with protein A, elution of the IgG-labeled compounds by mechanical compression yielded higher recovery rates without affecting the proliferation capacity of the stem cells.

#### 4.1.3 Tandem approaches using antibodies and protein A and G

Several tandem approaches have been described for the removal of antibodies and other high-abundant proteins

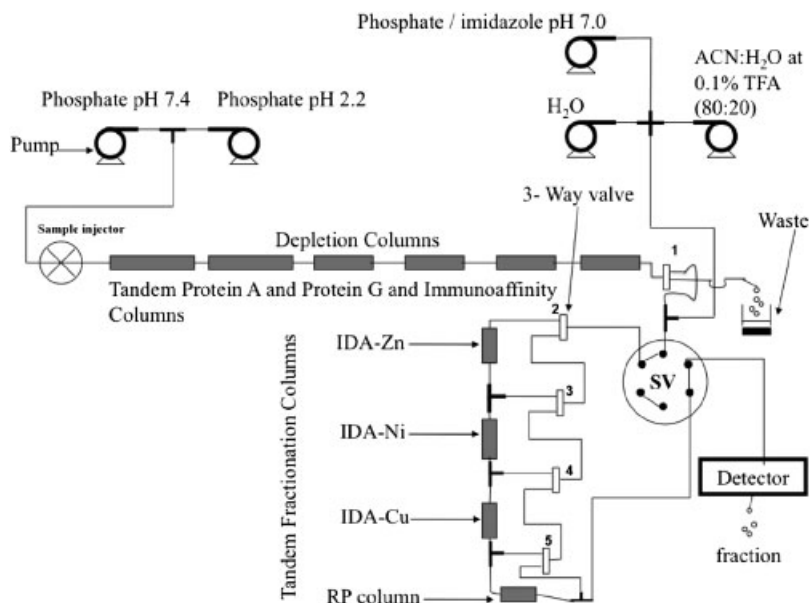


**Figure 5.** Setup of a multidimensional LC system for the integrated depletion of high-abundant proteins with a subsequent fractionation and concentration of medium- and low-abundant proteins (reproduced with permission from [89], copyright 2009, Am. Chem. Soc.).

from human serum or protein mixtures mimicking serum [87–89]. The monolithic affinity columns were functionalized with protein A and genetically engineered protein G' and polyclonal antibodies against HSA, human transferrin, human haptoglobulin, human  $\alpha_1$ -antitrypsin, and human  $\alpha_2$ -macroglobulin. After *online* depletion of high-abundant serum proteins, coupling of the affinity columns with a monolithic trypsin reactor [87], RP column [88], and/or monolithic immobilized metal ion affinity chromatography (IMAC) columns (Fig. 5) [89] allowed an in-depth analysis of serum proteins. Thus, this strategy has the potential to serve as basis for a fully automated analysis of serum samples.

## 4.2 Bioaffinity chromatography

Methods that rely on the interactions between biomolecules and their ligands are often summarized as “bioaffinity” methods. A comprehensive overview of these applications using MSPs is summarized in Table 2.

### 4.2.1 Lectins and carbohydrates

Glycosylation is one of the most common post-translational modifications of proteins and altered glycosylation patterns have been related to various diseases [90–92] underlining their biological importance [91, 93]. Due to the complexity of glycosylation, the investigation of their composition and structure remains a daunting analytical task [94], with many of the analytical approaches relying on an enrichment of glycoproteins and -peptides [95].

Sugars have been immobilized on monolithic supports by two strategies, namely immobilization via a spacer [96] and direct copolymerization of vinyl-terminated sugars [40]. The resulting affinity columns captured lectins, such as concavacalin A (Con A) and a lectin from *Arachis hypogaea*,

but the binding capacity of the sugar monoliths prepared by copolymerization was lower compared with that of those in which the carbohydrate had been attached via a spacer. Kinetic constants of the interaction between Con A and  $\alpha$ -mannose were determined by frontal analysis.

For the enrichment of antithrombin III, heparin was immobilized on monolithic discs and the influence of the spacer length was investigated [97]. The amounts of retained antithrombin III were not affected by the length of the introduced spacer, but the protein's activity was higher when using the short spacer. Influenza A virus particles were captured by targeting hemeagglutinin, the main antigen. Different carbohydrate ligands for hemeagglutinin were evaluated and sialyllactose yielded optimum results for capturing virus particles [98].

Lectin AC relies on the specificity of sugar-binding proteins toward defined carbohydrate residues (see above) [99–101]. Silica monoliths with immobilized Con A and wheat germ agglutinin (WGA) were successfully applied for separating glycoproteins based on their glycosylation patterns [102]. A methacrylate monolith modified with iminodiacetic acid (IDA) for the  $\text{Cu}^{2+}$ -mediated immobilization of Con A was used for the enrichment of glycoproteins from diluted urine [103]. Analysis with nano-HPLC/ESI-MS enabled the identification of 46 glycoproteins – almost three times more than with Con A that had been immobilized on agarose particles.

Macroporous monolithic cryogels with immobilized Con A have been successfully applied to capture yeast cells [50, 51] without compromising the ability of the captured yeast cells to metabolize glucose. Subsequent elution of the captured yeast cells was performed by mechanical [50] or temperature-induced [51] compression of the soft monolithic cryogels.

Boronate AC makes use of the interaction of boronic acids with *cis*-diol-containing compounds, such as sugars

**Table 2.** Applications of bioaffinity chromatography using monolithic supports

Ligand	Analyte	Monolithic support	Ref.
Con A, WGA	Glycoproteins	Silica	[102]
Con A	Glycoproteins <sup>a)</sup>	GMA/EDMA	[103]
Con A	Yeast cells	Cryogel	[50, 51]
Carbohydrates	Lectins	HEMA/PDA/DATD	[40, 96]
Sialyllactose, etc.	Hemeagglutinin, influenza A virus	GMA/EDMA	[98]
Heparin	Antithrombin III	NAT/GMA/EDMA	[97]
Boronic acid	Nucleosides	VPBA/EDMA	[18]
Boronic acid	Nucleosides	<i>m</i> -Aminophenylboronic acid/ 1,6-hexamethylenediamine/TEPIC	[39]
Boronic acid	Glycoproteins	VPBA/Bis	[105]
Boronic acid	Glycopeptides, glycoproteins	APBA/EDMA	[16]
Boronic acid	Glycoproteins	BSPBA/Bis	[106]
Boronic acid	Catecholamines	VBPA/EDMA	[107]
Streptavidin	Biotinylated antibodies <sup>b)</sup>	GMA/EDMA	[70]
Streptavidin	Biotinylated aptamers <sup>b)</sup>	GMA/TRIM	[109, 110]
Avidin	Biotinylated cytochrome <i>c</i> , biotinylated peptides	GMA/EDMA	[111]
Nucleotides	Cytochrome <i>c</i> , thrombin	GMA/TRIM	[109, 110]
Nucleotides	Polycations	GMA/EDMA	[114]
Peptide	Plasmid DNA	GMA/EDMA	[115, 116]
MAH	Plasmid DNA	MAH cryogel	[117]
BSA	Naproxen	GMA/EDMA	[119]
HSA	Carbamazepine, <i>R</i> -warfarin	Silica	[42]
HSA	Warfarin, diazepam, etc.	Silica	[120]
HSA	Chiral separation of amino acids	GMA/EDMA	[125]
HSA	Chiral separation of amino acids and drugs	Silica, GMA/EDMA	[126]
$\alpha_1$ -Acid glycoprotein	Chiral separation of drugs	Silica, GMA/EDMA	[127]
Zr <sup>4+</sup>	Phosphopeptides	EGMP/Bis	[133]
IDA-Ti <sup>4+</sup>	Phosphopeptides	Silica	[134]
Fe <sup>3+</sup>	Phosphopeptides	Silica	[135]
Ni <sup>2+</sup> , Co <sup>2+</sup>	His-tagged vectors	GMA/EDMA, cryogel	[136]
Cu <sup>2+</sup> , Ni <sup>2+</sup>	His-tagged <i>E. coli</i>	IDA cryogel	[50]
Cu <sup>2+</sup>	Lysozyme	IDA cryogel	[137]
Cu <sup>2+</sup>	His-tagged lactate dehydrogenase, Microparticles	IDA cryogel	[51]
IDA-Zn <sup>2+</sup> , Ni <sup>2+</sup> , Cu <sup>2+</sup>	Serum proteins	GMA/EDMA	[89, 142]
Zn <sup>2+</sup> , Ni <sup>2+</sup>	BSA	IDA cryogel	[138]
Zn <sup>2+</sup>	Lysozyme, DNA	MAH cryogel	[139, 140]
Cu <sup>2+</sup>	Lectin <sup>a)</sup>	GMA/EDMA	[103]
Ni <sup>2+</sup> , Cu <sup>2+</sup>	Immunoglobulin	GMA/EDMA	[141]
Cysteine	Heavy metal ions	MAC/HEMA	[144]
Reactive Green	Heavy metal ions	Cryogel	[145]
IDA, DTPA	Heavy metal ions	Cryogel	[143]
IDA	Cu <sup>2+</sup>	Cryogel, agarose	[67]
Fe <sub>3</sub> O <sub>4</sub> -nanoparticles <sup>c)</sup>	BSA	Cryogel	[146]
TiO <sub>2</sub> -nanoparticles <sup>c)</sup>	Phosphopeptides	EDMA	[43]
TiO <sub>2</sub> , ZrO <sub>2</sub> -nanoparticles <sup>c)</sup>	Phosphopeptides	DVB	[147]
Hydroxyapatite-nanoparticles <sup>c)</sup>	Phosphoproteins, phosphopeptides	HEMA/EDMA	[57]
Au-nanoparticles <sup>d)</sup>	Cysteine peptides	GMA/EDMA	[56]
Cu <sup>2+</sup> -sporopollenin particles <sup>c)</sup>	HSA	Cryogel	[148]
Antibiotic	<i>E. coli</i>	PGGE	[153]
Benzensulfonamide, tacrolimus	Carbonic anhydrase II, calcineurin A and B	PEG-methacrylates	[152]
Soybean trypsin inhibitor	Trypsin-labeled particles	GMA/EDMA	[149, 150]
Antipyrine	Penicillin acylase	MAAP/EDMA	[151]

**Table 2.** Continued.

Ligand	Analyte	Monolithic support	Ref.
Human lactoferrin	Peptide displaying phages	Cryogel	[154]
Peptide displaying phages	Human lactoferrin, von Willebrand factor	Cryogel	[53]
Peptide epitope	IgM	GMA/EDMA	[155]
Cibracon Blue	HSA	Cryogel	[156]
Cibracon Blue	BSA	Cryogel	[67]

APBA, 3-Acrylamidophenylboronic acid; BSA, bovine serum albumin; BSPBA, 4-(3-butenylsulfonyl) phenylboronic acid; DATD, (+)-*N,N'*-diallyltartardiamide; DTPA, diethylenetriamine-*N,N,N',N'',N'''*-pentaacetic acid; DVB, divinylbenzene; EGMP, ethylene glycol methacrylate phosphate; HSA, human serum albumin; MAAP, methacryloyl antipyrine; NAT, *N*-acryloyl-tris(hydroxymethyl)aminomethane; PDA, piperazine diacrylamide; PGGE, polyglycerol-3-glycidyl ether; TEPIC, *tris*(2,3-epoxy-propyl)isocyanurate; TRIM, trimethylolpropane trimethacrylate; VPBA, 4-vinylphenylboronic acid; WGA, wheat germ agglutinin.

a) Immobilized by IMAC.

b) Used for immobilization.

c) Embedded in MSP.

d) Bound to MSP.

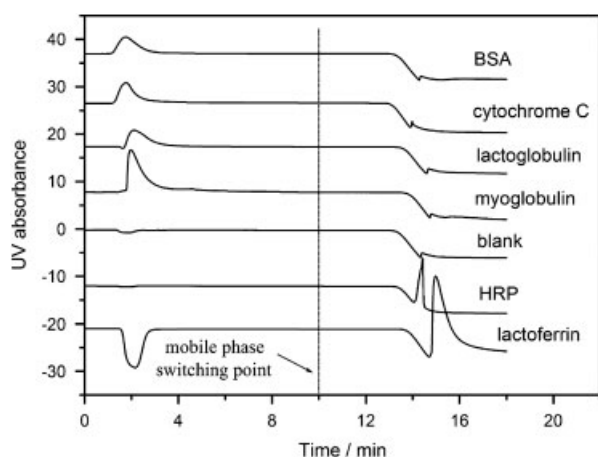


**Figure 6.** Specific capture of glycoproteins using a boronate affinity monolithic column. Nonglycosylated proteins were not retained (reproduced with permission from [105], copyright 2009, Elsevier).

[104], and is therefore frequently used for the enrichment of nucleosides [18, 39], glycopeptides, glycoproteins (Fig. 6) [105, 106] and catecholamines [107]. The performance of monolithic columns with phenylboronic acid derivatives as affinity ligands has been steadily improved [18, 39, 105]. Although the first affinity monolith was quite hydrophobic [18], nonspecific adsorption was decreased by employing hydrophilic monomers [39, 105]. The copolymerization of the synergistic monomer 1,6-hexamethylenediamine or the use of a sulfonylsubstituted phenylboronic acid with its lower  $pK_a$  value (7.0) allowed applying neutral pH values for the capture of analytes in contrast to the usually basic conditions, which might lead to decomposition of pH labile compounds [39, 106].

#### 4.2.2 Streptavidin–biotin and avidin–biotin interaction

The streptavidin/avidin–biotin complex is highly popular for the specific immobilization of biotinylated species due to its

high association constant ( $K_A = 10^{15} \text{ M}^{-1}$ ) [108]. Streptavidin on monolithic supports has been successfully used for the immobilization of biotinylated DNA aptamers, which then allow a specific capturing of proteins [109, 110] (Section 4.2.3) and an immobilization of antibodies (Section 4.1.1) [70]. Recently, MSPs with immobilized monomeric avidin ( $K_A = 10^7 \text{ M}^{-1}$  for the monomeric avidin–biotin complex) were prepared and used to enrich biotinylated cytochrome *c* and biotinylated cytochrome *c* peptides [111]. The monolithic columns showed better performance than commercially available monomeric avidin particles.

#### 4.2.3 Nucleotides and DNA

The interaction of DNA with polycations for gene delivery is still a topic of great interest [112, 113]. Poly(rC)- and poly(rA)-modified CIM discs have been used for studying the interactions with synthetic polycations for a potential application in gene therapy [114]. Also, DNA aptamers have been used for the enrichment of proteins [109, 110]. With a sandwich chromatographic assay, thrombin was analyzed in diluted plasma solutions at concentrations as low as 10 nM. Also, a 16-mer peptide that had been immobilized on a monolithic column permitted the purification of supercoiled plasmid DNA in a single step [115, 116]. Pseudoaffinity chromatography for the purification of plasmid DNA was performed with a monolithic cryogel with copolymerized *N*-methacryloyl-( $\iota$ )-histidine methylester [117].

#### 4.2.4 Protein–drug interactions

Affinity-based methods allow to screen for new drug targets, to evaluate drug candidates or to investigate drug effects *in vivo* [118]. The interaction with naproxen and serum proteins was characterized in respect to the binding constant, temperature, and thermodynamic parameters using monolithic CIM discs with immobilized BSA [119]. The interaction between the antiepileptic drug carbamazepine and the anticoagulant *R*-warfarin with HSA that had

been immobilized on silica monoliths and silica particles was the topic of another report [42]. HSA immobilized onto a silica monolith allowed the determination of dissociation constants of drug–HSA complexes using peak decay analysis [120]. Accurate results were obtained within 1 min due to the high flow rates applicable with monolithic columns.

#### 4.2.5 Chiral separations

Separation of chiral compounds is highly challenging due to the similar properties of enantiomers, but nevertheless, chiral drug candidates have to be separated from each other in order to get approval for a drug [121, 122]. Enantiomers are easily recognized by chiral biomolecules, such as carbohydrates or proteins [123, 124].

D-Amino acids were successfully separated from L-amino acids by immobilized HSA on a monolithic support [125]. The established method was subsequently used to determine enzymatic parameters of D-amino acid oxidase, which was incubated with a racemic mixture of tryptophan.

The separation of D-/L-tryptophan and R/S-warfarin was used for comparing HSA affinity media that had been prepared from monolithic silica, monolithic poly(GMA-co-EDMA), and silica particles [126]. Best results were obtained with the HSA silica monolith, whereas the methacrylate monolith and the silica particles with immobilized HSA yielded weaker results. Baseline separation of a racemic mixture of ibuprofen was achieved within 13 min. Similar results were obtained with  $\alpha_1$ -acid glycoprotein immobilized on silica particles, monolithic silica, and poly(GMA-co-EDMA) monolith [127]. R/S-Warfarin and R/S-propranolol were used as test compounds, for which the enantiomers could only be separated with the silica monolith.

#### 4.2.6 Metal chelators

Phosphorylation of proteins plays a major role in cellular signal trafficking and knowledge about phosphorylation events is of outstanding importance for a deeper understanding of all cellular processes and for the discovery of novel drug targets [128–130]. IMAC is the method of choice for an enrichment of phosphopeptides and phosphoproteins as it exploits the affinity of metal ions to phosphate groups. IMAC is also commonly used for the purification of recombinant His-tagged proteins [131, 132]. For IMAC, monoliths need to be modified with a chelator that complexes the metal ion for affinity capture of the desired analyte. An overview of IMAC applications with MSPs is summarized in Table 2.

For the enrichment of phosphopeptides monoliths with immobilized  $Zr^{4+}$  [133],  $Ti^{4+}$  [134] and  $Fe^{3+}$  ions [135] were used, resulting in improved enrichment efficiencies compared with particle-based enrichment methods [134]. His-tagged lentiviral vectors were captured using IDA-modified monolithic cryogels and monolithic CIM discs with  $Ni^{2+}$  and  $Co^{2+}$  ions as ligands [136]. Performance of

the CIM discs was superior compared with the cryogels in respect to binding capacity, concentration efficiency, and elution behavior. Capturing of His-tagged *Escherichia coli* cells [50] and virus-like particles [51] by  $Cu^{2+}$  and  $Ni^{2+}$  cryogel monoliths was achieved without affecting the viability of the bacteria. As described in Section 4.1, bound bacteria and virus-like particles were eluted by mechanical compression, which was also successful in eluting lysozyme [137].

Interestingly, IMAC using monolithic cryogels was successfully employed for the enrichment and purification of BSA [138], lysozyme [139], DNA [140], and IgG [141]. High recovery rates and excellent enrichment efficiencies were reported even from complex sample matrices. Poly-(GMA-co-EDMA) monolithic IMAC columns were used for *online* fractionation of proteins from serum samples, which had been depleted of high-abundant proteins by immunoaffinity chromatography [89], and after pretreatment using the peptide beads library technology (ProteoMiner™) [142].

Additionally, metal chelating monoliths have become increasingly interesting for the removal of heavy metal ions from aqueous solutions. In addition to the common chelator IDA [67, 143], N-methacryloyl-(L)-cysteine methylester (MAC) [144] and the dye Reactive Green HE-4BD [145] were used for preparing MSPs for capturing metal ions. Heavy metal ions were either removed in continuous mode by passing the solution through the monolithic column [144] or in batch mode by stirring monolithic cryogel discs, carriers filled with monolithic cryogel or monolithic agarose in solution [67, 143, 145].

Metal oxide nanoparticles embedded in monolithic supports have also been used repeatedly, e.g., BSA was enriched on  $Fe_3O_4$  nanoparticles embedded in a monolithic cryogel [146]. Pipet tips filled with  $TiO_2$  and  $ZrO_2$  nanoparticles in monoliths [43, 147] as well as a monolithic column with embedded hydroxyapatite nanoparticles [57] were used for the enrichment of phosphopeptides (Fig. 7). Monolithic columns with surface-bound gold nanoparticles were successfully applied for the enrichment of cysteine (SH group)-containing peptides [56]. Recently, the preparation of a monolithic cryogel with embedded  $Cu^{2+}$ -sporopollenin particles was reported [148]. The resulting monolithic IMAC-column was successfully employed for the adsorption of HSA from human plasma.

#### 4.2.7 Miscellaneous ligands

Last but not least, complexes between enzymes and their inhibitors are one of the major systems targeted by AC. Monolithic supports with immobilized soybean trypsin inhibitor were used to capture virus-like particles that had been modified with trypsin [149, 150]. Another report described the purification of penicillin acylase from crude extracts of *Penicillium* cultures by immobilized antipyrine [151].

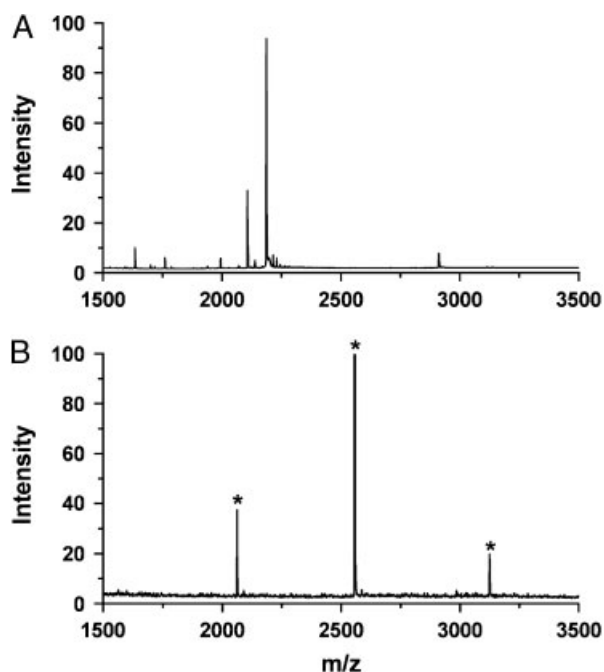


**Figure 7.** Tryptic digestion mixture of  $\beta$ -casein analyzed by MALDI-MS (A) before and (B) after phosphopeptide enrichment (reproduced with permission from [57], copyright 2010, Am. Chem. Soc.). Phosphopeptides are marked with an asterisk.

The influence of the spacer length for immobilizing benzenesulfonamide was investigated for the enrichment of carbonic anhydrase II from rat brain lysate [152], resulting in better results for the monolithic affinity medium compared with commercial particles. The optimized immobilization conditions were subsequently applied to the enrichment of the tacrolimus-binding proteins calcineurin A and calcineurin B.

Macroporous monoliths with immobilized polymyxin B were successfully used to capture gram-negative bacteria (Fig. 8) [153]. Although polymyxin B is cytotoxic, *E. coli* cells were enriched without impairing their viability.

Cryogels with immobilized human lactoferrin allowed identifying novel peptide ligands by peptide-displaying phages [154]. Without elution, the captured phages were used afterward for the infection of *E. coli* cells. Immobilized peptide-displaying phages with a high affinity for human lactoferrin and von-Willebrand factor were used to enrich these two proteins from complex sample matrices [53]. Compared with a monolithic cryogel with an immobilized antibody specific for von-Willebrand factor, enrichment efficiency with the immobilized peptide-displaying phage was superior. Immobilization of a peptide epitope onto monolithic CIM discs enabled the quantification of IgM from mammalian cell culture medium [155].

A monolithic cryogel with immobilized Cibracon Blue F3GA was used for dye-AC of HSA [156], resulting in an efficient depletion of HSA from human serum.

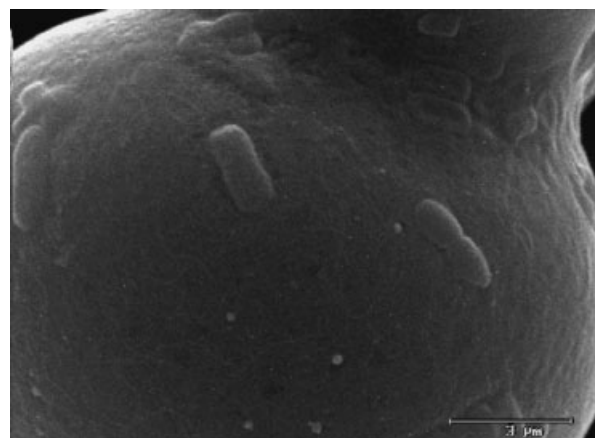


**Figure 8.** Scanning electron microscopy image of *E. coli* cells captured by polymyxin B immobilized on an MSP (reproduced with permission from [153], copyright 2009, Elsevier).

**Table 3.** Applications of molecularly imprinted MSPs

Template	Monolithic support	Ref.
Bupivacaine	TRIM <sup>a)</sup>	[158]
Ciprofloxacin	MAA/AAm/EDMA	[159]
Norfloxacin	HEMA/EDMA	[160]
Metribuzin	MAA/EDMA	[161]
Protocatechuic acid	AAm/TRIM	[162]
Tosyl-L-Phe	MAA/EDMA	[163]
(+)-Nilvadipine <sup>b)</sup>	4-Vinylpyridine/EDMA	[164]
S(-)-Amlodipine	MAA/EDMA	[165]
17 $\beta$ -Estradiol	4-Vinylpyridine/EDMA <sup>c)</sup>	[55]
Bilirubin	MAT/EDMA <sup>c)</sup>	[54]
Fe <sup>3+</sup>	MAC/HEMA/EDMA	[166, 167]
Fe <sup>3+</sup>	MAC-cryogel	[168]
Ni <sup>2+</sup>	MAH/HEMA	[169]
Cytochrome <i>c</i>	Methacrylamide/MAA/PDA	[170]
BSA, lysozyme	Silica <sup>d)</sup>	[63]

MAT, *N*-methacryloyl-(L)-tyrosine methylester; PDA, piperazine diacrylamide.

a) Grafted with MAA/EDMA.

b) *N*-Cbz-L-Trp as cotemplate.

c) Crushed monolith particles embedded in cryogel.

d) Grafted with AAm/Bis.

### 4.3 Molecularly imprinted monoliths

For molecular recognition, antibodies are the gold standard due to the high selectivity and stability of the antibody–antigen complexes. As the production of antibodies is a tedious process [35], molecular imprinting has been developed as an alternative strategy to recognize antigens because the stationary phase itself possesses an affinity for the target molecule [12]. Molecular imprinting relies on mixing the target molecule (template) with a polymerization mixture of monomers that are able to form a complex with the template. During the polymerization process, a cavity is formed containing the template molecule [17, 157]. After the

template has been removed from the polymer, the molecularly imprinted phase (MIP) is used for enrichment of the template molecule and structural analogues. An

overview of applications using molecularly imprinted monoliths is summarized in Table 3.

Performance of MIPs with the local anesthetic bupivacaine that has either been prepared from a crushed monolith, from grafted silica beads, from microparticles, or from a grafted monolith was investigated recently [158]. Although the imprinted microparticles prepared by precipitation polymerization yielded low imprinting factors, the other MIPs showed a significantly increased retention of the template molecule. Optimum results were obtained for the imprinted crushed monolith and the imprinted monolith column.

Preparation of MIPs was reported using ciprofloxacin [159], norfloxacin [160], metribuzin [161], and protocatechuic acid (3,4-dihydroxybenzoic acid) [162] as templates. The presence of both high- and low-affinity binding sites for the template molecule ciprofloxacin was determined by Scatchard analysis (Fig. 9) [159]. Structurally related compounds eluted earlier than the template molecules proving the high specificity of the molecularly imprinted monoliths. This high specificity is also impressively demonstrated by the separation of enantiomers using

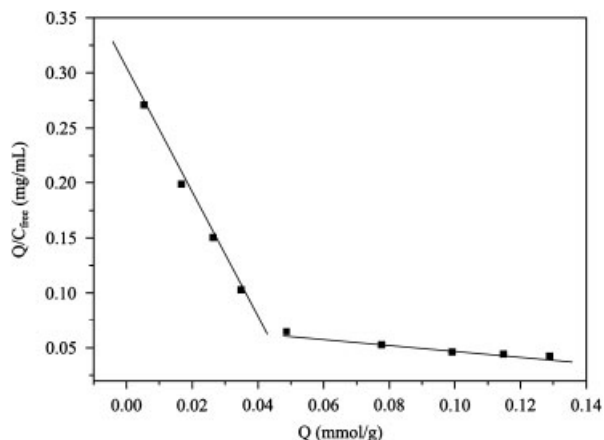


**Figure 9.** Scatchard analysis of ciprofloxacin-imprinted MSP (reproduced with permission from [160], copyright 2009, Springer).

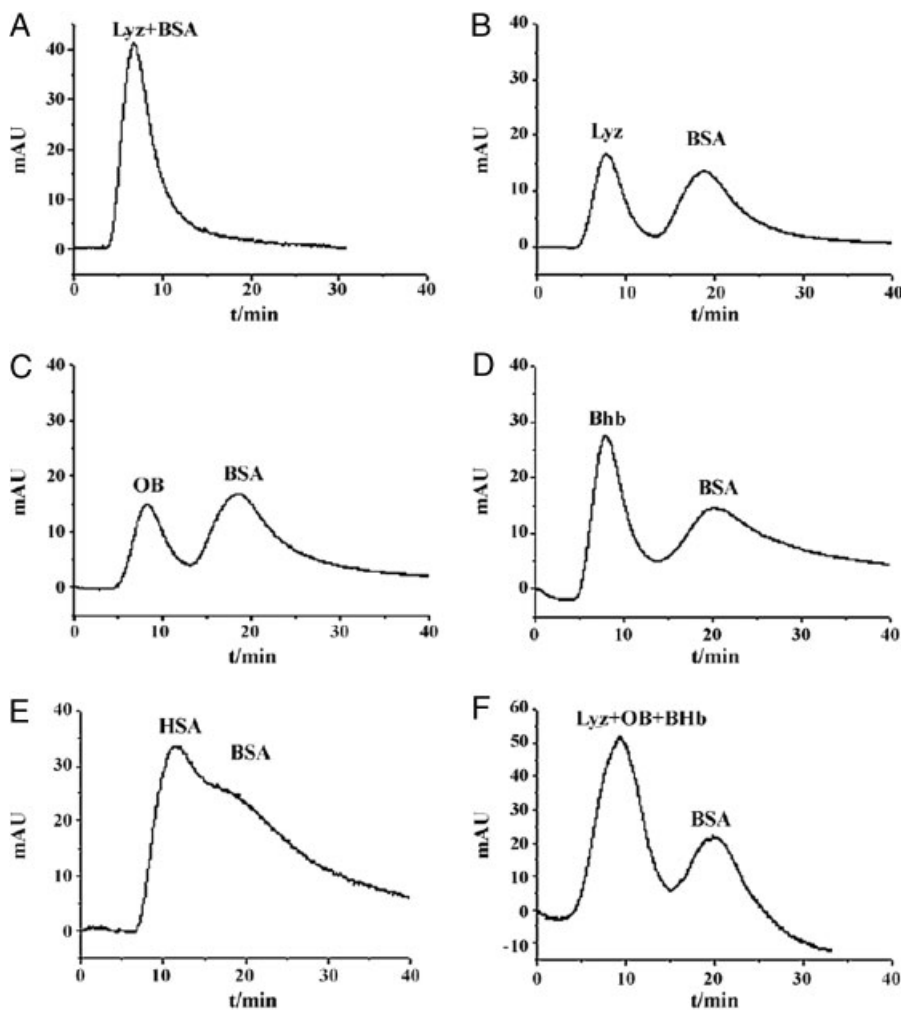


**Figure 10.** Separation of proteins and BSA on (A) a nonimprinted silica monolith and (B–F) a BSA-MIP monolith; Lyz, lysozyme; BHb, bovine hemoglobin; OB, ovalbumin (reproduced with permission from [63], copyright 2009, Elsevier).

monolithic MIPs. Using tosyl-L-Phe [163], (+)-nilvadipine [164], and *S*(-)-amlodipine [165] as templates, these compounds were separated from their corresponding enantiomers. In addition to modifying the polymerization conditions by changing the porogens [163], adding a chiral compound as cotemplate proved to be beneficial for both the preparation of the monolithic MIP and the separation efficiency [164].

The preparation and subsequent crushing of monolithic MIPs and embedding the resulting particles into cryogels is a strategy that was pursued by several groups. Such hybrid materials were prepared using 17 $\beta$ -estradiol [55] and bilirubin [54] as templates resulting in the enrichment of both compounds from complex sample matrices.

Also, ion-imprinted MSPs using monomers with chelating abilities have been prepared, such as a Fe<sup>3+</sup>-imprinted methacrylate monolith [166, 167], a Fe<sup>3+</sup>-imprinted monolithic cryogel [168], and a Ni<sup>2+</sup>-imprinted methacrylate monolith [169]. Due to its higher surface area, the binding capacity of the ion-imprinted methacrylate monolith was higher compared with the ion-imprinted monolithic cryogel. Competitive adsorption of a solution containing several metal ions showed a high selectivity for the Ni<sup>2+</sup> template ion [169].

It should be noted that template molecules for MIPs are usually small; yet, molecular imprinting of proteins on MSPs has been successfully demonstrated for cytochrome *c* [170], lysozyme, and BSA [63]. For the latter two proteins, a monolithic silica skeleton was grafted in the presence of lysozyme or BSA in order to obtain the imprinted stationary phase. High imprinting factors were determined for both templates resulting in the separation of these proteins from a mixture – but only when using monolithic materials (Fig. 10).

## 5 Concluding remarks

The multitude of applications discussed herein demonstrates that the field of AC using monolithic supports is still growing. The advantages associated with monolithic materials are numerous: (i) Monoliths can be prepared in a variety of sizes ranging from several centimeters down to micrometers making them suitable for both preparative and analytical needs. (ii) Monoliths are easily prepared in a column format that allows their straightforward implementation into LC systems. Coupling of monolithic AC with mass spectrometry further increases information about the analyte. (iii) The availability of different monomers for monolith preparation enables the creation of stationary phases that are compatible with complex matrices, such as blood or serum, with only minimal nonspecific adsorption. “Smart” monomers, as they are used for the preparation of cryogels, allow the application of softer elution methods by temperature-induced or mechanical compression. (iv) The high mass transfer and the convective flow of monoliths enable an intense interaction of analytes in the mobile phase with immobilized ligands, thus increasing the

separation efficiency and/or shortening analysis times. A comparison of monolithic with particle-based stationary phases for AC separations shows a superior performance of MSPs with lower nonspecific binding and therefore higher analyte enrichment.

The most commonly used monolithic supports are prepared from (meth)acrylates, and as such, GMA is currently the most common functional monomer. Monolithic discs prepared from EDMA and GMA are also commercially available and are widely used for AC applications. For cryogels, AGE is the mainly used functional monomer. In general, AC with inorganic silica monoliths guarantees a higher enrichment efficiency than with organic monoliths because of the higher surface area of silica monoliths.

The ease of preparation of MSPs and the multitude of functionalization techniques, which have matured during the past years, make monoliths interesting for an ever increasing number of analytical questions. The emergence of applications of monolithic affinity media for the enrichment and purification of large analytes, including cells and bacteria, as well as an extension to alternative affinity ligands, such as polynucleotides, indicate that the field is immensely vital and makes us look forward to a multitude of exciting applications in the near future.

*J. S. is indebted to Aleš Svatoš and Alexandr Muck for the introduction into monolithic supports.*

*The authors have declared no conflict of interest.*

## 6 References

- [1] Urban, J., Jandera, P., *J. Sep. Sci.* 2008, 31, 2521–2540.
- [2] Peters, E. C., Svec, F., Frechet, J. M. J., *Adv. Mater.* 1999, 11, 1169–1181.
- [3] Kobayashi, H., Ikegami, T., Kimura, H., Hara, T., Tokuda, D., Tanaka, N., *Anal. Sci.* 2006, 22, 491–501.
- [4] Nordborg, A., Hilder, E. F., *Anal. Bioanal. Chem.* 2009, 394, 71–84.
- [5] Li, Y., Tolley, H. D., Lee, M. L., *J. Chromatogr. A* 2010, 1217, 8181–8185.
- [6] Mallik, R., Hage, D. S., *J. Sep. Sci.* 2006, 29, 1686–1704.
- [7] Josic, D., Buchacher, A., *J. Biochem. Biophys. Methods* 2001, 49, 153–174.
- [8] Krenkova, J., Svec, F., *J. Sep. Sci.* 2009, 32, 706–718.
- [9] Sproß, J., Sinz, A., *Anal. Chem.* 2010, 82, 1434–1443.
- [10] Ma, J. F., Zhang, L. H., Liang, Z., Zhang, W. B., Zhang, Y. K., *Anal. Chim. Acta* 2009, 632, 1–8.
- [11] Tetala, K. K. R., van Beek, T. A., *J. Sep. Sci.* 2010, 33, 422–438.
- [12] Haginaka, J., *J. Sep. Sci.* 2009, 32, 1548–1565.

- [13] Haginaka, J., *J. Chromatogr. B* 2008, 875, 12–19.
- [14] Porath, J., Carlsson, J., Olsson, I., Belfrage, G., *Nature* 1975, 258, 598–599.
- [15] Ewings, K. N., Doelle, H. W., *Aust. J. Biol. Sci.* 1981, 34, 125–132.
- [16] Chen, M., Lu, Y., Ma, Q., Guo, L., Feng, Y.-Q., *Analyst* 2009, 134, 2158–2164.
- [17] Matsui, J., Kato, T., Takeuchi, T., Suzuki, M., Yokoyama, K., Tamiya, E., Karube, I., *Anal. Chem.* 1993, 65, 2223–2224.
- [18] Ren, L. B., Liu, Z., Dong, M. M., Ye, M. L., Zou, H. F., *J. Chromatogr. A* 2009, 1216, 4768–4774.
- [19] Trinkle-Mulcahy, L., Boulon, S., Lam, Y. W., Urcia, R., Boisvert, F. M., Vandermoere, F., Morrice, N. A., Swift, S., Rothbauer, U., Leonhardt, H., Lamond, A., *J. Cell Biol.* 2008, 183, 223–239.
- [20] Green, N. M., Toms, E. J., *Biochem. J.* 1973, 133, 687–698.
- [21] Ernst-Cabrera, K., Wilchek, M., *Anal. Biochem.* 1986, 159, 267–272.
- [22] Eeltink, S., Svec, F., *Electrophoresis* 2007, 28, 137–147.
- [23] Gritti, F., Piatkowski, W., Guiochon, G., *J. Chromatogr. A* 2003, 983, 51–71.
- [24] Stachowiak, T. B., Svec, F., Frechet, J. M. J., *J. Chromatogr. A* 2004, 1044, 97–111.
- [25] Ro, K. W., Nayalk, R., Knapp, D. R., *Electrophoresis* 2006, 27, 3547–3558.
- [26] Okanda, F. M., El Rassi, Z., *Electrophoresis* 2007, 28, 89–98.
- [27] Zhang, Z. B., Wu, R. A., Wu, M. H., Zou, H. F., *Electrophoresis* 2010, 31, 1457–1466.
- [28] Roberts, M. W. H., Ongkudon, C. M., Forde, G. M., Danquah, M. K., *J. Sep. Sci.* 2009, 32, 2485–2494.
- [29] Wu, R., Hu, L. G., Wang, F. J., Ye, M. L., Zou, H., *J. Chromatogr. A* 2008, 1184, 369–392.
- [30] Guiochon, G., *J. Chromatogr. A* 2007, 1168, 101–168.
- [31] Josic, D., Buchacher, A., Jungbauer, A., *J. Chromatogr. B* 2001, 752, 191–205.
- [32] Svec, F., Frechet, J. M. J., *Anal. Chem.* 1992, 64, 820–822.
- [33] Yang, W. C., Yu, M., Sun, X. H., Woolley, A. T., *Lab Chip* 2010, 10, 2527–2533.
- [34] Tennikova, T. B., Freitag, R., *HRC J. High Resolut. Chromatogr.* 2000, 23, 27–38.
- [35] Chen, H. X., Huang, T., Zhang, X. X., *Talanta* 2009, 78, 259–264.
- [36] Rohr, T., Hilder, E. F., Donovan, J. J., Svec, F., Frechet, J. M. J., *Macromolecules* 2003, 36, 1677–1684.
- [37] Vlach, E., Maksimova, E., Krasikov, V., Tennikova, T., *Poly. Sci. Ser. B* 2009, 51, 327–334.
- [38] Slabospitskaya, M. Y., Vlach, E. G., Saprykina, N. N., Tennikova, T. B., *J. Appl. Polym. Sci.* 2009, 111, 692–700.
- [39] Ren, L. B., Liu, Z., Liu, Y. C., Dou, P., Chen, H. Y., *Angew. Chem. Int. Ed.* 2009, 48, 6704–6707.
- [40] Tetala, K. K. R., Chen, B., Visser, G. M., van Beek, T. A., *J. Sep. Sci.* 2007, 30, 2828–2835.
- [41] Courtois, J., Szumski, M., Bystrom, E., Iwasiewicz, A., Shchukarev, A., Irgum, K., *J. Sep. Sci.* 2006, 29, 14–24.
- [42] Yoo, M. J., Hage, D. S., *J. Sep. Sci.* 2009, 32, 2776–2785.
- [43] Hsieh, H. C., Sheu, C., Shi, F. K., Li, D. T., *J. Chromatogr. A* 2007, 1165, 128–135.
- [44] Lozinsky, V. I., Plieva, F. M., Galaev, I. Y., Mattiasson, B., *Bioseparation* 2001, 10, 163–188.
- [45] Dainiak, M. B., Kumar, A., Galaev, I. Y., Mattiasson, B., *Proc. Natl. Acad. Sci. USA* 2006, 103, 849–854.
- [46] Kumar, A., Bhardwaj, A., *Biomed. Mater.* 2008, 3, 1–11.
- [47] Chen, Z. Y., Xu, L., Liang, Y., Wang, J. B., Zhao, M. P., Li, Y. Z., *J. Chromatogr. A* 2008, 1182, 128–131.
- [48] Laemmli, U. K., *Nature* 1970, 227, 680–685.
- [49] Jungbauer, A., Hahn, R., *J. Chromatogr. A* 2008, 1184, 62–79.
- [50] Dainiak, M. B., Galaev, I. Y., Mattiasson, B., *Enzyme Microb. Technol.* 2007, 40, 688–695.
- [51] Galaev, I. Y., Dainiak, M. B., Plieva, F., Mattiasson, B., *Langmuir* 2007, 23, 35–40.
- [52] Minakuchi, H., Nakanishi, K., Soga, N., Ishizuka, N., Tanaka, N., *J. Chromatogr. A* 1997, 762, 135–146.
- [53] Noppe, W., Plieva, F. M., Vanhoorelbeke, K., Deckmyn, H., Tuncel, M., Tuncel, A., Galaev, I. Y., Mattiasson, B., *J. Biotechnol.* 2007, 131, 293–299.
- [54] Baydemir, G., Bereli, N., Andac, M., Say, R., Galaev, I. Y., Denizli, A., *React. Funct. Polym.* 2009, 69, 36–42.
- [55] Le Noir, M., Plieva, F., Hey, T., Guieysse, B., Mattiasson, B., *J. Chromatogr. A* 2007, 1154, 158–164.
- [56] Xu, Y., Cao, Q., Svec, F., Frechet, J. M. J., *Anal. Chem.* 2010, 82, 3352–3358.
- [57] Krenkova, J., Lacher, N. A., Svec, F., *Anal. Chem.* 2010, 82, 8335–8341.
- [58] Minakuchi, H., Nakanishi, K., Soga, N., Ishizuka, N., Tanaka, N., *Anal. Chem.* 1996, 68, 3498–3501.
- [59] Ishizuka, N., Minakuchi, H., Nakanishi, K., Soga, N., Hosoya, K., Tanaka, N., *HRC J. High Resolut. Chromatogr.* 1998, 21, 477–479.
- [60] Massolini, G., Calleri, E., Lavecchia, A., Lolodice, F., Lubda, D., Temporini, C., Fracchiolla, G., Tortorella, P., Novellino, E., Caccialanza, G., *Anal. Chem.* 2003, 75, 535–542.
- [61] Calleri, E., Temporini, C., Perani, E., Stella, C., Rudaz, S., Lubda, D., Mellerio, G., Veuthey, J. L., Caccialanza, G., Massolini, G., *J. Chromatogr. A* 2004, 1045, 99–109.
- [62] Hage, D. S., *J. Chromatogr. B* 2002, 768, 3–30.
- [63] Lin, Z. A., Yang, F., He, X. W., Zhao, X. M., Zhang, Y. K., *J. Chromatogr. A* 2009, 1216, 8612–8622.
- [64] Tanaka, N., Kobayashi, H., Ishizuka, N., Minakuchi, H., Nakanishi, K., Hosoya, K., Ikegami, T., *J. Chromatogr. A* 2002, 965, 35–49.
- [65] Jin, W., Brennan, J. D., *Anal. Chim. Acta* 2002, 461, 1–36.

- [66] Sakai-Kato, K., Kato, M., Toyo'oka, T., *Anal. Chem.* 2002, **74**, 2943–2949.
- [67] Plieva, F. M., Mattiasson, B., *Ind. Eng. Chem. Res.* 2008, **47**, 4131–4141.
- [68] Rober, M., Walter, J., Vlach, E., Stahl, F., Kasper, C., Tennikova, T., *Anal. Chim. Acta* 2009, **644**, 95–103.
- [69] Brne, P., Lim, Y. P., Podgornik, A., Barut, M., Pihlar, B., Strancar, A., *J. Chromatogr. A* 2009, **1216**, 2658–2663.
- [70] Delmotte, N., Kobold, U., Meier, T., Gallusser, A., Strancar, A., Huber, C. G., *Anal. Bioanal. Chem.* 2007, **389**, 1065–1074.
- [71] Sinitsyna, E. S., Sergeeva, Y. N., Vlach, E. G., Saprikin, N. N., Tennikova, T. B., *React. Funct. Polym.* 2009, **69**, 385–392.
- [72] Yang, W. C., Sun, X. H., Pan, T., Woolley, A. T., *Electrophoresis* 2008, **29**, 3429–3435.
- [73] Sun, X. H., Yang, W. C., Pan, T., Woolley, A. T., *Anal. Chem.* 2008, **80**, 5126–5130.
- [74] Mönster, A., Hiller, O., Grüger, D., Blasczyk, R., Kasper, C., *J. Chromatogr. A* 2011, **1218**, 706–710.
- [75] Faure, K., Delaunay, N., Alloncle, G., Cotte, S., Rocca, J. L., *J. Chromatogr. A* 2007, **1149**, 145–150.
- [76] Calleri, E., Marrubini, G., Brusotti, G., Massolini, G., Caccialanza, G., *J. Pharm. Biomed. Anal.* 2007, **44**, 396–403.
- [77] Li, L., Wang, J. B., Zhou, S. A., Zhao, M. P., *Anal. Chim. Acta* 2008, **620**, 1–7.
- [78] Liang, Y., Zhou, S., Hu, L., Li, L., Zhao, M., Liu, H., *J. Chromatogr. B* 2010, **878**, 278–282.
- [79] Lönnberg, M., Dehnes, Y., Drevin, M., Garle, M., Lamon, S., Leuenberger, N., Quach, T., Carlsson, J., *J. Chromatogr. A* 2010, **1217**, 7031–7037.
- [80] Lindmark, R., Thorentolling, K., Sjöquist, J., *J. Immun. Meth.* 1983, **62**, 1–13.
- [81] Akerström, B., Björck, L., *J. Biol. Chem.* 1986, **261**, 240–247.
- [82] Petric, T. C., Brne, P., Gabor, B., Govednik, L., Barut, M., Strancar, A., Kralj, L. Z., *J. Pharm. Biomed. Anal.* 2007, **43**, 243–249.
- [83] Ralla, K., Anton, F., Scheper, T., Kasper, C., *J. Chromatogr. A* 2009, **1216**, 2671–2675.
- [84] Armenta, J. A., Gu, B. H., Thulin, C. D., Lee, M. L., *J. Chromatogr. A* 2007, **1148**, 115–122.
- [85] Tscheliessnig, A., Jungbauer, A., *J. Chromatogr. A* 2009, **1216**, 2676–2682.
- [86] Kumar, A., Srivastava, A., *Nat. Protoc.* 2010, **5**, 1737–1747.
- [87] Jmeian, Y., El Rassi, Z., *J. Proteome Res.* 2007, **6**, 947–954.
- [88] Jmeian, Y., El Rassi, Z., *Electrophoresis* 2008, **29**, 2801–2811.
- [89] Jmeian, Y., El Rassi, Z., *J. Proteome Res.* 2009, **8**, 4592–4603.
- [90] Funakoshi, Y., Suzuki, T., *Biochim. Biophys. Acta* 2009, **1790**, 81–94.
- [91] Helenius, A., Aebi, M., *Annu. Rev. Biochem.* 2004, **73**, 1019–1049.
- [92] Zhao, Y. Y., Takahashi, M., Gu, J. G., Miyoshi, E., Matsumoto, A., Kitazume, S., Taniguchi, N., *Cancer Sci.* 2008, **99**, 1304–1310.
- [93] Haltiwanger, R. S., Lowe, J. B., *Annu. Rev. Biochem.* 2004, **73**, 491–537.
- [94] Dell, A., Morris, H. R., *Science* 2001, **291**, 2351–2356.
- [95] Lisowska, E., Szeliga, W., Duk, M., *FEBS Lett.* 1976, **72**, 327–330.
- [96] Tetala, K. K. R., Chen, B., Visser, G. M., Maruska, A., Kornysova, O., van Beek, T. A., Sudholter, E. J. R., *J. Biochem. Biophys. Methods* 2007, **70**, 63–69.
- [97] Arrua, R. D., Moya, C., Bernardi, E., Zazur, J., Strumia, M., Igarzabal, C. I. A., *Eur. Polym. J.* 2010, **46**, 663–672.
- [98] Kalashnikova, I., Ivanova, N., Tennikova, T., *Anal. Chem.* 2008, **80**, 2188–2198.
- [99] Surolia, A., Bishayee, S., Ahmad, A., Balasubramanian, K. A., Thambi-Dorai, D., Podder, S. K., Bachhawat, B. K., *Adv. Exp. Med. Biol.* 1975, **55**, 95–115.
- [100] Dulaney, J. T., *Mol. Cell. Biochem.* 1978, **21**, 43–63.
- [101] Nilsson, C. L., *Anal. Chem.* 2003, **75**, 348A–353A.
- [102] Zhong, H. W., El Rassi, Z., *J. Sep. Sci.* 2009, **32**, 1642–1653.
- [103] Feng, S., Yang, N., Pennathur, S., Goodison, S., Lubman, D. M., *Anal. Chem.* 2009, **81**, 3776–3783.
- [104] Bouriotis, V., Galpin, I. J., Dean, P. D. G., *J. Chromatogr.* 1981, **210**, 267–278.
- [105] Ren, L. B., Liu, Y. C., Dong, M. M., Liu, Z., *J. Chromatogr. A* 2009, **1216**, 8421–8425.
- [106] Liu, Y. C., Ren, L. B., Liu, Z., *Chem. Commun.* 2011, **47**, 5067–5069.
- [107] Cakal, C., Ferrance, J. P., Landers, J. P., Caglar, P., *Anal. Chim. Acta* 2011, **690**, 94–100.
- [108] Green, N. M., *Biochem. J.* 1963, **89**, 609–620.
- [109] Zhao, Q., Li, X. F., Le, X. C., *Anal. Chem.* 2008, **80**, 3915–3920.
- [110] Zhao, Q., Li, X. F., Shao, Y. H., Le, X. C., *Anal. Chem.* 2008, **80**, 7586–7593.
- [111] Sproß, J., Sinz, A., submitted.
- [112] O'Rorke, S., Keeney, M., Pandit, A., *Prog. Polym. Sci.* 2010, **35**, 441–458.
- [113] Cavazzana-Calvo, M., Fischer, A., *J. Clin. Invest.* 2007, **117**, 1456–1465.
- [114] Platonova, G. A., Nazarova, O. V., Tennikova, T. B., *J. Sep. Sci.* 2009, **32**, 2674–2681.
- [115] Han, Y., Forde, G. M., *J. Chromatogr. B* 2008, **874**, 21–26.
- [116] Han, Y., You, G. L., Pattenden, L. K., Forde, G. M., *Process Biochem.* 2010, **45**, 203–209.
- [117] Percin, I., Saglar, E., Yavuz, H., Aksoz, E., Denizli, A., *Int. J. Biol. Macromol.* 2011, **48**, 577–582.
- [118] Bantscheff, M., Scholten, A., Heck, A. J. R., *Drug Discov. Today* 2009, **14**, 1021–1029.
- [119] Zacharis, C. K., Kalaitzantonakis, E. A., Podgornik, A., Theodoridis, G., *J. Chromatogr. A* 2007, **1144**, 126–134.
- [120] Yoo, M. J., Hage, D. S., *J. Chromatogr. A* 2011, **1218**, 2072–2078.

- [121] Sui, J. J., Zhang, J. H., Tan, T. L., Ching, C. B., Chen, W. N., *Mol. Cell. Proteomics* 2008, 7, 1007–1018.
- [122] Lu, H., *Expert Opin. Drug Metab. Toxicol.* 2007, 3, 149–158.
- [123] Debowski, J., Sybilska, D., Jurczak, J., *J. Chromatogr.* 1982, 237, 303–306.
- [124] Gubitz, G., Schmid, M. G., *Biopharm. Drug Dispos.* 2001, 22, 291–336.
- [125] Yao, C. H., Qi, L., Qiao, J. A., Zhang, H. Z., Wang, F. Y., Chen, Y., Yang, G. L., *Talanta* 2010, 82, 1332–1337.
- [126] Mallik, R., Hage, D. S., *J. Pharm. Biomed. Anal.* 2008, 46, 820–830.
- [127] Mallik, R., Xuan, H., Hage, D. S., *J. Chromatogr. A* 2007, 1149, 294–304.
- [128] Yu, L. R., Issaq, H. J., Veenstra, T. D., *Proteomics Clin. Appl.* 2007, 1, 1042–1057.
- [129] Rozengurt, E., *Physiology* 2011, 26, 23–33.
- [130] Kondoh, K., Torii, S., Nishida, E., *Chromosoma* 2005, 114, 86–91.
- [131] Porath, J., Axen, R., Ernback, S., *Nature* 1967, 215, 1491–1492.
- [132] Thingholm, T. E., Jensen, O. N., Larsen, M. R., *Proteomics* 2009, 9, 1451–1468.
- [133] Dong, J., Zhou, H., Wu, R., Ye, M., Zou, H., *J. Sep. Sci.* 2007, 30, 2917–2923.
- [134] Hou, C. Y., Ma, J. F., Tao, D. Y., Shan, Y. C., Liang, Z., Zhang, L. H., Zhang, Y. K., *J. Proteome Res.* 2010, 9, 4093–4101.
- [135] Feng, S., Pan, C. S., Jiang, X. G., Xu, S. Y., Zhou, H. J., Ye, M. L., Zou, H. F., *Proteomics* 2007, 7, 351–360.
- [136] Cheeks, M. C., Kamal, N., Sorrell, A., Darling, D., Farzaneh, F., Slater, N. K. H., *J. Chromatogr. A* 2009, 1216, 2705–2711.
- [137] Plieva, F. M., De Seta, E., Galaev, I. Y., Mattiasson, B., *Sep. Purif. Technol.* 2009, 65, 110–116.
- [138] Wang, L. H., Shen, S. C., He, X. J., Yun, B. X., Yao, K. J., Yao, S. J., *Biochem. Eng. J.* 2008, 42, 237–242.
- [139] Derazshamshir, A., Ergun, B., Pesint, G., Odabasi, M., *J. Appl. Polym. Sci.* 2008, 109, 2905–2913.
- [140] Odabasi, M., Baydemir, G., Karatas, M., Derazshamshir, A., *J. Appl. Polym. Sci.* 2010, 116, 1306–1312.
- [141] Prasanna, R. R., Vijayalakshmi, M. A., *J. Chromatogr. A* 2010, 1217, 3660–3667.
- [142] Selvaraju, S., El Rassi, Z., *Electrophoresis* 2011, 32, 674–685.
- [143] Önnby, L., Giorgi, C., Plieva, F. M., Mattiasson, B., *Biotechnol. Progr.* 2010, 26, 1295–1302.
- [144] Uzun, L., Turkmen, D., Yilmaz, E., Bektas, S., Denizli, A., *Colloids Surf. A* 2008, 330, 161–167.
- [145] Arpa, C., Bereli, N., Ozdil, E., Bektas, S., Denizli, A., *J. Appl. Polym. Sci.* 2010, 118, 2208–2215.
- [146] Yao, K. J., Shen, S. C., Yun, J. X., Wang, L. H., Chen, F., Yu, X. M., *Biochem. Eng. J.* 2007, 36, 139–146.
- [147] Rainer, M., Sonderegger, H., Bakry, R., Huck, C. W., Morandell, S., Huber, L. A., Gjerde, D. T., Bonn, G. K., *Proteomics* 2008, 8, 4593–4602.
- [148] Erzenin, M., Ünlü, N., Odabasi, M., *J. Chromatogr. A* 2011, 1218, 484–490.
- [149] Kalashnikova, I. V., Ivanova, N. D., Evseeva, T. G., Menshikova, A. Y., Vlach, E. G., Tennikova, T. B., *J. Chromatogr. A* 2007, 1144, 40–47.
- [150] Kalashnikova, I. V., Ivanova, N. D., Tennikova, T. B., *Russ. J. Appl. Chem.* 2008, 81, 867–873.
- [151] Kecili, R., Say, R., Ersoz, A., Yuvuz, H., Denizli, A., *Sep. Purif. Technol.* 2007, 55, 1–7.
- [152] Iwaoka, E., Mori, T., Shimizu, T., Hosoya, K., Tanaka, A., *Bioorg. Med. Chem. Lett.* 2009, 19, 1469–1472.
- [153] Peskoller, C., Niessner, R., Seidel, M., *J. Chromatogr. A* 2009, 1216, 3794–3801.
- [154] Noppe, W., Plieva, F., Galaev, I. Y., Pottel, H., Deckmyn, H., Mattiasson, B., *Biomed. Chromatogr. Biotechnol.* 2009, 9, 9.
- [155] Neff, S., Jungbauer, A., *J. Chromatogr. A* 2011, 1218, 2374–2380.
- [156] Demiryas, N., Tuzmen, N., Galaev, I. Y., Piskin, E., Denizli, A., *J. Appl. Polym. Sci.* 2007, 105, 1808–1816.
- [157] Sellergren, B., *J. Chromatogr. A* 1994, 673, 133–141.
- [158] Oxelbark, J., Legido-Quigley, C., Aureliano, C. S. A., Titirici, M. M., Schillinger, E., Sellergren, B., Courtois, J., Irgum, K., Dambies, L., Cormack, P. A. G., Sherrington, D. C., De Lorenzi, E., *J. Chromatogr. A* 2007, 1160, 215–226.
- [159] Yan, H. Y., Row, K. H., *Biomed. Chromatogr.* 2008, 22, 487–493.
- [160] Yan, H. Y., Qiao, F. X., Row, K. H., *Chromatographia* 2009, 70, 1087–1093.
- [161] Zhang, S. J., Yang, G. L., Zheng, Z. S., Chen, Y., *Chromatographia* 2009, 69, 615–619.
- [162] Li, H., Nie, L. H., Li, Y. N., Zhang, Z. H., Shi, H., Hu, W. B., Zhang, Y. K., *Sep. Sci. Technol.* 2009, 44, 370–385.
- [163] Sirc, J., Bosakova, Z., Coufal, P., Michalek, J., Pradny, M., Hobzova, R., Hradil, J., *e-Polymers* 2007, 117, 1–15.
- [164] Haginaka, J., Futagami, A., *J. Chromatogr. A* 2008, 1185, 258–262.
- [165] Amut, E., Fu, Q., Fang, Q., Liu, R., Xiao, A. P., Zeng, A. G., Chang, C., *J. Polym. Res.* 2010, 17, 401–409.
- [166] Özkara, S., Say, R., Andac, C., Denizli, A., *Ind. Eng. Chem. Res.* 2008, 47, 7849–7856.
- [167] Özkara, S., Andac, M., Karakoc, V., Say, R., Denizli, A., *J. Appl. Polym. Sci.* 2011, 120, 1829–1836.
- [168] Asliyüce, S., Bereli, N., Uzun, L., Onur, M. A., Say, R., Denizli, A., *Sep. Purif. Technol.* 2010, 73, 243–249.
- [169] Demiralay, E. C., Andac, M., Say, R., Alsancak, G., Denizli, A., *J. Appl. Polym. Sci.* 2010, 117, 3704–3714.
- [170] Liu, J. X., Deng, Q. L., Yang, K. G., Zhang, L. H., Liang, Z., Zhang, Y. K., *J. Sep. Sci.* 2009, 33, 2757–2761.

# Monolithic columns with immobilized monomeric avidin: preparation and application for affinity chromatography

Jens Sproß · Andrea Sinz

Received: 12 November 2011 / Revised: 11 December 2011 / Accepted: 15 December 2011 / Published online: 20 January 2012  
© Springer-Verlag 2012

**Abstract** A poly(glycidyl methacrylate-*co*-acrylamide-*co*-ethylene dimethacrylate) monolith and a poly(glycidyl methacrylate-*co*-ethylene dimethacrylate) monolith were prepared in fused silica capillaries (100 µm ID) and modified with monomeric avidin using the glutaraldehyde technique. The biotin binding capacity of monolithic affinity columns with immobilized monomeric avidin (MACMAs) was determined by fluorescence spectroscopy using biotin (5-fluorescein) conjugate, as well as biotin- and fluorescein-labeled bovine serum albumin (BSA). The affinity columns were able to bind 16.4 and 3.7 µmol biotin/mL, respectively. Columns prepared using the poly(glycidyl methacrylate-*co*-ethylene dimethacrylate) monolith retained 7.1 mg BSA/mL, almost six times more than commercially available monomeric avidin beads. Protocols based on MALDI-TOF mass spectrometry monitoring were optimized for the enrichment of biotinylated proteins and peptides. A comparison of enrichment efficiencies between MACMAs and commercially available monomeric avidin beads yielded superior results for our novel monolithic affinity columns. However, the affinity medium presented in this work suffers from a significant degree of nonspecific binding, which might hamper the analysis of more complex mixtures. Further modifications of the monolith's surface are envisaged for the future development of monoliths with improved enrichment characteristics.

**Keywords** Monolithic column · Affinity purification · Avidin · Biotin · Protein identification

## Abbreviations

AAM	acrylamide
ACN	acetonitrile
B-5F	biotin (5-fluorescein) conjugate
EDMA	ethylene dimethacrylate
FA	formic acid
Gdm HCl	guanidinium hydrochloride
GMA	glycidyl methacrylate
HEPES	4-(2-hydroxyethyl)-1-piperazineethanesulfonic acid
ID	inner diameter
MACMA	monolithic affinity column with immobilized monomeric avidin
MALDI	matrix-assisted laser desorption/ionization
MS	mass spectrometry
MS/MS	tandem mass spectrometry
NHS	N-hydroxysuccinimide
OD	outer diameter
TFA	trifluoroacetic acid
Tris HCl	tris(hydroxymethyl)aminomethane hydrochloride
TOF	time-of-flight

**Electronic supplementary material** The online version of this article (doi:10.1007/s00216-011-5670-3) contains supplementary material, which is available to authorized users.

J. Sproß · A. Sinz (✉)

Department of Pharmaceutical Chemistry & Bioanalytics,  
Institute of Pharmacy, Martin Luther University Halle-Wittenberg,  
Wolfgang-Langenbeck-Str. 4,  
06120 Halle (Saale), Germany  
e-mail: andrea.sinz@pharmazie.uni-halle.de

## Introduction

The exploitation of highly specific interactions between biological compounds is the basis of all affinity chromatographic techniques [1, 2]. The most commonly used systems comprise interactions between antibodies and antigens [3, 4], lectins and sugars [5, 6], and avidin and biotin [7, 8]. The high stability and specificity of the avidin/biotin complex makes it

one of the most popular systems for affinity purification strategies [9, 10]. However, despite the extremely high association constant of  $10^{15} \text{ M}^{-1}$  for the avidin/biotin complex being a distinct advantage for the purposes of affinity chromatography, this feature of the reaction can hamper the elution of biotin or biotinylated species from avidin affinity matrices under physiological conditions [11]. Several strategies have been developed to reduce the binding affinity between avidin and biotin with the aim of improving the release of bound ligands. These strategies are mentioned only briefly herein, as a large body of literature exists on this topic.

1. The association of biotin and monomeric avidin ( $K_A=10^7 \text{ M}^{-1}$ ) is significantly lower compared with that of biotin and tetrameric avidin [7, 12]. Tetrameric avidin can be monomerized under denaturing conditions [e.g., 6 M guanidinium hydrochloride (Gdm HCl)], but prevention of spontaneous re-association of monomeric avidin requires immobilization of avidin prior to the monomerization process.
2. Chemical modification of the native avidin tetramer, such as the oxidation of tryptophans or the nitration of tyrosine in the biotin binding site of avidin (captavidin) leads to a reduction in the affinity of the avidin/biotin complex [11, 13].
3. Site-directed mutagenesis of avidin has also resulted in engineered variants with lower affinity towards biotin [14].
4. Biotin analogues, such as desthiobiotin or 2-iminobiotin, have been developed and these exhibit lower affinities towards avidin [15, 16].

In this work, we have combined the advantages of monomeric avidin with monolithic stationary phases. To date, only particle-based materials have been reported as supports for the immobilization of avidin and its subsequent monomerization [7, 17, 18]. Monoliths possess several advantages over particulate chromatography systems, including a fast mass transfer, high porosity, low back pressure at high flow rates, a high loading capacity, and a straightforward preparation in microfluidic devices [4, 19–22]. Monoliths prepared from glycidyl methacrylate (GMA) and ethylene dimethacrylate (EDMA) have proved popular for use in affinity chromatography. In recent years poly(GMA-co-EDMA) monoliths have proved most popular [2].

The influences of several factors that affect monolith preparation have been intensively studied. Some of these include polymerization temperature, the monomer content of the polymerization mixture, as well as the effect of the nature and amount of the porogenic solvent on the pore size distribution. Other factors that have to be considered include the surface area and amount of the immobilized ligand used [4, 23–26]. Although a great variety of polymerization processes have been developed over the years, the most

commonly employed techniques involve initiation of the reaction process by heat or UV light [26]. One of the major advantages of poly(GMA-co-EDMA) monoliths is the huge variety of immobilization strategies that are available [1, 2]. Consequently, a specific monolithic matrix can be used for the immobilization of different ligands without the need to optimize the monolith for each particular application. Poly(GMA-co-EDMA) monoliths have also been used as templates in stationary phases using photografting to selectively modify the monolith's surface [27]. The variety of potential modifications has been significantly extended using this technique [28]. However, more time-consuming procedures, such as the glutaraldehyde technique, have also yielded reproducible results [29].

In this work, we report for the first time the immobilization and subsequent monomerization of avidin onto two monolithic stationary phases. The biotin binding capacities of the **Monolithic Affinity Columns with immobilized Monomeric Avidin (MACMAs)** described in this study were determined by a newly developed assay using fluorescence spectroscopy and the affinity columns were successfully used to enrich biotinylated proteins and peptides. Comparison of the MACMAs with commercially available monomeric avidin beads revealed a superior enrichment of biotinylated species using the monolithic material.

## Experimental

### Materials and reagents

Fused silica capillaries (OD 360  $\mu\text{m}$ , ID 100  $\mu\text{m}$ ) were obtained from Ziemer Chromatographie (Mannheim, Germany). Ethylene dimethacrylate (EDMA, 98%),  $\gamma$ -methacryloxypropyl trimethoxysilane (98%), cyclohexanol (99%), glutaraldehyde solution (50%), avidin (chicken egg white), cytochrome *c* (horse heart), lysozyme (chicken egg white), myoglobin (horse heart), tris(hydroxymethyl) aminomethane hydrochloride (Tris HCl, 99%), sodium phosphate (monobasic and dibasic, 98+%), ammonium bicarbonate (99%), ammonium acetate (98%), 4-(2-hydroxyethyl)-1-piperazineethanesulfonic acid (HEPES, 99.5%), dimethyl sulfoxide (DMSO, 99.5%), biotin (99%), biotin (5-fluorescein) conjugate (B-5F, 96%), formic acid (FA, mass spectrometry grade),  $\alpha$ -cyano-4-hydroxycinnamic acid (>98%), sodium azide, *N*-(5-fluoresceinyl)maleimide, sinapinic acid, and 2,5-dihydroxybenzoic acid (gentisic acid, 99+%) were purchased from Sigma (Taufkirchen, Germany). Benzamidine hydrochloride (97%) was obtained from Calbiochem (Darmstadt, Germany). Acrylamide (AAM, 99.5%), glycidyl methacrylate (GMA, 97%), sodium cyanoborohydride (>95%),  $\alpha, \alpha'$ -azobisisobutyronitrile (AIBN, 98%), and 1-dodecanol (99.5%) were purchased

from Fluka (Buchs, Switzerland). AIBN was purified by recrystallization from ethanol. Ammonia solution (30–33%) and guanidinium hydrochloride (Gdm HCl, 99%) were from Roth (Karlsruhe, Germany). Trypsin gold (mass spectrometry grade) was obtained from Promega (Madison, WI, USA). Urea (99.5%), glycine (for CE), trifluoroacetic acid (TFA, UvaSolv<sup>®</sup>), and acetonitrile (ACN, LiChroSolv<sup>®</sup>) were from Merck (Darmstadt, Germany). Potassium hydroxide (85%) was obtained from Grüssing (Filsun, Germany). NHS-PEG<sub>4</sub>-biotin and Monomeric Avidin UltraLink Resin were obtained from Pierce Inc. (Rockford, IL, USA). Water was purified using a Milli-Q5 system (Millipore) and Amicon Ultra (0.5 mL, cutoff 10 kDa) filtration units were from Millipore (Schwalbach, Germany). All mixtures are given in volume per volume unless specified otherwise.

### Preparation of monolithic stationary phases

Fused silica capillaries were prepared according to previous reports [29, 30]. The compositions of polymerization mixtures M-1 and M-2 were published elsewhere [5, 29, 31]. For monolith M-1, GMA 9 wt%, EDMA 15 wt%, AAm 6 wt%, cyclohexanol 59.5 wt%, and 1-dodecanol 10.5 wt% and for monolith M-2 GMA 18 wt%, EDMA 12 wt%, cyclohexanol 58.8 wt%, and 1-dodecanol 11.2 wt% were mixed and sonicated for 15 min. Both mixtures contained the initiator AIBN (1 wt% in respect to monomers). Three batches consisting of three columns each were prepared from mixtures M-1 and M-2. The solutions were manually filled into the pretreated 30-cm-long capillaries using a syringe. Both ends of the capillaries were sealed with silicon rubber stoppers and the capillaries were heated in a water bath for 16 h at 55 °C (M-1) or 50 °C (M-2). After polymerization was completed, each column was inspected under a light microscope to evaluate the homogeneity of the monolith. ACN was flushed through the monoliths to remove porogenic solvents and compounds that had not reacted. A closer investigation of the monolithic support was performed by scanning electron microscopy (SEM) using a JEOL JSM-7401F scanning electron microscope (JEOL, Tokyo, Japan).

### Immobilization of avidin

All steps were performed at room temperature using glass syringes from ILS (Stützerbach, Germany). A Fusion400 syringe pump from Chemyx (Stafford, TX, USA) was used to deliver liquid through the capillaries. Avidin was immobilized on the monolithic support according to an existing procedure that was used with slight modifications [29]. The monolithic columns were flushed overnight with 15% ammonia solution containing 50% ACN. Excess ammonia was removed with

25% ACN solution (8 h), after which a 10% glutaraldehyde solution in 25% ACN was pumped through the columns overnight. The activated support was washed with water for 8 h before avidin (2.5 mg/mL) in 100 mM sodium phosphate buffer (pH 7.0) was continuously flushed through the capillaries overnight. Afterwards, the labile Schiff base and unreacted aldehyde groups were reduced with 80 mM sodium borohydride solution (6 h) (Fig. S2 Electronic Supplementary Material). Monomeric avidin was prepared directly in the columns by introducing a 6 M Gdm HCl solution containing 0.2 M potassium chloride (pH 1.5) [18] for 66 h. Unbound avidin was eluted from the matrix, whereas immobilized subunits remained on the monolith. Excess Gdm HCl was removed by flushing the columns with 0.1 M ammonium bicarbonate solution. The capillaries were cut to a length of 6.5 cm (for monolith M-1) or 20 cm (for monolith M-2). Irreversible biotin binding sites were blocked by washing the columns with 0.4 mM biotin in 50 mM Tris HCl (pH 7.5). Reversible binding sites were regenerated with elution buffer (50% ACN containing 0.4% FA). A glutaraldehyde column (monolith M-2) was prepared without avidin to estimate the degree of nonspecific binding. Columns were equilibrated with 50 mM Tris HCl (pH 7.5) and stored in a buffer composed of 50 mM Tris HCl (pH 7.5) and 0.02% sodium azide at 4 °C until use.

### Biotin and protein binding capacity

The biotin binding capacity of the MACMAs was determined by fluorescence spectroscopy using B-5F. Additionally, protein binding capacity was evaluated using PEG<sub>4</sub>-biotinylated and fluorescein-labeled bovine serum albumin (BSA, see Electronic Supplementary Material). Briefly, MACMAs were saturated with fluorescein-labeled sample, excess analyte was removed by washing, and bound analyte was eluted with 50% ACN containing 0.4% FA. The collected eluates were diluted with 0.1 M Tris HCl (pH 8.0) and analyzed by using a MPF-44 fluorescence spectrophotometer (PerkinElmer, MA, USA). The fluorescence emission of fluorescein at 523 nm served to calibrate the instrument and to calculate binding capacities (Electronic Supplementary Material).

### In-solution digestion of cytochrome *c*

A 30- $\mu$ L aliquot of a 10  $\mu$ M PEG<sub>4</sub>-biotinylated cytochrome *c* solution (NHS-PEG<sub>4</sub>-biotin, 30 min reaction time; Electronic Supplementary Material) was mixed with 60  $\mu$ L of a 0.2 M ammonium acetate solution. *In-solution* digestion was performed by adding trypsin at an enzyme-to-substrate ratio of 1:60 (w/w) and incubating the mixture at 37 °C for 16 h. The digestion was stopped by adding benzamidine to a final concentration of 4  $\mu$ M.

### Enrichment of biotinylated cytochrome *c* on MACMAs

Biotinylated cytochrome *c* solution (NHS-PEG<sub>4</sub>-biotin, 5 min reaction time; [Electronic Supplementary Material](#)) was mixed 1:1 or 2:1 with unmodified cytochrome *c* solution giving a final protein concentration of 5 μM in 0.1 M ammonium acetate. A 5-μL aliquot of the solution was loaded onto each MACMA at a flow rate of 500 nL/min. To evaluate the optimum composition of the washing solution (22.5 μL) several conditions were tested [0.1 M ammonium acetate (pH 7.0); 5% ACN (pH 3.0, 3.5, 4.0); pH 4.0 (12.5% ACN, 20% ACN, 40% ACN)]. Bound cytochrome *c* was eluted with 50% ACN, 0.4% FA. Fractions were collected for MALDI-TOF-MS analysis. Desalting of samples prior to MS analysis was performed with C4-ZipTips (Millipore) according to the manufacturer's protocol. All experiments were conducted in triplicate.

### Enrichment of biotinylated cytochrome *c* peptides on MACMAs

In-solution digestion mixtures of cytochrome (10 μL) were loaded onto the MACMAs. Removal of nonspecifically bound peptides was performed with 22.5 μL of a 0.1 M ammonium acetate solution (pH 7.0, containing 0%, 10%, 15% or 20% ACN) or 5% ACN (pH 4.0). Bound peptides were eluted with 50% ACN containing 0.4% FA. All steps were performed at a flow rate of 500 nL/min. Fractions were collected for MALDI-TOF-MS analysis and desalted with C18-ZipTips (Millipore) using the manufacturer's protocol prior to MS analysis. Each experiment was performed in triplicate.

### Enrichment of biotinylated peptides using monomeric avidin beads

Enrichment of PEG<sub>4</sub>-biotinylated cytochrome *c* peptides was additionally performed using Monomeric Avidin UltraLink® Resin (Pierce) using an established protocol with slight modifications [32]. First, the beads were successively washed with 0.1 M sodium phosphate buffer (pH 7.5), 0.1 M glycine buffer (pH 2.8), 0.1 M sodium phosphate buffer (pH 7.5), 2 mM biotin in 0.1 M sodium phosphate buffer (pH 7.5), 0.1 M glycine buffer (pH 2.8), 15% ACN containing 0.1 M ammonium acetate (pH 7.0), and 0.1 M sodium phosphate buffer (pH 7.5). To 14 μL of beads, 14 μL of water and 10 μL of PEG<sub>4</sub>-biotin-labeled cytochrome *c* from the in-solution digestion mixture were added and the mixtures were incubated for 3 h at room temperature in the dark. The supernatant was collected and the beads were washed three times with 25 μL 0.1 M sodium phosphate buffer (pH 7.5). The beads were then washed twice with 25 μL 0.1 M ammonium acetate (pH 7.0) or 25 μL 15% ACN containing 0.1 M ammonium acetate (pH 7.0). Bound peptides were eluted by adding 25 μL of 50%

ACN containing 0.4% FA twice. The supernatant, sodium phosphate buffer fractions, and ACN/ammonium acetate fractions were desalted using C18-ZipTips (Millipore) and all fractions were analyzed by MALDI-TOF/TOF-MS/MS.

### Mass spectrometry

MALDI-TOF-MS and MALDI-TOF/TOF-MS/MS analyses were performed with an Ultraflex III MALDI mass spectrometer equipped with a 200 Hz SmartBeam™ laser (Bruker Daltonik, Bremen, Germany). MALDI-TOF-MS analyses of intact biotinylated cytochrome *c* were performed in the linear and positive ionization mode. Samples were mixed with 2 μL of matrix solution (50 mg/mL 2,5-dihydroxybenzoic acid in 50% ACN containing 0.1% TFA) and spotted onto a polished stainless steel target (384 spots, Bruker Daltonik). A total of 4,000 laser shots in the *m/z* range 5,000–30,000 were accumulated into one mass spectrum. Mass spectra of labeled BSA were recorded in the *m/z* range 10,000–100,000 (4,000 shots) using sinapinic acid as matrix (saturated solution in 50% ACN containing 0.1% TFA). External calibration of mass spectra was performed using a mixture of cytochrome *c* and myoglobin or Protein Calibration Standard II (Bruker Daltonik). Biotinylated cytochrome *c* peptides were analyzed in the positive ionization and reflectron mode. Samples were mixed with 2 μL of matrix solution (0.7 mg/mL α-cyano-4-hydroxycinnamic acid in 95% ACN containing 0.1% TFA, 1 mM NH<sub>4</sub>H<sub>2</sub>PO<sub>4</sub>). Mixtures were spotted onto a 384 MTP 800 μm AnchorChip™ target (Bruker Daltonik). MALDI-TOF-MS analyses were performed by accumulating 2,000 laser shots in the range *m/z* 700–5,500 into one mass spectrum. Mass spectra were externally calibrated using Peptide Calibration Standard II (Bruker Daltonik). Precursor ion selection for laser-induced fragmentation (MS/MS) was performed manually. Data acquisition and data processing were manually performed with FlexControl 3.3 and FlexAnalysis 3.3 software (both Bruker Daltonik).

### Protein identification

Analysis of peptide mass fingerprints was conducted with BioTools 3.2 (Bruker Daltonik) using the Mascot software and the Swissprot database ([www.expasy.ch](http://www.expasy.ch)). A mass deviation of 50 ppm was allowed for MS data. For database searches of digested cytochrome *c*, heme modification (formal charge of +1, formula C<sub>34</sub>H<sub>31</sub>N<sub>4</sub>O<sub>4</sub>Fe, mass 615.1694) and PEG<sub>4</sub>-biotinylation (formula C<sub>21</sub>H<sub>35</sub>N<sub>3</sub>O<sub>7</sub>S, mass 473.2196) were included as modifications.

### Enrichment of biotinylated species

Five cytochrome *c* peptides (Table 1) were chosen for the evaluation of the enrichment performance of the MACMAs.

**Table 1** Cytochrome *c* peptides and their corresponding biotinylated species selected for the evaluation of enrichment

<i>m/z</i>	Amino acid number	Amino acid sequence
1,168.622	28–38	TGPNLHGLFGR
1,433.776	26–38	HKTGPNLHGLFGR
1,906.996		H <b>K</b> TGPNLHGLFGR
1,922.991		H <b>K</b> TGPNLHGLFGR
1,598.781	39–53	KTGQAPGFYTDANK
2,072.000		<b>K</b> TGQAPGFYTDANK
2,087.995		<b>K</b> TGQAPGFYTDANK
1,735.011	86–99	KKTEREDLIAYLKK
2,208.231	87–100	KKTEREDLIAYL <b>KK</b>
2,224.226		KKTEREDLIAYL <b>KK</b>
1,606.916	87–99	KTEREDLIAYLKK
2,080.136	88–100	KTEREDLIAYL <b>KK</b>
2,096.131		KTEREDLIAYL <b>KK</b>
1,478.821	88–99	TEREDLIAYLKK
1,952.041	89–100	TEREDLIAYL <b>KK</b>
1,968.036		TEREDLIAYL <b>KK</b>

Amino acid sequences were confirmed by MS/MS. Lysine residues that are most likely to be modified with PEG<sub>4</sub>-biotin are highlighted in bold italics

The unmodified cytochrome *c* peptide TGPNLHGLFGR (*m/z* 1,168.622, amino acids 28–38) was used as the reference peptide as it was present in all fractions under investigation. The most abundant biotinylated cytochrome *c* peptide (*m/z* 1,906.996, aa 26–38) resulted from a missed tryptic cleavage at biotinylated Lys-28. The chromatographic behavior of both peptides (aa 26–38 and 28–38) should be comparable during the enrichment steps on the MACMAs. *Signal-to-noise* ratios of six unmodified and ten biotinylated cytochrome *c* peptides [PEG<sub>4</sub>-biotin and oxidized PEG<sub>4</sub>-biotin (confirmed by MS/MS, Fig. S4 Electronic Supplementary Material)] were manually extracted from the mass spectra. Peptides labeled with PEG<sub>4</sub>-biotin and oxidized PEG<sub>4</sub>-biotin were treated as single species and their *S/N* values were added. All peptide signal intensities were normalized to the intensity of the reference peptide at *m/z* 1,168.622. The arithmetic mean and standard deviations were calculated from the average normalized intensities obtained from triplicate measurements.

## Results and discussion

### Preparation of MACMAs

Polymerization mixtures optimized by Duan et al. (designated as M-1) [29, 31] and Okanda et al. (designated as M-2) [5] were used for the preparation of MACMAs. M-1 was chosen on the basis of our experience using this monolith in a

**Table 2** Intra- and interbatch reproducibility of the biotin binding capacity for the MACMAs prepared from mixtures M-1 and M-2

	M-1		M-2	
	<i>c<sub>n</sub></i> (pmol/cm)	RSD (%)	<i>c<sub>n</sub></i> (pmol/cm)	RSD (%)
Batch 1	364	3.6	92	10.8
Batch 2	386	8.7	79	9.5
Batch 3	408	7.1	86	9.6
Interbatch	386	4.6	86	6.1

Each batch comprised 3 columns; B-5F binding was repeated 3 times; fluorescence measurements were performed 5 times

previous investigation [29], whereas M-2 was chosen because of the absence of nonspecific interactions as reported by Okanda et al. [5] GMA was incorporated into the monoliths to facilitate avidin immobilization. Monolith M-1 contained AAm, which is copolymerized to yield a more hydrophilic surface. This should lead to a better affinity chromatographic performance due to a lower amount of nonspecifically bound analytes. SEM images of both monoliths showed comparable morphologies (Fig. S1 Electronic Supplementary Material). The monoliths are anchored to the inner wall of the fused silica capillary, showing microglobules of similar sizes. The MACMAs (ID 100 μm) can be operated at the high salt concentrations required for monomerization of native tetrameric avidin. A flow rate of 500 nL/min was chosen for the experiments. This was a compromise between performing a fast analysis and allowing sufficiently long contact times of the analytes with the stationary phase; however, it should be noted that higher flow rates are possible.

Immobilization of proteins on GMA-based monoliths makes use of the reactivity of the oxirane ring (Fig. S2 Electronic Supplementary Material). Several strategies taking advantage of this reactivity have been developed, including the direct attachment of the protein via the amine group (created by ring-opening of the epoxide), as well as time-consuming multistep procedures [1, 2, 33–35]. The glutaraldehyde technique used here belongs to the latter group of strategies. Nevertheless, compared with single-step strategies, larger protein amounts can be immobilized

**Table 3** Intra- and interbatch reproducibility of the protein binding capacities for MACMAs prepared from mixture M-2

	<i>c<sub>n</sub></i> (pmol/column)	RSD (%)
M-2 batch 4	43.2	15.2
M-2 batch 5	54.4	9.4
M-2 interbatch	48.8	13.4
Glutaraldehyde	26.9	6.2

Each batch comprised 3 columns. Nonspecific binding was determined using a column (glutaraldehyde modification without avidin) prepared from mixture M-2. All experiments were performed in triplicate

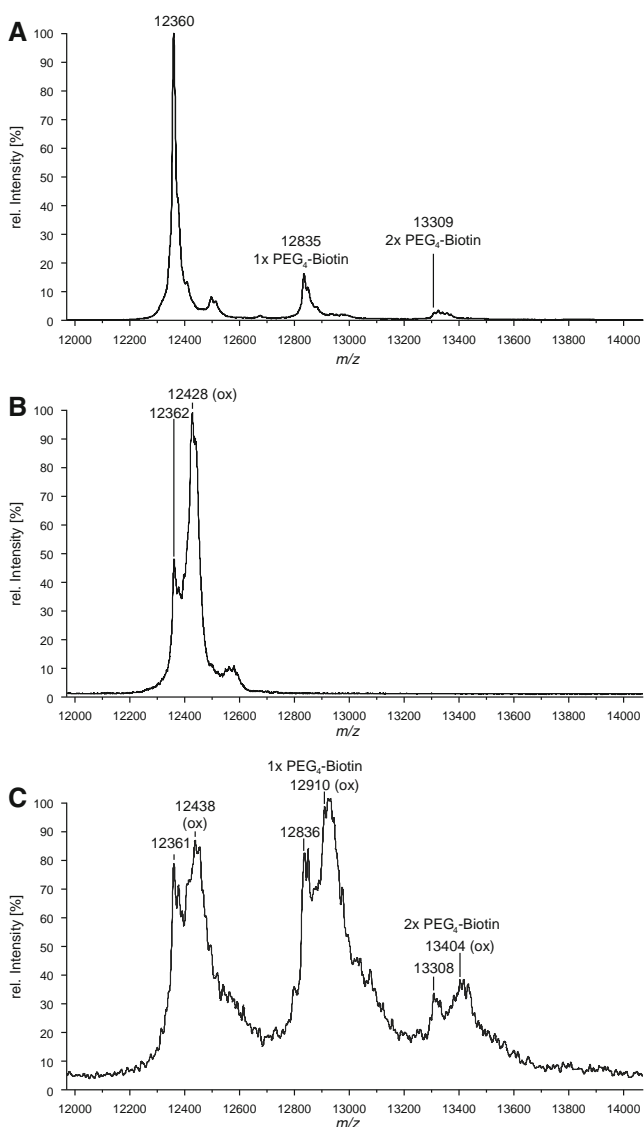


**Fig. 1** MALDI-TOF mass spectra of PEG<sub>4</sub>-biotinylated cytochrome *c* **a** before the enrichment on MACMA (prepared from mixture M-2); **b** the flow-through fraction contained exclusively unmodified cytochrome *c*; **c** biotinylated species eluted with 50% ACN containing 0.4% FA

on the monolith and the activity of immobilized enzymes is higher, probably due to better accessibility of the active site because of the glutaraldehyde spacer [35, 36]. During the monomerization of avidin the presence of reducing agents such as mercaptoethanol had to be avoided because of avidin's disulfide bridge (Cys4–Cys83), which is essential for the correct refolding of the avidin monomer after Gdm HCl has been removed [12].

### Binding capacity of MACMAS

The reproducibility of the preparation process was investigated on the basis of the biotin binding capacities of the MACMAS using the fluorescent compound B-5F. The

MACMAS were saturated with B-5F and nonspecifically bound dye was removed by washing steps with 2.5% ACN (pH 3.5). Bound B-5F was eluted with 50% ACN containing 0.4% FA and the eluate was collected for fluorescence spectroscopy. MACMAS prepared from mixture M-1 were expected to have a lower biotin binding capacity compared with MACMAS prepared from mixture M-2 because of the lower amount of GMA in mixture M-1.

MACMAS prepared from mixture M-2 had biotin binding capacities of 79–92 pmol per cm column length [pmol/cm; intrabatch, relative standard deviation (RSD) 9.5–10.8%] with an average binding capacity of 86 pmol/cm (interbatch, RSD 6.1%, Table 2). The 20 cm MACMA retained a total of 1.7 nmol of biotin. Surprisingly, the biotin binding capacities of the MACMAS prepared from mixture M-1 were significantly higher, although the GMA content of mixture M-1 was lower than that of mixture M-2. Biotin binding capacities were determined to be 364–408 pmol/cm (intrabatch, RSD 3.6–8.7%), corresponding to an average binding capacity of 386 pmol/cm (interbatch, RSD 4.6%, Table 2). Although MACMAS obtained from mixture M-1 were only 6.5 cm in length, they retained 2.5 nmol of biotin. We assume that the amide group of the acrylamide in mixture M-1 also reacted with glutaraldehyde during the immobilization procedure and thus served as an additional attachment site next to the amine groups that were created by aminolysis of the oxirane rings. Recent experiments conducted by Duan et al. indicated that acrylamide might participate in the reaction with glutaraldehyde, thereby resulting in additional anchor sites for the immobilized protein [31]. As early as 1933 Noyes and Forman described the reaction of aldehydes with acetamide proving that a reaction between glutaraldehyde and acrylamide might be possible [37]. A better accessibility or even a preferential location of epoxy groups on the surface of the AAM-containing monolithic material M-1 might also be possible, but in our opinion the increase of the biotin binding capacity of MACMAS prepared from mixture M-1 cannot be solely explained by this mechanism. However, this problem should be investigated in the future in more detail.

In summary, MACMAS prepared from mixture M-2 bound approximately 3.7  $\mu\text{mol}$  biotin/mL, whereas MACMAS prepared from mixture M-1 bound approximately 16.4  $\mu\text{mol}$  biotin/mL. Biotin binding capacities of particle-based affinity materials have been reported to be significantly lower (4 nmol/mL [17] and 5.3 nmol/mL [18]). Estimating the binding capacities for biotinylated proteins is clearly more challenging. MACMAS prepared from mixture M-2 were saturated with BSA that had been doubly labeled with fluorescein and biotin. Nonspecifically bound BSA was removed by extensive washing with 10% ACN containing 0.1 M ammonium acetate (pH 7.0) and bound BSA was eluted with a mixture of 50% ACN containing 0.4% FA. Fluorescence spectroscopy revealed a reversible binding capacity of 48.8 pmol

BSA per column (RSD 13.4%, Table 3) corresponding to approximately 7.1 mg BSA/mL. This is almost six times higher than the binding capacity of 1.2 mg biotinylated BSA/mL resin provided for commercially available Monomeric Avidin UltraLink® Resin (Pierce). These agarose particles have a size ranging from 50–80  $\mu\text{m}$  and a surface area greater than 250  $\text{m}^2/\text{g}$ . Unfortunately, comparable data are not available for the monoliths used in this study; however, the surface area of monoliths prepared from similar mixtures range between 10 and 120  $\text{m}^2/\text{g}$  and median pore diameters of approximately 900 nm have been reported [4, 23, 38]. The ligand density on the surface of the monolith is therefore higher compared with that on particles.

The protein binding capacity was also determined for a MACMA with the glutaraldehyde modification because poly(GMA-*co*-EDMA) monoliths are known to be susceptible to nonspecific binding [27]. The contribution of nonspecific binding was found to be up to 55% (Table 3) and pretreatment of the columns with BSA did not significantly reduce the amount of nonspecific binding. It is important to note, however, that comparable data are not available for the commercial UltraLink® Resin.

#### Enrichment of biotinylated cytochrome *c*

Unmodified cytochrome *c* was mixed with singly and doubly PEG<sub>4</sub>-biotinylated cytochrome *c* and applied to the MACMAs (Fig. 1A). The flow-through contained only unmodified cytochrome *c* (Fig. 1B). Different conditions were evaluated for the washing procedure including changing the pH or the amount of ACN in the solution. Elution fractions that were obtained after washing the columns at  $\text{pH} < 4.0$  showed no, or only low-intensity, signals of biotinylated protein (data not shown). The use of more than 5% acetonitrile in the washing solution hampered the recovery of biotinylated cytochrome *c*. Optimum results were obtained by washing the MACMAs with 5% ACN (pH 4.0) or 0.1 M ammonium acetate (pH 7.0). Elution fractions were not completely depleted of unmodified protein, yet signals of singly and doubly PEG<sub>4</sub>-biotinylated cytochrome *c* were clearly visible in MALDI-TOF mass spectra (Fig. 1C).

The enrichment of biotinylated species was also influenced by the chemistry of the monolithic support. Although monoliths prepared from mixture M-1 should be more hydrophilic due to the presence of AAm in the polymerization mixture (Table 1), the recovery of biotinylated cytochrome *c* was lower compared with that of monoliths M-2. Therefore, MACMAs prepared from polymerization mixture M-1 were excluded from further experiments. MALDI-TOF mass spectra showed shifts towards higher  $m/z$  values for both biotinylated and unmodified cytochrome *c*, which corresponded to the presence of oxidation products, probably

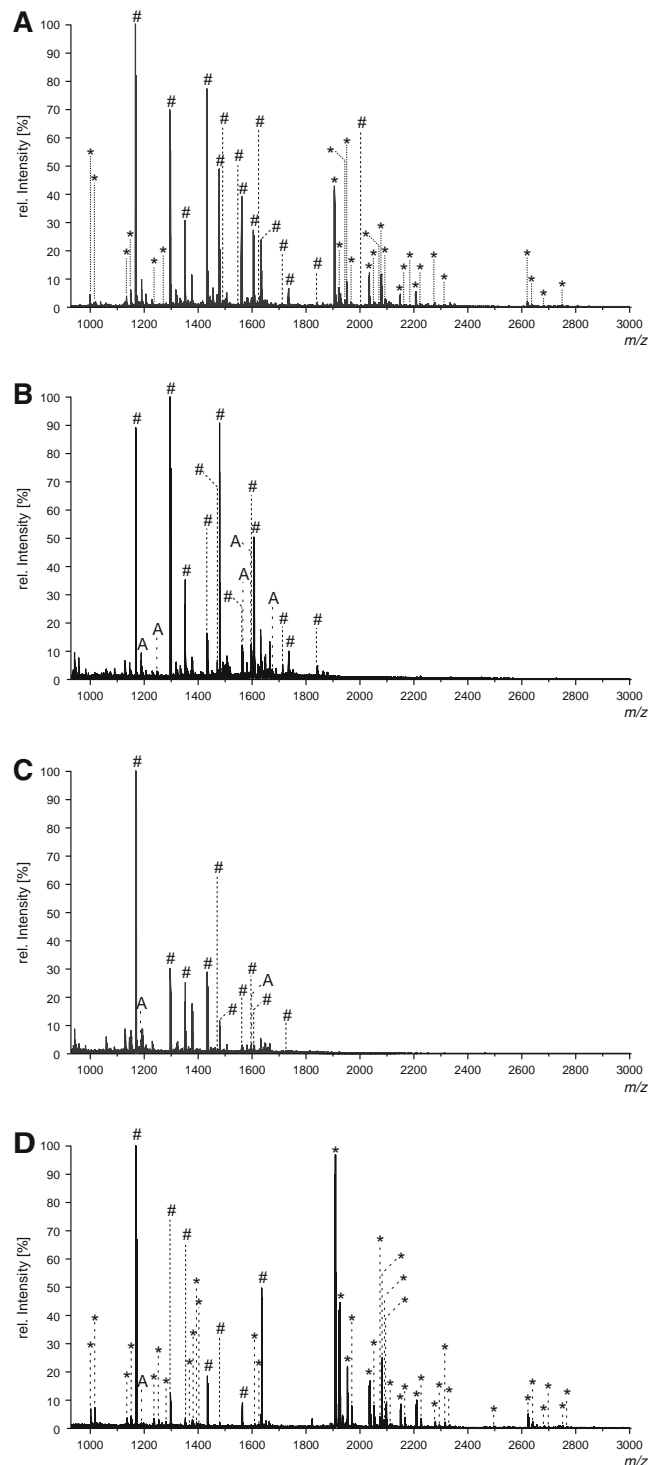


**Fig. 2** Mass spectra of **A** in-solution digest, **B** flow-through, **C** washing fraction (15% ACN containing 0.1 M ammonium acetate, pH 7.0), and **D** the elution fraction from a MACMA enrichment of PEG<sub>4</sub>-biotinylated cytochrome *c* peptides. # unmodified cytochrome *c* peptides, \* PEG<sub>4</sub>-biotinylated cytochrome *c* peptides, A avidin peptides. The MACMA was prepared from mixture M-2

originating from auto-oxidation induced by the heme group in cytochrome *c*. This hypothesis is supported by the observation that no formation of oxidation products was observed

for hen egg lysozyme, whereas the heme-containing protein myoglobin was also oxidized when passed through the MACMA (Fig. S3 Electronic Supplementary Material).

#### Enrichment of biotinylated cytochrome *c* peptides

PEG<sub>4</sub>-biotinylated cytochrome *c* digested in solution (Fig. S4 Electronic Supplementary Material) was subjected to MACMAs from mixture M-2 in order to optimize the washing procedure with the aim of minimizing nonspecific binding of peptides. Signals due to unmodified cytochrome *c* peptides were observed in MALDI-TOF mass spectra from all fractions, and were most abundant in the flow-through and washing fractions (Fig. 2). The complete depletion of non-biotinylated peptides was not possible. In

particular, hydrophobic cytochrome *c* peptides were present in all fractions of the affinity purification. Nevertheless, biotinylated cytochrome *c* peptides were highly abundant in the elution fractions and only rarely identified in mass spectra of flow-through and washing fractions (Fig. 3A).

The results obtained for the five most abundant cytochrome *c* peptides provide a more detailed view of the enrichment efficiencies of the MACMAs (Fig. 3 and Electronic Supplementary Material Figs. S6-1 to 3). Before the affinity enrichment, ratios of unmodified/biotinylated peptides ranged between 2:1 and 1:2 (Fig. 3A). In the flow-through and washing fractions unmodified cytochrome *c* peptides were abundant, whereas biotinylated peptides were present as only minor species. In the elution fraction, the

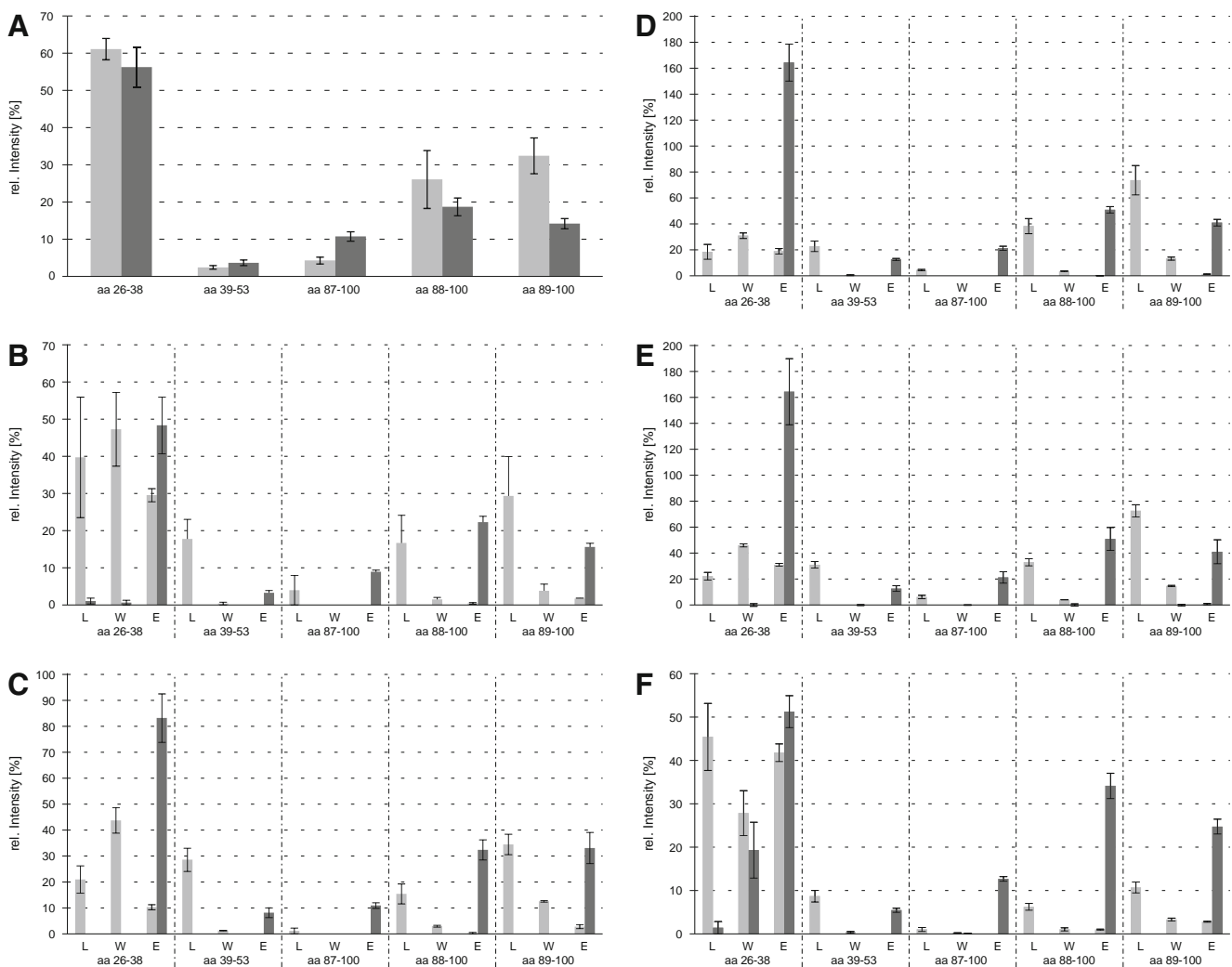


**Fig. 3** **A** *S/N* values of unmodified and biotinylated cytochrome *c* peptides before affinity chromatography. **B–F** Enrichment performance of five biotinylated cytochrome *c* peptides on a MACMA (mixture M-2) under different washing conditions: **B** 0.1 M ammonium acetate, pH 7.0; **C** 10% ACN containing 0.1 M ammonium acetate, pH 7.0; **D** 15% ACN containing 0.1 M ammonium acetate, pH 7.0; **E** 20% ACN

containing 0.1 M ammonium acetate, pH 7.0; and **F** 5% ACN, pH 4.0. Elution was performed with 50% ACN containing 0.4% FA. *Light gray* unmodified cytochrome *c* peptides, *dark gray* PEG<sub>4</sub>-biotinylated cytochrome *c* peptides, *L* load, *W* washing fractions, *E* elution fractions. Intensities were normalized to *S/N* value of the peptide at *m/z* 1,168.622. All experiments were performed in triplicate

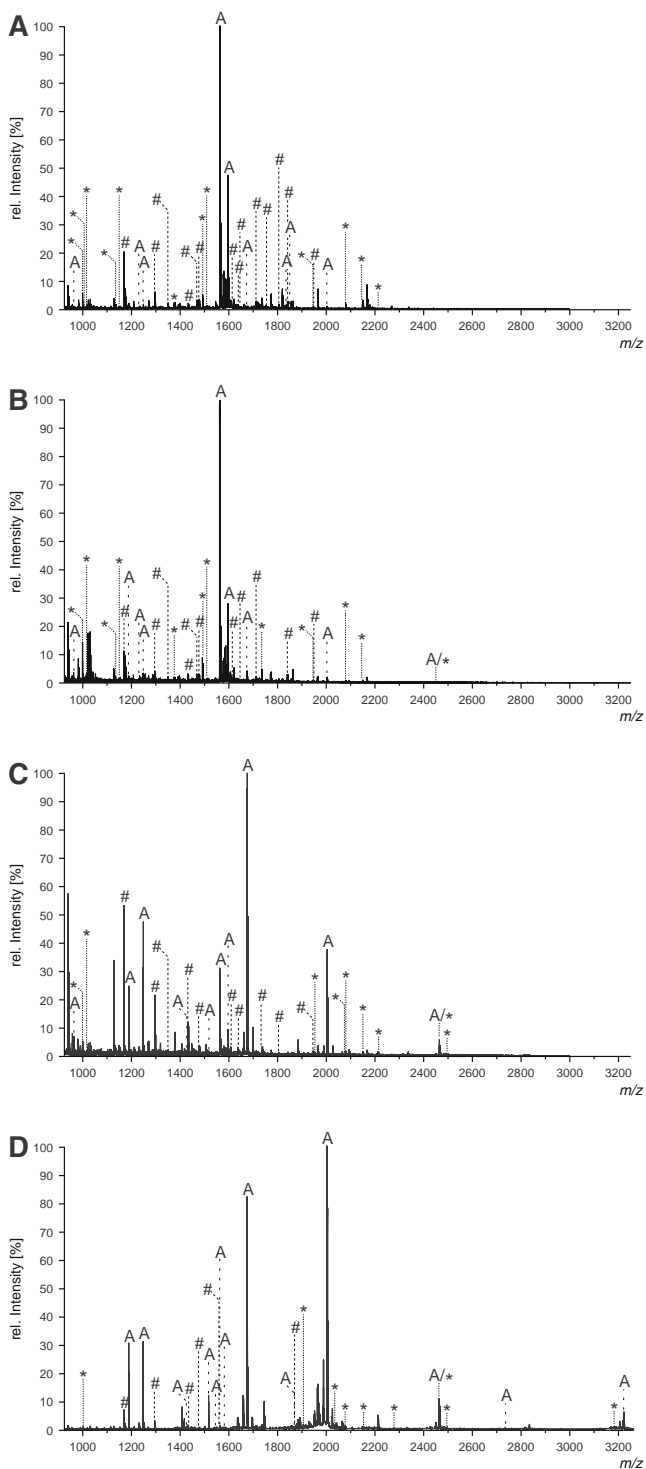


**Fig. 4** Mass spectra of **A** supernatant, **B** washing fraction with 0.1 M sodium phosphate buffer (pH 7.5), **C** washing fraction with 15% ACN containing 0.1 M ammonium acetate pH 7.0, and **D** elution of PEG<sub>4</sub>-biotinylated cytochrome *c* peptides (50% ACN containing 0.4% FA) using monomeric avidin beads. # unmodified cytochrome *c* peptides, \* PEG<sub>4</sub>-biotinylated cytochrome peptides, *A* avidin peptides. Compare also to Fig. 2A

ratios of unmodified/biotinylated peptides exceeded 1:4. It should be noted that in most cases the complete depletion of

their unmodified counterparts was successful. Increasing the ACN content in the washing solution from 5 to 15% yielded higher signal intensities for biotinylated peptides, whereas ACN contents greater than 15%, together with acidic pH values, led to the elution of biotinylated peptides in the washing steps. Optimum results were obtained by washing the MACMAs with 15% ACN containing 0.1 M ammonium acetate (pH 7.0, Fig. 3D).

The main cause of the rather high degree of nonspecific binding observed in this study was probably due to the high degree of hydrophobic interactions of the analytes with the monolithic support. The higher the amount of organic modifier in the elution buffer, the lower the specific enrichment of biotinylated species. A more hydrophilic monolithic surface would potentially result in less nonspecific binding and increase the performance of the affinity column. Modification of the monolith's surface, e.g., by photografting with poly(ethylene glycol) methacrylate, or preparing the monolithic support with hydrophilic monomers is envisaged for the future development of monoliths with improved enrichment characteristics [27, 39].

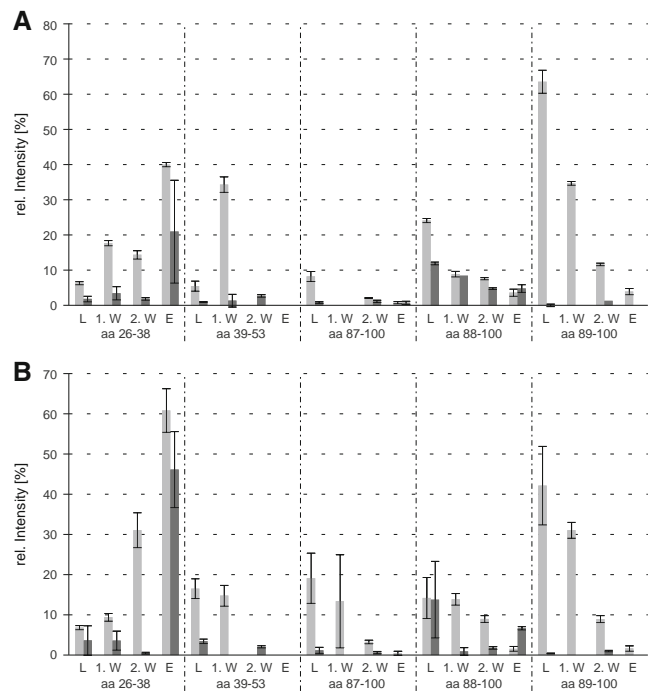


**Fig. 5** Enrichment performance of five biotinylated cytochrome *c* peptides on monomeric avidin beads using different wash conditions in the second wash step: **a** 0.1 M ammonium acetate, **b** 15% ACN containing 0.1 M ammonium acetate. Elution was performed with 50% ACN containing 0.4% FA. Light gray unmodified cytochrome *c* peptides, dark gray PEG<sub>4</sub>-biotinylated cytochrome *c* peptides, *L* load, *W* washing fractions, *E* elution fractions. Intensities were normalized to *S/N* value of the peptide at *m/z* 1,168.622. Affinity purifications were repeated three times each. Compare also to Fig. 3a

### Comparison of MACMAs with monomeric avidin beads

The affinity enrichment performance of the MACMAs is superior compared with that of commercially available monomeric avidin beads. Mass spectra of the flow-through (supernatant), washing, and elution fractions from monomeric avidin beads contained both unmodified and biotinylated peptides (Fig. 4). It should be noted that although the agarose beads are more hydrophilic than the monolithic support they also showed a rather high degree of nonspecific binding. Ratios of unmodified/biotinylated peptides never exceed the values obtained for the untreated in-solution digestion mixture (Fig. 5). Despite the blocking of residual trypsin with benzamidine after in-solution digestion, signals of avidin peptides were still detected. When using the MACMAs, we found that the intensities of the avidin signals were rather low and mass spectra were dominated by signals of biotinylated and unmodified cytochrome *c* peptides (Fig. 2B–D). On the other hand, mass spectra from all fractions of the affinity enrichment using monomeric avidin beads were dominated by tryptic avidin peptides (Fig. 4). This indicates that either trypsin or the tryptic avidin peptides were nonspecifically retained on the beads causing the appearance of avidin peptides in all fractions. Most of these peptides originated from the C-terminal 28 amino acids of avidin, with the majority of peptides from the C-terminal 17 amino acids. This drastically impairs the enrichment performance of monomeric avidin beads, as well as compromising their reuse due to a potential loss of biotin binding after proteolysis of avidin. Therefore, the lifetime of monomeric avidin beads (10 cycles according to the manufacturer) can be considered much lower compared with that of the MACMAs, which were operated for more than 1 year during this study.

### Conclusions

The MACMAs described herein have proven to be highly efficient for enriching biotinylated proteins and peptides. The combination of monomeric avidin and monolithic columns allows for a higher biotin binding capacity and a better enrichment of biotinylated compounds compared with commercially available particle-based affinity media. An interaction time of 132 s was shown to be sufficient for the complete attachment of biotinylated tryptic cytochrome *c* peptides using the MACMAs, whereas for commercially available particle-based monomeric avidin beads, biotinylated peptides were still present in the supernatant after an incubation time of 3 h. This can be explained by the fast mass transfer of the monolithic material, a distinctive feature of monolithic stationary phases and a consequence of the convective flow within monolithic supports, thus enabling

an efficient interaction of immobilized monomeric avidin and biotinylated species in the mobile phase. The stability of monomeric avidin on a monolithic support is enhanced compared with particle-based monomeric avidin beads, from which the avidin peptides were eluted. However, the affinity medium presented in this work suffers from a significant degree of nonspecific binding, which might hamper the analysis of more complex samples. Further modifications of the monolith's surface are envisaged to allow the further development of monoliths with improved enrichment characteristics.

**Acknowledgements** The authors thank Dr. P. Miclea for providing SEM images, Dr. C.H. Ihling for assistance with MS, and Dr. H.H. Rüttinger for assistance with fluorescence spectroscopy. Ms. B. Brandt and Ms. S. Knies are acknowledged for excellent technical support. Prof. G. Sawers is acknowledged for critical reading of the manuscript. J.S. indebted to Dr. A. Svatoš and Dr. A. Muck for the introduction to monolithic supports.

### References

- Mallik R, Hage DS (2006) *J Sep Sci* 29(12):1686–1704
- Sproß J, Sinz A (2011) *J Sep Sci* 34(16–17):1958–1973
- Weller MG (2000) *Fresenius J Anal Chem* 366(6–7):635–645
- Jiang T, Mallik R, Hage DS (2005) *Anal Chem* 77(8):2362–2372
- Okanda FM, El Rassi Z (2006) *Electrophoresis* 27(5–6):1020–1030
- Bedair M, El Rassi Z (2004) *J Chromatogr A* 1044(1–2):177–186
- Green NM, Toms EJ (1973) *Biochem J* 133(4):687–698
- Diamandis EP, Christopoulos TK (1991) *Clin Chem* 37(5):625–636
- Wilchek M, Bayer EA (1988) *Anal Biochem* 171(1):1–32
- Nicoli R, Bartolini M, Rudaz S, Andrisano V, Veuthey JL (2008) *J Chromatogr A* 1206(1):2–10
- Green NM (1963) *Biochem J* 89(3):599–609
- Green NM (1963) *Biochem J* 89(3):609–620
- Garcia-Aljaro C, Munoz FX, Baldrich E (2009) *Analyst* 134(11):2338–2343
- Laitinen OH, Nordlund HR, Hytonen VP, Uotila STH, Marttila AT, Savolainen J, Airene KJ, Livnah O, Bayer EA, Wilchek M, Kulomaa MS (2003) *J Biol Chem* 278(6):4010–4014
- Green NM (1966) *Biochem J* 101(3):774–780
- Hirsch JD, Eslamizar L, Filanoski BJ, Malekzadeh N, Haugland RP, Beechem JM (2002) *Anal Biochem* 308(2):343–357
- Henrikson KP, Allen SHG, Maloy WL (1979) *Anal Biochem* 94(2):366–370
- Gravel RA, Lam KF, Mahuran D, Kronis A (1980) *Arch Biochem Biophys* 201(2):669–673
- Urban J, Jandera P (2008) *J Sep Sci* 31(14):2521–2540
- Svec F, Frechet JM (1992) *Anal Chem* 64(7):820–822
- Guiochon G (2007) *J Chromatogr A* 1168(1–2):101–168
- Gritti F, Piatkowski W, Guiochon G (2003) *J Chromatogr A* 983(1–2):51–71
- Svec F, Frechet JM (1995) *Chem Mater* 7(4):707–715
- Eeltink S, Svec F (2007) *Electrophoresis* 28(1–2):137–147
- Nischang I, Brueggemann O, Svec F (2010) *Anal Bioanal Chem* 397(3):953–960
- Svec F (2010) *J Chromatogr A* 1217(6):902–924

27. Krenkova J, Lacher NA, Svec F (2009) *Anal Chem* 81(5):2004–2012
28. Eeltink S, Hilder EF, Geiser L, Svec F, Frechet JM, Rosing GP, Schoenmakers PJ, Kok WT (2007) *J Sep Sci* 30(3):407–413
29. Sproß J, Sinz A (2010) *Anal Chem* 82(4):1434–1443
30. Courtois J, Szumski M, Bystrom E, Iwasiewicz A, Shchukarev A, Irgum K (2006) *J Sep Sci* 29(2):325–325
31. Duan JC, Liang Z, Yang C, Zhang J, Zhang LH, Zhang WB, Zhang YK (2006) *Proteomics* 6(2):412–419
32. Sinz A, Kalkhof S, Ihling C (2005) *J Am Soc Mass Spectrom* 16(12):1921–1931
33. Petro M, Svec F, Frechet JM (1996) *Biotechnol Bioeng* 49(4):355–363
34. Calleri E, Temporini C, Perani E, De Palma A, Lubda D, Mellerio G, Sala A, Galliano M, Caccialanza G, Massolini G (2005) *J Proteome Res* 4(2):481–490
35. Nicoli R, Gaud N, Stella C, Rudaz S, Veuthey JL (2008) *J Pharm Biomed Anal* 48(2):398–407
36. Bartolini M, Cavrini V, Andrisano V (2005) *J Chromatogr A* 1065(1):135–144
37. Noyes WA, Forman DB (1933) *J Am Chem Soc* 55(8):3493–3494
38. Merhar M, Podgornik A, Barut M, Zigon M, Strancar A (2003) *J Sep Sci* 26(3–4):322–330
39. Ren LB, Liu YC, Dong MM, Liu Z (2009) *J Chromatogr A* 1216(47):8421–8425

# Multidimensional nano-HPLC coupled with tandem mass spectrometry for analyzing biotinylated proteins

Jens Sproß · Sebastian Brauch · Friedrich Mandel ·  
Moritz Wagner · Stephan Buckenmaier ·  
Bernhard Westermann · Andrea Sinz

Received: 28 February 2012 / Revised: 12 April 2012 / Accepted: 16 April 2012 / Published online: 29 May 2012  
© Springer-Verlag 2012

**Abstract** Multidimensional high-performance liquid chromatography (HPLC) is a key method in shotgun proteomics approaches for analyzing highly complex protein mixtures by complementary chromatographic separation principles. Here, we describe an integrated 3D-nano-HPLC/nano-electrospray ionization quadrupole time-of-flight mass spectrometry system that allows an enzymatic digestion of proteins followed by an enrichment and subsequent separation of the created peptide mixtures. The *online* 3D-nano-HPLC system is composed of a monolithic trypsin reactor in the first dimension, a monolithic affinity column with immobilized monomeric avidin in the second dimension, and a reversed phase C18 HPLC-Chip in the third dimension that is coupled to a nano-ESI-Q-TOF mass spectrometer. The 3D-LC/MS setup

is exemplified for the identification of biotinylated proteins from a simple protein mixture. Additionally, we describe an *online* 2D-nano-HPLC/nano-ESI-LTQ-Orbitrap-MS/MS setup for the enrichment, separation, and identification of cross-linked, biotinylated species from chemical cross-linking of cytochrome *c* and a calmodulin/peptide complex using a novel trifunctional cross-linker with two amine-reactive groups and a biotin label.

**Keywords** Affinity enrichment · Avidin · Biotin · Monolithic column · Multidimensional HPLC · Protein identification

## Abbreviations

ACN	Acetonitrile
BSA	Bovine serum albumin
CaM	Calmodulin
DMSO	Dimethyl sulfoxide
ESI-Q-TOF	Electrospray ionization quadrupole time-of-flight
FA	Formic acid
HEPES	4-(2-hydroxyethyl)-1-piperazineethanesulfonic acid
IMER	Immobilized monolithic enzyme reactor
MACMA	Monolithic affinity column with immobilized monomeric avidin
MS	Mass spectrometry
MS/MS	Tandem mass spectrometry
NHS	<i>N</i> -hydroxysuccinimide
RP	Reversed phase
skMLCK	Skeletal muscle myosin light chain kinase
TFA	Trifluoroacetic acid
TOF	Time-of-flight
Tris-HCl	Tris(hydroxymethyl) aminomethane hydrochloride
Ugi-4CR	Ugi-4-component reaction

Published in the topical collection *Monolithic Columns in Liquid Phase Separations* with guest editor Luis A. Colon.

**Electronic supplementary material** The online version of this article (doi:10.1007/s00216-012-6057-9) contains supplementary material, which is available to authorized users.

J. Sproß (✉) · A. Sinz (✉)  
Department of Pharmaceutical Chemistry and Bioanalytics,  
Institute of Pharmacy, Martin-Luther University Halle-Wittenberg,  
Wolfgang-Langenbeck-Str. 4,  
06120 Halle (Saale), Germany  
e-mail: jens.spross@pharmazie.uni-halle.de  
e-mail: andrea.sinz@pharmazie.uni-halle.de

S. Brauch · B. Westermann  
Department of Bioorganic Chemistry,  
Leibniz Institute of Plant Biochemistry,  
Weinberg 3,  
06120 Halle (Saale), Germany

F. Mandel · M. Wagner · S. Buckenmaier  
Agilent Technologies,  
Hewlett-Packard-Str. 8,  
76337 Waldbronn, Germany

## Introduction

Mass spectrometry-based identification of proteins is usually performed in a “bottom-up” fashion relying on an enzymatic digestion of proteins, followed by reversed-phase (RP) chromatographic separation of the peptides, tandem mass spectrometric analysis, and database searching. However, complex biological samples as they are analyzed in proteomics require more potent separation techniques, namely, chromatographic techniques possessing high peak capacities [1–3]. One-dimensional RP-high-performance liquid chromatography (HPLC) approaches exhibit only limited peak capacities, whereas coupling of two columns with complementary separation principles leads to a dramatic increase in peak capacities [4, 5]. Ion exchange chromatography relies on a separation of peptides based on their charge and is therefore often used as first dimension for multidimensional HPLC separation in shotgun proteomics approaches [5, 6]. Also, the combination of hydrophilic interaction chromatography with RP-LC [7, 8] as well as the coupling of two RP separations, which are operated at different pH values [9, 10], have proven beneficial for analyzing protein mixtures. In case affinity chromatography is used as the first dimension, specific peptides can be targeted [11]: immobilized metal ion affinity chromatography is routinely used for the enrichment of phosphopeptides [12–14], immobilized lectins or boronate groups target glycoproteins and glycopeptides [15, 16], antibodies recognize specific antigens [17, 18], and (strept-)avidin is used for the enrichment of biotinylated species [19, 20].

As the enzymatic digestion step in “bottom-up” protein analysis is prone to introduce contaminations by manual sample handling, it is favorable to automatize the digestion procedure. Excellent results have been obtained by utilizing immobilized proteases, such as trypsin, chymotrypsin, and pronase in *online* digestion reactors [21–23]. Additional advantages of these enzyme reactors are the reduction of digestion times due to an increased enzymatic activity and a higher localized concentration of the immobilized enzyme as well as a direct transfer of peptides onto the separation column, thereby minimizing potential sample loss.

In functional proteomics studies, specific interactions of proteins with their binding partners, such as proteins, fatty acids, or nucleic acids, are investigated with the aim to elucidate biochemical pathways in the cell. An emerging strategy for studying protein assemblies is chemical cross-linking of interacting proteins followed by a mass spectrometric analysis of the created reaction products [24]. The proteins are cross-linked to their binding partners by chemical reagents that connect amino acid side chains within a defined distance before the cross-linked proteins are enzymatically digested and the cross-linked products are analyzed by LC/MS/MS. The cross-linker acts as a kind of

molecular ruler as the bridged distance is defined by the spacer length of the reagent [25]. In order to increase the amount of structural information from one cross-linking experiment, enrichment of cross-linked species has been performed by strong cation exchange chromatography [2, 3]. The use of trifunctional cross-linkers with an additional biotin moiety is another strategy to specifically enrich cross-linked species [26, 27]. In case biotinylated cross-linkers are used, monolithic affinity columns with immobilized monomeric avidin (MACMAs) have proven highly efficient for a rapid and efficient enrichment of cross-linked products [20].

In this paper, we describe a fully automated *online* 3D-nano-HPLC system coupled to nano-electrospray ionization quadrupole time-of-flight mass spectrometry (ESI-Q-TOF-MS) for an integrated tryptic digestion of proteins, an affinity enrichment of biotinylated peptides with monomeric avidin, peptide separation by RP-HPLC, and their subsequent identification by MS/MS. The digestion and affinity chromatography steps rely on the use of monolithic material. Biotinylated cytochrome *c* peptides were successfully identified from a simple protein mixture. Additionally, we established an *online* 2D-nano-HPLC/nano-ESI-LTQ-Orbitrap-MS/MS system composed of a monolithic monomeric avidin column as first dimension and a RP column as second dimension. A novel trifunctional cross-linker containing two amine-reactive *N*-hydroxysuccinimide (NHS) esters and a biotin group was used to cross-link cytochrome *c* and a calmodulin (CaM)/skeletal muscle myosin light chain kinase target peptide (skMLCK) complex. After an *in-solution* digestion, the created cross-linked products were readily enriched on the monomeric avidin column and identified by MS/MS.

## Experimental section

**Materials and reagents** Cytochrome *c* (horse heart), lysozyme (chicken egg white), myoglobin (horse heart),  $\beta$ -lactoglobulin (bovine milk), bovine serum albumin (BSA), tris(hydroxymethyl) aminomethane hydrochloride (Tris-HCl, 99 %), ammonium bicarbonate (99 %), ammonium acetate (99 %), 4-(2-hydroxyethyl)-1-piperazineethanesulfonic acid (HEPES; 99.5 %), calcium chloride (99 %), dimethyl sulfoxide (DMSO; 99.5 %), formic acid (FA; mass spectrometry grade), 2,2,2-trifluoroethanol, and 2,5-dihydroxy benzoic acid (gentisic acid, 99+%) were purchased from Sigma (Taufkirchen, Germany). Bovine CaM and benzamidine hydrochloride (97 %) were obtained from Calbiochem (Darmstadt, Germany). Trypsin gold (mass spectrometry grade) was obtained from Promega (Madison, WI, USA). Urea (99.5 %), and trifluoroacetic acid (TFA, UvaSolv<sup>®</sup>) were from Merck (Darmstadt, Germany). Acetonitrile (ACN, LiChroSolv<sup>®</sup> and for Mass Spectrometry) was obtained from Merck and JT Baker. NHS-PEG<sub>4</sub>-biotin was obtained from ThermoFisher Scientific (Rockford, IL, USA). Water was purified using a

Milli-Q5 system (Millipore) and Amicon Ultra (0.5 mL, cut-off 10 kDa) filtration units were from Millipore (Schwalbach, Germany). The trifunctional cross-linker PEG<sub>4</sub>-biotin-(NHS)<sub>2</sub> was synthesized *in-house* (Electronic Supplementary Material). The skMLCK peptide was synthesized by Dr. O. Jahn, Göttingen, Germany. All mixtures are given in *v/v* unless specified otherwise.

**Preparation of the monolithic trypsin reactor and monolithic avidin affinity column** Preparation of the immobilized monolithic enzyme reactor (IMER) [21] and the MACMA [20] was performed as described previously. Columns were stored in 50 mM Tris-HCl (pH 7.5), 0.02 % sodium azide at 4 °C before use.

**Synthesis of the trifunctional cross-linker PEG<sub>4</sub>-biotin-(NHS)<sub>2</sub>** For detailed information on the synthesis of PEG<sub>4</sub>-biotin-(NHS)<sub>2</sub> please refer to the Electronic supplementary material (ESM). The building blocks methyl 4-aminobutyrate hydrochloride and methyl 4-isocyanobutanoate were synthesized from  $\gamma$ -aminobutyric acid. The backbone of the cross-linker was subsequently synthesized in a one-pot four-component reaction with the additional building blocks *i*-butyraldehyde and 15-[D(+)-biotinylamino]-4,7,10,13-tetraoxapentadecanoic acid in the presence of triethylamine. Deprotection of carboxylic acid groups and coupling with NHS yielded PEG<sub>4</sub>-biotin-(NHS)<sub>2</sub> (Fig. 1) with an overall yield of 20 %.

**Biotinylation and cross-linking of cytochrome *c* and a CaM/skMLCK peptide complex** The biotinylation of cytochrome *c* was performed as reported previously with a reaction time of 5 min [20]. Cross-linking of cytochrome *c* and a CaM/skMLCK peptide complex was performed with the trifunctional cross-linker PEG<sub>4</sub>-biotin-(NHS)<sub>2</sub>. To a solution of cytochrome *c* (10  $\mu$ M) or a solution containing CaM

(10  $\mu$ M), skMLCK peptide (10  $\mu$ M), and 1 mM CaCl<sub>2</sub> (preincubated for 30 min), both in 20 mM HEPES (pH 7.5), a 60-fold molar excess of PEG<sub>4</sub>-biotin-(NHS)<sub>2</sub> (Fig. 1) in DMSO was added to give a total volume of 300  $\mu$ L; 100- $\mu$ L aliquots were taken after 15, 30, and 60 min, and the cross-linking reactions were terminated by adding ammonium bicarbonate to a final concentration of 20 mM. Excess NHS-PEG<sub>4</sub>-biotin or PEG<sub>4</sub>-biotin-(NHS)<sub>2</sub> was removed by Amicon Ultra filtration units (cut-off 10 kDa) according to the manufacturer's protocol (Millipore). Cross-linking reactions were monitored by MALDI-TOF-MS (Ultraflex III, Bruker Daltonik, Bremen) (Fig. 2) using 2,5-dihydroxy benzoic acid as matrix and the previously described parameters [20].

**Sample preparation for 3D-nano-HPLC/nano-ESI-Q-TOF-MS/MS** The concentration of biotinylated cytochrome *c* was adjusted to 2  $\mu$ M for experiments where only cytochrome *c* was present. In the protein mixture concentration of BSA, lysozyme and *b*-lactoglobulin was 2  $\mu$ M, whereas biotinylated cytochrome *c* had a concentration of 1  $\mu$ M. Both mixtures contained 2 M urea, 10 % ACN, and 0.1 M NH<sub>4</sub>HCO<sub>3</sub> to achieve optimal digestion performance.

**In-solution digestion of proteins** Thirty microliters of cross-linked cytochrome *c* or CaM/skMLCK peptide solution (10  $\mu$ M each) were mixed with 59  $\mu$ L of ammonium acetate (0.2 M) and 11  $\mu$ L urea (8 M) solutions. Trypsin was added to an enzyme-to-substrate ratio of 1:60 (*w/w*) and the mixtures were incubated at 37 °C for 16 h. Enzymatic digestion was stopped by adding benzamidine (4  $\mu$ M final concentration).

**3D-nano-HPLC/nano-ESI-Q-TOF-MS/MS setup** The HPLC system was composed of a micro-wellplate sampler (8- $\mu$ L injection needle), a capillary pump, two nano-pumps (all 1200 series, Agilent Technologies, Waldbronn, Germany), a nano-pump (1260 Infinity series, Agilent Technologies), and a column thermostat (1290 Infinity series, Agilent Technologies). The column oven was operated at a temperature of 37 or 50 °C. Switching between the first dimension (trypsin IMER, 210-mm column length) and the second dimension (MACMA, 200-mm column length) was performed via a six-port micro-switching valve (1100 series, Agilent Technologies). Directly after the second dimension (MACMA), the flow of the loading pump (6  $\mu$ L/min, 0.1 % (*v/v*) FA) was added to the flow from the MACMA via a T-shaped connection, and the enriched fraction of the digestion mixture was loaded onto the C18 trapping column of the HPLC-Chip. A ProtID-Chip-43 packed with 5  $\mu$ m 300 Å StableBond C18 particles (Agilent Technologies) was used for peptide separation in the third dimension (43-mm column length). The HPLC system was coupled to a 6530 Q-TOF mass spectrometer (Agilent Technologies) via a HPLC-Chip

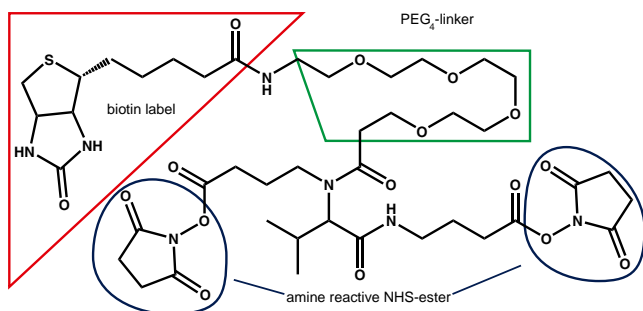


**Fig. 1** Chemical structure of the trifunctional, biotinylated cross-linker PEG<sub>4</sub>-biotin-(NHS)<sub>2</sub>. The biotin group (*triangle*) enables the enrichment of cross-linked species by affinity chromatography using monomeric avidin; the PEG-linker (*square*) enhances solubility; NHS esters (*circles*) react with nucleophilic groups of amino acid side chains, e.g.,  $\epsilon$ -amine groups of lysines

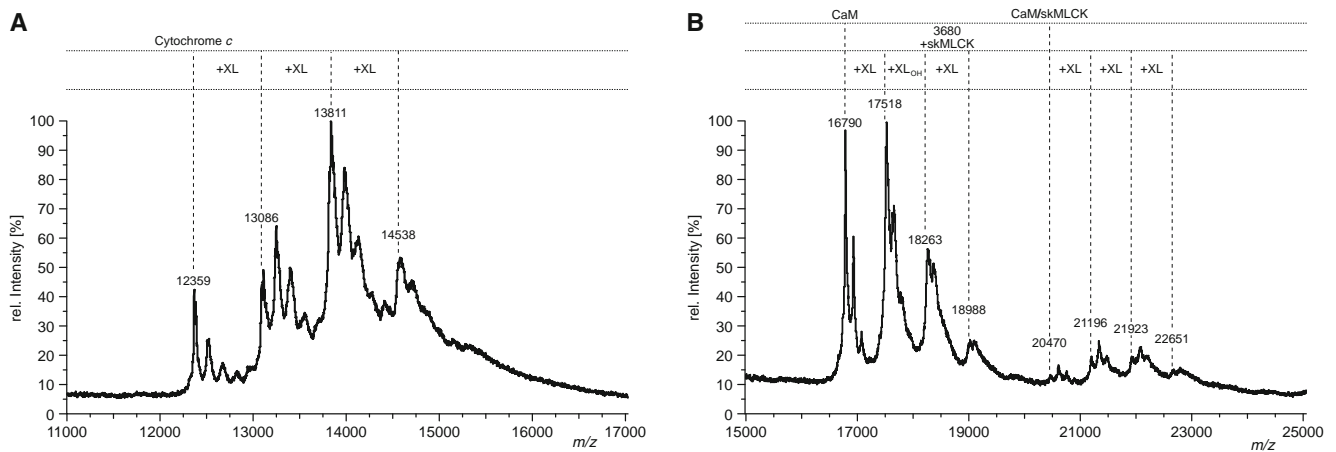


**Fig. 2** MALDI-TOF mass spectra of (A) cytochrome c and (B) CaM/skMLCK peptide complex cross-linked with the trifunctional, biotinylated cross-linker PEG<sub>4</sub>-biotin-(NHS)<sub>2</sub>, 15-min reaction time

Cube Nanospray ion source (Agilent Technologies). A schematic representation of the 3D-nano-HPLC/nano-ESI-Q-TOF-MS/MS system is shown in Fig. 3A.

In the Load 1 gradient step (Table 1), 5  $\mu$ L of protein solution were injected and digested on the trypsin reactor (IMER). Directly after the digestion, enzymatic peptides were subjected to the avidin affinity column (MACMA). After 45 min, the six-port micro-valve was switched from “load” to “wash/elute” to remove nonbound peptides using nano-pump 2. Meanwhile, the trapping column and separation column of the HPLC-Chip was set to “analysis” and were washed with a linear gradient.

The elution of biotinylated peptides from the MACMA was initiated by the injection of the injection of 5  $\mu$ L water, pH 7.6 (Elution1 gradient, Table 1). The six-port micro-valve was switched to “wash/elute” and the second nano-pump delivered 50 % ACN containing 0.4 % formic acid for 30 min. The HPLC-Chip was set to “enrichment” to enable trapping of biotinylated peptides eluting from the MACMA on the trapping column.

After 30 min the HPLC-Chip was set to “analysis” and bound peptides were separated on the analytical column using a linear 15-min gradient and analyzed with the Q-TOF instrument.

For ESI-MS, a spray voltage of 1.85 kV was employed and the temperature of the drying gas (nitrogen) was set to 350  $^{\circ}$ C at a flow rate of 3 L/min. MS data were acquired over 25 min in data-dependent MS/MS mode and in profile (MS) and centroid (MS/MS) data format. Survey MS scans ( $m/z$  100–2,000) were followed by product ion scans of the five most intense signals in the survey MS scan (isolation window 4 u). The collision energy for MS/MS (collision-induced dissociation) was determined using equation ( $E=(3.6*m/z)/100-4.8$ ) and singly charged signals were rejected from fragmentation. Precursor ions that had been fragmented were subjected to an active exclusion (0.8 s duration; exclusion window 10 ppm). The Q-TOF analyzer was operated in the Extended Dynamic Range mode. Chromatograms of the total ion current, MS, and MS/MS data were recorded on a PC with MassHunter Acquisition software B.04 (Agilent Technologies). External mass

**Fig. 3** Schematic representations of (A) online 3D-nano-HPLC/nano-ESI-Q-TOF-MS/MS (switching valve in “load” position), and (B) online 2D-nano-HPLC/nano-ESI-LTQ-Orbitrap-MS/MS (switching valve in “wash” position) setups. LP loading pump, NP nano-pump

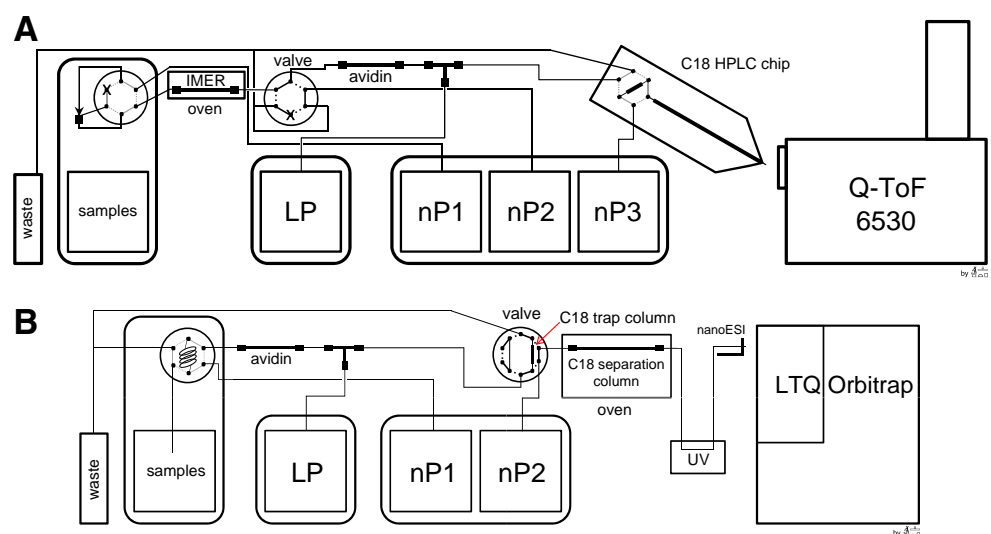


**Table 1** Load and elution gradients for the *online* 3D-nano-HPLC/nano-ESI-Q-TOF-MS/MS experiments

Time (min)	LP	nP1	nP2			nP3		Valve
	A1 (%)	B1 (%)	C1 (%)	D1 (%)	E1 (%)	F1 (%)	G1 (%)	
<b>Load 1</b>								
0	100	100	100	0	0	95	5	"Load"
20						65	35	
22						20	80	
26						20	80	
26.1						95	5	
39			100	0				"Wash/elute"
40			70	30				
45								
69			70	30				
70			100	0		95	5	
<b>Elution 1</b>								
0	100	100	0	0	100	95	5	"Wash/elute"
30					100	95	5	
31			100	0	0			
45						65	35	
47						20	80	
51						20	80	
51.1						95	5	
55						95	5	

Flow rate LP, 6  $\mu\text{L}/\text{min}$ ; flow rate nP1 and nP3, 300  $\text{nL}/\text{min}$ ; flow rate nP2, 500  $\text{nL}/\text{min}$ . A1, water with 0.1 % FA; B1, water, pH 7.6; C1, 0.1 M ammonium acetate, pH 7.0; D1, 50 % ACN, 0.1 M ammonium acetate, pH 7.0; E1, 50 % ACN containing 0.4 % formic acid; F1, water with 0.1 % FA; G1, ACN with 0.1 % FA. Compare also with Fig. 3A

LP loading pump, nP nano-pump

calibration and tuning of the mass spectrometer were performed in the positive ionization mode using the JetStream ESI source by direct infusion of a calibration mixture supplied from the manufacturer (Agilent Technologies). Internal mass calibration was performed by nebulizing a mixture of hexakis(1H,1H,3H-tetrafluoropropoxy)phosphazene ( $m/z$  922.0098) and purine ( $m/z$  121.0509) in the nano-ESI-source.

**2D-nano-HPLC/nano-ESI-LTQ-Orbitrap-MS/MS setup**  
*Online* enrichment and analysis of cross-linked, biotinylated peptides were performed on a nano-HPLC system consisting of a Famos autosampler (5- $\mu\text{L}$  sample loop), a Switchos II (loading pump and valves), an Ultimate™ system (two nano-HPLC pumps and a column oven operated at 35 °C, all Dionex/LC Packings, Idstein, Germany), and an U3000 variable wavelength UV detector (Dionex). The full-loop program was used for sample injection. Directly after the first dimension (MACMA), the flow of the loading pump (6  $\mu\text{L}/\text{min}$ , 0.1 % ( $v/v$ ) TFA) was added to the flow from the MACMA via a T-shaped connection, and the enriched peptides were loaded onto the C18 trapping column. A schematic representation of the 2D-nano-HPLC/nano-ESI-LTQ-Orbitrap-MS/MS setup is shown in Fig. 3B.

First, the in-solution digestion mixtures of the cross-linked cytochrome *c* or CaM/skMLCK peptide complex

were loaded onto the affinity column (200-mm column length) and nonbound peptides were removed by washing with 15 % ACN containing 1 mM ammonium acetate, pH 7.0 (Load 2 gradient, Table 2). In the meantime the C18 trapping column (Acclaim PepMap, C18, 100  $\mu\text{m} \times 20$  mm, 5  $\mu\text{m}$ , 100 Å, Dionex) and the separation column (Acclaim PepMap, C18, 75  $\mu\text{m} \times 150$  mm, 3  $\mu\text{m}$ , 100 Å, Dionex) were washed using a linear gradient.

Biotinylated cross-linked peptides were eluted by injecting 5  $\mu\text{L}$  of 50 % ACN containing 0.4 % formic acid (Elution 2 gradient, Table 2). Directly after the injection the ten-port switching valve was switched to enable the loading of the eluted cross-linked peptides onto the trapping column. After 25 min, the switching valve was switched again to enable the separation and analysis of the enriched biotinylated, cross-linked peptides. The separation was performed using a linear 45-min gradient. Peptides were detected by their UV absorption at 214 nm. Nano-ESI-LTQ-Orbitrap-MS/MS was performed on a LTQ-Orbitrap XL mass spectrometer (ThermoFisher Scientific) using the previously described parameters [21].

**Protein identification** Peptide mass fingerprint analysis and peptide fragment fingerprint analysis were conducted with MassHunter Qualitative Analysis B.04 (build 4.0.479.5 SP2)

**Table 2** Load and elution gradients for the *online* 2D-nano-HPLC/nano-ESI-LTQ-Orbitrap-MS/MS experiments

Time (min)	LP	nP1			nP2			Valve
	A2	B2	C2	D2	E2	F2		
<b>Load 2</b>								
0	100	100	0	100	0	0	“Wash”	
0.1		0	100					
15				100	0	0		
30		0	100					
31		100	0					
35				60	40	0		
36				60	25	15		
39				5	5	90		
40				5	5	90		
41				100	0	0		
45				100	0	0		
<b>Elution 2</b>								
0	100	100	0	100	0	0	“Elute”	
25				100	0	0	“Wash”	
70				60	40	0		
71				60	25	15		
80				5	5	90		
85				5	5	90		
86				100	0	0		
90				100	0	0		

Flow rate LP, 6  $\mu\text{L}/\text{min}$ ; flow rate nP1, 500 nL/min; flow rate nP2, 300 nL/min. A2, water with 0.1 % TFA; B2, 1 mM ammonium acetate, pH 7.0; C2, 15 % ACN, 1 mM ammonium acetate, pH 7.0; D2, 5 % ACN, 0.1 % FA; E2, 80 % ACN, 0.1 % FA; F2, 80 % ACN, 5 % 2,2,2-trifluoroethanol, 0.1 % FA. Compare also with Fig. 3B

LP loading pump, nP nano-pump

and BioConfirm (Agilent Technologies). A mass deviation of 10 ppm was allowed for MS data acquired with the Q-TOF instrument. The heme group (formal charge: +1;  $\text{C}_{34}\text{H}_{31}\text{N}_4\text{O}_4\text{Fe}$  mass: 615.1694), PEG<sub>4</sub>-biotinylation ( $\text{C}_{21}\text{H}_{35}\text{N}_3\text{O}_7\text{S}$  mass: 473.2196), and oxidized PEG<sub>4</sub>-biotinylation ( $\text{C}_{21}\text{H}_{35}\text{N}_3\text{O}_8\text{S}$  mass: 489.2145) were included as modifications for database searches of digested cytochrome *c*. Six missed cleavage sites and oxidation of methionine were additional parameters. Identification of cross-links with PEG<sub>4</sub>-biotin-(NHS)<sub>2</sub> ( $\text{C}_{34}\text{H}_{55}\text{N}_5\text{O}_{10}\text{S}$  mass: 725.3670) was performed with StavroX software version 2.0.6 [28] using mgf files (generated with Proteome Discoverer 1.2, ThermoFisher Scientific). Visualization of cross-links was performed with The PyMOL Molecular Graphics System, Version 1.3, Schrödinger, LLC (<http://www.pymol.org>).

## Results and discussion

*Enrichment of biotinylated cytochrome c peptides by 3D-nano-HPLC/nano-ESI-Q-TOF-MS/MS* Cytochrome *c* that had been modified with NHS-PEG<sub>4</sub>-biotin [20] was selected as model system for establishing the *online* 3D-nano-HPLC setup (Fig. 3A) as it is a small globular protein composed of 104 amino acids. Its *N* terminus is acetylated and a heme-group is attached to cysteines 14 and 21 via a thioether linkage. In total, 19 lysines can potentially be modified, but when using previously established optimized reaction conditions with NHS-PEG<sub>4</sub>-biotin, on average one biotin molecule is introduced per cytochrome *c* molecule [20]. If we expect four missed cleavage sites during *online* digestion of biotinylated cytochrome *c* using the IMER and assume a homogenous distribution of the biotinylation site, ca. 100 biotinylated peptides will be created in the mass range between 500 and 3,250 Da, with an average concentration of 100 fmol/biotinylated peptide.

Protein digestion using the monolithic trypsin reactor (IMER) and enrichment of biotinylated species on the MACMA have already been optimized in previous studies [20, 21]. Biotinylated peptides were loaded onto the MACMA in the presence of 0.1 M ammonium acetate (pH 7.0), whereas an efficient digestion of proteins on the monolithic trypsin reactor required a solution composed of 2 M urea, 10 % ACN, and 0.1 M ammonium bicarbonate to adjust the pH to 8.0. As it was unknown whether the MACMA would be able to capture biotinylated peptides under these harsh denaturing conditions, a 2D-nano-HPLC system consisting of a MACMA and a C18-RP HPLC-Chip was used to evaluate the compatibility of the digestion conditions with the affinity enrichment step. This step was essential for establishing the 3D-nano-HPLC system as the latter required a direct transfer of the eluate from the IMER to the MACMA without a previous desalting step. Loading of 5  $\mu\text{L}$  of an in-solution digest containing 3  $\mu\text{M}$  PEG<sub>4</sub>-biotinylated cytochrome *c*, 2 M urea, 10 % ACN, and 0.1 M ammonium bicarbonate revealed that mainly unbiotinylated peptides were present in the flow-through and washing fractions from the MACMA but that not all biotinylated peptides were retained on the affinity column. However, biotinylated peptides dominated the elution fraction—both by number and intensity—and most of the biotinylated peptides present in the flow-through and washing fractions were also detected in the elution fractions (data not shown). As the optimized digestion conditions did not significantly impair the enrichment performance of the MACMA, they were also employed for the *online* 3D-nano-HPLC system.

Five-microliter PEG<sub>4</sub>-biotinylated cytochrome *c* (2  $\mu\text{M}$ ) in the optimized buffer were injected. To ensure a complete transfer of the digested protein from trypsin reactor onto the affinity column, the valve separating the first and the second dimension (Fig. 3A) was switched after 45 min. The

**Table 3** Identified peptides in *online* 3D-nano-HPLC/nano-ESI-Q-TOF-MS/MS experiments

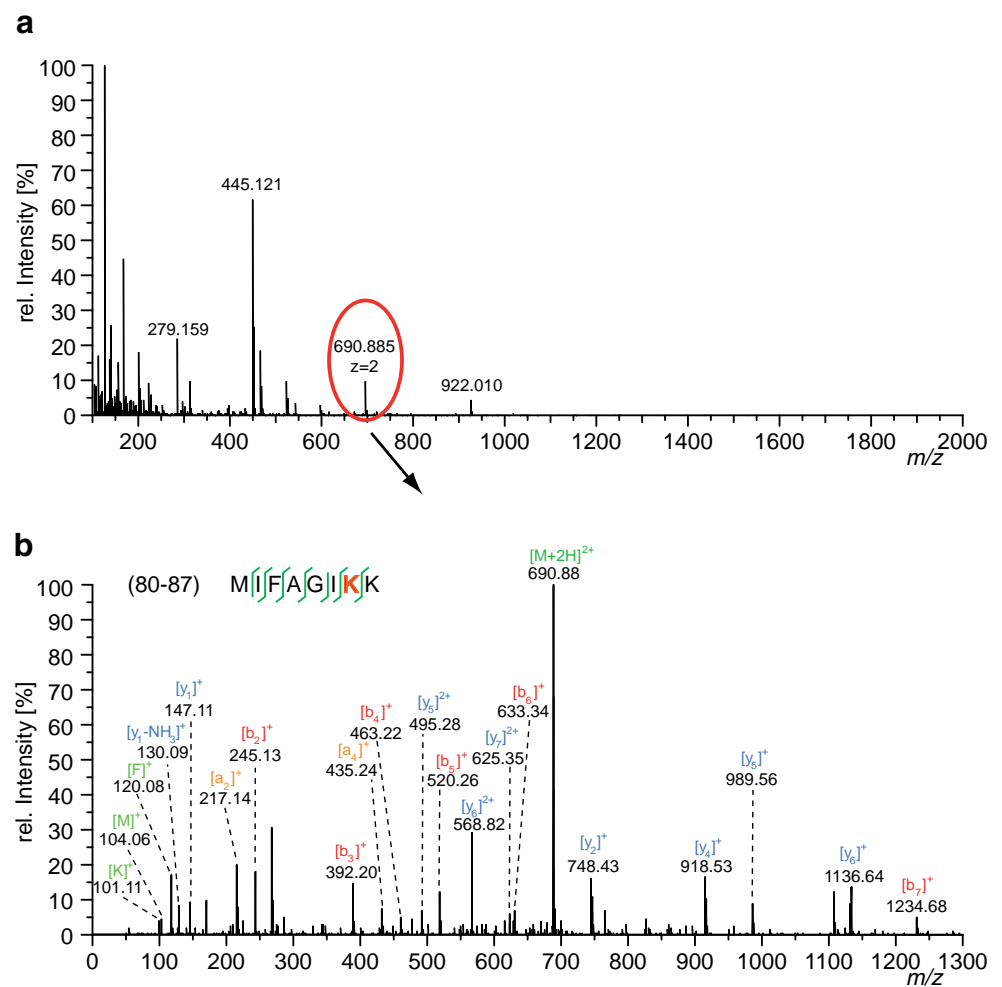
Protein	Digestion Temp. (°C)	# peptides	# biotinylated peptides	Sequence coverage
Cytochrome <i>c</i>	37	20±3	18±3	99±1
Cytochrome <i>c</i>	50	35±4	34±4	100±0
Cytochrome <i>c</i>	37	25±4	23±3	99±1
Lysozyme		0	n.a.	0
β-lactoglobulin		1±0.5	n.a.	11±8
BSA		0	n.a.	0
Cytochrome <i>c</i>	50	20±2	19±2	97±0
Lysozyme		1±0.8	n.a.	8±6
β-lactoglobulin		1±0	n.a.	20±0
BSA		0	n.a.	0

All experiments were performed in triplicates

MACMA was directly switched to washing conditions (15 % ACN, 0.1 M ammonium acetate) to remove nonspecifically bound peptides. This step was performed at a flow rate of 500 nL/min, which is higher than that of the previous digestion step. Flow-through and washing fraction were not

analyzed by MS. After a blank injection, nano-pump 2 was used to pump the elution mixture (50 % ACN, 0.4 % formic acid) through the MACMA. The eluate was trapped on the trapping column of the HPLC separation chip and subsequently separated and analyzed by nano-ESI-Q-TOF-MS/

**Fig. 4** MS analysis of biotinylated cytochrome *c*. **(a)** Survey mass spectrum at 43.7 min, **(b)** fragment ion mass spectrum of the 2<sup>+</sup>-charged precursor ion at *m/z* 690.885. The location of the PEG<sub>4</sub>-biotin modification was successfully identified as Lys86. The first dimension was operated at 50 °C



MS. On average, 20 cytochrome *c* peptides were identified, 18 of them were biotinylated (Table 3). Because of the detection of intact biotinylated cytochrome *c* we increased the digestion temperature of the first dimension from 37 to 50 °C. The activity of the immobilized trypsin was further enhanced resulting in the identification of 35 cytochrome *c* peptides on average, 34 of them being biotinylated and intact biotinylated cytochrome *c* was not detected (Table 3; Fig. 4). A sequence coverage of 100 % was obtained. Interestingly, oxidized PEG<sub>4</sub>-biotin modifications were only

present in cytochrome *c* peptides with heme modification, thus supporting our hypothesis of an involvement of the heme group in the oxidation of the PEG<sub>4</sub>-biotin modification [20]. In almost all cases, unmodified cytochrome *c* peptides contained the heme group indicating that mainly hydrophobic peptides were retained by the MACMA. Figure 4 shows a result of a typical 3D-LC/MS/MS experiment for cytochrome *c*.

Using these optimized conditions, a simple protein mixture comprised of biotinylated cytochrome *c* (1 μM), BSA,

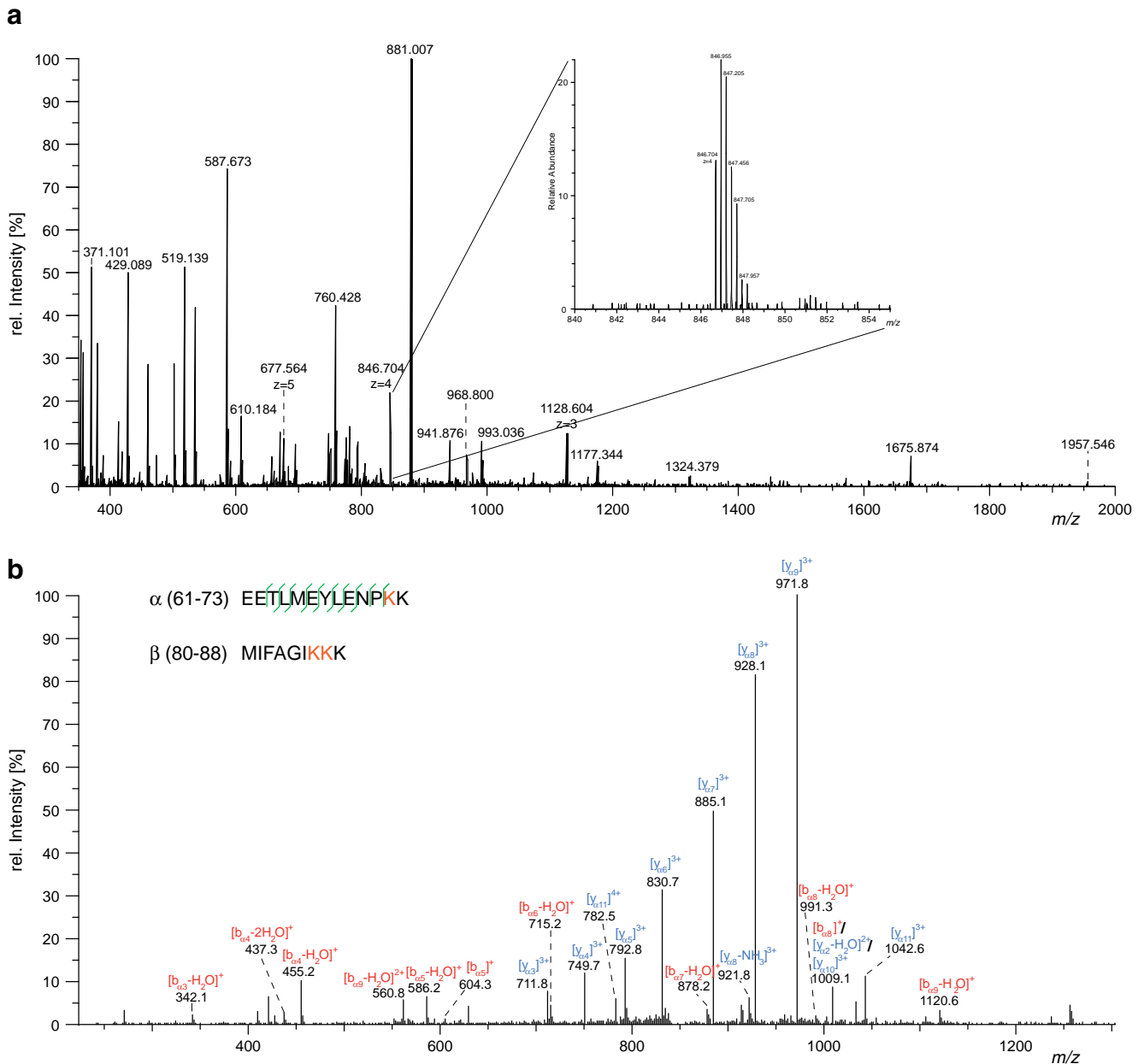


**Fig. 5** MS analysis of cross-linked cytochrome *c*. **(a)** Survey mass spectrum at 69.6 min, **(b)** fragment ion mass spectrum of the 4+ charged precursor ion at *m/z* 846.704. Fragment ion mass spectra

of an additional charge state allowed narrowing down cross-linked amino acids to K72 and K86/87

**Table 4** Intramolecular cross-linked products within cytochrome *c*, identified with the 2D-nano-HPLC/nano-ESI-LTQ-Orbitrap-MS/MS system

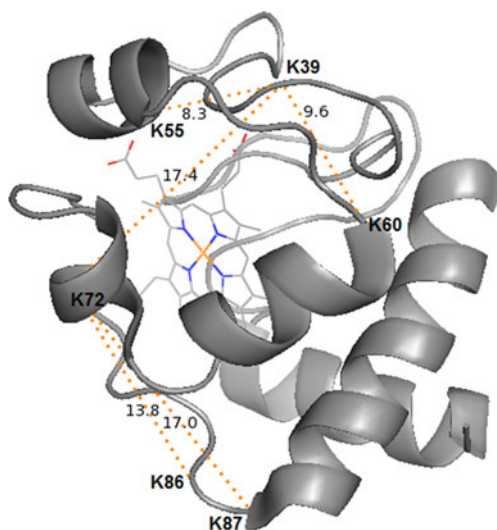
[M+H] <sup>+</sup> calculation	<i>z</i>	$\Delta$ (ppm)	Cyt <i>c</i> sequence A	Cyt <i>c</i> sequence B	C $\alpha$ distance (Å)
3,383.790	4/5	0.8/0.1	61–73 [K72]	80–88 [K86/87]	13.8/17.0
3,875.996	4	1.5	40–55 [K53]	74–86 [K79]	11.6
4,532.259	3/4/5	1.3/1.7/1.2	56–73 [60]	39–53 [K39]	9.6
4,646.306	4/5	1.3/0.5	56–72 [K72]	39–55 [K39]	17.4
4,774.399	4/5/6	–0.1/0.3/0.2	54–73 [K55/72]	39–53 [K39]	8.3/17.4

lysozyme, and  $\beta$ -lactoglobulin (2  $\mu$ M each) was analyzed (injection volume 5  $\mu$ L). When operating the trypsin reactor at 37 °C, on average 25 cytochrome *c* peptides were identified, with 23 being biotinylated (Table 3). Only one  $\beta$ -lactoglobulin peptide was identified in some of the analyses. However, intact biotinylated cytochrome *c* and  $\beta$ -lactoglobulin were detected which was overcome by increasing the temperature in the first dimension to 50 °C. 20 cytochrome *c* peptides, 19 of them being biotinylated were identified using these conditions. One  $\beta$ -lactoglobulin peptide was identified in all LC/MS analyses, whereas one lysozyme peptide was merely present in a single LC/MS analysis. BSA peptides were never detected in both experiments proving the excellent performance of the 3D-nano-HPLC/nano-ESI-Q-TOF-MS/MS setup in simple protein mixtures. Nonbiotinylated peptides were effectively depleted and almost exclusively biotinylated peptides were transferred to the third dimension (RP-LC) and MS analysis.

**Synthesis of the cross-linker PEG<sub>4</sub>-biotin-(NHS)<sub>2</sub>** Based on the modular design of trifunctional cross-linking reagents [29] we envisioned synthesis of an amine-reactive and biotinylated cross-linker in a one-pot multicomponent

reaction, such as the Ugi-4-component reaction (Ugi-4CR). The Ugi-4CR enables the synthesis of structural highly diverse peptoids by simply combining one equivalent each of an amine, a carbonyl compound (aldehyde or ketone), a carboxylic acid, and an isocyanide in one step with water as the sole by-product (Scheme S1 in the ESM), whereas common synthetic approaches exhibit a much higher synthetic effort [30–32]. Moreover, the Ugi-4CR enables a fast synthesis of structurally diverse cross-linking reagents by simply varying one of the components and is not relying on toxic and/or expensive coupling reagents [33].

The synthesis of the cross-linker started with the combination of all four building blocks of the Ugi-4CR (*i*-butyraldehyde, methyl 4-aminobutyrate hydrochloride, methyl 4-isocyanobutanoate, and 15-[D(+)-biotinylamino]-4,7,10,13-tetraoxapentadecanoic acid) in the presence of equimolar amounts of triethylamine yielding the protected precursor PEG<sub>4</sub>-biotin-(COOMe)<sub>2</sub>. Subsequent alkaline cleavage of the methyl ester and treatment of the resulting dicarboxylic acid PEG<sub>4</sub>-biotin-(COOH)<sub>2</sub> with NHS under classical coupling conditions lead to the formation of the activated PEG<sub>4</sub>-biotin-(NHS)<sub>2</sub> (Fig. 1).

**Fig. 6** X-ray structure of cytochrome *c* (pdb entry: 1HRC). Cross-links: orange dotted lines; the heme group is shown as sticks. Distances are given in Å (visualized with The PyMOL Molecular Graphics System, Version 1.3, Schrödinger, LLC)

**Enrichment of cross-linked cytochrome *c* peptides by 2D-nano-HPLC/nano-ESI-LTQ-Orbitrap-MS/MS** For the analysis of cross-linked cytochrome *c*, we employed the trifunctional, biotinylated cross-linker PEG<sub>4</sub>-biotin-(NHS)<sub>2</sub>. The cross-linking reaction was monitored by MALDI-TOF-MS and an average incorporation of two cross-linkers per cytochrome *c* was observed (Fig. 2A). Cross-linked proteins require longer digestion times due to stabilization of their 3D-structures by the introduced cross-links. The short

**Table 5** Intermolecular cross-linked products between calmodulin and skMLCK, identified with the 2D-nano-HPLC/nano-ESI-LTQ-Orbitrap-MS/MS system

[M+H] <sup>+</sup> calculation	<i>z</i>	$\Delta$ (ppm)	CaM sequence	skMLCK sequence	Distance (Å)
2,380.290	4/5	3.8/3.3	75–77 [K75]	21–33 [K21]	15.3
3,438.742	4	2.0	75–86 [K75]	21–33 [K21]	15.3
3,870.092	5/6	4.9/4.0	14–21 [K21]	1–18 [K3]	20.6

digestion times of the IMER, i.e., 231 s, are not sufficient for a complete digestion of cross-linked protein, therefore we chose to perform an in-solution digestion prior to *online* 2D-LC/MS/MS analysis. Enrichment and separation of the cross-linked peptides was performed using an *online* 2D-nano-HPLC/MS set-up with a monomeric avidin monolithic affinity column in the first dimension and a C18 particle column for RP-separation in the second dimension (Fig. 3B). Eluted cross-linked, biotinylated peptides were analyzed by nano-ESI-LTQ-Orbitrap-MS/MS to identify cross-linked amino acids within cytochrome *c* (Fig. 5). We were able to identify five cross-links with  $C_{\alpha}$ - $C_{\alpha}$  distances ranging between 8.3 and 17.4 Å (Table 4, Fig. 6), which agree well with the X-ray structure of cytochrome *c* (pdb: 1HRC) [34]. Due to the relatively large number (19) of lysine residues and the presence of three lysine clusters in cytochrome *c* the assignment of involved lysine residues was sometimes not unambiguous; however, MS fragmentation data enabled to narrow down potentially cross-linked residues (Fig. 5C). PEG<sub>4</sub>-biotin-(NHS)<sub>2</sub> possess a spacer length of approximately 16.5 Å and because of the flexibility of amino acid side chains a  $C_{\alpha}$ - $C_{\alpha}$  distance of 25.5 Å or even 31.5 Å can be assumed as constraint for cross-linked lysine residues. All identified cross-links bridge distances below this limit and extend the number of previously identified cross-links [35].

*Enrichment of cross-linked CaM/skMLCK peptides by 2D-nano-HPLC/nano-ESI-LTQ-Orbitrap-MS/MS* Using the optimized setup we analyzed a 20 kDa complex of the calcium-activated signal transduction protein CaM with a peptide derived from the skMLCK. The trifunctional cross-linker PEG<sub>4</sub>-biotin-(NHS)<sub>2</sub> allowed us to identify three cross-links after affinity enrichment (Table 5, Fig. S1 in the ESM). The distances between CaM and the peptide are within the range that can be bridged by the cross-linker (Fig. S2 in the ESM) [36] and are in agreement with the cross-links that have previously been identified with alternative amine- and photo-reactive cross-linkers (Schaks et al., unpublished data).

## Conclusions

An *online* 3D nano-HPLC/nano-ESI-Q-TOF-MS/MS system was established that allows a fully automated digestion, enrichment, separation, and MS/MS analysis of biotinylated proteins. The depletion of nonbiotinylated peptides was highly efficient in the cases where biotinylated cytochrome *c* or a simple protein mixture were analyzed. The introduction of the trifunctional cross-linker PEG<sub>4</sub>-biotin-(NHS)<sub>2</sub> presents a valuable expansion of the existing entity of cross-linking reagents available for protein structure analysis. The biotin group enables an efficient enrichment of

cross-linked species and enhances their MS identification as demonstrated in an *online* 2D-nano-HPLC system, composed of an affinity and a RP-chromatographic separation, coupled to nano-ESI-LTQ-Orbitrap-MS/MS. Further studies will be necessary to evaluate the applicability of our setups for more complex sample mixtures.

**Acknowledgments** J.S. acknowledges the “*Mass Spec Research Summer 2011*” award (Agilent Technologies) of the DGMS (German Society for Mass Spectrometry). The authors thank Dr. C.H. Ihling for assistance with MS and Dr. O. Jahn for synthesis of the skMLCK peptide. J.S. thanks Dr. A. Svatoš and Dr. A. Muck for the introduction to monolithic supports.

## References

- Schley C, Altmeyer MO, Swart R, Muller R, Huber CG (2006) *J Proteome Res* 5(10):2760–2768
- Chen ZA, Jawhari A, Fischer L, Buchen C, Tahir S, Kamenski T, Rasmussen M, Lariviere L, Bukowski-Wills JC, Nilges M, Cramer P, Rappsilber J (2010) *EMBO J* 29(4):717–726
- Fritzsche R, Ihling CH, Gotze M, Sinz A (2012) *Rapid Commun Mass Spectrom*: RCM 26(6):653–658
- Dugo P, Cacciola F, Kumm T, Dugo G, Mondello L (2008) *J Chromatogr A* 1184(1–2):353–368
- Karty JA, Running WE, Reilly JP (2007) *J Chromatogr B* 847(2):103–113
- Wolters DA, Washburn MP, Yates JR (2001) *Anal Chem* 73(23):5683–5690
- Boersema PJ, Divecha N, Heck AJR, Mohammed S (2007) *J Proteome Res* 6(3):937–946
- Mihailova A, Malerod H, Wilson SR, Karaszewski B, Hauser R, Lundanes E, Greibrokk T (2008) *J Sep Sci* 31(3):459–467
- Gilar M, Olivova P, Daly AE, Gebler JC (2005) *J Sep Sci* 28(14):1694–1703
- Delmotte N, Lasasoa M, Tholey A, Heinze E, Huber CG (2007) *J Proteome Res* 6(11):4363–4373
- Sproß J, Sinz A (2011) *J Sep Sci* 34(16–17):1958–1973
- Dong J, Zhou H, Wu R, Ye M, Zou H (2007) *J Sep Sci* 30(17):2917–2923
- Feng S, Pan CS, Jiang XG, Xu SY, Zhou HJ, Ye ML, Zou HF (2007) *Proteomics* 7(3):351–360
- Hou CY, Ma JF, Tao DY, Shan YC, Liang Z, Zhang LH, Zhang YK (2010) *J Proteome Res* 9(8):4093–4101
- Ren LB, Liu YC, Dong MM, Liu Z (2009) *J Chromatogr A* 1216(47):8421–8425
- Zhong HW, El Rassi Z (2009) *J Sep Sci* 32(10):1642–1653
- Sun XH, Yang WC, Pan T, Woolley AT (2008) *Anal Chem* 80(13):5126–5130
- Yang WC, Sun XH, Pan T, Woolley AT (2008) *Electrophoresis* 29(16):3429–3435
- Delmotte N, Kobold U, Meier T, Gallusser A, Strancar A, Huber CG (2007) *Anal Bioanal Chem* 389(4):1065–1074
- Sproß J, Sinz A (2012) *Anal Bioanal Chem* 402(7):2395–2405
- Sproß J, Sinz A (2010) *Anal Chem* 82(4):1434–1443
- Ponomareva EA, Kartuzova VE, Vlakh EG, Tennikova TB (2010) *J Chromatogr B* 878(5–6):567–574
- Temporini C, Dolcini L, Abee A, Calleri E, Galliano M, Caccialanza G, Massolini G (2008) *J Chromatogr A* 1183(1–2):65–75
- Sinz A (2006) *Mass Spectrom Rev* 25(4):663–682
- Green NS, Reisler E, Houk KN (2001) *Protein Sci* 10(7):1293–1304

26. Sinz A, Kalkhof S, Ihling C (2005) *J Am Soc Mass Spectrom* 16 (12):1921–1931
27. Hurst GB, Lankford TK, Kennel SJ (2004) *J Am Soc Mass Spectrom* 15(6):832–839
28. Götze M, Pettelkau J, Schaks S, Bosse K, Ihling C, Krauth F, Fritzsche R, Kühn U, Sinz A. *J Am Soc Mass Spectrom* 1–12
29. Trester-Zedlitz M, Kamada K, Burley SK, Fenyo D, Chait BT, Muir TW (2003) *J Am Chem Soc* 125(9):2416–2425
30. Dömling A, Ugi I (2000) *Angew Chem Int Ed* 39(18):3169–3210
31. Dömling A (2006) *Chem Rev* 106(1):17–89
32. Westermann B, Dörner S (2005) *Chem Commun* 16:2116–2118
33. Brauch S, Henze M, Osswald B, Naumann K, Waessjohann LA, van Berkel SS, Westermann B (2012) *Org Biomol Chem* 10:958–965
34. Bushnell GW, Louie GV, Brayer GD (1990) *J Mol Biol* 214(2):585–595
35. Dihazi GH, Sinz A (2003) *Rapid Commun Mass Spectrom* 17 (17):2005–2014
36. Ikura M, Clore GM, Gronenborn AM, Zhu G, Klee CB, Bax A (1992) *Science* 256(5057):632–638

## Acknowledgement

Zu allererst geht mein Dank an Frau Prof. Dr. Andrea Sinz, für die Möglichkeit ein Thema zu bearbeiten, das in eine etwas andere Richtung ging, als zuerst geplant. Vielen Dank für die Aufnahme in ihre Arbeitsgruppe, die exzellenten Arbeitsbedingungen, für die Möglichkeit Ergebnisse und Probleme zu diskutieren, die herausragende Zusammenarbeit beim Verfassen der Publikationen, die fortwährende Motivation und ihr Vertrauen in das selbständige wissenschaftliche Arbeiten.

Allen Mitgliedern der AG Sinz danke ich für das herzliche und freundschaftliche Arbeitsklima, an das ich immer mit viel Freude zurückdenken werde. Für die vielen fruchtbaren Diskussionen, Ratschläge, Grillabende und den Kuchen bei den Donnerstagsseminaren bedanke ich mich vor allem bei den 206lern Mathias, Stefan, Bine, Konny und Romy, sowie Christian, Knut, Fabian, dem kleinen Jens, Michael, Rico, Bärbel, Dirk, Frau Peters, Frau Knies, Frau Brandt und Frau Nishnik. Außerdem vielen Dank für die Geduld, wenn ich mal wieder die Orbitrap mit Beschlag belegt hatte.

Für die Übernahme der Zweit- und Drittgutachten danke ich Prof. Dr. Hans-Herrmann Rüttinger und Prof. Dr. Frank-Michael Matysik vielmals.

Dr. Christian Ihling danke ich für die Einweisung und die wertvollen Tipps bei der Bedienung und dem Arbeiten mit den nano-HPLC Anlagen und den Massenspektrometern, die viele Ergebnisse dieser Arbeit erst ermöglicht haben. Prof. Dr. Hans-Herrmann Rüttinger danke ich für die Möglichkeit, Messungen mit den CE-Geräten und dem Fluoreszenzspektroskop durchzuführen, wodurch die Charakterisierung der monolithischen Säulen erst möglich wurde.

Der Deutschen Gesellschaft für Massenspektrometrie danke ich für die Verleihung des Preises des *Mass Spec Research Summer*, gesponsert von der Firma Agilent Technologies. Vielen Dank auch an alle Verantwortlichen von Agilent Technologies, vor allem Dr. Volker Gnau,

Dr. Friedrich Mandel, Dr. Moritz Wagner, Dr. Stephan Buckenmaier und Claudia Meyer, für die Organisation und Betreuung während meines zweimonatigen Aufenthalt in Waldbronn.

Sebastian Brauch und Prof. Dr. Bernhard Westermann danke ich für die Synthese des neuen Cross-Linkers PEG<sub>4</sub>-Biotin-(NHS)<sub>2</sub> und die nette sowie erfolgreiche Kooperation. Für die Entwicklung der Auswertesoftware StavroX danke ich Michael Götze, eine wahre Erleichterung bei den großen Datenmengen. Nadja, Ulla und Sir Joseph danke ich für die zuverlässige Zusammenarbeit.

Dr. Aleš Svatoš und Dr. Alexandr Muck danke ich für die Unterstützung und Ratschläge während meiner Diplomarbeitszeit in der ich erste Erfahrungen mit monolithischen Säulen sammeln konnte.

Außerdem danke ich German Erenkamp und Dr. Alexandr Muck für die Unterstützung bei der Suche nach Fehlern in dieser Arbeit und Christina Lehmann für die Überprüfung des finalen Layouts. Alle verbleibenden Fehler gehen auf mein Konto.

Ganz besonders möchte ich mich bei meiner Freundin für ihre jahrelange Geduld, ihre Ermutigungen, Unterstützung und die notwendigen Ablenkung danken. Ich danke auch meinen Eltern und den Pöbneckern für ihre vielfältige Unterstützung während meiner Promotionszeit.

## Publication List

## Patent:

Monolithische Säule mit immobilisiertem monomeren Avidin zur Anreicherung und Identifizierung biotinylierter Spezies; Patent application on 09. October 2008; file number DE 10 2008 050 588.9

## Publications in peer-reviewed journals:

**Sproß, J.** and Sinz, A., Immobilized Monolithic Enzyme Reactors for Application in Proteomics and Pharmaceutics. *Anal. Bioanal. Chem.* **395**, 1583–1588 (2009) [Trend article]

**Sproß, J.** and Sinz, A., A Capillary Monolithic Trypsin Reactor for Efficient Protein Digestion in Online and Offline Coupling to ESI and MALDI Mass Spectrometry. *Anal. Chem.* **82**, 1434–1443 (2010)

**Sproß, J.** and Sinz, A., Monolithic media for applications in affinity chromatography. *J Sep Sci.* **34**, 1958–1973 (2011) [Review]

**Sproß, J.** and Sinz, A., Monolithic columns with immobilized monomeric avidin: preparation and application for affinity chromatography. *Anal. Bioanal. Chem.* **402**, 2395–2405 (2012)

**Sproß, J.**, Brauch, S., Mandel, F., Wagner, M., Buckenmaier, S., Westermann, B. and Sinz, A., Multidimensional Nano-HPLC Coupled with Tandem Mass Spectrometry for Analyzing Biotinylated Proteins. *Anal. Bioanal. Chem.* **405**, 2163-2173 (2013)

## Publications in journals without peer-review:

**Sproß, J.** and Sinz, A., HPLC mit monolithischen Säulen. *Deutsche Apotheker-Zeitung* **149**, 3390–3392 (2009)

Conference contributions

Oral presentations:

Nano-Flow Monolithic Enzyme Reactors with Immobilized Trypsin for Proteomics Applications. *18<sup>th</sup> International Mass Spectrometry Convention* (2009), Bremen

Ein monolithischer Reaktor mit immobilisiertem Trypsin für Anwendungen in der Pharmazie und Proteomik. *Jahrestagung der Deutschen Pharmazeutischen Gesellschaft* (2010), Braunschweig

Herstellung monolithischer Säulen zur LC/MS/MS Analyse von Proteinen und Arzneistoffen. *Jahrestagung der Deutschen Pharmazeutischen Gesellschaft* (Fachgruppe Pharmazeutische Analytik) (2010), Braunschweig

Monolithischen Säulen mit immobilisiertem monomeren Avidin zur Affinitätsanreicherung. *44. Jahrestagung der Deutschen Gesellschaft für Massenspektrometrie* (2011), Dortmund

Monomeric Avidin Immobilized on a Monolithic Column for Affinity Purification of Biotinylated Proteins and Peptides. *Doktorandentagung der Deutschen Pharmazeutischen Gesellschaft* (2011), Heringsdorf

Digestion, Enrichment, and Separation of Proteins – Establishing an online 3D nano-HPLC/MS/MS System for Protein Analysis. *45. Jahrestagung der Deutschen Gesellschaft für Massenspektrometrie* (2012), Poznan

Poster:

Identification of protein interaction partners using different cross-linkers and affinity purification combined with MALDI-TOF/TOF-MS. *First International Meeting of the GRK 1026* (2008), Halle (Saale) und *41. Jahrestagung der Deutschen Gesellschaft für Massenspektrometrie* (2008), Gießen

Monolithic Enzyme Reactor with Immobilized Trypsin for Proteomics Applications.  
*42. Jahrestagung der Deutschen Gesellschaft für Massenspektrometrie* (2009), Konstanz

A Monolithic Trypsin Reactor for Protein Digestion by *off-line* and *on-line* Nano-LC/MS.  
*43. Jahrestagung der Deutschen Gesellschaft für Massenspektrometrie* (2010), Halle (Saale)

Monomeric Avidin Immobilized on a Monolithic Column for Affinity Purification of Biotinylated Proteins and Peptides. *Second International Meeting of the GRK 1026* (2011), Halle (Saale) und *ANAKON 2011*, 2011 Zürich

## Curriculum Vitae

<b>Name</b>	Jens Sproß
<b>Date of birth</b>	20. November 1981
<b>Place of birth</b>	Villingen-Schwenningen
<b>Education</b>	Gymnasium am Deutenberg 1992 - 1999 Gymnasium am Romäusring 1999 - 2001 (Abitur)
<b>Military service</b>	Basic military service 01.07.2001 – 31.03.2002
<b>Diploma thesis</b>	Diploma studies: Chemistry, Friedrich-Schiller-University Jena, 2002 – 2007 Student-employments at the Max-Planck Institute (MPI) for Chemical Ecology in the Departments NMR (Dr. Bernd Schneider) and MS (Dr. Aleš Svatoš), 2002 – 2006 Completion of the diploma thesis ( <i>Monolithic columns for nanoLC-ESI-MS analysis of proteins and peptides</i> ) at the MPI for Chemical Ecology in the MS department under the supervision of Dr. Aleš Svatoš (MPI for Chemical Ecology) and PD Dr. Gerhard Mohr (Institute for Physical Chemistry, FSU Jena), Prof. Dr. Georg Pohnert, (referee; Institute for Inorganic and Analytical Chemistry, FSU Jena)
<b>Doctoral thesis</b>	Since 09/2007 Department “Pharmaceutical Chemistry and Bioanalytics”, Institute of Pharmacy, Martin-Luther-University Halle-Wittenberg under the supervision of Prof. Dr. Andrea Sinz.  08/2011 – 09/2011: Research stay at Agilent Technologies (Waldbronn) ( <i>Agilent Mass Spec Research Summers 2011</i> )
<b>Professional life</b>	Since 06/2012: employed at the Department of Chemistry, Institute of Organic Chemistry I, University of Bielefeld as head of the MS department.

## Selbständigkeitserklärung

Ich versichere hiermit, die vorliegende Dissertation selbständig und ohne unerlaubte fremde Hilfe angefertigt zu haben. Ich habe keine anderen als die im Literaturverzeichnis angeführten Quellen genutzt und sämtliche Textstellen, die wörtlich oder sinngemäß aus veröffentlichten oder unveröffentlichten Schriften entnommen wurden, und alle Angaben, die auf mündlichen Auskünften beruhen, als solche kenntlich gemacht. Ebenfalls sind alle von anderen Personen bereitgestellten Materialien oder erbrachten Dienstleistungen als solche gekennzeichnet. Für alle verwendeten Abbildungen, die von anderen Personen erstellt wurden, wurde die Erlaubnis zur Veröffentlichung in dieser Arbeit eingeholt. Bei der Auswahl und Auswertung des Materials, bei der Herstellung des Manuskripts, sowie bei der geistigen Herstellung der vorgelegten Arbeit waren keine anderen Personen beteiligt. Insbesondere wurde weder die Hilfe eines Promotionsberaters in Anspruch genommen, noch haben Dritte von mir unmittelbar oder mittelbar geldwerte Leistungen für Arbeiten erhalten, die im Zusammenhang mit dem Inhalt der vorgelegten Dissertation stehen. Die vorgelegte Arbeit ist weder im Inland noch im Ausland in gleicher oder ähnlicher Form einer anderen Prüfungsbehörde zum Zweck einer Promotion oder eines anderen Prüfungsverfahrens vorgelegt worden. Ich habe keine früheren erfolglosen Promotionsversuche unternommen.

Halle (Saale), den 03. September 2012

Jens Sproß

Cover: composed by Jens Sproß.

Background: SEM image of M-1 and M-2, adapted with permission from [10], copyright 2012, Springer.

Front: “Monolith Monsters” movie poster was created by Reynold Brown, copyright 1958 by Universal Pictures Co., Inc. Modification was performed by Jens Sproß. Protein visualization was performed with The PyMOL Molecular Graphics System, Version 1.3, Schrödinger, LLC (<http://www.pymol.org>). Back: MS spectrum, MS/MS spectrum, and protein structure with cross-links were adapted with permission from [11], copyright 2012, Springer.